NASA CR-165,829, V.1

NASA Contractor Report 165829

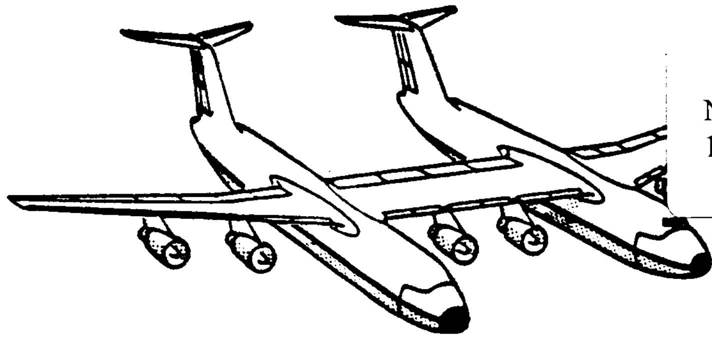

MULTIBODY AIRCRAFT STUDY
VOLUME I

J. W. Moore; E. P. Craven;
B. T. Farmer; J. F. Honrath;
R. E. Stephens; R. T. Meyer

LOCKHEED-GEORGIA COMPANY
A Division of Lockheed Corporation
Marietta, Georgia 30063

Contract No. NAS1-15927
JULY 1982

NASA
National Aeronautics and
Space Administration

Langley Research Center
Hampton, Virginia 23665

NASA Contractor Report 165829

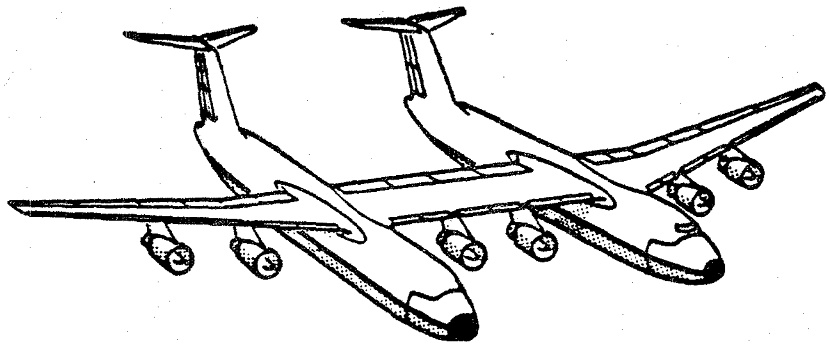

MULTIBODY AIRCRAFT STUDY
VOLUME I

J. W. Moore; E. P. Craven;
B. T. Farmer; J. F. Honrath;
R. E. Stephens; R. T. Meyer

LOCKHEED-GEORGIA COMPANY
A Division of Lockheed Corporation
Marietta, Georgia 30063

Contract No. NAS1-15927
JULY 1982

NASA
National Aeronautics and
Space Administration

Langley Research Center
Hampton, Virginia 23665

N82-32344 #

This Page Intentionally Left Blank

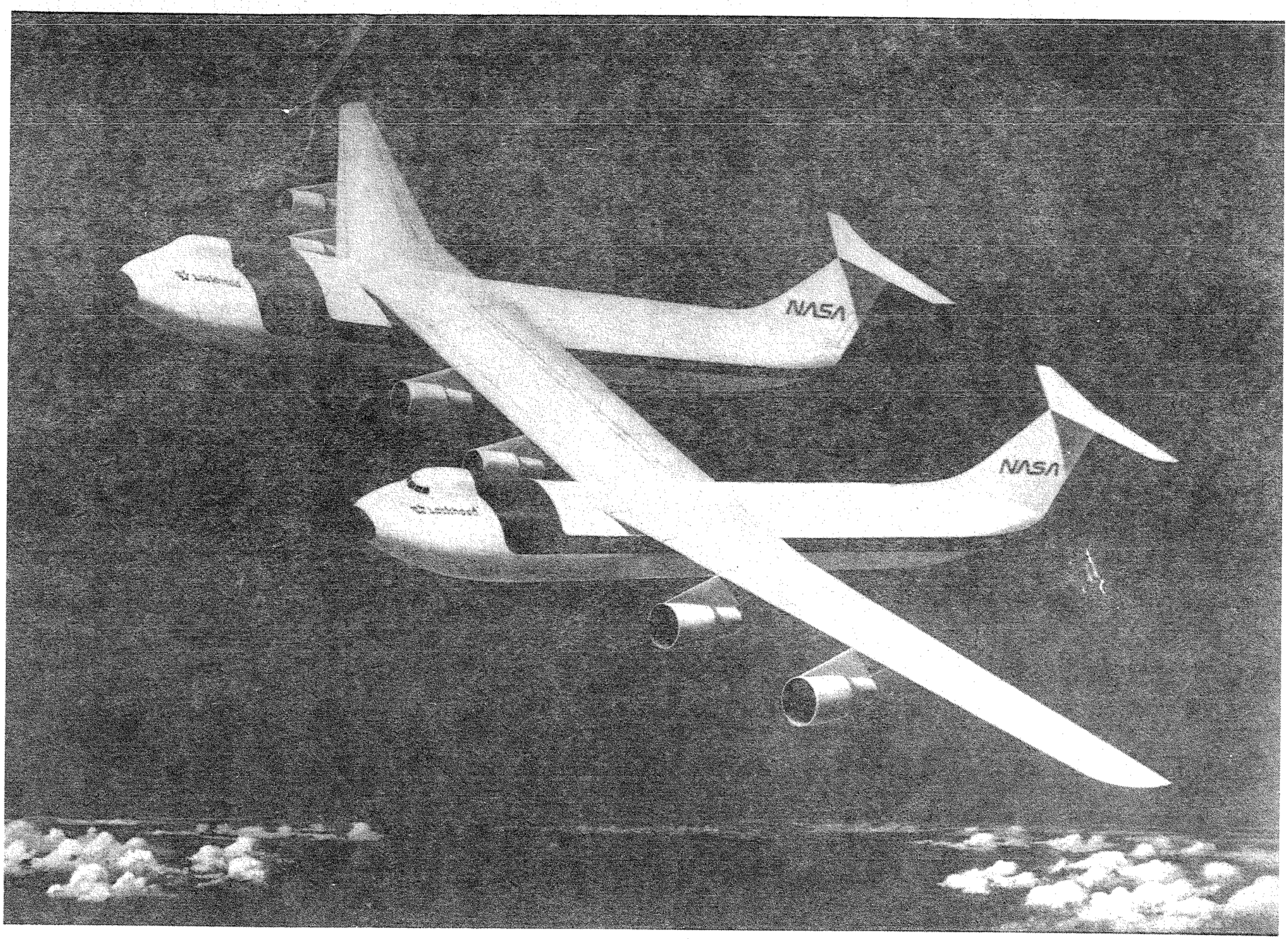
NASA
NASA

This Page Intentionally Left Blank

FOREWORD

The data contained herein are furnished in response to NASA-Langley Research Center Contract NAS1-15927, "Multibody Aircraft Study," September 1979 through September 1981. The technical response, contained in this single volume, was prepared in direct response to the required contractual effort and contains the basic multibody point design study. The appendix, Volume II, to the technical response contains the fuselage sizing analysis, wing planform selection, flutter analyses, and stability and control simulator data packs.

The International System of Units (SI) are presented as primary, and customary units are in parentheses. Customary units were used for the principal measurements and calculations. Report No. NAS SP-7012, "SI Units, Physical Constants and Conversion Factors," 2nd Revision, E.A. Mechtly, was used as a basis for conversion.

The NASA program manager of the Multibody Aircraft Study was D. V. Maddalon. The Lockheed effort was under the direction of J. W. Moore. Those persons and their area of responsibility for the analyses and results contained within this report are:

Design	E. P. Craven
	B. T. Farmer
Aerodynamics	J. F. Honrath
Structures	R. E. Stephens
	C. E. Bronson, Jr.
Stability & Control	R. T. Meyer
	J. H. Hogue
Noise Analysis	G. Swift

In addition to the authors listed, acknowledgement of their contributions to the aerodynamic analysis is given to J.M. Wilson, Jr.; J.E. Viney; C.E. Izurieta; and J. L. Crosas.

Credit for the technical illustrations is fully accorded to R.J. Stevens.

Program management of the Multibody Aircraft Study resides in the Advanced Concepts Department, R. H. Lange, Manager, of the Lockheed-Georgia Advanced Design Division, Marietta, Georgia.

TABLE OF CONTENTS

TABLE OF CONTENTS (Cont'd)

TABLE OF CONTENTS (Cont'd)

TABLE OF CONTENTS (Cont'd)

TABLE OF CONTENTS (Cont'd)

This Page Intentionally Left Blank

LIST OF FIGURES

LIST OF FIGURES (Cont'd)

LIST OF FIGURES (Cont'd)

LIST OF FIGURES (Cont'd)

LIST OF FIGURES (Cont'd)

LIST OF FIGURES (Cont'd)

LIST OF FIGURES (Cont'd)

LIST OF FIGURES (Cont'd)

LIST OF FIGURES (Cont'd)

LIST OF FIGURES (Cont'd)

LIST OF FIGURES (Cont'd)

LIST OF FIGURES (Cont'd)

LIST OF FIGURES (Cont'd)

LIST OF FIGURES (Cont'd)

LIST OF FIGURES (Cont'd)

LIST OF FIGURES (Cont'd)

LIST OF FIGURES (Cont'd)

LIST OF FIGURES (Cont'd)

LIST OF FIGURES (Cont'd)

LIST OF FIGURES (Cont'd)

LIST OF FIGURES (Cont'd)

SUMMARY

Large span-distributed-load aircraft, designed to reduce wing bending moment, offer a potential for both production cost reduction and performance improvements realized by weight reduction. NASA in-house and contracted study efforts, References 1 through 4, directed to fully span-distributed-load, all wing cargo aircraft have shown that cost reductions can be achieved through savings in structural weight and in reduction in the number of unique structural parts. These savings are particularly evident for very large payloads of the order of 272,155 kg (600,000 pounds), or greater. Preliminary studies have indicated that a multibody aircraft concept may offer benefits similar to the span-distributed-load aircraft yet retain configurational and operational characteristics more like those of a conventional transport aircraft.

The reduced wing root bending moment of the multibody concept should offer savings in both weight and cost. Multibody designs which emphasize part commonality in the fuselage and empennage should result in reduced first cost and lower overall operating cost.

Many technical unknowns, however, exist concerning this type of aircraft. Basic questions which arise relate to the wing efficiency obtainable, structural characteristics, and stability and control behavior. Moreover, wind tunnel data on multibody aircraft are minimal, giving rise to numerous uncertainties when standard analytical methods are used to design multibody concepts.

The objective of this study is twofold; first, to quantify and provide technical substantiation of multibody aircraft potential benefits by weight, performance, and cost comparison to conventional single body aircraft; second, to provide guidance in the area of technology development necessary to validate the multibody concept. To accomplish this objective, detailed point design analyses are conducted for one, two, and three-body aircraft designs to common performance and cost groundrules. Based upon the results of these analyses, concept comparison data and technology development recommendations are provided.

A 1985 level of technology readiness is used in the design of these aircraft with direct operating cost (DOC) used as the primary figure-of-merit to select among design alternatives. An initial inservice date is assumed to be 1990 to 1995 thus allowing for the incorporation of those advanced technologies expected to be available for production usage in 1985.

A single-leg, international flight serves as the design mission for all study aircraft. Performance requirements for the mission are as follows:

Payload	350,000 kg (771,618 lb)
Range	6482.0 km (3500 nm)
Cruise Speed	Mach 0.80
Initial Cruise Altitude	9753.6 m (32,000 ft)
Field Length	3200.4 m (10,500 ft)
Approach Speed (Max)	77.2 m/sec (150 kts)

Other performance requirements such as second-segment climb gradient and fuel reserves are as defined by FAR Part 25.

All aircraft are sized based upon the payload being transported within civil containers 2.44 x 2.44 x 3.05 or 6.10 m (8 x 8 x 10 or 20 feet) in width, height, and length, respectively. Revenue payload (aircraft payload minus container tare weight) design density is 160.2 kg/m^3 (10 lb/ft^3). The aircraft are designed to maintain a minimum cargo compartment pressure equivalent to an altitude of 5,486.4m (18,000 ft), as opposed to 2438.4m (8000 ft) for current transport aircraft, thus providing the weight advantage of an oval shaped fuselage.

The 1967 Air Transportation Association (ATA) equations with coefficients updated to reflect widebody transport experience are used to calculate direct operating cost (DOC).

Other DOC constants used are an average annual utilization of 4000 hours per aircraft, a crew of 3, a 15-year straight-line depreciation with a 10 percent residual value, and a hull insurance rate of 2 percent. Maintenance labor rate is 14.40 dollars per hour, and crew costs are escalated by a factor of 2.58 to 1981 levels. The point design analysis uses a fuel price of 34.34 ¢/liter (1.30 $/gallon); however, sensitivity studies are performed for fuel prices of 17.17, 51.51, and 68.68 ¢/liter (0.65, 1.95, and 2.60 $/gallon).

Aircraft production quantity is defined by the productivity, or throughput, requirement of 76.4 billion revenue Mg-km/yr (45.5 billion revenue ton-nm/yr) at an aircraft load factor of 60 percent. For the point design aircraft payload of 350,000 kg (771,618 lb), 107 aircraft are required to provide this productivity capability. For payloads of 75,000, 167,000 and 258,000 kg (165,347, 368,172 and 568,793 lb) used within the payload sensitivity study, production quantities are 500, 224, and 145, respectively.

Aircraft development and manufacturing costs, as well as propulsion system acquisition costs, are stated in January 1981 dollar values and are estimated by Lockheed's in-house methods.

Three multibody and one single body reference aircraft are defined based on the use of supercritical aerodynamics, advanced aluminum alloys, graphite-epoxy composites, advanced turbofan engines, and active controls providing relaxed static stability. The lateral separation distance of the main landing gear is 39.6 m (130 ft). A 35.1 m (115 ft) gear separation distance is also evaluated.

Due to the absence of an experimental data base, studies of multibody aircraft require that aerodynamic and structural analyses be made for a series of two and three-body aircraft configurations.

In the absence of a transonic code capable of modeling the aerodynamics of off-centerline bodies, initial estimates of span efficiency and loading were made using the Hess subsonic code and various vortex lattice methods. The Vorlax Vortex Latice was the selected method. Although the Hess code provides the more accurate results, study resources prevented its continued use.

The single body span load and resulting efficiency given by these analytical methods are less than those achieved for existing single body aircraft. Consequently, a method was developed to adjust the single body analytical results to more realistic values. This method essentially assumes a percentage reduction in the single body lift loss in order to produce known achievable efficiencies. Having determined this change in single body lift loss, a corresponding correction is applied to the multibody analytical load distribution. This procedure results in multibody span efficiencies, as a function of body location, which are comparable to the levels achieved in practice for single body aircraft. The resulting span loads and efficiencies used for the single body and multibody aircraft are 0.95 and 0.936, respectively.

Although test data results were not available at the time the above estimates were made, a representative multibody configuration and a clean wing were subsequently tested in the Lockheed Compressible Flow Wind Tunnel. Force, pressure, and flow visualization data were obtained at representative angles of attack for Mach numbers up to 0.82. The primary goal of the test was to determine the effect of the multibody fuselage on induced drag. Force data plots show wing efficiency values to be 0.96 for the multibody and 0.98

for the clean wing. Pressure data plots show these respective values to be 0.96 and 0.99. These data compare favorably and correlate well with the values used in the initial estimates.

Since transonic codes capable of analyzing the impact on the design of wings with large bodies mounted along the semispan are not available, wing camber and twist distributions are not developed for the multibody configurations. There is, however, a twist schedule included in the initial Hess code runs. Proper variations of the wing camber and twist are implicitly included in the results of this study since the thickness ratios defined for these configurations correlate very well with the characteristics of well designed wings.

Weight estimating methods used are a combination of statistical and analytical techniques. The stability and control influence is designed to ensure good flying qualities by the selection of empennage and controls of sufficient size, shape, and aerodynamic loading to be compatible with a given aircraft configuration. All cost data are produced using a parametric estimating approach which employs various types of cost estimating relationships. The sizing analysis of the point design aircraft is conducted using the Lockheed Generalized Aircraft Sizing and Performance (GASP) program. The GASP program controls the interaction of the program modules provided by the various technical disciplines and the inputs provided by the specific configuration.

Four wing planforms are evaluated at three body locations with the selection based on achieving a balance between the wing areas inboard and outboard of the fuselage bodies. These planforms are: 1) swept wing with trailing edge bat; 2) reduced sweep center section; 3) unswept center section; 4) straight taper. Aircraft sizing data indicate that performance, structural, and control capability characteristics of planform 3 and 4 above are improved when compared to the other two planforms. These planforms also optimize at lower DOC values and each is selected for a two-body point design aircraft. Planform 4 is also selected for the single body aircraft. Since only one three-body aircraft is analyzed within the point design study, planform 3 is selected. Although it does not have the minimum DOC, it does have the best ratio of outer wing area to total wing area, tip chord to root chord ratio, and wing break chord and thickness are maximized.

Based upon the study design requirements, advanced technology applications, and the aircraft sizing criteria and methods, aircraft are sized for

each multibody concept. Preliminary structure, aerodynamic, and stability and control analyses are performed on these aircraft. Using the results of these analyses, required revisions are made to the sizing criteria and the cycle repeated. This cycle is repeated numerous times prior to aircraft point design definition. During these initial point design definition cycles, a number of configuration trade studies are performed for configuration concept evaluation, such as engine location, empennage configuration, and wing sweep. These studies show that wing mounted engines are preferred to aft fuselage mounted engines and that a twin tee-tail is the preferred empennage configuration.

Four empennage configurations are evaluated: twin tee, canted slab, high slab, and low slab. The horizontal slab tails have the highest aspect ratios and, therefore, the highest C_{L_α} values. The thickness (t/c) of the horizontal surfaces is selected to avoid drag rise at the cruise Mach number of 0.80. Thus the 0.44 rad (25 degrees) sweep of the tee-tail allows a t/c of 0.08 as compared to 0.064 for the unswept slab tail. The mid-span average skin thicknesses required to react the limit loads are 0.66 cm (0.26 in.) for the twin tee-tail and 2.84 cm (1.12 in.) for the high slab tail. The relatively high skin thickness of the slab tail is influenced by its greater span and lower chord thickness as compared to the tee-tail configuration. The horizontal high and low slab tails have increased weights of 3129.8 and 3492.7 kg (6900 and 7700 lb), respectively, relative to the tee-tail. Since aircraft weight, cost, and DOC are minimized by the twin tee-tail, it is the selected concept. However, it is noted that this analysis does not include the influence of dynamic loads. It is possible the slab tail arrangement could offer a benefit when considering this influence.

A further impact on empennage weight reduction is the use of an active control system to allow relaxed static stability and thus permit a smaller horizontal tail. The negative eight percent static margin chosen allows a decrease of approximately 25 percent in tail size. Although this resulting decrease in weight of the tail is a very low percentage of overall weight, the synergistic effect of savings due to each pound of operating weight empty is significant. The selected level of instability is such that in the event of total augmentation failure, the pilot would still be able to safely fly and land the aircraft. Requirements of the active control system are considered to be within the present state-of-the-art.

Based on trade study results, a relatively high sweep angle of the wing, 0.61 rad (35 degrees), is selected for the single body and straight taper wing multibody configurations. The results show that as sweep is increased from 0.44 rad (25 degrees) to 0.61 rad (35 degrees), DOC decreases by 1.3 and 0.3 percent for the single body and two-body configurations, respectively. These data indicate that the aerodynamic penalty which occurs as sweep increases is offset by the reduced wing weight resulting from significant increases in allowable wing thickness.

In these configuration trade studies, the preferred, and hence selected, configuration alternative results in lower gross weight, acquisition cost, and DOC. The aircraft are then resized incorporating all selected alternatives, thus defining the initial point design aircraft.

A point design analysis is performed on each of the initial point design aircraft. This analysis investigates the aircraft characteristics relating to aerodynamics, structures, weight and balance, and stability and control. Upon completion, a final resizing of the aircraft is performed where required. These aircraft are used as the bases for sensitivity studies of variations in cruise power setting, payload, body spanwise location, and fuel price. Also included are the results of a comprehensive flutter analysis conducted on each of the point design aircraft.

The two-body MB2 (unswept center section wing) and the single body reference aircraft are used in the sensitivity studies. Reductions in trip cost are very small over the range of variations in cruise power settings. As the payload is increased from 75,000 kg (165,347 lb) to 350,000 kg (771,618 lb), DOC of the two-body aircraft decreases from 9.54 ¢/AMgkm (16.03 ¢/ATNM) to 6.32 ¢/AMgkm (10.61 ¢/ATNM). In the fuel price sensitivity study, DOC of the two-body aircraft is 10.7 percent less than that of the single body reference aircraft at the lowest fuel price and 12.0 percent less at the highest fuel price, 0.69 ¢/l (2.60 $/gal).

The multibody baseline aircraft is configured with a body centerline separation distance of 35.1m (115 ft), or as a function of percent wing semispan, the bodies are located at 28 percent. To define the influence of body location on aircraft characteristics, three additional body locations are evaluated: 17, 39, and 50 percent semispan. Wing stiffness corrections required as a result of the flutter optimization analysis are incorporated into the aircraft evaluated at these various body locations.

The aircraft are optimized to provide minimum DOC when sized for each of the body locations. The primary benefit to be realized by the multibody concept is a reduction in the magnitude of the cruise mode wing bending moment and thereby a reduction in wing weight. It would also be expected that, as body semispan location increases, this bending relief would also increase and wing weight would decrease. However, the multibody aircraft wing weight decreases for locations out to approximately 40 percent then begins to increase as the body is located further outboard.

Both wing up bending and down bending moment cases are evaluated for the critical load conditions, 2.5g flight maneuver and 2.0g taxi, respectively. The peak bending moment at the outboard side of the body decreases for both flight and taxi conditions as the body is moved outboard from the 17 to 50 percent semispan location. However, as the body is moved from the 39 percent location to the 50 pecent location, the flight bending moment imposed on the wing center section changes from an up bending moment to a down bending and exceeds the taxi down bending moment at the 50 percent body location. This wing center section moment reversal, coupled with a reduction in center wing chord and thickness that occurs as the body is moved outboard, results in the wing weight increase when the body is located outboard of the 39 percent body location.

Although the wing span efficiency increases as the bodies are moved outboard, the cruise lift-to-drag ratio decreases from 23.4 to 23.0 for the 39 to the 50 percent body location, respectively. Wing aspect ratio also decreases from 11.5 to 10.9 when the body is relocated from the 39 to the 50 percent semispan location, off-setting the increased span efficiency.

The optimum body location based upon direct operating cost (DOC) is approximately 39 percent semispan. It is noted, however, that the aircraft evaluated by this analysis have coincident fuselage and landing gear centerlines. Thus, the 39 percent body location aircraft with a wing span of 128.0m (420 ft) would require a runway width greater than 50.0m (164 ft).

The severity of the lateral control problem is shown by noting the tradeoffs that occur and the resulting aircraft response as the bodies move outboard. Ailerons are used on the outboard 30 percent of the semispan and their area remains relatively constant. However, the roll control spoilers extend from the outboard side of the body to 70 percent semispan and the area available is a direct function of body location. As body position moves from

19 to 50 percent semispan, the available rolling moment decreases by approximately 55 percent while the required rolling moment, represented by the inertia, increases.

It is obvious that roll control becomes increasingly difficult with fuselages located off the aircraft centerline. MIL-Spec 8785B quantifies roll capability by specifying the time required to bank 30 degrees. The ability to reach 30 degrees of bank in approximately 5 seconds appears to be a reasonable guide. A cross plot of these data show body locations in the area of 32 percent semispan will meet this requirement.

Based upon the above data, the baseline aircraft body location of 28 percent semispan is considered within the optimum body location range. To better define the optimum location requires additional investigations such as wind tunnel tests, flight simulator evaluation, and detailed structural analyses.

Figure 1 shows an efficiency comparison of the four point design aircraft. The three stick multibody aircraft show an improvement in fuselage efficiency relative to the four stick single body aircraft. This is a function of stick width since for each stick added, the fuselage cross sectional area increases at a faster rate than does the container cross sectional area. That is, a

EFFICIENCY PARAMETER	SINGLE BODY REFERENCE (SBR)	MULTIBODY TWO-BODY (MB1)	MULTIBODY TWO-BODY (MB2)	MULTIBODY THREE-BODY (MB3)
FUSELAGE (CONTAINER X-SECT. AREA/ FUSELAGE X-SECT AREA)	0.335	0.402	0.402	0.402
FUEL-Mgkm/l (TON-NM/GAL)	9.34 (21.04)	9.91 (22.32)	10.79 (24.31)	9.69 (21.84)
AERODYNAMIC - ML/D	17.45	17.17	17.92	17.18
ECONOMIC - DOC ¢/AMgkm @ 0.34 $/l (¢/ATNM @ 1.30 $/GAL)	7.09 (11.91)	6.47 (10.87)	6.29 (10.56)	6.69 (11.24)

Figure 1. Efficiency Comparison - Point Design Aircraft

single stick configuration would have the highest fuselage efficiency. Fuel efficiency is reflected in the direct operating cost, with the two-body MB2 aircraft showing the better performance in both of these categories. This is a result of the lower weight, cost, and cruise drag of this aircraft. The higher aerodynamic efficiency of the two-body MB2 is indicated by the higher ML/D value resulting from improved drag characteristics.

Each of the final point design multibody aircraft is compared to the single body reference aircraft to define the potential benefits of the multibody concept. The multibody aircraft show decreases in gross weight ranging from 4.8 to 6.9 percent, in fly-away-cost from 8.6 to 13.4 percent, and in DOC from 5.6 to 11.3 percent.

The results of a multibody versus a spanloader aircraft comparison show that the multibody aircraft has improved performance and a significantly lower DOC. Both of these aircraft benefit from reduced wing weight resulting from a reduction of the cruise mode wing bending moment; however, the multibody retains more conventional characteristics and is not as restricted in ground operations and handling.

Other study results and/or observations are:

- Reasonable span efficiencies can be obtained for multibody configurations, however, transonic code development and wind tunnel tests are required to optimize the configuration. This code, along with additional test data, can be used to develop wing camber and twist variations, wing-body filleting, and wing spanwise variations which will optimize the aerodynamic configuration for a prescribed fuselage size, shape, and location.
- Multibody aircraft have a lower drag level than single body aircraft sized for the same mission capability. Lower induced drag levels are due to higher wing aspect ratios. The profile drag level is reduced because external landing gear housings are not required.
- Flying qualities criteria are not specified for extremely large aircraft. This first became a concern with the C-5 size aircraft at 340,194 kg (750,000 lb) and will be an even greater concern with aircraft at gross weights of 907,185 kg (2,000,000 lb).
- Present control criterion limits the fuselage outboard semispan location to a position slightly

less than that desired from a weight saving viewpoint. The designs shown for the selected configurations show the crew station located within a main fuselage. However, the crew location may be limited to aircraft centerline of rotation if acceptable ride qualities are to be achieved. Further investigations are required to fully define the performance and weight penalties associated with this crew location concept.

- A competitive advantage is offered by the multibody study aircraft only at payload values in excess of 258,000 kg (568,793 lb). Compared to the single body reference aircraft, the advantage in DOC at this payload is about 4 percent and is approximately 11 percent at a payload of 350,000 kg (771,618 lb). Other multibody advantages are reductions in fly-away-cost of from about 9 to 15 percent, greater loading flexibility due to multiple cargo loading access, and cargo floor heights compatible with existing loading equipment.

Considerable research and development is required before a multibody configuration can be placed in service. Test programs are required to define the basic lift, drag, stability, and loads characteristics for a systematic variation of multibody configurations in order to assure that all parameters of potential significance are evaluated and that resulting configurations will be properly selected. These data are required for cruise performance evaluation as well as for evaluation of low speed performance, control, and handling characteristics. Other research and development recommendations are for transonic code modifications for modeling the aerodynamics of off-centerline bodies; flight simulation for guidance in defining design criteria; detailed structures studies pertaining to dynamic loads, load alleviation, flutter analysis, unsymmetrical loadings, and material application.

1.0 INTRODUCTION

Future large transport aircraft replacement programs face severe economic hurdles related to development and operational cost of new aircraft. The continuing rise in such costs, as influenced by inflation and increasing fuel price, dictate that the next generation of large transport aircraft offer the means to minimize development cost and to reduce fuel consumption. High payload capability innovative transport aircraft concepts incorporating advanced technologies may offer a potential solution.

Large span-distributed-loads aircraft, designed to reduce wing bending moment, offer a potential for both production cost reduction and performance improvements realized by weight reduction. NASA in-house and contracted study efforts, References 1 through 4, directed to fully span-distributed-load, all wing cargo aircraft have shown that cost reductions can be achieved through savings in structural weight and in reduction in the number of unique structural parts. These savings are particularly evident for very large payloads of the order of 272,155 kg (600,000 pounds), or greater. Preliminary studies have indicated that a multibody aircraft concept may offer benefits similar to the span-distributed-load aircraft yet retain configurational and operational characteristics more like those of a conventional transport aircraft.

The reduced wing root bending moment of the multibody concept should offer savings in both weight and cost. Multibody designs which emphasize part commonality in the fuselage and empennage should result in reduced first cost and lower overall operating cost.

Many technical unknowns, however, exist concerning this type of aircraft. Basic questions which arise relate to the wing efficiency obtainable, structural characteristics, and stability and control behavior. Moreover, wind tunnel data on multibody aircraft are minimal, giving rise to numerous uncertainties when standard analytical methods are used to design multibody concepts.

The intent of this report is to present the results of a detailed analysis of both multibody and single body aircraft. The objective of the analysis is to quantify and provide technical substantiation of the potential multibody aircraft benefits when compared to single body aircraft and to identify technology development requirements.

The analysis consists of three elements: (1) a detailed point design analysis of selected one, two, and three-body aircraft; (2) sensitivity

studies are performed on the design parameters (payload, body location, and fuel price) which have a major influence on the definition of the aircraft; and (3) recommendations are made as to required research and technology requirements which are needed to fully validate the multibody concept. A 1985 level of technology readiness is used in the design of these aircraft with direct operating cost (DOC) used as the primary figure-of-merit (FOM) to select among design alternatives.

The point design studies consist of detailed performance, weight, stability and control, and cost investigations of four aircraft; two, two-body concepts; one, three-body concept; and a single body reference aircraft. These aircraft are analyzed at a payload value of 350,000 kg (771,618 lb) and a maximum body centerline separation distance of 39.6m (130 ft) such that landing gear tread width is compatible with a 45.7m (150 ft) runway width. Economic data are based upon 1981 dollars and a fuel price of 34.34 ¢/liter (1.30 $/gal). Sensitivity studies are performed for payload values between 75,000 an 350,000 kg (165,347 and 771,618 lb) and body locations between 17 and 50 percent wing semispan. The influence of fuel price over a range of 17.17 to 68.68 ¢/liter (0.65 to 2.60 $/gal) is also determined.

2.0 POINT DESIGN AIRCRAFT DEFINITION

The procedure used to define, analyze, and evaluate the multibody and single body aircraft is illustrated in Figure 2. Had a well defined design data base been available for multibody aircraft, defining the multibody point design aircraft would have been a straightforward process, as illustrated by this flow diagram, without the two iterative loops. However, as this data base was not available, many iterations were required before arriving at final point design aircraft. Based upon the study design requirements, advanced technology application, and the aircraft sizing criteria and methods (sections 2.1, 2.2, and 2.3), aircraft were sized (section 2.4) for each multibody concept. Preliminary structural, aerodynamic, and stability and control analyses were performed on these aircraft. Using these preliminary analyses, required revisions were made to the sizing criteria and the cycle repeated. This cycle was repeated numerous times prior to point design definition. Therefore, the initial point design aircraft definitions given (section 2.5) represent the major results of these iterations.

During the initial point design definition cycle, a number of configuration trade studies (section 2.6) were also performed where configuration concept questions arose, such as wing sweep, engine location, etc. The aircraft were then resized based upon the study selected alternative, thus establishing a revised initial point design aircraft.

Upon completion of the point design analysis, a final resizing of the aircraft was performed (section 4.0), where required, to incorporate any conclusions of the analysis which were not included in the iterative process. These final aircraft were then used as the bases of the sensitivity studies (section 3.0) and the benefit summary (section 5.0).

2.1 DESIGN REQUIREMENTS

The design requirements upon which all study aircraft are based were defined by the NASA or were adopted by Lockheed based upon experience in the design of transport aircraft. An initial inservice date of 1990 to 1995 is assumed thus allowing for the incorporation of those advanced technologies expected to be mature and available for production usage in 1985. Current requirements of the Federal Aviation Regulations (FAR Part 25) for Transport Category Aircraft are assumed to be applicable to aircraft with an initial operational capability in the

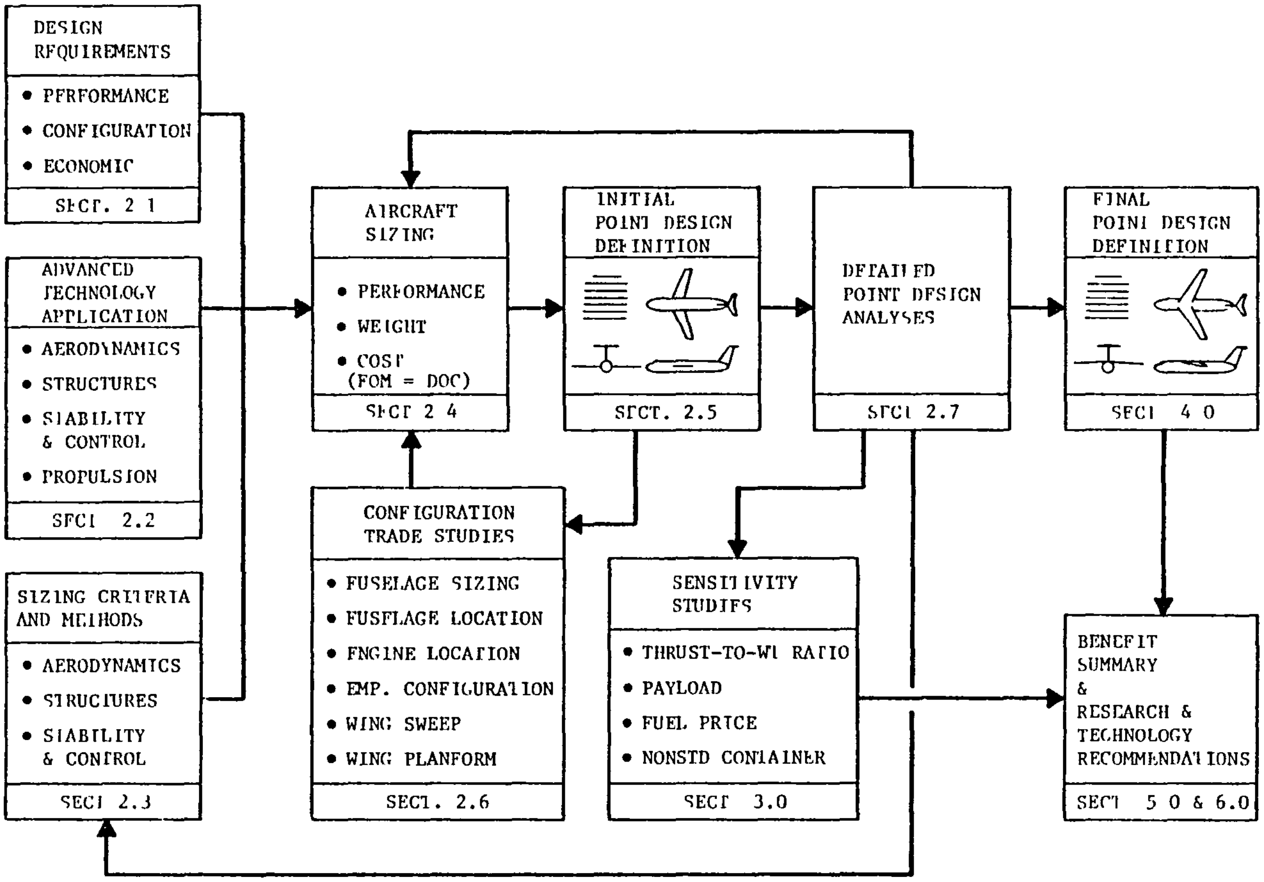

Figure 2. Definition Cycle - Point Design Aircraft

early 1990s, and are satisfied by the study aircraft.

2.1.1 Performance Requirements

A single-leg, international flight serves as the design mission for all study aircraft. Performance requirements for the mission are as follows:

Payload	350,000 kg (771,618 lb)
Range	6482.0 km (3500 nm)
Cruise Speed	Mach 0.80
Initial Cruise Altitude	9753.6 m (32,000 ft)
Field Length	3200.4 m (10,500 ft)
Approach speed (max)	77.2 m/sec (150 kts)

Other performance requirements such as second-segment climb gradient and fuel reserves are as defined by FAR Part 25.

2.1.2 Configuration Requirements

The configuration concept used incorporates many features of today's cargo transport aircraft. All of the payload is carried in the fuselage and is loaded straight-in through a nose visor door. The wing is mounted sufficiently high on the fuselage at approximately mid-fuselage length so that it does not compromise the cargo compartment design. Other pertinent features of the basic configuration include conventional fuselage-mounted landing gear and engines attached to the underside of the wing. Pitch and directional flight controls are provided by aft-fuselage-mounted tee-tail empennage configurations. All aircraft are sized based upon the payload being transported within civil containers 2.44 x 2.44 x 3.05 or 6.10 m (8 x 8 x 10 or 20 feet) in width, height, and length, respectively. Revenue payload (aircraft payload minus container tare weight) design density is 160.2 kg/m^3 (10 lb/ft^3). The aircraft are designed to maintain a minimum cargo compartment pressure equivalent to an altitude of 5,486.4 m (18,000 ft) and a minimum temperature of 283°k (50°F) at maximum cruise altitude. Fuselage sizing and selection based upon these requirements are given in Appendix A.

Two, two-body aircraft are analyzed. One of these aircraft has a 35.1 m (115 ft) fuselage centerline separation distance with the nose and main landing gear centerlines coincident with the fuselage centerline. The other two-body aircraft has a 39.6 m (130 ft) fuselage centerline separation. The landing gear and fuselage centerlines are also coincident. Fifty percent of the total payload is contained in each fuselage. Twin tee-tail arrangements are used. The wing planform concept selection data for these aircraft are given in Appendix C.

A single three-body aircraft is analyzed with an outboard fuselage centerline separation distance of 39.6 m (130 ft). The main landing gear centerlines are coincident with the outboard fuselage centerlines. One-third of the total payload is contained in each of the three fuselages. A twin tee-tail arrangement is also used for this aircraft and wing planform data are also contained in Appendix C.

2.1.3 Economic Guidelines

The 1967 Air Transportation Association (ATA) equations with coefficients updated to reflect widebody transport experience are used to calculate direct operating cost (DOC). These coefficients relating to airframe and engine maintenance are derived from 1979 CAB airline reported data and are as follows:

- o Airframe maintenance labor cost [0.52]

- o Airframe maintenance material cost [0.68]

- o Engine maintenance labor cost - [0.62]

- o Engine maintenance material cost [1.31]

Other DOC constants used are an average annual utilization of 4000 hours per aircraft, a crew of 3, a 15-year straight-line depreciation with a 10 percent residual value, and a hull insurance rate of 2 percent. Maintenance labor rate is 14.40 dollars per hour, and crew costs are escalated by a factor of 2.58 to 1981 levels. The point design analysis uses a fuel price of 34.34 ¢/liter (1.30 $/gallon); however, sensitivity studies are performed for fuel prices of 17.17, 51.51, and 68.68 ¢/liter (0.65, 1.95, and 2.60 $/gallon).

Aircraft production quantity is defined by the productivity, or throughput, requirement of 76.4 billion revenue Mg-km/yr (45.5 billion revenue ton-nm/yr) at an aircraft load factor of 60 percent. For the point design aircraft payload of 350,000 kg (771,618 lb), 107 aircraft are required to provide this productivity capability. For payloads of 75,000, 167,000, and 258,000 kg (165,347, 368,172, and 568,793 lb) used within the payload sensitivity study, production quantities are 500, 224, and 145, respectively.

Aircraft development and manufacturing costs, as well as propulsion system acquisition costs, are stated in January 1981 dollar values and are estimated by Lockheed's in-house methods.

2.2 ADVANCED TECHNOLOGY APPLICATION

The aircraft designs produced as a result of this study are based on an inservice date of 1990. The technologies incorporated in the aircraft, with the objective of improving performance and reducing costs, are those projected to be mature by 1985. Five years are allowed for aircraft design and production between technology maturity and aircraft inservice date.

These technologies include the use of supercritical aerodynamics, advanced aluminum alloys, graphite-epoxy composites, advanced turbofan engines, and active controls providing relaxed static stability. The definition and use of these technologies are expanded in the following paragraphs.

2.2.1 Aerodynamics

The basic airfoils used in this study incorporate supercritical technology. Lockheed has defined and wind-tunnel tested supercritical airfoil sections with thickness ratios between 10 and 20 percent, which is the basis for the airfoil performance characteristics used. Typical variations in the allowable wing thickness ratio for fixed wing sweep angles are shown as a function of design cruise Mach number and lift coefficient in Figure 3. These data are based upon a compressible drag rise of 10 counts.

A maximum cruise lift coefficient of 0.530, based on total wing area, is used for all configurations. This value is representative of wing capabilities for the design cruise speed of Mach 0.80 and the technology time frame of 1985. It is possible that lower C_L values would more appropriately reflect the decrements in span load distribution caused by the additional bodies at a fixed angle of attack. However, it is assumed that extensive wing-body filleting and careful attention to airfoil design and the wing twist schedule will eliminate this potential lift loss.

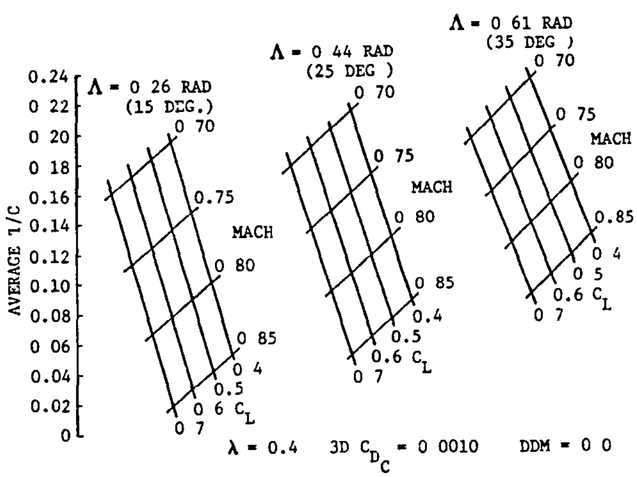

Figure 3. Supercritical Airfoil Technology

Wing twist and camber variations were not explicitly considered in this study; however, proper variations of these parameters and other characteristics important to overall transonic design of wings is implicitly included in the study results. This is assured by the very good correlation of the thickness ratios shown for moderate sweep angles in Figure 3 with the characteristics of well designed wings.

Development of the camber and twist characteristics for each of the configurations examined is outside the scope of the study and is, in fact, impossible since transonic codes capable of analyzing the impact on the wing design of large bodies mounted along the wing semispan are not available. NASA-Langley has been funding development of codes capable of this analysis and further investigations of this problem are dependent on these codes.

An analysis, included in this study, and discussed in Secton 2.3.1.1, indicates that the 0.00 Rad (0 degree) sweep data are overly conservative for

the high Mach number, low lift coefficient condition appropriate to the unswept center panel multibody airfoil sections and are therefore not shown in Figure 3. Zero sweep thickness ratios are determined as described in Section 2.3.1.1.

2.2.2 Structures and Materials

Lockheed projects that, by 1985, composites can be used for the design of a significant portion of an aircraft structure. For this study, it is assumed that graphite/epoxy is used in most of the secondary structure. For the wing and empennage, this includes leading and trailing edges, control surfaces, tips, fairings, and access doors. Fuselage applications include doors, fairings, and other miscellaneous parts. The nacelle/pylon has composite doors and fairings where temperature is not a problem. Applications to the landing gear are limited to fairings and miscellaneous parts. The wing and fuselage primary structure is selectively reinforced with boron/epoxy. On the wing, reinforcement is applied to the covers, spar caps, and bulkheads, while the fuselage has reinforced stringers, frames, and rings. The horizontal and vertical stabilizers are almost all graphite/ epoxy.

This material utilization results in weight reductions, when compared to current aluminum material application, for the various structural components of the aircraft. Figure 4 summarizes material application for each component and shows the weight savings realized by that application. The maximum composite utilization is applied to the empennage where about 85 percent of the structure is graphite/epoxy. This results in a 27 percent reduction in weight. The wing, fuselage, and nacelle/pylon show a smaller weight

COMPONENT	MATERIAL APPLICATION PERCENT BY WEIGHT			WEIGHT SAVING - PERCENT
	ALUMINUM	GRAPHITE/EPOXY	BORON/EPOXY	
WING	80.7	14.6	4.7	18
FUSELAGE	86.8	12.5	0.7	12
EMPENNAGE	15	85	0	27
NACELLE/PYLON	77	23	0	11
LANDING GEAR	95	5	0	2

Figure 4. Structural Material Application

reduction due to a lesser application of composites. The landing gear has the least composite application and, therefore, the least weight reduction.

The material application for the multibody study is not considered overly optimistic and can be supported by various material development programs funded in the past by government and industry. Many secondary structure applications are considered state of the art today. Lockheed, for example, has built and tested composite designs for slats, leading edge panels, doors, and fairings for several different aircraft. Some of these programs produced flight articles. Other companies have designed and built various other components. There should be no significant problems, therefore, for incorporating composite secondary structure into a 1985 aircraft design.

The use of boron-reinforced primary structure is supported by the C-130 reinforced center wing program. There are currently several C-130s which have boron/epoxy-reinforced center wing cover panels. These aircraft are in service and are part of a continuing evaluation program. This program has been very successful in establishing manufacturing methods, reducing wing stress levels, and improving the service life of the aircraft. It is projected that by 1985 this same philosophy can be applied to the fuselage. This would involve reinforced stringers, frames, underfloor bulkheads, and floor structure.

The all-composite empennage is very close to becoming a mature technology. Under NASA programs, several contractors are building and testing horizontal and vertical tail boxes for which the major material usage is graphite/epoxy. Lockheed has designed and built such a vertical stabilizer box for an L-1011. The structure is undergoing structural tests now and will be flight tested in the near future. The results of these programs will be available to support a 1985 design effort.

2.2.3 Stability and Control

The technology level assumed for this study will be easily attainable for the 1985 to 1990 time frame. A main stability and control feature which impacts this study is the use of longitudinal relaxed static stability (RSS). A horizontal tail designed for RSS can be smaller than for conventional aircraft and thus provide a considerable weight savings. The design of an advanced flight control system is not part of this study effort, but current similar Lockheed designs of flight control systems for future aircraft such as the C-X assures the credibility

of such a philosophy. The technologies of the study assume an integrated stability augmentation, flying qualities, and ride qualities type system.

The directional stability level assumes a level consistent with current Lockheed designs known to produce good flying qualities. Thus any unknown adversities of multibody directional stability or instability (although believed to be easily predictable) can be easily overcome.

The lateral mode is also designed with conventional technologies. Since this is expected to be one of the most difficult areas due to extremely large inertias, a conservative approach is again taken to provide credence to the feasibility of the designs. An advanced augmentation system as well as innovative control concepts provide a further hedge for unforeseen difficulties in this area.

Aeroelastic effects on stability and control are not evaluated in this study. The effects would be large for very large aircraft such as these. To be meaningful, however, a fairly detailed structural design would have to be made to predict aeroelastic distortions. The approach taken in this study is to base decisions on stability changes and control effectiveness on experience gained from Lockheed's present flying large aircraft - the C-5A.

2.2.4 Propulsion

The advanced technology turbofan engine selected as representative of 1985 technology is based on the Pratt and Whitney (P&W) STF477. This is a paper engine resulting from NASA-contracted studies of "Advanced Turbofan Engines Designed for Low Energy Consumption." The P&W estimated certification date for an STF 477 is 1998; however, by adjustments to specific fuel consumption and weight furnished by P&W as shown in Figures 5 and 6, performance related to an earlier certification date is obtained. The 1990 engine certification date shown on these figures for the multibody aircraft assumes a 1985 technology cut-off date. The upper thrust scaling limit of STF 477 performance, as defined by P&W, is 444,822 N (100,000 lb).

Inlet, nozzle, thrust reverser flows, and interference potential between airframe and power plants are qualitatively assessed, as is the application of advanced acoustical material and treatment of nacelles and pylons.

2.3 AIRCRAFT SIZING CRITERIA AND METHODS

The sizing of multibody aircraft requires a number of modifications to be made to the data base used for the siz-

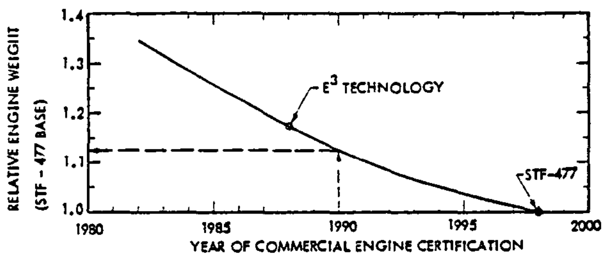

Figure 5. Technology vs Engine Weight - High Bypass Ratio Turbofan

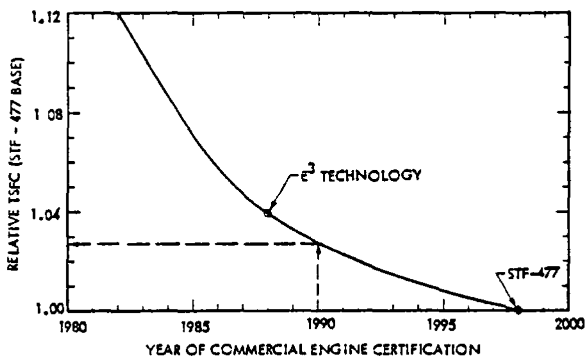

Figure 6. Technology vs Engine TSFC - High Bypass Ratio Turbofan

ing of conventional single body aircraft. These modifications are discussed in the following paragraphs grouped under the technical areas of aerodynamics, structures, stability and control, and cost.

2.3.1 Aerodynamics

The primary criteria upon which the multibody concept has an influence, as related to aerodynamics, are spanwise thickness distribution, span efficiency, and span load distribution.

2.3.1.1 Spanwise Thickness Distribution

The wing thickness definition used in the sizing of conventional aircraft is based on the allowable thickness ratio (t/c) selected from Figure 3 as a function of cruise Mach number, lift coefficient, wing sweep angle, and a compressible drag rise of 10 counts. The value obtained from this figure is the average thickness ratio for the wing as represented by its basic trapezoidal planform. This method has demonstrated very close agreement with the results obtained in more detailed design of various advanced transport wings.

As many as six control chords along the wing semispan are used to define the thickness distribution. A constant thickness ratio is used for single body configurations, but spanwise variations are used for the multibody configurations. These variations are used to adequately account for variations in parameters, such as local sweep angle and lift coefficient, which result from the multibody multipanel wing planforms.

The outer panel thickness of the two-panel multibody wing is defined based upon a constant t/c value ob-

tained from Figure 3. The center panel thickness is derived using a number of spanwise control stations where both local section lift coefficients and sweep angle values are used to replace the nominal wing values. The local lift coefficient values are defined based upon the assumption that an elliptical load distribution is achieved.

Where the center section sweep angle is low, an additional thickness ratio increment is added to the results obtained from the above analysis. The data contained in NASA TM X-73940, dated August 1976, indicate that thickness ratios higher than those obtained from Figure 3 are acceptable for unswept wing panels. Using the wing planform as defined in the above report, an analysis using conventional supercritical airfoil assumptions and computer codes was conducted to define the wing thickness ratio. A lift coefficient of 0.4 and a cruise Mach number of 0.84 were used for this analysis. The results indicate that a 7.5 percent thick section will provide an acceptable drag rise.

This thickness ratio is greater (by approximately 0.03) than is obtained by the use of Figure 3. The mismatch is not unexpected as the center panel design case for the multibody aircraft is considerably different from the typical transport design spectrum in terms of sweep angle and section lift coefficient.

Multibody configurations analyzed include several center wing panel planforms which result in a significant variation in panel sweep angle. Therefore, based upon the above analysis, a thickness correction is applied at the mid-chord sweep, which is representative of the expected wing chordwise shock position. The thickness increment defined below is added to the thickness defined in Figure 3.

$$\Delta t/c_{center} = \left[1 - \left(\frac{c/2\ \text{center}}{c/2\ \text{outer}}\right)\right] 0.03$$

$$(\text{Valid @ } \Lambda \leq 25^{o})$$

2.3.1.2 Wing Span Efficiency and Load Distribution

In the absence of a transonic code capable of modeling the aerodynamics of off-centerline bodies, initial estimates of span efficiency and loading are made using the Hess subsonic code described in Reference 5 and various vortex lattice methods. The Vorlax Vortex Lattice method given in Reference 6 is the selected method. The representation of Figure 7 which employs a flatplate at zero incidence with lower surface fences for the body is used with VORLAX. Although the Hess code provides the more accurate results,

study resources prevented its continued use. Figure 8 compares typical results from both these code methods for single body and multibody aircraft.

The single body span load and resulting efficiency given by these analytical methods are obviously less than those achieved for existing single body aircraft. Consequently, a method was developed to adjust the single body analytical results to more realistic values. This method, described in Appendix B, essentially assumes a percentage reduction in the single body lift loss in order to produce known achievable efficiencies. Having determined this change in single body lift loss, a corresponding correction is applied to the multibody analytical load distribution. This procedure results in multibody span efficiencies, as a function of body location, which are comparable to the levels achieved in practice for single body aircraft.

Although test data were not available at the time these estimates were made, a representative semispan multibody configuration was subsequently tested in the Lockheed Compressible Flow Wind Tunnel. A geometric definition of the model is presented in Figure 9. The body is located at 40 percent wing semispan. Figure 10 shows the model installed in the test facility.

The primary goal of the test was to determine the effect of the multibody fuselage on induced drag. Force, pressure, and flow visualization data were obtained at representative angles of attack for Mach numbers up to 0.82 at three and six million Reynold's number based on the mean aerodynamic chord of 4.825 inches.

Two methods are available for determining span efficiencies from test data; one using force data and the other using pressure data. The force data is used by plotting the square of the lift coefficient (C_L^2) versus the drag coefficient (C_D) as shown in Figure 11. The efficiency factor e is determined from the slope of these curves by the equation:

$$e = 1 \div \left[AR \left(\frac{dC_D}{dC_L^2} \right) \right]$$

The resulting values, as noted in Figure 11, are 0.98 for the clean wing and 0.96 for the multibody.

Using pressure data, span efficiencies can also be obtained from a plot of the loading, $CC_l \,/\, C_{avg}$ as a function of the semispan as shown in Figure 12. Hess analytical results are included for comparison with clean wing and multibody data from the test. For the condition shown here, the lift coeffic-

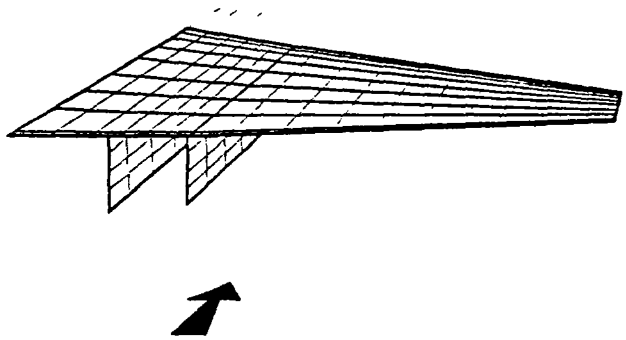

Figure 7. General Arrangement - Wing + Flat Fuselage with Vertical Fences

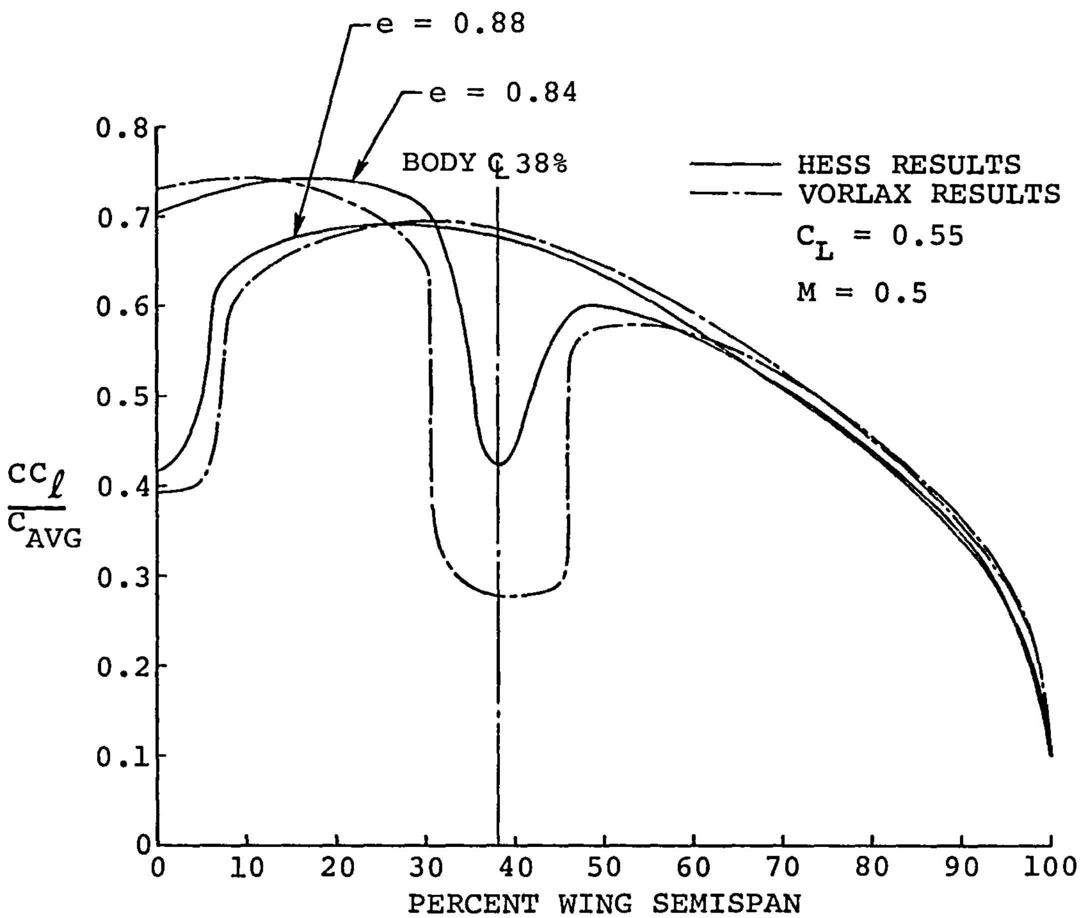

Figure 8. Hess and Vorlax Span Loading Comparisons for Different Body Locations

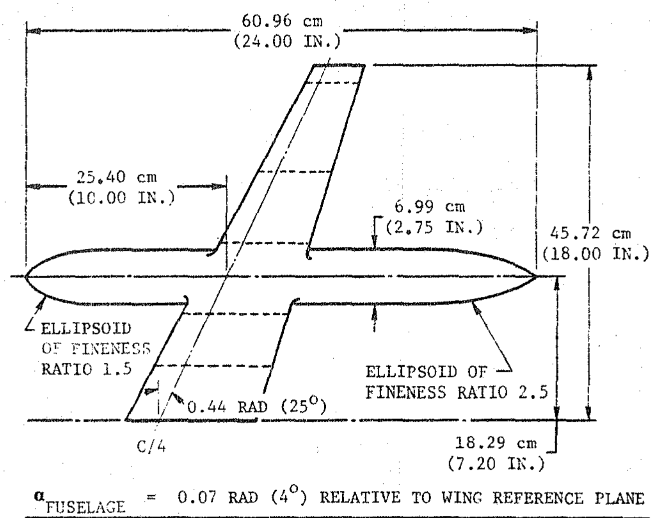

Figure 9. Multibody Model

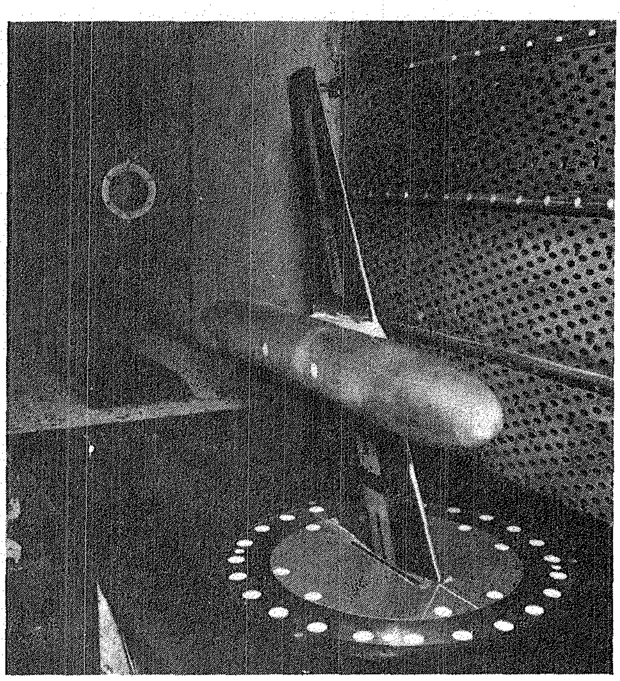

Figure 10. Semispan Multibody Model Installed in Lockheed Compressible Flow Wind Tunnel

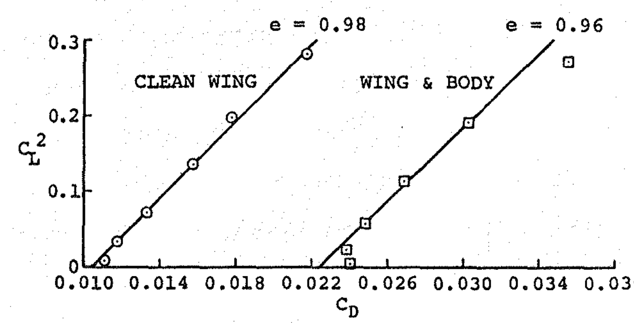

Figure 11. Experimental Span Efficiencies - Force Data

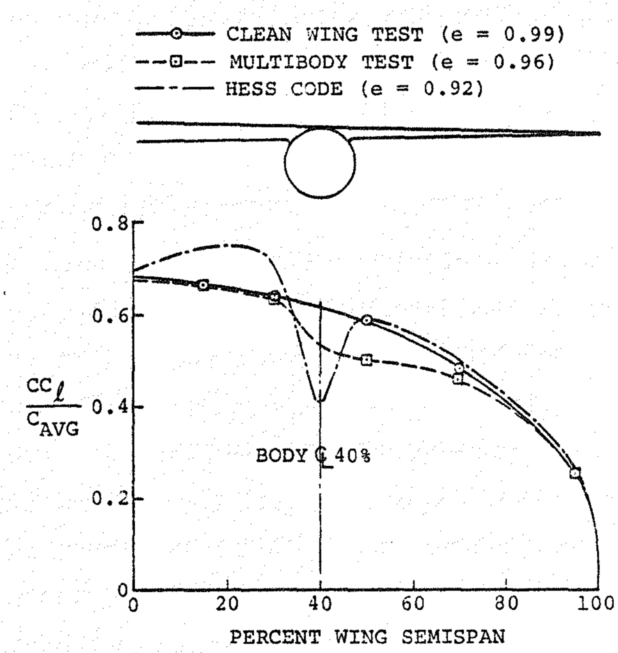

Figure 12. Experimental Span Efficiencies - Pressure Data

ients of the clean wing and the multibody are not equal. The clean wing C_L is 0.534 while that for the multibody is 0.505. Still, a comparison of the resulting span efficiencies is meaningful. The value of e for the clean wing is 0.99 and that of the multibody is 0.96. Both values compare favorably with the results from the force data.

Difficulties, such as determining the exact slope of the C_L^2 versus C_D curve, and the lack of pressure data near the body, prevent an accurate estimate of spanload efficiency. However, the results of this test clearly indicate that no serious span efficiency problems exist for a high wing multibody configuration. Figure 13, which is a typical upper surface isobar plot from the wind tunnel pressure data, also supports this conclusion.

The span efficiency yielded by the load distribution of Figure 12 is higher than that initially provided by the Vorlax analysis. However, the way in which the data are faired on each side of the body has a significant effect on e. Alternate fairings of the load distribution and the C_L^2 versus C_D curve produced e values of approximately 0.92, rather than the 0.96 shown in Figure 12. This range of values clearly encompasses the Vorlax values. Therefore, it can be concluded that the test results substantiate the validity of span efficiency values used for the multibody aircraft.

2.3.1.3 Empennage Sweep and Thickness

Flight safety requires that empennage sweep angles and thickness ratios be selected such that flow separation and loss of control will not occur during overspeed conditions due to upset. At the same time, based on appearance and historical trends, horizontal tail sweep angles generally agree with the sweep angle selected for the wing. The thickness ratios and sweep relationships used are based on these considerations and are shown in Figure 14.

2.3.1.4 Component Drag Buildup

Total aircraft drag is estimated on a component buildup basis. That is, the wing, fuselage, horizontal tail, etc., are treated individually. The skin friction drag is determined for the wetted area and the characteristic Reynolds number for each component, and is then referenced to the wing area. Next, shape factors are applied to the skin friction drag to obtain the profile drag for each component, and these are combined to obtain the basic profile drag. The drag increments listed in Figure 15 are then added to obtain the total profile drag. An allowance

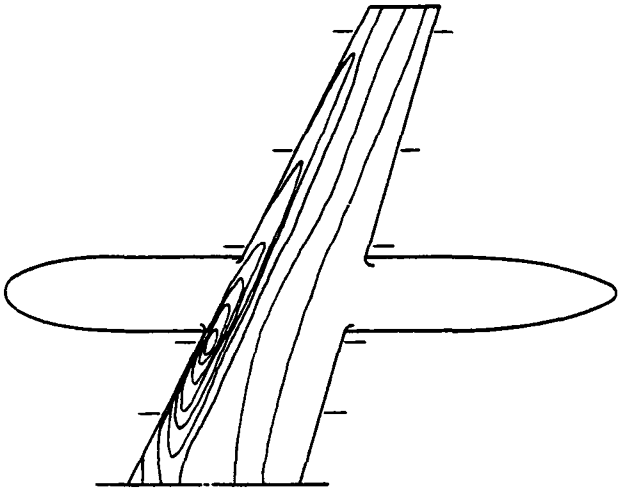

Figure 13. Typical Isobar Plot - Multibody Model Wing Upper Surface Test Data

	T TAIL		SLAB TAIL
WING SWEEP	0 44 RAD (25 DEG)	0 61 RAD (35 DEG)	0 44 RAD (25 DEG)
HORIZONTAL SWEEP	0.44 RAD (25 DEG)	0 61 RAD (35 DEG)	0 RAD (0 DEG)
HORIZONTAL t/c	0 0800	0 1150	0 0640
VERTICAL SWEEP	0.61 RAD (35 DEG)	0 61 RAD (35 DEG)	0 61 RAD (35 DEG)
VERTICAL t/c	0 1050	0 1050	0 1050

Figure 14. Empennage Configuration Data

ELEMENT	VALUATION		
	SINGLE BODY	TWO-BODY	THREE-BODY
ROUGHNESS (% OF BASIC PROFILE DRAG)	5	5	5
INTERFERENCE (% OF BASIC PROFILE DRAG)	6	10	12
TRIM - COUNTS	4	4	4
COMPRESSIBILITY DRAG - COUNTS	10	10	10
MISCELLANEOUS DRAG - COUNTS	4	4	4

Figure 15. Drag Increments

for drag resulting from steps/gaps, rivets, antennas, and other proturberances is provided by the roughness factor. Additional drag due to interference between components is used to provide better correlation between the drag data estimates of the sizing program and flight test results. The nominal level used for the conventional configuration is increased for the multibody aircraft to account for the greater number of surface intersections.

The induced drag is determined based on the Hess/Vorlax analyses which are discussed in section 2.3.1.2.

Profile drag variations, correlated with test results of configurations utilizing supercritical airfoils, are included in the drag values at lift coefficients other than the design value.

2.3.1.5 High-Lift System Description

The high-lift system incorporates a 27 percent chord Fowler flap and a 12 percent chord leading edge device. Corrections for wing sweep and exposed flap span are applied as appropriate. The outer flap semispan is at $\eta = 0.70$ for all configurations.

2.3.2 Structural Criteria and Methods

The structural criteria used are typical of large commercially operated transports. In particular, FAR Part 25 is used to establish design criteria wherever applicable. The aircraft are designed to a 2.5g limit load factor with no alternate load factors defined. Figure 16 presents the speed versus altitude envelope used for all designs. The cruise Mach number of 0.80 is chosen for compatibility with commercial traffic. Figure 17 summarizes the gust load requirements from the FAR. The requirements define a specific gust velocity for a given aircraft speed and altitude. Each of these points is analyzed.

The FAR requires that the aircraft be flutter free for all points on an envelope 20 percent larger than the one given in Figure 16. A maximum wing tension stress level of 310,251 kN/m^2 (45,000 psi) is used to give a structural life of 60,000 hours.

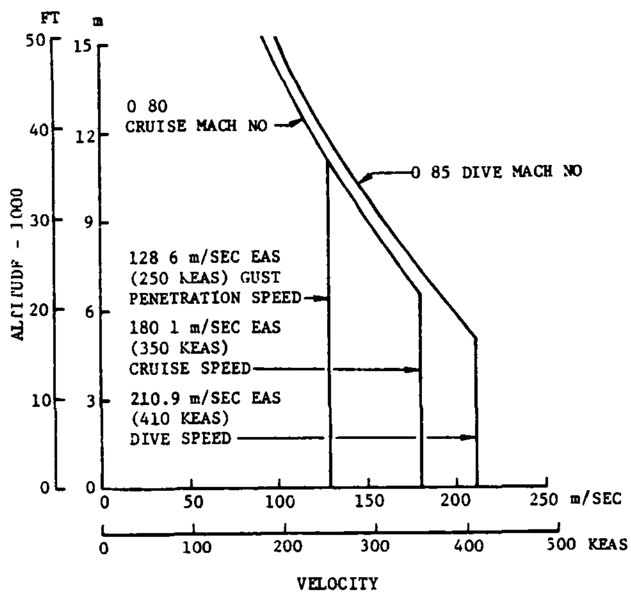

Figure 16. Speed vs Altitude

GUST VELOCITY		AIRCRAFT SPEED		ALTITUDE	
m/SEC	FT/SEC	m/SEC	KEAS	m	FT
15.2	50	180.1	350	6,096	20,000
7.6	25	92.3	179.5	15,240	50,000
7.6	25	196.2	381.3	6,096	20,000
3.8	12.5	98.1	190.7	15,240	50,000
20.1	66	128.6	250	10,973	36,000

Figure 17. FAR Gust Load Requirements

The weight estimating methods used are a combination of statistical and analytical techniques. During parametric studies GASP is used extensively. Since GASP is such a large program and since a great many data points are examined, the routines for each principal discipline must be simple enough to analyze many configurations very rapidly. For this reason the weight estimating methods are statistical in nature. The methods are based on large transport aircraft and they are modified as necessary for unusual configurations.

After an aircraft is first defined by a parametric analysis, more detailed analytical methods are used to either verify or modify the aircraft weight. The most detailed analysis is done on the wing structure. This involves a load survey to determine critical loads, a structural analysis with a beam theory program, and a flutter analysis to determine optimum torsional stiffness requirements.

2.3.3 Stability and Control

The stability and control influence in the Generalized Aircraft Sizing and Performance (GASP) program is designed to ensure that it is feasible for all configurations to achieve good flying qualities. This is attained by select-

ing the empennage and controls with sufficient size, shape, and aerodynamic loading capability to be compatible with the selected fuselage, wing, and center of gravity combinations for a given configuration.

The horizontal tail is sized using relaxed static stability criteria and an optimum center of gravity (cg) travel. The aft cg position is thus set by stability. The level of relaxed longitudinal stability selected is an eight percent negative static margin. This criterion is estimated to produce the most adverse unaugmented response with a time to double amplitude of five seconds or greater. The stability augmentation system is designed to achieve an equivalent positive five percent static margin for normal operation and therefore provides good flying qualities. To assure safety of flight, the aircraft would remain controllable should a total system failure occur even at the most adverse condition. The most forward cg is checked for trim adequacy for the full flap low-speed landing approach condition and for control adequacy during nose wheel lift off with takeoff flaps. The tail selection chooses the most critical of those conditions using a maximum lift coefficient of 1.0 for the tail, which should be easily achieveable.

The computerized tail sizing routine accounts for such things as: shifts of the neutral point due to fuselage location based on Royal Aeronautical Society (RAS) data sheet methods; lift curve slope of the horizontal based on DATCOM methods and flight test data; and downwash at the horizontal tail and its efficiency factor as a function of position based on Lockheed empirical methods. The iterative process of the GASP program continually updates the selection process with proper stall speeds, rotation speeds, gear locations, and required cg travel to evaluate the critical conditions.

The vertical tail is sized for the most critical condition between control of an outboard engine failure on takeoff and a minimum level of directional static stability. Effectiveness of the vertical tail as a lifting surface is determined using DATCOM and Lockheed empirical methods. Directional instability due to the fuselages is obtained from published empirical methods. A minimum level of "tail on" directional stability is chosen to assure a C_{n_β} of +0.0015. This criterion has been found to provide good lateral directional characteristics for large transport type aircraft.

Lateral control is provided during the aircraft sizing procedure by allocating the outer 30 percent of the wing

semispan for ailerons. Spoilers are to be used in conjunction with the ailerons for conventional control.

The above assumptions and methods are used in the GASP program for initial aircraft sizing. Point design selections are then analyzed in detail to verify these methods and/or assumptions.

2.3.4 RTD&E and Production Cost

All cost data produced for the point design aircraft are developed using the Lockheed Advanced Design Acquisition Cost Model. This model uses a parametric estimating approach which employs various types of cost estimating relationships (CER) for the various levels of function and of the work breakdown structure (WBS). The CERs are based upon historical relationships among aircraft and program parameters (independent variables). CERs are composed of one dependent variable and a combination of one or more independent variables. The CERs may take the form of linear, log, or exponential equations, hours or dollars per pound, and percentages of other program elements.

2.3.4.1 Development CERs

Independent variables used in the development phase CERs generally take a form which describes size, compactness, technology advancement, speed, and schedule. Size is generally a predominant variable and is described by various terms such as weight or thrust. Aircraft density (kg/m^3) (lb/ft^3) is a variable used to define design and test problems associated with compactness. Technology advancement is usually a subjective estimate of "state of the art" (SOA). This factor incorporates a range from one (for "off-the-shelf" programs) to three (for production programs requiring maximum innovation and invention). A data bank of SOA data from historical programs has been developed as a guide. Speed is used where it is an independent factor and not a measure of SOA or compactness. Various schedule and military-commercial related factors are also used. Some elements have been estimated using vendor prices or estimates, or by best judgement of informed personnel.

Takeoff gross weight, manufacturers empty weight, airframe weight, and structural weight are used in various CERs. The calculated values for these reflect the weight of the advanced materials. Since the CERs used in calculating development costs are based upon current technology aircraft, the calculated weights are adjusted to equivalent aluminum weights for estimating development costs utilizing advanced materials technology.

The design SOAs are developed at a system level (wing, tail, electrical, etc.) for each configuration and summed to an average structure and average total design SOA. The design support SOAs are estimated at a function level (aerodynamics, loads, stress, reliability, etc.) for each configuration and summed to an average design support SOA as reflected in the premise. Total program SOAs are weighted sums of design and support SOAs.

2.3.4.2 Production CERs

Airframe manufacturing elements are estimated using CERs which develop cumulative average hour/cost per kilogram (pound) values for 100 units for each major aircraft component or system. Costs are projected for development and production quantities using cumulative average theory equations and appropriate learning curve factors. Airframe manufacturing CERs are developed separately for labor hours and material dollars and are a function of weight and SOA for each component/system defined by the group weight statement.

Airframe manufacturing support functions such as quality assurance, sustaining tooling and engineering are estimated as a percent of manufacturing hours.

2.3.4.3 Point Design Estimates

Parametric estimating theory presumes that relationships defined from historical programs may be used to project the cost of new programs. This, of course, assumes that the independent variables selected for historical programs will also define the peculiar characteristics of the new program, or that adjustments are made in the CERs to reflect the new characteristics. Where there is a distinct difference in the data related to aircraft size or type, the data is split and separate CERs are derived or a parameter in the equation is added which adjusts the equation to reflect the proper application.

Three factors are developed which are used to compute the SOA for each aircraft component for material and labor, respectively. These factors are all relative to an aluminum technology data base and address materials technology, size, and commonality within the aircraft relative to conventional aluminum aircraft. In all cases, the materials technology factors assume 1985 technology using boron/epoxy reinforcements in primary structure and graphite/epoxy in secondary structure. The sizing and commonality factors are developed for each point design configuration. The material cost tech-

nology factors used for all point design aircraft are shown in Figure 18.

The method used to define these material cost technology factors is illustrated in Figure 19.

2.4 AIRCRAFT SIZING

The sizing analysis for the point design aircraft is conducted using the Lockheed GASP Program; the methodology of this program is outlined in Figure 20. Design data, such as basic engine characteristics, the required mission, atmospheric data, and geometric characteristics, including fuselage characteristics developed for the specified payload, are required inputs. The GASP program controls the interaction of the program modules provided by the various technical disciplines and the inputs provided for the specific configuration, then generates a component build-up of drag and weight and integrates these results into total aircraft drag and weight. Propulsion system size is selected by matching cruise thrust requirements, or, if required, by mismatching these requirements so as to oversize the engine at cruise to provide additional takeoff thrust. The aircraft size required for the mission is defined by an iterative process.

The data given in Figures 21 through 24 illustrate the sizing process for the single body and the two-body aircraft. These data are constrained by the required 3200.4 m (10,500 ft) field length and second segment climb gradient of 0.03. Wing loading is iterated at a given aspect ratio to meet both of these constraints for the configurations shown. The flap setting is allowed to increase to the maximum value which will allow the climb gradient to be met since this will result in the shortest takeoff distance. An increase in aspect ratio is accompanied by a decrease in wing loading and an increase in takeoff flap deflection for the aircraft which meet these constraints.

Aircraft are sized over a range of wing aspect ratio values with the aspect ratio which provides the minimum DOC (or trip cost), Figures 21 and 23, selected as the optimum. As seen from Figure 21 where trip cost, which is directly proportional to DOC, is plotted vs aspect ratio, the sensitivity of DOC to aspect ratio is relatively small for the two-body aircraft at the baseline fuel price of 34.34 ¢/l (1.30 $/gallon). At the "bucket" of the curve, DOC remains constant over an approximate aspect ratio range of 10.5 to 11.1 when DOC is determined to two significant decimal places, 6.29 ¢/AMgkm (10.57 ¢/ATNM). Over the aspect ratio range given, DOC varies by a maximum of 2.6 percent.

	MATERIAL*	LABOR
WING	1.752	1.110
FUSELAGE	1.310	1.064
EMPENNAGE	4.780	1.607
LANDING GEAR	1.133	1.034
NACELLE/PYLON	1.437	1.113

*BORON @ 90.72 $/kg(200 $/LB)
GRAPHITE @ 17.69 $/kg(39 $/LB)

Figure 18. Material Cost Technology Factors

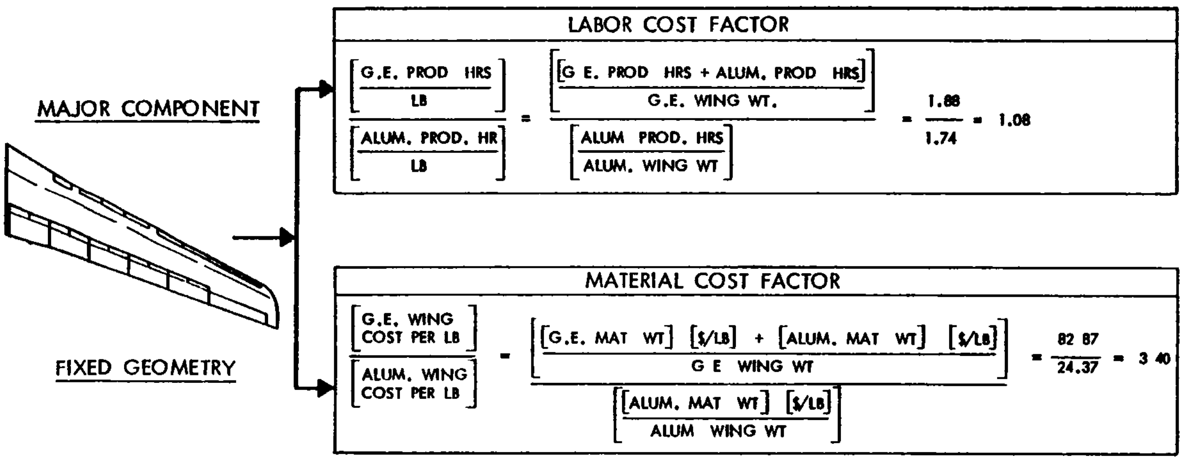

ALUMINUM @ 4.5/6.0 $/LB
GRAPHITE EPOXY @ 30 $/LB

Figure 19. Material Cost Technology Factor Method

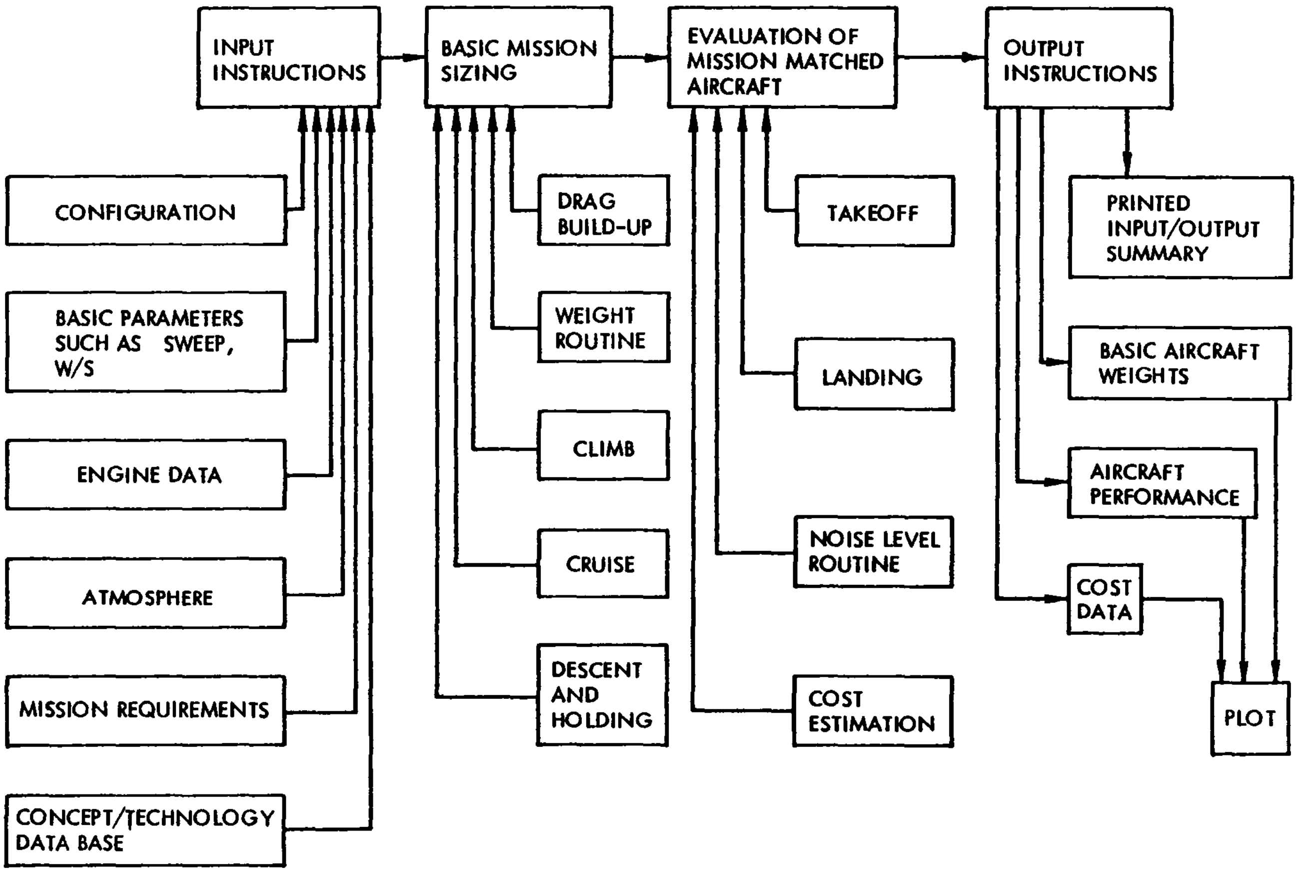

Figure 20. Generalized Aircraft Sizing and Performance (GASP) Program

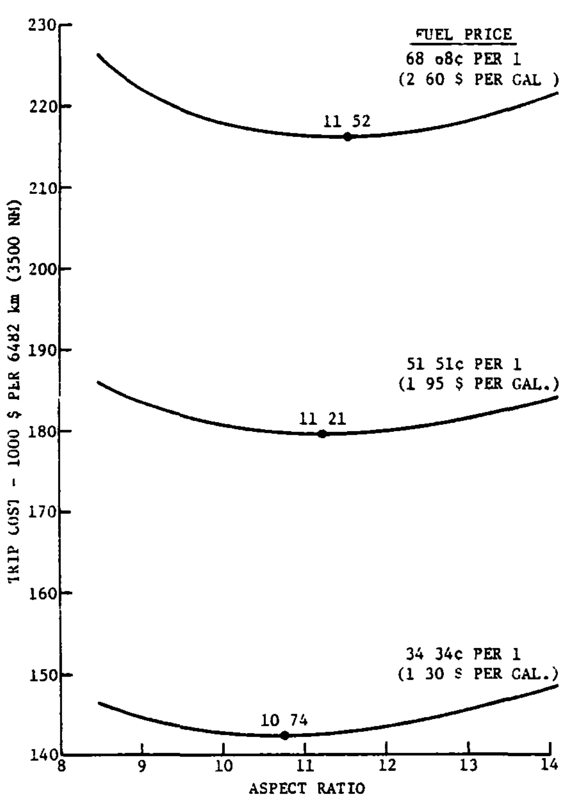

Figure 21. Aspect Ratio Selection - Two-Body Aircraft

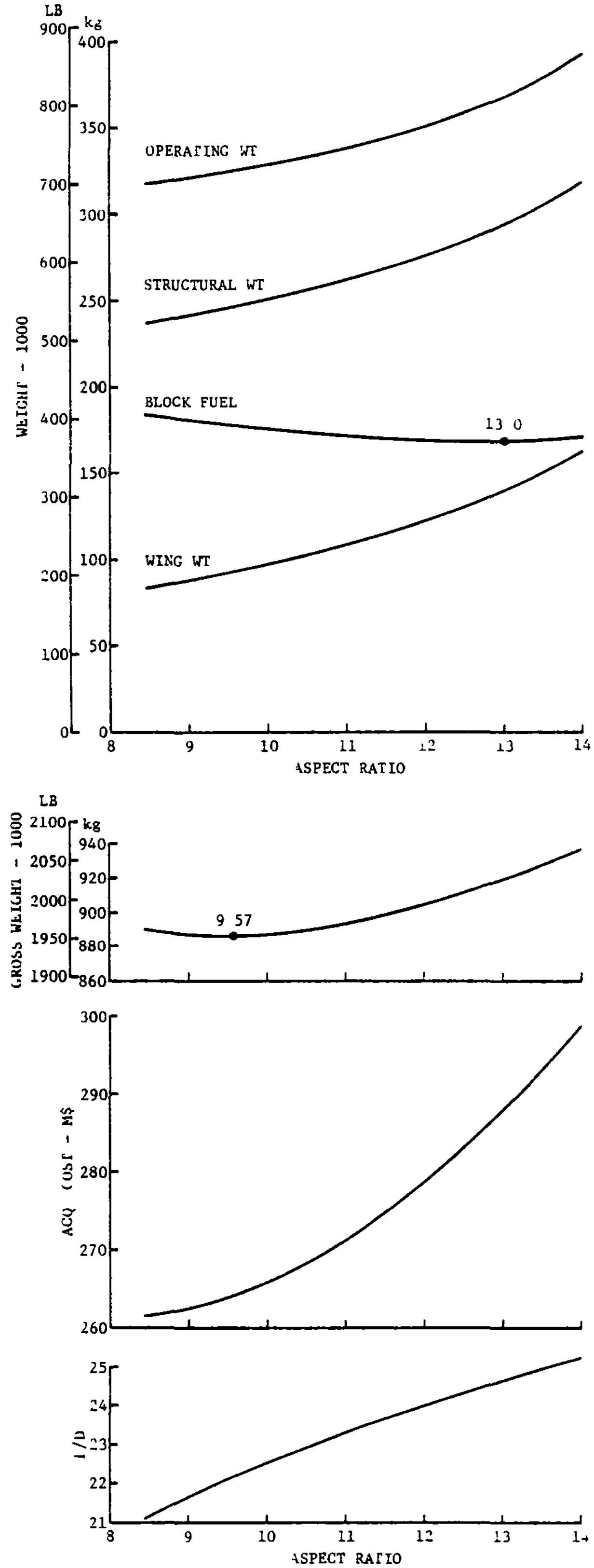

Figure 22. Aircraft Characteristics vs Aspect Ratio - Two-Body

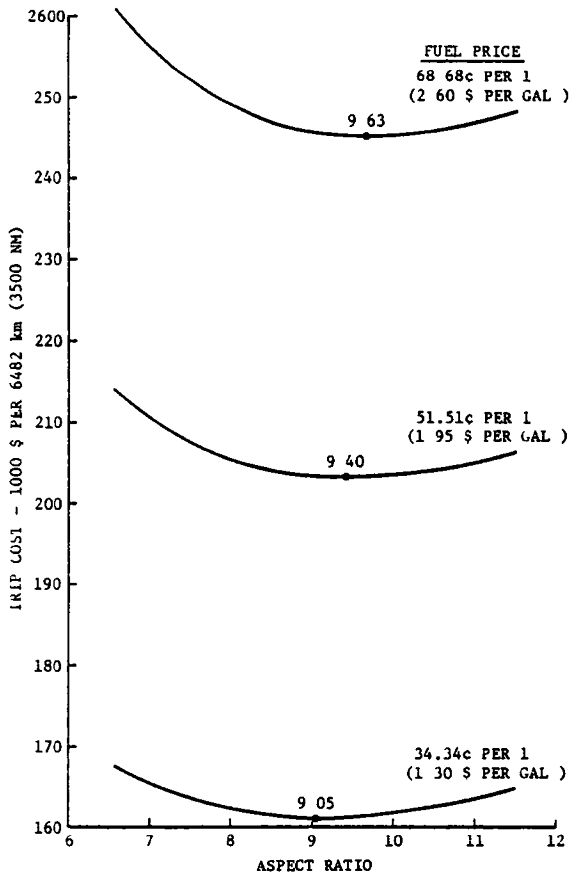

Figure 23. Aspect Ratio Selection - Single Body Reference Aircraft

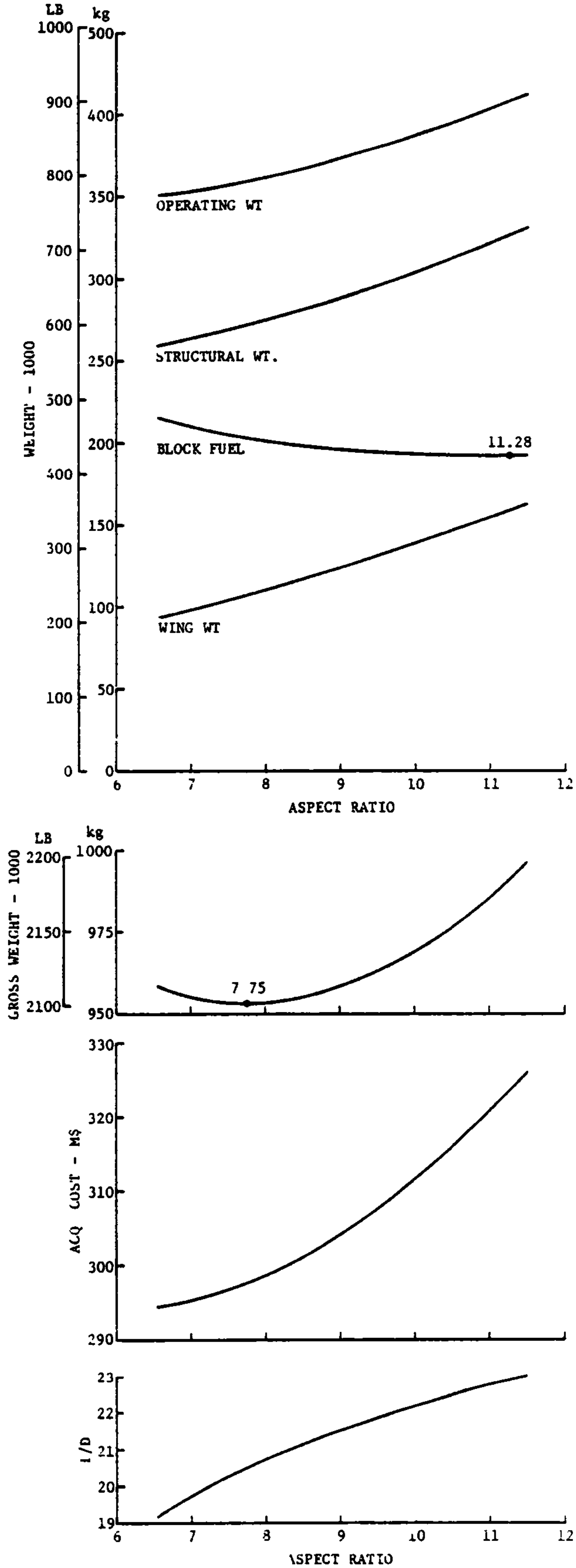

Figure 24. Aircraft Characteristics vs Aspect Ratio - Single Body Reference

This lack of DOC sensitivity requires the analysis of a great number of aircraft data points to arrive at the DOC "bucket." Where sensitivity studies are to be performed throughout the study (payload, body locations, etc.), the minimum DOC band is defined and aspect ratios within this band are selected; however, finding the exact bucket is not accomplished and is not felt to be necessary. Inspection of the data in Figure 22 indicates that other aircraft parameters are somewhat more sensitive to aspect ratio variation. For example, over the aspect ratio range of 10.5 to 11.1 where DOC remains relatively constant, wing weight varies by 5.5 percent and structural weight varies by 2.3 percent. When performing sensitivity studies, not locating the exact bucket of the DOC curve when optimizing the aspect ratio selection can result in data point scatter for other aircraft parameters. This scatter is not felt to be significant and is removed by using point averaging curves.

The single body aircraft DOC is slightly more sensitive to aspect ratio selection. A maximum change of 3.7 percent occurs between the DOC curve "bucket" and the maximum DOC resulting over an aspect ratio range of 7 to 11.

The aspect ratio values investigated for these two aircraft encompass the values of aspect ratio at which block fuel and gross weight are optimized. Optimum block fuel aspect ratio values are 13.0 and 11.28 and optimum gross weight values are 9.5 and 7.75, respectively, for the two-body and single body aircraft.

2.5 INITIAL POINT DESIGN AIRCRAFT

The point design aircraft upon which the detailed analyses of Section 2.7 are based are shown in Figures 25, 26, 27, and 28. Two, two-body aircraft are analyzed, Figures 25 and 26, with the primary difference being wing planform and body/landing gear spanwise location. One, three-body aircraft, Figure 27, and one single body aircraft, Figure 28, are analyzed. Each of these aircraft is assigned a code identification as indicated on the figures, such as MB1 for the straight taper wing planform two-body aircraft. These codes are used throughout the report to represent a given type aircraft design.

A data summary of the point design aircraft characteristics are presented in Figure 29. General descriptions of each of these aircraft follow. Fuselage sizing data are given in Appendix A; however, a fuselage data summary is presented in Figure 30.

2.5.1 Two-Body MB1 and MB2 Aircraft

The two-body MB1 aircraft has a gross weight of 893,214 kg (1,969,200

SPEED	0 80 MACH
PAYLOAD	350,000 kg (771,618 LB)
RANGE	6,482 km (3,500 NM)
OPERATING WEIGHT	323,547 kg (713,300 LB)
GROSS WEIGHT	893,214 kg (1,969,200 LB)
BLOCK FUEL	183,796 kg (405,200 LB)
ASPECT RATIO	9.70
DOC	6.47 ¢/AMgkm @ 34.34¢ PER LITER
	(10.87 ¢/ATNM @ 1.30$ PER GAL.)

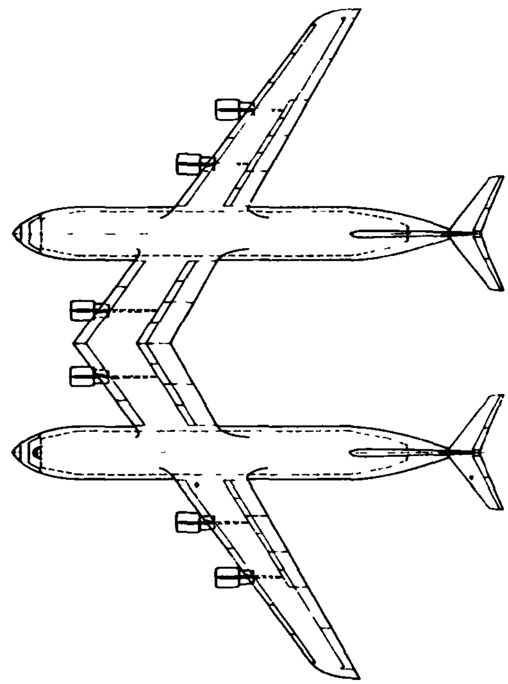

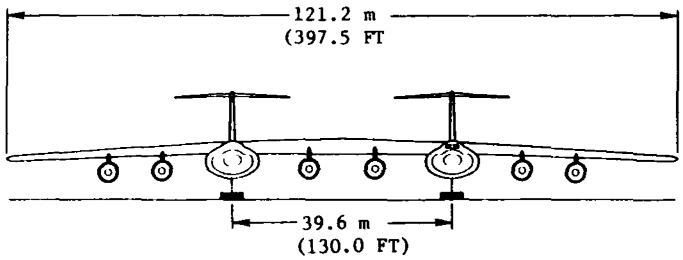

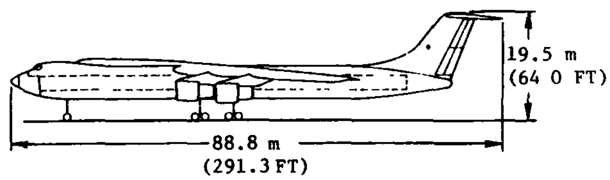

Figure 25. Two-Body MB1 Aircraft - Point Design

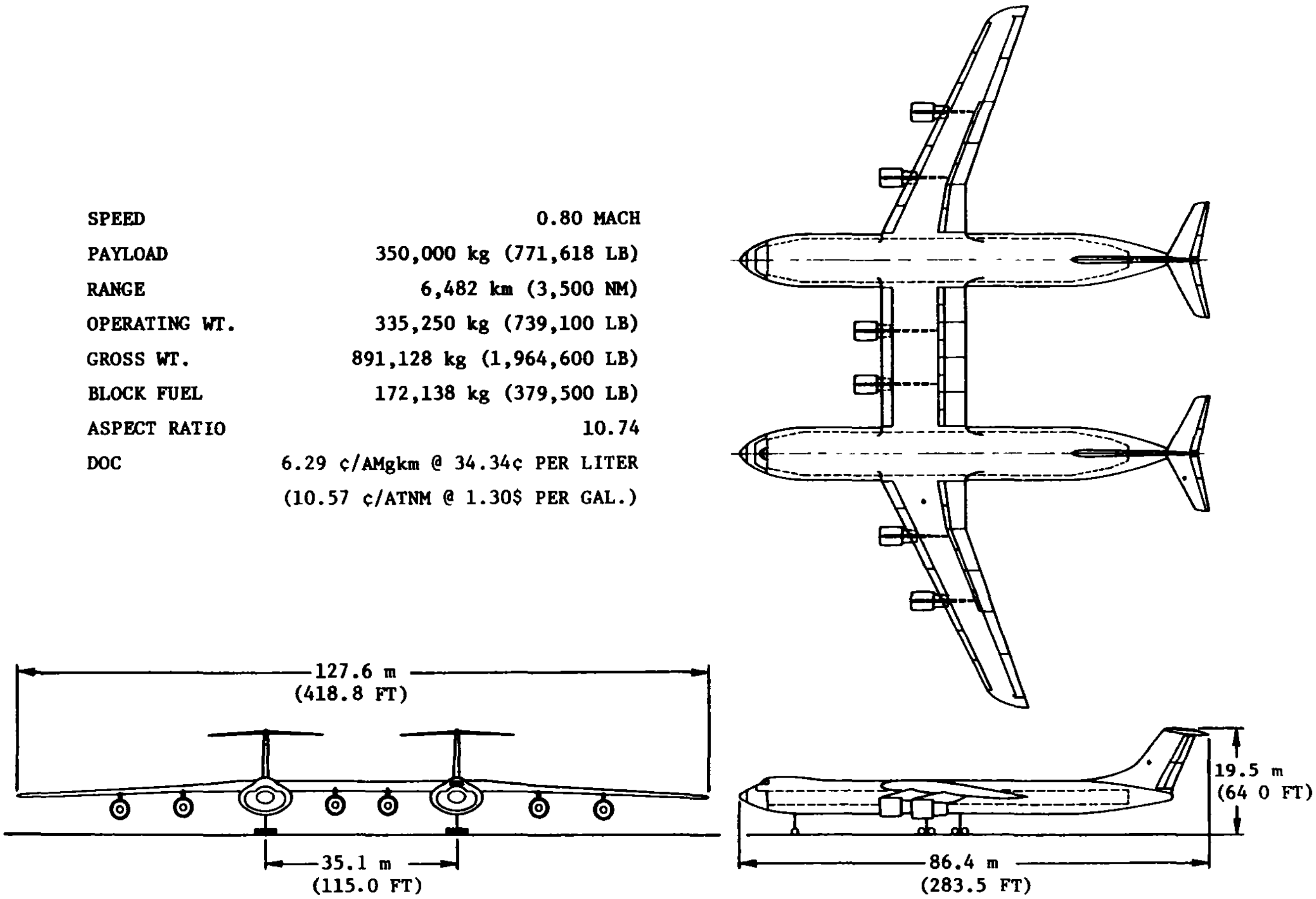

Figure 26. Two-Body MB2 Aircraft - Point Design

SPEED	0 80 MACH
PAYLOAD	350,000 kg (771,618 LB)
RANGE	6,482 km (3,500 NM)
OPERATING WT	335,613 kg (739,900 LB)
GROSS WT	905,234 kg (1,995,700 LB)
BLOCK FUEL	183,660 kg (404,900 LB)
ASPECT RATIO	12 54
DOC	6.58 ¢/AMgkm @ 34 34¢ PER LITER (11.06 ¢/ATNM @ 1.30$ PER GAL)

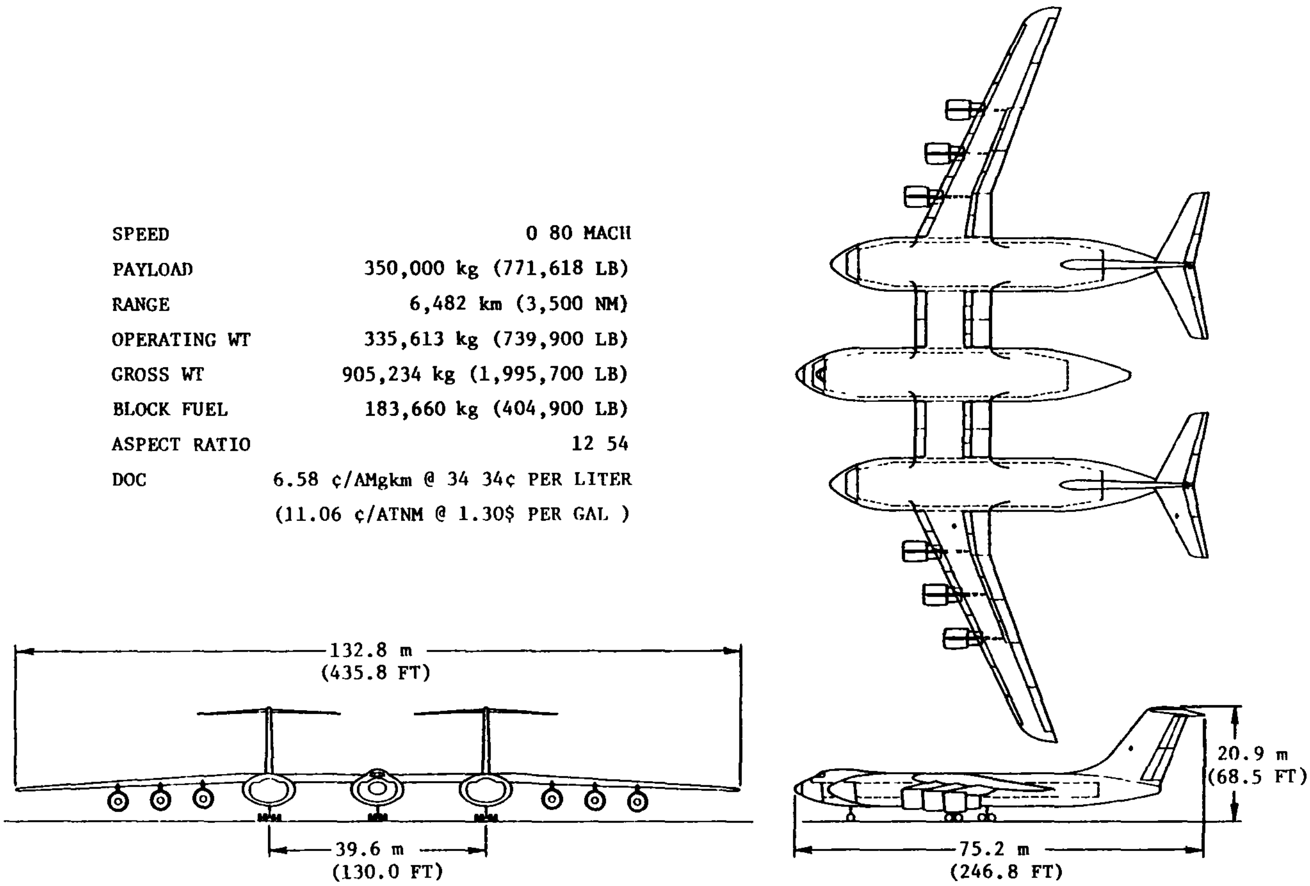

Figure 27. Three-Body MB3 Aircraft - Point Design

SPEED	0.80 MACH
PAYLOAD	350,000 kg (771,618 LB)
RANGE	6,482 km (3,500 NM)
OPERATING WT	372,354 kg (820,900 LB)
GROSS WT.	957,851 kg (2,111,700 LB)
BLOCK FUEL	196,950 kg (434,200 LB)
ASPECT RATIO	8 93
DOC	7.10 ¢/AMgkm @ 34.34¢ PER LITER
	(11.93 ¢/ATNM @ 1.30$ PER GAL.)

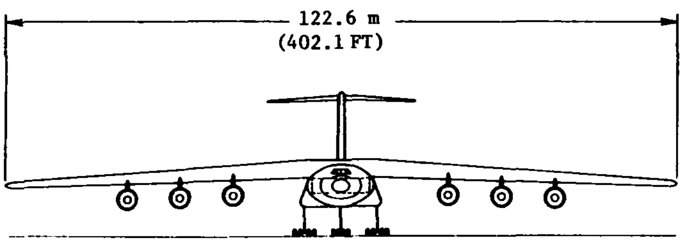

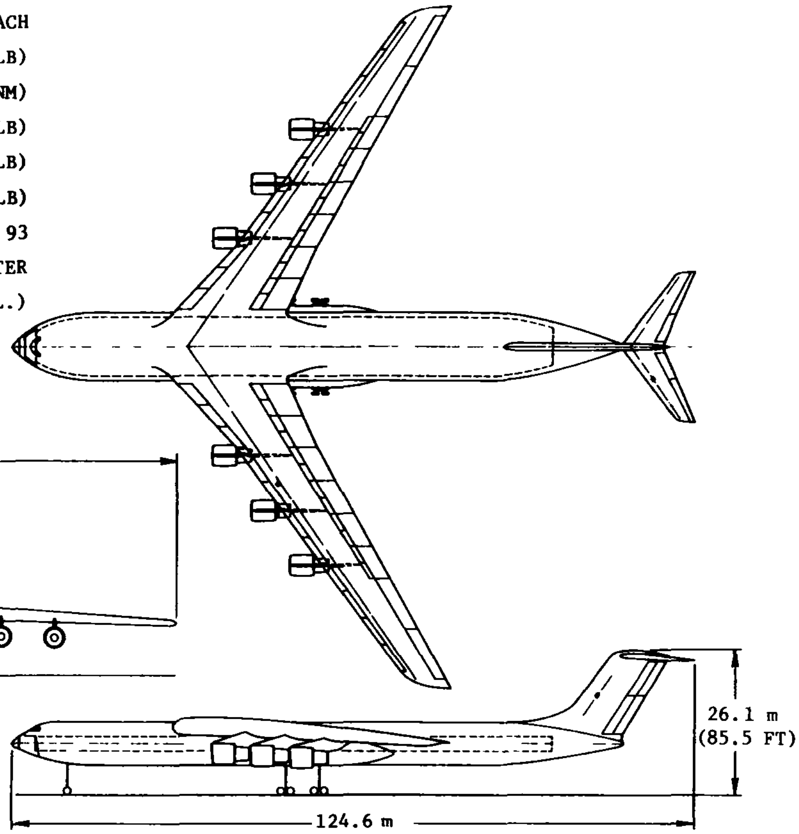

Figure 28. Single Body Reference SBR Aircraft - Point Design

ITEM ↓ / AIRCRAFT →	SINGLE BODY SBR	MULTIBODY MB1	MULTIBODY MB2	MULTIBODY MB3
Wing				
Aspect Ratio	8.93	9.70	10.74	12.54
Area - SQ. m	1617.7	1454.3	1457.6	1352.2
Sweep - Radians	0.610	0.610	0.436	0.436
Loading - kN/SQ.m	5.66	5.87	5.84	6.40
Span - m	120.15	118.17	125.15	130.24
Weight - kg	122,901	89,512	105,555	101,850
Weight - kg/SQ. m	76.0	61.6	72.4	75.3
Fuselage				
Length - m	111.53	79.61	79.61	60.87
Width - m	12.25	9.60	9.60	9.60
Height - m	7.71	6.00	6.00	6.00
Weight - kg	105,025	107,116	107,175	102,929
Weight - kg/SQ. m	34.3	31.3	31.3	27.5
Floor Height Above Ground - m	7.77	5.39	5.41	4.11
Empennage				
Area - SQ. m	310.8	347.9	354.5	540.8
Weight - kg	7,911	8,469	8,568	11,617
Weight - kg/SQ. m	25.4	24.4	24.2	21.5
Propulsion				
Engines - Number	6	6	6	6
Thrust/Eng. - 1000 N	330.8	308.8	285.6	307.1
System Wt. - kg	53,447	49,741	45,731	49,278
Cruise Power Setting η	0.95	0.95	0.95	0.95
Landing Gear				
Max. Tread Width - m	16.98	43.30	38.77	43.30
Weight - kg	42,733	29,710	29,892	30,168
Aircraft Weight - 1000 kg				
Structure	287.9	243.6	259.3	255.3
Operating	372.4	323.5	335.3	335.6
Fuel	235.5	219.6	205.9	219.6
Gross	957.9	893.2	891.1	887.1
Performance				
Cruise L/D	21.48	21.46	23.14	21.85
Block Fuel - 1000 kg	196.9	183.8	172.0	183.7
Mg km/l - Fuel	9.25	9.91	10.58	9.92
Ferry Range - km	9,930	10,206	9,988	9,895
Ecomonic				
Aircraft Price - $M	303.8	264.8	269.6	277.3
DOC-¢/AMgkm @ $0.34/l	7.10	6.47	6.29	6.58
Efficiency Factors				
Fuselage	0.335	0.402	0.402	0.402
ML/D	17.18	17.17	18.51	17.48
Aircraft Price/Payload - $/kg	869	756	769	791

Figure 29. Aircraft Characteristics Summary - Point Design (Metric Units)(Sheet 1 of 2)

ITEM \ AIRCRAFT	SINGLE BODY SBR	MULTIBODY MB1	MB2	MB3
Wing				
Aspect Ratio	8.93	9.70	10.74	12.54
Area - SQ. FT.	17,413	15,654	15,689	14,555
Sweep - Degree	35	35	25	25
Loading - LB/SQ. FT.	118.2	122.6	122.0	133.6
Span - FT.	394.2	387.7	410.6	427.3
Weight - LB.	270,950	197,340	232,710	224,540
Weight - LB./SQ. FT.	15.56	12.61	14.83	15.43
Fuselage				
Length - FT.	365.9	261.2	261.2	199.7
Width - FT.	40.2	31.5	31.5	31.5
Height - FT.	25.3	19.7	19.7	19.7
Weight - LB.	231,540	236,150	236,280	226,920
Weight - LB/SQ. FT.	7.02	6.41	6.42	5.64
Floor Height Above Ground - FT.	25.50	17.67	17.74	13.50
Empennage				
Area - SQ. FT.	3,345	3,745	3,816	5,821
Weight - LB.	17,440	18,670	18,890	25,610
Weight - LB./SQ. FT.	5.21	5.00	4.95	4.40
Propulsion				
Engines - Number	6	6	6	6
Thrust/Eng. - LB.	74,360	69,410	64,200	69,040
System Wt. - LB.	117,830	109,660	100,820	108,640
Cruise Power Setting η	0.95	0.95	0.95	0.95
Landing Gear				
Max. Tread Width - FT.	55.7	142.2	127.2	142.2
Weight - LB.	94,210	65,500	65,900	66,510
Aircraft Weight - 1000 LB.				
Structure	634.8	537.0	571.7	562.8
Operating	820.9	713.3	739.1	739.9
Fuel	519.2	484.2	453.9	484.2
Gross	2,111.7	1,969.2	1,964.6	1,955.7
Performance				
Cruise L/D	21.48	21.46	23.14	21.85
Block Fuel - 1000 LB.	434.2	405.2	379.1	404.9
Ton NM/GAL, Fuel	20.84	22.32	23.84	22.34
Ferry Range - NM	5,362	5,511	5,393	5,343
Economic				
Aircraft Price - $M	303.8	264.8	269.6	277.3
DOC - ¢/ATNM @ 1.30 $/GAL	11.93	10.87	10.57	11.06
Efficiency Factors				
Fuselage	0.335	0.402	0.402	0.402
ML/D	17.18	17.17	18.51	17.48
Aircraft Price/Payload - $/LB	394	343	349	359

Figure 29. Aircraft Characteristics Summary - Point Design (Customary Units) (Sheet 2 of 2)

IDENTIFICATION → / ↓ ITEM	SINGLEBODY	MULTIBODY	
	SBR	MB1 & MB2	MB3
NO. FUSELAGES	1	2	3
CONTAINERS PER FUSELAGE	112	56	37
NET PAYLOAD DENSITY kg/CU.m. (LB/CU.FT.)	159.86 (9.98)	159.86 (9.98)	161.63 (10.09)
FUSELAGE EFFICIENCY A_c/A_f	0.3347	0.4022	0.4022
COMPARTMENT DIMENSIONS-m (FT)			
LENGTH	94.36 (309.58)	66.24 (217.33)	44.37 (145.58)
WIDTH	10.52 (34.50)	7.92 (26.00)	7.92 (26.00)
HEIGHT	2.64 (8.67)	2.64 (8.67)	2.64 (8.67)
FUSELAGE DIMENSIONS-m (FT)			
LENGTH	111.53 (365.91)	79.60 (261.17)	44.37 (145.58)
WIDTH	12.24 (40.17)	9.60 (31.50)	9.60 (31.50)
HEIGHT	7.72 (25.33)	6.00 (19.67)	6.00 (19.67)
MAX X-SECT AREA-SQ.m. (SQ.FT.)	71.07 (764.95)	44.35 (477.43)	44.35 (477.43)
WETTED AREA-SQ.m. (SQ.FT.)	3,064.22* (32,983)* 3,064.22* (32,983)*	1,710.72 (18,414) 3,422.36* (36,838)*	1,246.11(13,413) 3,737.32*(40,239)*
PRESSURIZED VOLUME CU.m. (CU.FT.)	6,347.39* (224,156)* 6,347.39* (224,156)*	2,860.88(101,031) 5,721.76*(202,062)*	1,950.29 (68,874) 5,850.88* (206,622)*

*TOTAL PER AIRCRAFT

Figure 30. Fuselage Data Summary

lb). Each fuselage accommodates 50 percent of the 350,000 kg (771,618 lb) payload which is loaded/unloaded straight in at cargo floor height through a nose visor door opening. The fuselages are oval in cross section, accommodate three sticks of cargo containers, are laterally spaced 39.6 m (130 ft) (32.7 percent wing semispan) between centerlines, and are identical except for crew compartment accommodations and wing carry through structure. A high tee-tail is mounted on the afterbody of each fuselage. The wing has a constant taper and a sweep of 0.61 rad (35 degrees) at the quarter chord. Total wing area is 1454.3m^2 (15,654 ft^2). Two of the six engines are located between the fuselages and two are outboard of each fuselage. Each has a thrust of 308,751 N (69,410 lb) and is pylon mounted to the lower wing surface structure.

The cargo floor has integral rails, rollers, and restraint mechanisms and is 5.23 m (17.17 ft) above ground level when the aircraft is at maximum gross weight. The landing gear arrangement consists of a two-wheel nose gear and two, eight-wheel tandem bogie main

gears on the centerline of each fuselage.

The two-body MB2 aircraft has a gross weight of 891,128 kg (1,964,600 lb). The fuselages are laterally spaced 35.1 m (115 ft) (27.5 percent wing semispan) between centerlines and each engine has a thrust of 285,576 N (64,200 lb). The outer wing panel has a 0.44 rad (25 degrees) quarter chord sweep, the center panel has an aft bat, and the inner panel is unswept. Total wing area is 1458 m^2 (15,689 ft^2). In all other respects, this aircraft has the same general arrangement as the MB1.

2.5.2 Three-Body MB3 Aircraft

The three-body MB3 aircraft has a gross weight of 905,234 kg (1,995,700 lb) of which 350,000 kg (771,618 lb) is payload, with each fuselage accommodating one-third. The payload is loaded/unloaded straight in at cargo floor height through a nose visor door opening. The fuselages are oval in cross section, accommodate three sticks of cargo, and are identical except that the center one has a flight deck, each of the outboard ones has a high tee-tail empennage configuration, and there is a slight difference in wing attach structure. Each of the outboard fuselages are 19.8 m (65.0 ft) from the center one, for a total lateral spacing of 39.6 m (130 ft) (29.8 percent wing semispan). The outer wing panel has a 0.44 rad (25 degrees) quarter chord sweep, the center panel has an aft bat, and the inner panel is unswept. Total wing area is 1352.2 m^2 (14,555 ft^2). Six engines, each having a thrust of 307,105 N (69,040 lb), are pylon mounted to the lower wing surface structure, three being located outboard of each outboard fuselage. The cargo floor has integral rails, rollers, and cargo restraint mechanisms and is 4.1 m (13.5 ft) above ground level when the aircraft is at maximum gross weight. The landing gear arrangement consists of a four-wheel nose gear on the center fuselage and two, eight-wheel tandem bogie main gears on the centerline of each outboard fuselage.

2.5.3 Single Body Reference SBR Aircraft

The single body reference SBR aircraft has a four-stick oval fuselage and a gross weight of 957,851 kg (2,111,700 lb) of which 350,000 kg (771,618 lb) is payload. The payload is loaded/unloaded straight in at cargo floor height through a nose visor door opening. It has a high tee-tail and a 0.61 rad (35 degrees) quarter chord swept wing which has an area of 1617.7 m^2 (17,413 ft^2). Six engines, each having a thrust of 330,770 N (74,360

lb), are pylon mounted to the lower wing surface structure. The cargo floor has integral rails, rollers, and cargo restraint mechanisms and is 7.8 m (25.5 ft) above ground level when the aircraft is at maximum gross weight. The landing gear arrangement consists of a four-wheel nose gear and two, eight-wheel tandem bogie main gears on each side, laterally spaced about the aircraft centerline at a distance of 13.3 m (43.5 ft).

2.6 CONFIGURATION TRADE STUDIES

A number of configuration trade studies were performed during the course of defining the point design aircraft. These configuration alternatives include items such as major component locations (engine and fuselage), wing sweep and planform, and empennage configuration. With the exception of the fuselage location study which relates to the fore and aft location of the three-body aircraft fuselages with respect to the wing, all of the studies are performed for the MB1 or MB2 type two-body configuration with the results assumed to be equally applicable to the MB3 type configuration.

2.6.1 Engine Location

The maximum engine thrust to which the STF477 engine can be scaled is assumed to be 444,822 N (100,000 lb). With the total thrust requirements for the point design aircraft approximating 1,779,289 N (400,000 lb), six engine configurations are selected for the initial point design aircraft so as to maintain maximum single engine thrust well below the scaling limit. This also enhances one engine out performance relative to a four-engine installation.

Two engine location configurations are evaluated. The MB2 aircraft where all engines are wing pylon mounted as shown in Figure 26 is used as the baseline configuration. The alternate configuration relocates the center wing engines to the aft-fuselage, using an installation similar to that of the L-1011 aircraft.

Comparing these two configurations, both weight and cost are increased by the alternate configuration as shown in Figure 31. Relocating the two engines from the wing to the fuselage reduces wing bending relief and thereby increases wing weight. Fuselage weight is also increased due to increased aft-fuselage loads. Total propulsion system weight increases due to increased system complexity and increased surface wetted area required to house the inlet duct, engine, and exhaust system. These increased weights result in the requirement for additional fuel. The end effect of these weight incre-

	*INCREASE	PERCENT CHANGE
WEIGHTS kg (LB)		
WING	340 (750)	0.3
HORIZONTAL TAIL	930 (2,050)	19.1
FUSELAGE	3,937 (8,680)	1.9
PROPULSION SYSTEM	1,347 (2,970)	2.5
OPERATING	7,575 (16,700)	2.3
FUEL	4,536 (10,000)	2.2
GROSS	12,111 (26,700)	1.4
COSTS		
ACQUISITION	5,303,000 $	2.0
DOC	0.12 ¢/AMgkm (0.21 ¢/ATNM)	2.0

*WEIGHT INCREASE DUE TO AFT FUSELAGE MOUNTED ENGINES

Figure 31. Engine Location Summary Data

ments is an increase in DOC of two percent. Thus, the wing mounted engine configuration is chosen for the point design aircraft.

2.6.2 Empennage Configuration

The "twin tee-tail" empennage configuration used on the initial point design multibody aircraft is selected based upon a comparison of the four configurations shown in Figure 32.

The canted slab, configuration 4, was not evaluated in detail. It showed no real advantage from a stability and control viewpoint for the following reasons. Control effectiveness for this concept is a function of the horizontal and vertical plane projected area; therefore, for equivalent capability, the physical surface area must

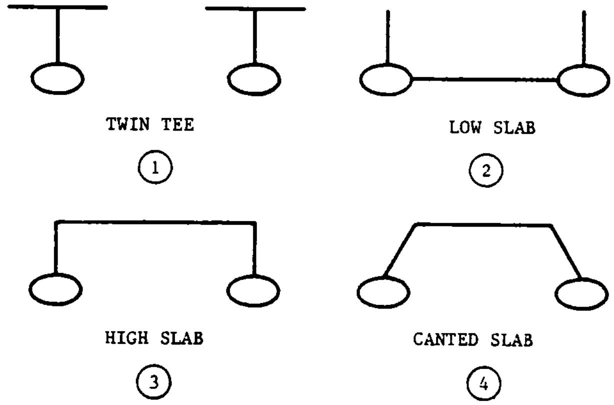

Figure 32. Empennage Configuration Alternatives

be greater than the required effective area. Control system complexity is also increased as rudder surface deflection results in a cross coupling force in the longitudinal or pitch mode. Additional complexity occurs when horizontal and vertical surface controls are deflected simultaneously, as flow interference occurs. Thus the effectiveness of each control surface is a function of the degree of deflection of the other surface. Directional control effectiveness is influenced by both a downwash and a sidewash flow field.

The foregoing are reasons for not desiring a canted vertical configuration. If further study proved that a canted tail would serve other functions, such as restraining large elastic modes of the fuselages, it would be acceptable from a stability and control standpoint. Since as noted in the following paragraphs no benefit was derived from the slab concept, the canted

vertical with the slab arrangement was not evaluated any further.

Aircraft are sized using the twin tee, high slab, and low slab tail configurations (configurations 1 through 3 in Figure 32) with the resulting geometric, weights, and cost data given in Figure 33.

The high slab tail requires the least horizontal area and the low slab tail requires the maximum area. The minimum and maximum vertical areas are required by the low slab and twin tee-tails, respectively. These area variations are a result of the combined effect of tail arm lengths, surface volume coefficients, and wing characteristics.

The horizontal slab tails have the highest aspect ratios; therefore, they also have the highest C_L values. As a result, these surfaces require the minimum volume coefficients. The low horizontal slab tail coefficient is the highest of the two as the surface is immersed in a turbulent downwash. Stability and control requirements dictate the following ranking of the three concepts in relation to decreasing volume coefficient magnitude: twin tee, low slab, and high slab. The shorter tail arm of the low slab tail results in its area being larger than that of the twin tee.

Limit load for the twin tee and high slab horizontal tails are estimated as 308,896 and 328,854 kg (681,000 and 725,000 lb), respectively. Midspan average skin thicknesses required to react these loads are 0.66 cm (0.26 in.) for the tee-tail and 2.84 cm (1.12 in.) for the high slab tail. The relatively high skin thickness of the slab tail is influenced by its span of 35.1 m (115 ft) and chord maximum thickness of 0.29 m (0.95 ft) as compared to a span of 20.96m (68.78 ft) and a chord maximum thickness of 0.48m (1.57 ft) for the tee-tail. The t/c of the horizontal surfaces is selected to avoid drag rise at the cruise mach number of 0.80. Thus the 0.44 rad (25 degrees) sweep of the tee-tail allows a t/c of 0.08 as compared to 0.064 for the unswept slab tail. Comparison of the low slab and tee-tail skin thickness requirements provide similar results. Based upon these skin thickness requirements, the horizontal high and low slab tails have increased weights, compared to the tee-tail, of 3129.8 and 3492.7 kg (6,900 and 7,700 lb), respectively.

The vertical surfaces for each of the empennage configurations as ranked in order of decreasing aerodynamic efficiency are twin tee, high slab, and low slab. However, due to the differences in wing areas and tail arm lengths, the required vertical areas, and therefore the surface weights, are in the reverse order. The weight dif-

ITEM \ EMPENNAGE CONFIGURATION	TWIN TEE (1)		HIGH SLAB (2)		LOW SLAB (3)	
	METRIC UNITS	CUSTOMARY UNITS	METRIC UNITS	CUSTOMARY UNITS	METRIC UNITS	CUSTOMARY UNITS
HORIZONTAL						
ASPECT RATIO	5.0	5.0	7.8	7.8	6.3	6.3
*AREA - m^2, FT^2	176	1892	158	1702	195	2098
SPAN - m, FT	21.0	68.8	35.1	115	35.1	115
C_r - m, FT	6.0	19.7	4.5	14.8	5.6	18.3
C_t - m, FT	2.4	7.9	4.5	14.8	5.6	18.3
TAIL ARM - m, FT	48.0	157.6	46.6	152.8	40.1	131.7
VOLUME COEFFICIENT	0.4592	0.4592	0.3882	0.3882	0.4187	0.4187
t/c	0.08	0.08	0.064	0.064	0.064	0.064
Λ @ 1/4 CHORD-RAD, DEG.	0.44	25	ZERO	ZERO	ZERO	ZERO
VERTICAL						
*AREA - m^2, FT^2	179	1923	169	1820	167	1797
SPAN - m, FT	10.8	35.4	10.5	34.4	10.4	34.2
TAIL ARM - m, FT	41.5	136.1	42.1	138.0	42.1	138.0
VOLUME COEFFICIENT	0.0406	0.0406	0.038	0.038	0.038	0.038
t/c	0.105	0.105	0.105	0.105	0.105	0.105
WEIGHTS - kg, LB						
HORIZONTAL	4867	10,730	7979	17,590	8328	18,360
VERTICAL	3701	8160	3565	7860	2717	5990
WING	105,555	232,710	106,136	233,990	107,928	237,940
STRUCTURE	259,319	571,700	263,088	580,010	264,540	583,210
OPERATING	335,259	739,120	339,423	748,300	341,256	752,340
FUEL	205,881	453,890	206,121	454,420	207,133	456,650
GROSS	891,137	1,964,620	895,546	1,974,340	898,390	1,980,610
COST						
AIRCRAFT PRICE - $M	269.6	269.6	273.7	273.7	274.6	274.6
DOC-¢/AMgkm, ¢/ATNM	6.29	10.57	6.33	10.64	6.36	10.68

*TOTAL AREA PER AIRCRAFT

Figure 33. Empennage Data Comparison Summary

ferences between the vertical surfaces are relatively insignificant.

Based upon aircraft weight, cost, and DOC being minimized by the twin tee-tail configuration, it is the selected concept; however, a dynamic loads analysis, which was outside the scope of this study, will be required before a final empennage configuration selection can be validated.

2.6.3 Wing Sweep

The advantage of the 0.61 rad (35 degree) wing sweep angle used on the single body reference and two-body MB1 aircraft is a combined result of the aerodynamic and structural characteristics of the wing. Figure 3, presented previously in Section 2.2, shows a substantial increase in allowable thickness ratio (t/c) results as wing sweep increases from 0.44 rad (25 degrees) to 0.61 rad (35 degrees). For example, at Mach 0.8 and 0.5 lift coefficient, the incremental t/c increase is about 0.034 for this 40 percent increase in wing sweep. Although this results in an increase in wing profile drag, wing weight decreases.

Figure 34 tabulates the characteristics of the 0.61 rad (35 degrees) sweep single body (SBR-35) and two-body (MB1-35) aircraft along with the 0.44 rad (25 degrees) sweep comparison aircraft, SBR-25 and MB1-25. These aircraft are sized to provide a five percent thrust margin at the initial cruise point and the wing size is adjusted as necessary to compensate for sweep induced changes in the high-lift performance and the resulting airport performance. The higher sweep angle aircraft have lower lift coefficients and a greater wing area to achieve the required 3200.4 m (10,500 ft) takeoff distance. As a result of this constraint, the higher wing sweep aircraft have lower cruise lift coefficients and induced drag coefficients. Since the SBR-35 aircraft optimized at a lower aspect ratio than the SBR-25 aircraft, while the two multibody aircraft optimized at the same aspect ratio, the induced drag advantage of the SBR-35 is less than for its multibody counterpart. Also, the SBR-35 aircraft has a higher total drag coefficient than does the SBR-25 aircraft. On the other hand, because of its greater induced drag advantage, the MB1-35 configuration does maintain a slight total drag coefficient advantage relative to the MB1-25. In summary:

1. The SBR-35 and MB1-35 aircraft wing weights per unit of area are 15 to 16 percent less than those for the SBR-25 and MB1-25 aircraft.

2. The SBR-35 and MB1-35 aircraft have an increase in wing thickness ratio between 0.035 and 0.040 compared to the SBR-25 and MB1-25 aircraft.

IDENTIFICATION → / ↓ ITEM	SINGLEBODY			TWO-BODY		
	SBR-25	SBR-35	% CHANGE	MB1-25	MB1-35	% CHANGE
WING						
SWEEP @ ¼ CHORD-RAD.	0.44	0.61		0 44	0.61	
ASPECT RATIO	9.16	8.93	2.6	9.70	9.70	0.0
AREA - SQ.m.	1,618	1,617	0.1	1,398	1,454	- 3.8
LOADING - kN/SQ.m	5.79	5.66	2.4	6.17	5.87	5.2
AVERAGE THICKNESS - %	11.71	15.36	-23.8	11.70	15.54	-24.7
WEIGHT - kg	146,279	122,901	19.0	101,514	89,512	13.4
WEIGHT - kg/SQ.m.	90.42	75.97	19.0	72.65	61.57	18.0
SPAN - m	121.75	120 17	1.3	116.44	118.77	- 2.0
WEIGHTS - kg						
STRUCTURE	313,069	287,940	8.7	256,144	243,579	5.2
OPERATING	396,893	372,354	6.6	335,250	323,547	3.6
FUEL	233,872	235,505	- 0.7	217,361	219,629	- 1.0
GROSS	980,757	957,851	2.4	902,603	893,214	1.1
PERFORMANCE						
WING PROFILE DRAG - CTS	0.00533	0.00576	- 7.5	0.00496	0.00542	- 8.5
WING INDUCED DRAG - CTS	0.00864	0.00846	2.1	0.00900	0.00814	10.6
C_D - CTS	0.02251	0.02281	- 1.3	0.02283	0.02225	2.6
C_L	0.502	0.490	2.4	0.502	0.477	5.2
CRUISE L/D	22.28	21.48	3.7	21.99	21.46	2 5
$C_{L_{MAX_{TO}}}$	2.56	2.44	4.9	2.55	2.42	5.4
$\delta_{F_{TO}}$	19.6	26.1	-24.9	24.6	31.1	-20.9
$C_{L_{MAX_{LG}}}$	3.08	2.78	10.8	2.93	2.65	10.6
BLOCK FUEL - kg	195,453	196,950	- 0.8	181,845	183,796	- 1.1
Mg-km/kg FUEL	11.608	11.519	- 0.8	12.479	12.342	1.1
WING SPAN EFFICIENCY - %	0.95000	0.95000	0.0	0.91913	0.91913	0.0
COST						
ACQUISITION - $\$10^6$	316.5	303.8	4.2	270.7	264.8	2.2
DOC - ¢/AMgkm	7.20	7.10	1.3	6.49	6.47	0.3

$$* \ \% \text{ CHANGE} = \left[\frac{0.44 \text{ RAD.} \Lambda - 0.61 \text{ RAD.} \Lambda}{0.61 \text{ RAD } \Lambda}\right] 100$$

Figure 34. Wing Sweep Angle Comparison Data
(Metric Units)(Sheet 1 of 2)

ITEM \ IDENTIFICATION	SINGLEBODY			TWO-BODY		
	SBR-25	SBR-35	% CHANGE	MB1-25	MB1-35	% CHANGE
WING						
SWEEP @ ¼ CHORD-DEGREE	25	35		25	35	
ASPECT RATIO	9.16	8.93	2.6	9 70	9.70	0.0
AREA - SQ.FT.	17,420	17,410	0.1	15,050	15,650	- 3.8
LOADING - LB/SQ.FT.	121.02	118.20	2.4	128.95	122.60	5.2
AVERAGE THICKNESS - %	11.71	15.36	-23.8	11.70	15.54	-24.7
WEIGHT - LB	322,490	270,950	19.0	223,800	197,340	13.4
WEIGHT - LB/SQ.FT.^{2}	18.52	15.56	19.0	14.88	12.61	18.0
SPAN - FT.	399.45	394.25	1.3	382.02	389.67	- 2.0
WEIGHTS - LB.						
STRUCTURE	690,200	634,800	8.7	564,700	537,000	5.2
OPERATING	875,000	820,900	6.6	739,100	713,300	3.6
FUEL	515,600	519,200	- 0.7	479,200	484,200	- 1.0
GROSS	2,162,200	2,111,700	2.4	1,989,900	1,969,200	1.1
PERFORMANCE						
WING PROFILE DRAG - CTS	0.00533	0.00576	- 7.5	0.00496	0.00542	- 8.5
WING INDUCED DRAG - CTS	0.00864	0.00846	2.1	0.00900	0.00814	10.6
C_D - CTS	0.02251	0.02281	- 1.3	0.02283	0.02225	2.6
C_L	0.5020	0.490	2.4	0.502	0.477	5.2
CRUISE L/D	22.28	21.48	3.7	21.99	21.46	2.5
$C_{L_{MAX_{TO}}}$	2.56	2.44	4.9	2.55	2.42	5.4
$\delta_{F_{TO}}$	19.6	26.1	-24.9	24.6	31.1	-20.9
$C_{L_{MAX_{LG}}}$	3.08	2.78	10.8	2.93	2.65	10.6
BLOCK FUEL - LB	430,900	434,200	- 0.8	400,900	405,200	- 1.1
TNM/LB FUEL	3.134	3.110	0.8	3.369	3.332	1.1
WING SPAN EFFICIENCY - %	0.95000	0.95000	0.0	0.91913	0.91913	0.0
COST						
ACQUISITION - $\$10^6$	316.5	303.8	4.2	270.7	264.8	2.2
DOC - ¢/ATNM	12.09	11.93	1.3	10.90	10.87	0.3

$$* \ \% \text{ CHANGE} = \left[\frac{25^\circ\Lambda \quad - 35^\circ\Lambda}{35^\circ\Lambda}\right] 100$$

Figure 34. Wing Sweep Angle Comparison Data (Customary Units) (Sheet 2 of 2)

3. Although the MB1-35 aircraft has a lower aerodynamic efficiency (L/D) than the MB1-25, its trip cost is about 0.3 percent less. This trip cost advantage is more pronounced (1.3 percent) for the SBR-35 aircraft.

2.6.4 Fuselage Location-Three-Body Aircraft

The fore and aft location of the fuselage center of gravity relative to the wing elastic axis has an effect on wing weight, and the percent of fuselage length overhang from the wing elastic axis has an effect on fuselage weight. The wing weight effect is caused by changes in wing torsion as the fuselage center of gravity is changed relative to the wing elastic axis. The wing weight penalty, as a function of body CG and wing elastic axis displacement, is shown in Figure 35. The fuselage weight penalty is caused by changes in fuselage bending as the center of the fuselage moves forward or aft of the wing elastic axis. The fuselage weight penalty, as a function of a percent of fuselage length overhang from the wing elastic axis, is shown in Figure 36.

Studies are made to determine the fuselage and wing fore and aft relationship which give the lowest direct operating cost. The study is made by first fixing the location of the center fuselage center of gravity slightly aft of the wing elastic axis to minimize the wing and fuselage weight penalties associated with this fuselage. The outer fuselage are then moved fore and aft to determine the location which gives the lowest direct operating cost.

The results of moving the outer fuselage fore and aft, with the wing in a fixed position, are shown in Figures 37 through 39. As can be seen from these figures, none of the parameters is overly sensitive to fuselage movements. The optimal point for minimizing direct operating cost occurs when the outer fuselage center of gravity is located approximately 7.6 meters (25 ft) aft of the wing elastic axis. This location, therefore, is selected as the fore and aft location of the three-body MB3 aircraft outboard fuselages.

2.7 POINT DESIGN ANALYSIS

The lack of a well defined multibody aircraft data base requires a number of aircraft sizing iterations be performed prior to defining the point design aircraft. In fact, during these sizing iterations it is necessary to perform several preliminary detailed analyses such that correct inputs are made to the initial sizing process. An example of this activity is the development of the weight relationships for the multibody wing. Initial aircraft sizings are conducted using estimated

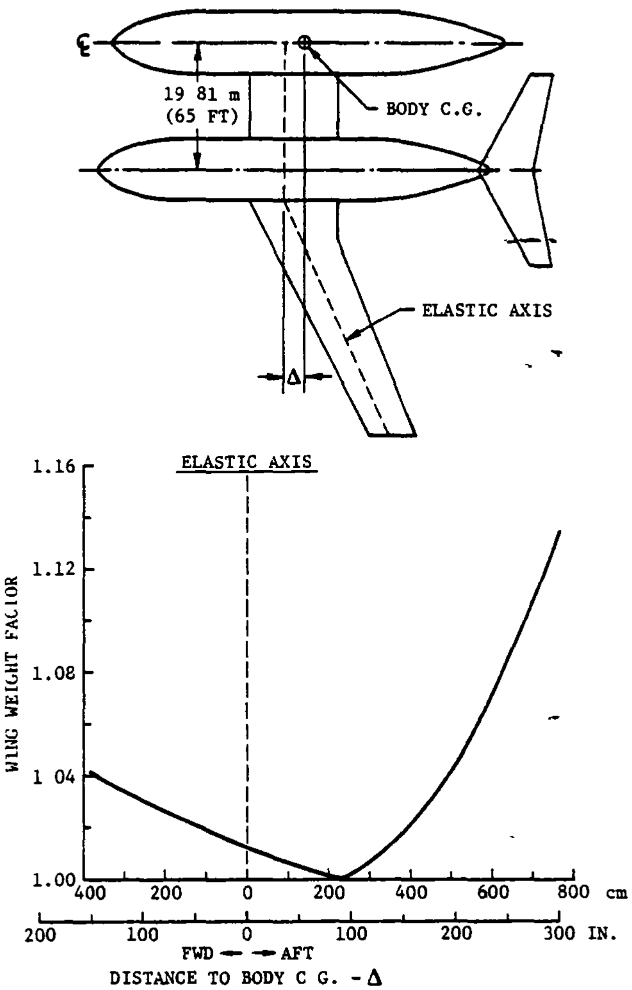

Figure 35. Wing Weight Factors - Unswept Center Section Planform

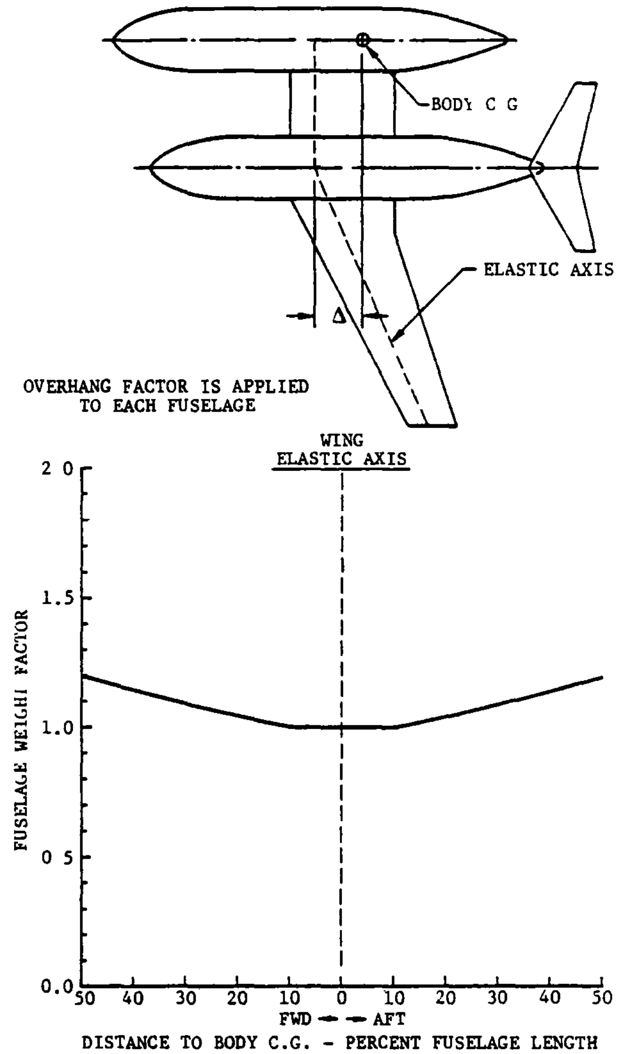

Figure 36. Weight Factor - Fuselage Overhang

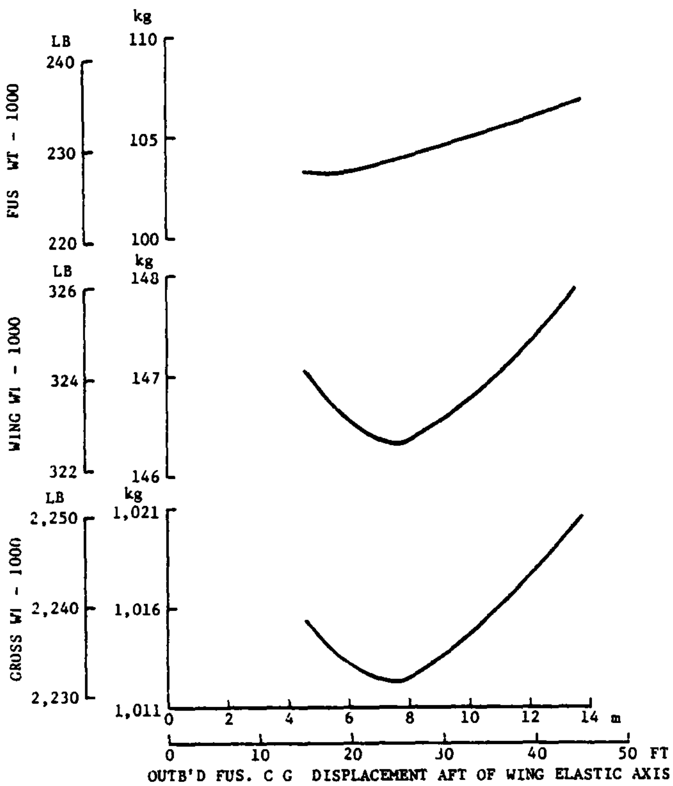

Figure 37. Fuselage Location vs Weight - Parametric Baseline 3 - Unswept Center Wing

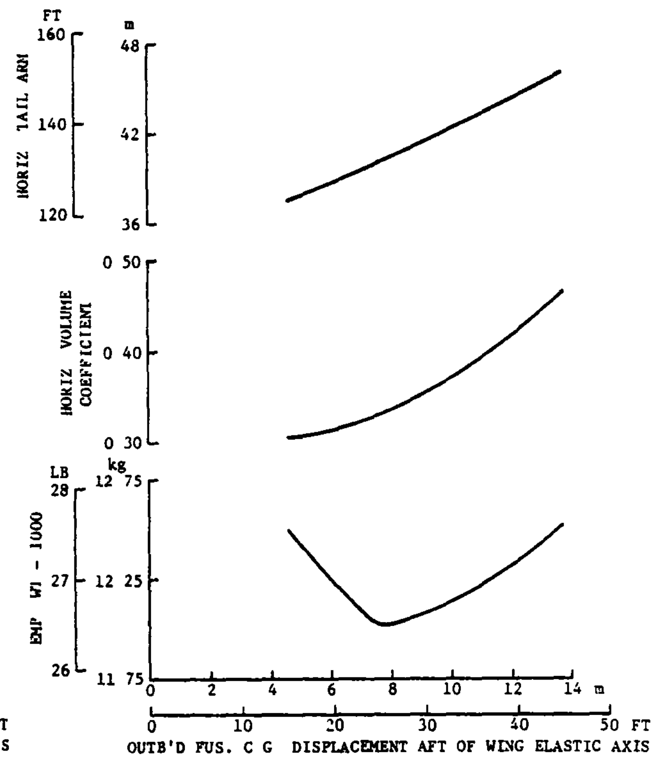

Figure 38. Fuselage Location vs Empennage - Parametric Baseline 3 - Unswept Center Wing

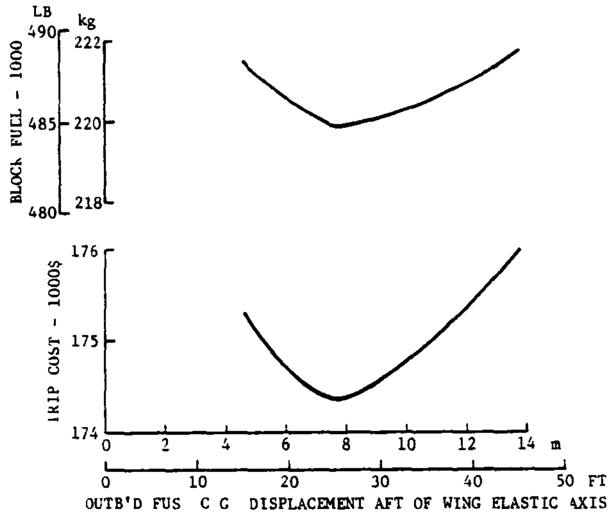

Figure 39. Fuselage Location vs Cost & Fuel - Parametric Baseline 3 - Unswept Center Wing

relationships. Using the aircraft produced by these sizings, detailed wing structural analyses are made. Based upon the results of these analyses, the wing weight relationships are adjusted. Several sizing and analysis iterations are required prior to obtaining agreement between the aircraft sizing analysis and the detailed structural analysis. Wing span efficiencies and stability and control requirements are other examples of items included in this iterative cycle. Using this method of defining the aircraft which are subjected to the point design analysis resulted in no major unknowns being discovered during the analysis. The one exception is wing stiffness as influenced by flutter requirements, which is not a consideration during initial sizing activities.

2.7.1 Aerodynamics

The point design analyses of these configurations are conducted using the methods and assumptions described earlier in Section 2.3.1. The resulting aerodynamic configuration and the estimated performance characteristics are discussed as follows. The impact of the three selected planform shapes on wing thickness is followed by the definition of the span efficiencies used for the point design aircraft. The cruise drag polars which reflect the span efficiencies are then detailed. The takeoff drag polars are then detailed and are followed by the resulting takeoff performance estimates. The resulting cruise performance data are then discussed.

2.7.1.1 Wing Thickness Distribution

The thickness distributions of the four point design aircraft are given in Figure 40. The corresponding local lift coefficients, C1, assuming an elliptic load distribution, are shown in Figure 41. A plot of the resulting physical thickness distribution of the wings is given in Figure 42. The thickness ratio shown is based on total local chord in all cases.

The single body reference aircraft wing has both a leading edge glove and

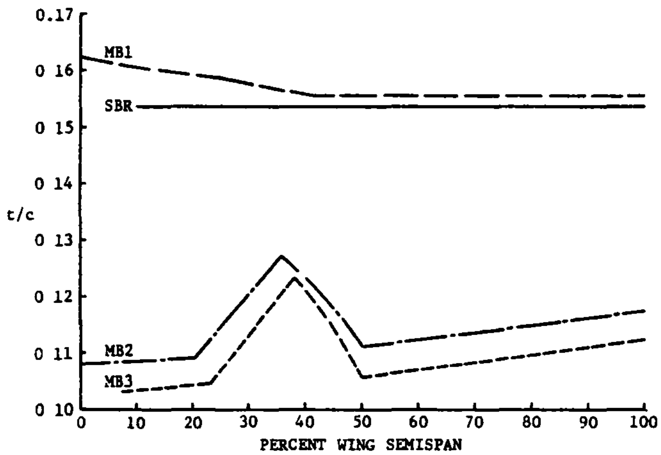

Figure 40. Spanwise Thickness Ratio Variation

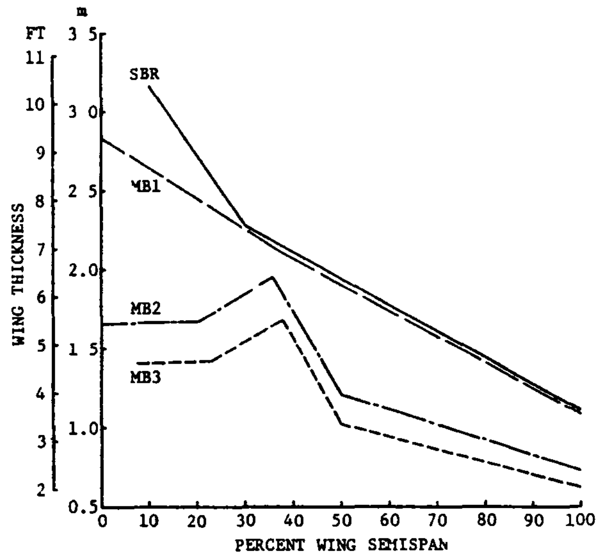

Figure 42. Wing Spanwise Thickness Variation

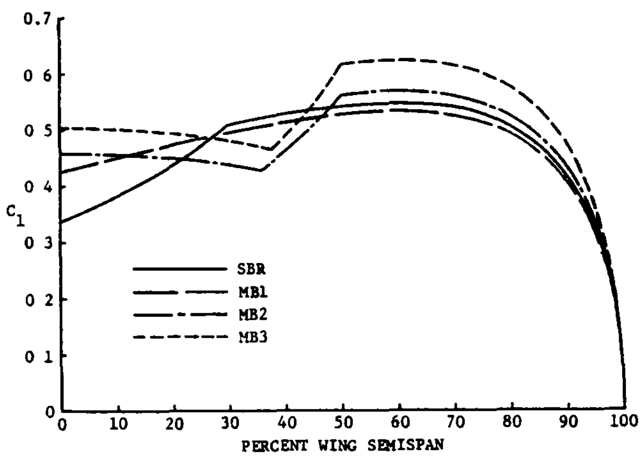

Figure 41. Section Lift Coefficient Distribution

a trailing edge bat; with a constant spanwise t/c this translates into substantial increases in actual wing thickness in the wing root area as shown in Figure 42.

The two-body MB1 aircraft wing has a trapezoidal planform (no localized chord extensions). Based on the procedure defined in Section 2.3.1, the thickness ratio of the inner panel is somewhat greater than on the outer panel because of the reduced local lift coefficient in this area.

Because of the impact of wing sweep angle shown in Section 2.3.1, the single body reference and two-body MB1 aircraft, which have a wing sweep angle of 0.61 rad (35 degrees), have substantially larger thickness ratios than do the two-body MB2 and three-body MB3

aircraft which have a wing sweep angle of 0.44 rad (25 degrees).

The data for the two-body MB2 and three-body MB3 aircraft are very similar since both have unswept center sections, 0.44 rad (25 degrees) sweep on the outer panel, and a wing trailing edge bat extending from the outer body side to the 0.5 semispan location. The relatively lower t/c on the inner panel results from the lack of sweep relief on this panel; the small increase in t/c moving from the centerline toward the inner side of the body is caused by the decrease in local lift coefficient which results if an elliptical loading is provided with a constant chord wing. The substantial increase in thickness at the outer side of the body reflects the relatively low local lift coefficient and the sweep relief of the outer panel. The rapid decrease in t/c moving outward to the mid semispan is a result of the increase in local lift coefficient shown in Figure 41.

The thickness ratio at the wing tip is equal to that defined at the mean aerodynamic chord (MAC) for the trapezoidal wing which incorporates the outer wing panel and which provides the correct lift for the aircraft at its design point. This MAC value is held constant across the entire outer span for the two-body MB1 aircraft. On the two-body MB2 and three-body MB3 aircraft the local lift coefficient at the 0.5 semispan location, where the wing reverts to the nominal trapezoidal planform, becomes quite high and, based on the method of Section 2.3.1, dictates a low local thickness ratio. As a result, the thickness ratio increases from mid semispan to the tip. Although this is a somewhat unorthodox thickness ratio distribution, the wing, as shown in Figure 42, is still substantially thicker at the mid semispan than at the tip. Perhaps a more realistic representation of the wing would include a constant t/c from mid semispan to the tip for these two aircraft. An anticipated reduction in wing weight would be countered to some extent by increased drag rise characteristics in the localized area near this juncture.

2.7.1.2 Span Efficiency and Spanload Distribution

The span efficiency and spanload distributions for the point design aircraft are defined by the process described in Section 2.3.1. The span efficiency factors for the four aircraft are as follows:

Aircraft	Span Efficiency (e)
Single Body (SBR)	0.95000
Two-Body (MB1)	0.91913
Two-Body (MB2)	0.93580

Three-Body (MB3) 0.85720

The spanload distributions for the above aircraft are given in Figures 43 through 46.

2.7.1.3 Cruise Drag Polars

Cruise drag polars for the point design aircraft are given as a function of Mach number and lift coefficient in Figures 47 through 50. A drag buildup for each aircraft is given in Figure

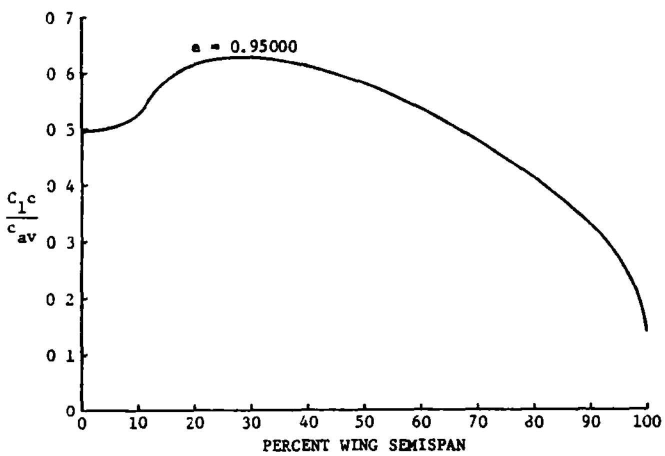

Figure 43. Spanload Distribution - Single Body Aircraft

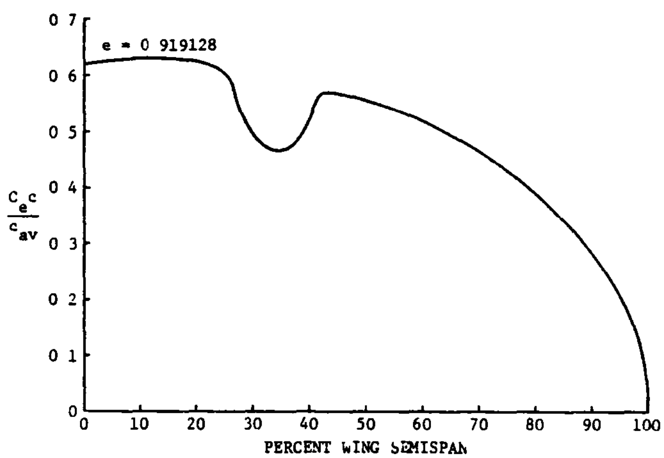

Figure 44. Spanload Distribution - Two-Body MB1 Aircraft

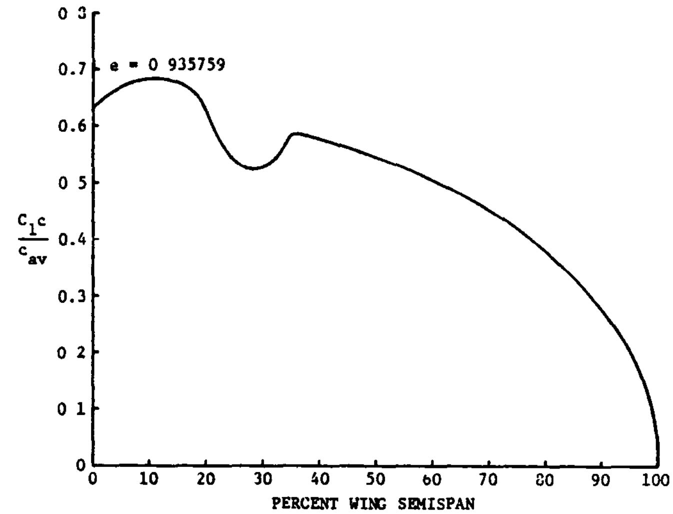

Figure 45. Spanload Distribution - Two-Body MB2 Aircraft

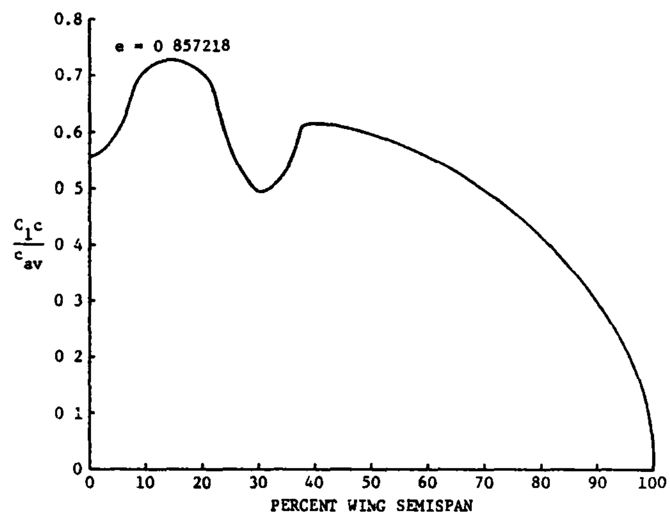

Figure 46. Spanload Distribution - Three-Body MB3 Aircraft

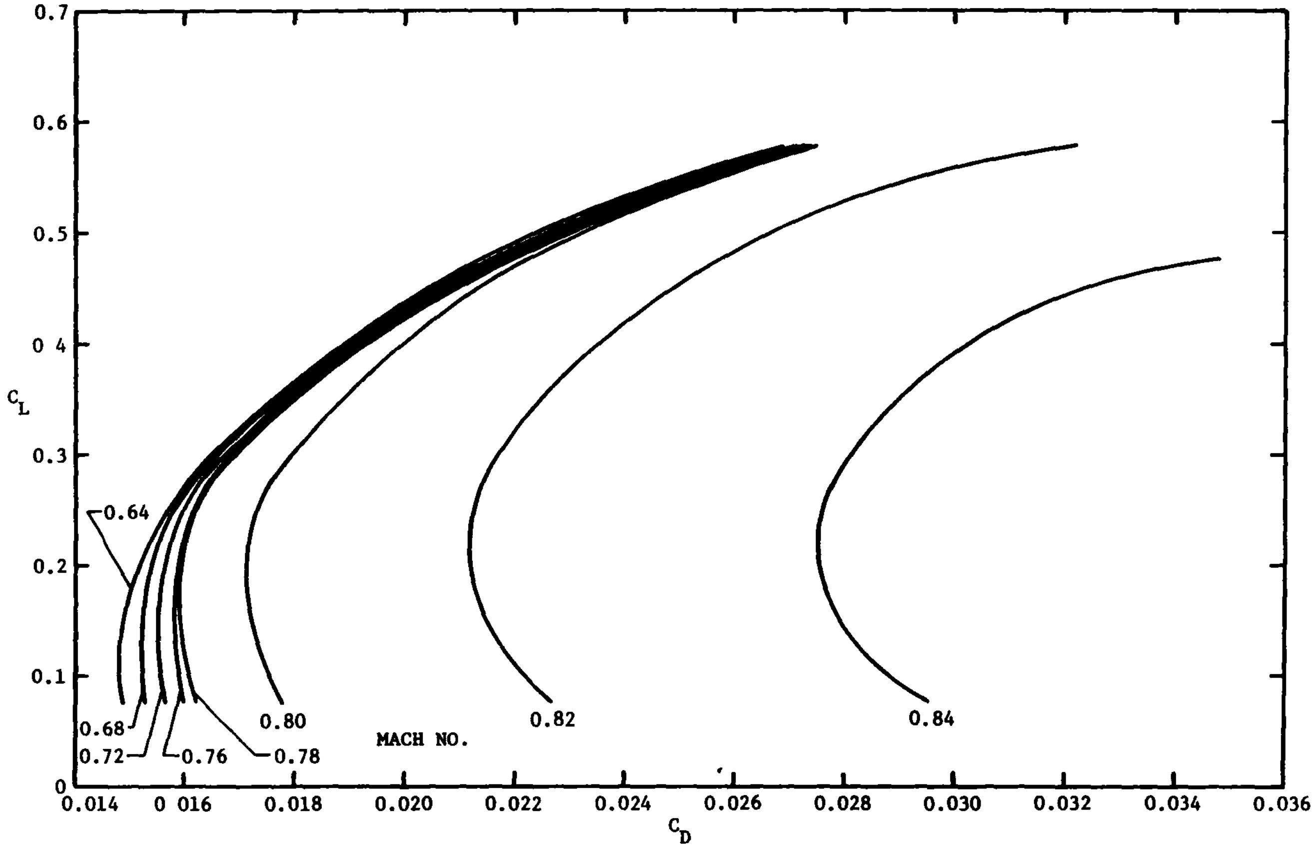

Figure 47. Cruise Drag Polar - Two-Body MB1 Aircraft

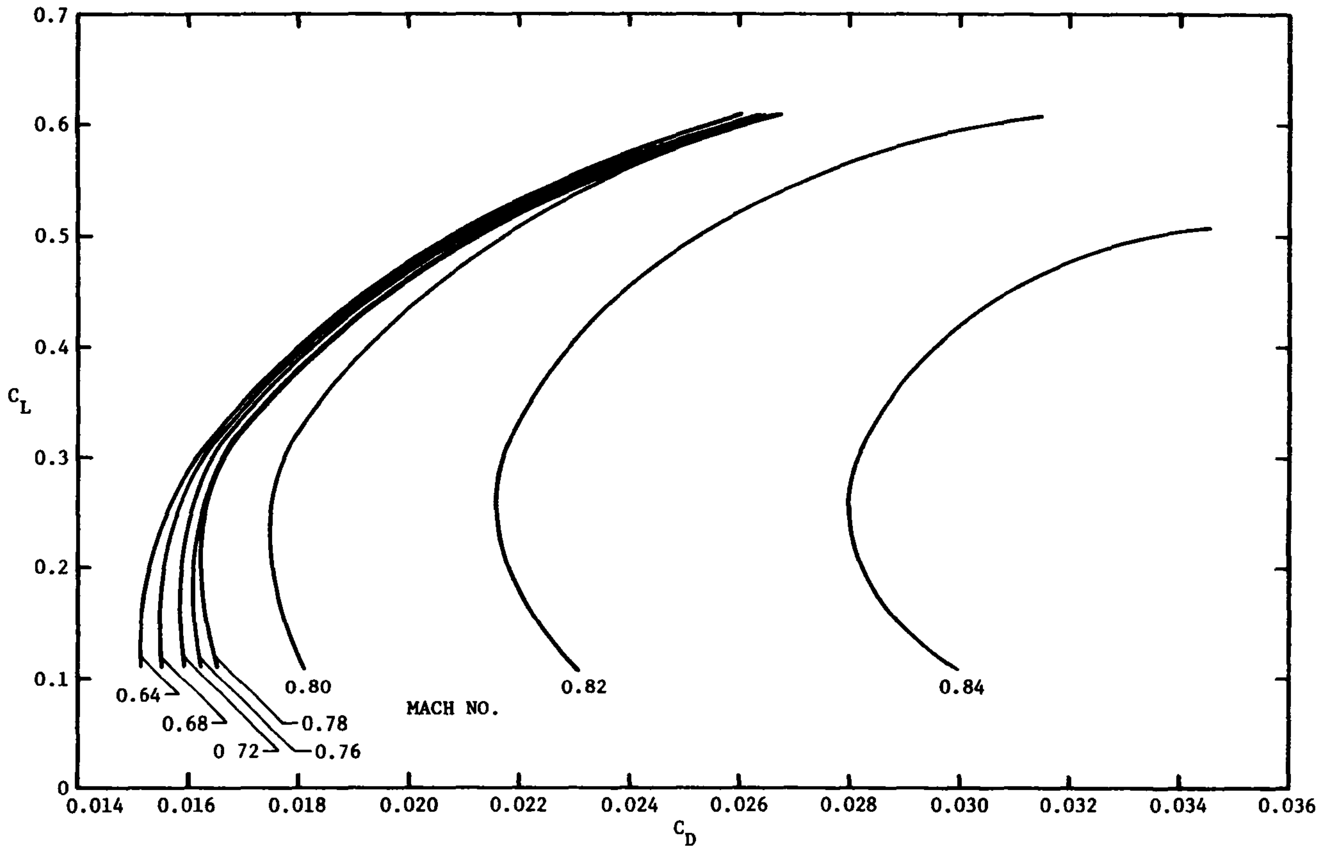

Figure 48. Cruise Drag Polar - Two-Body MB2 Aircraft

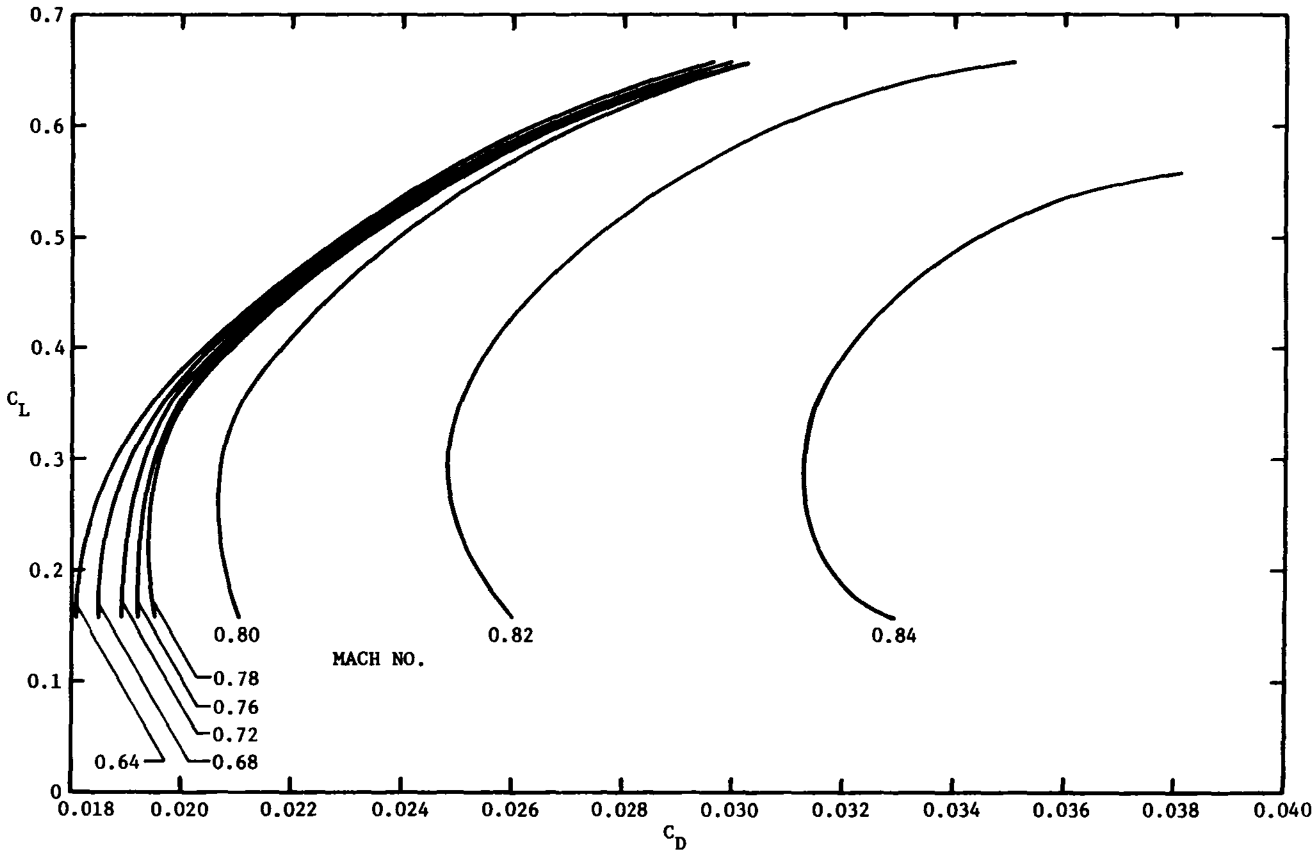

Figure 49. Cruise Drag Polar - Three-Body MB3 Aircraft

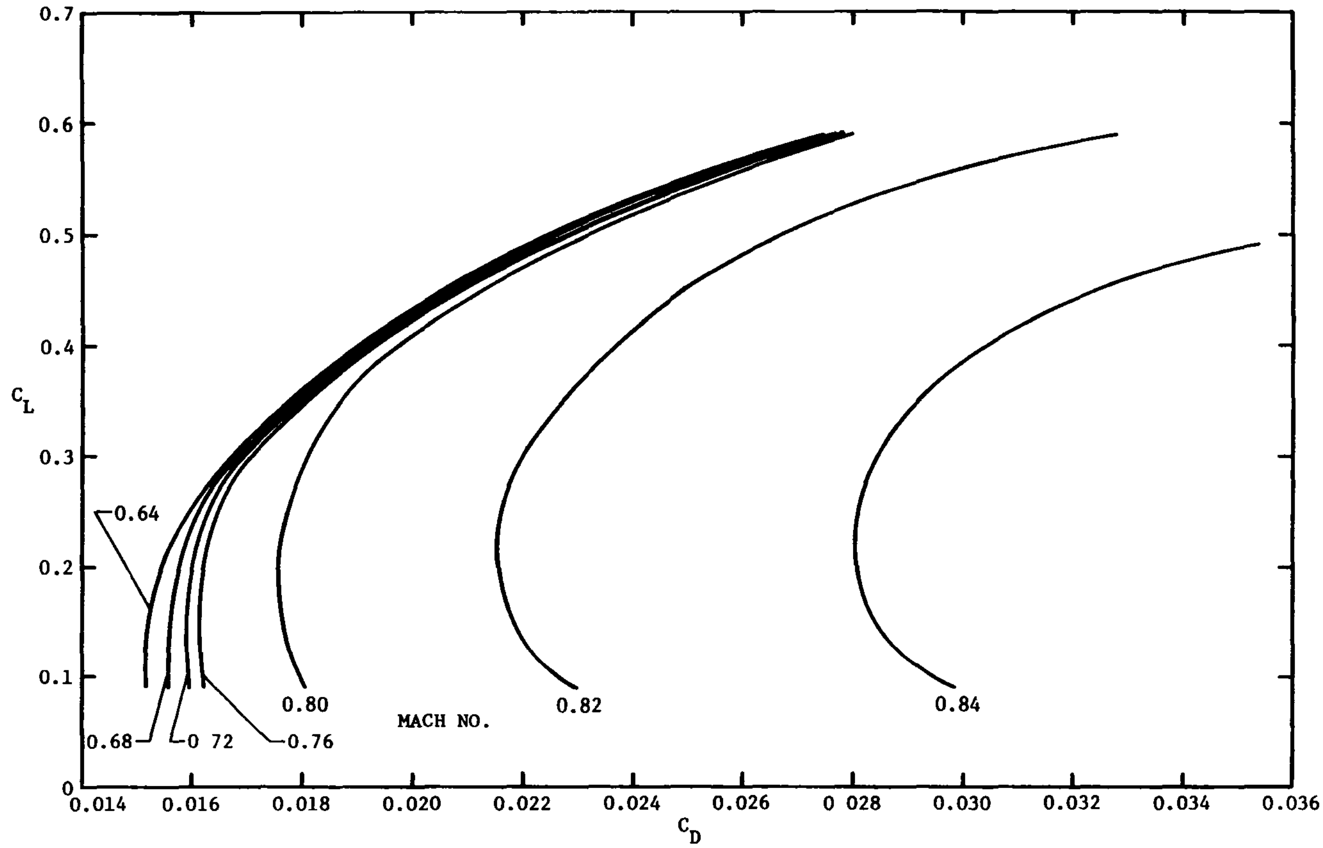

Figure 50. Cruise Drag Polar - Single Body Reference SBR Aircraft

51. These data are referenced to the basic trapezoidal planform area of the wing.

An overall comparison of the drag characteristics of the point design aircraft fuselages is shown in Figure 52. One item of particular interest is the additional drag of the multibody fuselages. This figure provides a comparison of the equivalent parasite drag, D/q ($=C_D S$), of the fuselages for each of the point design aircraft.

The data show approximately 10 and 30 percent drag increases for two-body and three-body aircraft fuselages, respectively, relative to the single body reference aircraft. This fuselage drag penalty is offset by the removal of gear pods on the multibody configurations. The single body reference aircraft, as configured, requires fuselage mounted pods to house the gear while the multibodies have sufficient space for gear storage within the fuselages. The D/q of the gear pod on the single body reference aircraft is $1.06 m^2$ ($11.45 ft^2$) which is about twice the additional drag attributed to the fuselage for the two-body MB1 and MB2 aircraft and slightly less than the additional fuselage drag of the three-body MB3 aircraft. Since the single body reference aircraft has external gear pods, while multibody aircraft do not require these pods, the additional aircraft fuselage drag does not result in a profile drag penalty relative to the single body reference aircraft, except in the case of the three-body MB3 aircraft.

A review of the general arrangement of the three-body MB3 aircraft, presented previously in Figure 27, shows that the bodies are quite close. This spacing is required in order to operate from 45.7 m (150 ft) wide runways. Three counts of drag have been added to the fuselage drag to account for the anticipated interference between fuselages.

The wing drag reductions of the multibody aircraft relative to the single body reference aircraft primarily reflect the wing wetted area reductions resulting from the wing area masked by the additional bodies.

The three-body MB3 aircraft has significantly more empennage drag than the other aircraft. This is largely because structural considerations dictate the wing-fuselage placement. As a result, this aircraft cannot be adjusted for a minimum tail size. Hence, a larger tail size is necessary to provide the required stability levels.

The induced drag characteristics reflect the lower span efficiency factors of the multibody aircraft and the counterbalancing influence of the

ITEM \ AIRCRAFT	SINGLE BODY SBR	TWO-BODY MB1	TWO-BODY MB2	THREE-BODY MB3
PROFILE DRAG (COUNTS)				
WING	60	55	53	50
FUSELAGE	33	38	40	52
EMPENNAGE	13	14	15	22
PYLONS	1	1	1	1
MAIN GEAR FAIRINGS	7	0	0	0
INTERFERENCE	6	11	11	15
ROUGHNESS	5	5	5	6
TRIM	4	4	4	4
TOTAL	129	128	129	150
TOTAL DRAG (COUNTS)				
PROFILE	129	128	129	150
INDUCED	85	81	77	86
COMPRESSIBILITY	10	10	10	10
MISCELLANEOUS	4	4	4	4
TOTAL	228	223	220	250
REFERENCE DATA				
CRUISE C_L	0.490	0.477	0.509	0.558
CRUISE L/D	21.49	21.39	23.14	22.32
REFERENCE WING				
• ASPECT RATIO	9.5	9.7	11.5	13.45
• SPAN EFFICIENCY	0.95	0.919	0.936	0.857
• AREA - m^2	1520.0	1454.3	1361.6	1261.0
• AREA - FT^2	16,361	15,654	14,656	13,573

Figure 51. Drag Summary

	POINT DESIGN AIRCRAFT			
	SINGLE BODY REFERENCE SBR	TWO-BODY		THREE -BODY MB3
		MB1	MB2	
D/q - FUSELAGE - m^2	5.02	5.52	5.45	6.56
D/q - FUSELAGE - FT^2	53.99	59.44	58.62	70.58
D/q - FUSELAGE AND GEAR POD - m^2	6.08	5.53	5.45	6.56
D/q - FUSELAGE AND GEAR POD - FT^2	65.44	59.49	58.62	70.58

Figure 52. Drag Summary - Fuselage - Point Design Aircraft

higher aspect ratios of these aircraft. The lift coefficient also varies between aircraft because of the necessity to adjust wing loading to achieve the specified field length with cruise matched engines.

As shown in Figure 51, the multibody aircraft generally have L/D's that are comparable to or better than that of the single body reference aircraft.

Figure 51 shows that the two-body and single body reference aircraft have essentially the same profile drag levels, while the profile drag of the three-body aircraft is considerably greater. The L/D improvements obtained by the multibody aircraft are a result of the higher aspect ratios and lower induced drag which are attributable to the structural advantages of the multibody aircraft.

2.7.1.4 Takeoff Drag Polars

The takeoff drag polars are shown in Figures 53 through 56. These polars are shown both in free air and in ground effect. Maximum flap deflection is used to allow the aircraft to meet the required second segment climb gradient of 0.03 at design gross weight. Pertinent data for the four point design aircraft in the climb-out configuration are shown in Figure 57.

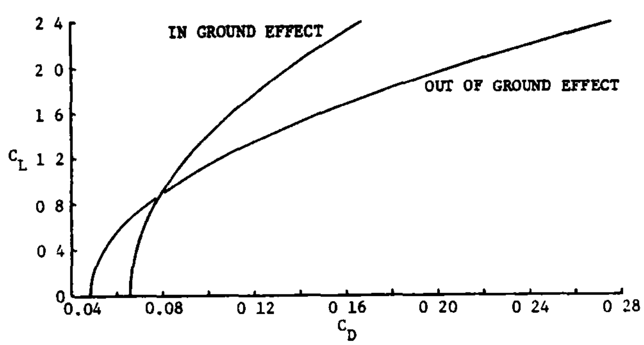

Figure 53. Takeoff Drag Polar - Single Body Reference SBR Aircraft

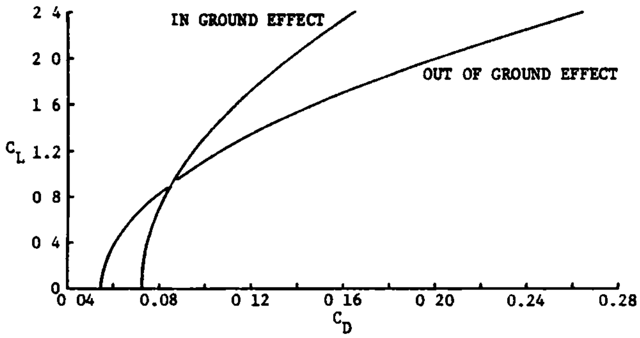

Figure 54. Takeoff Drag Polar - Two-Body MB1 Aircraft

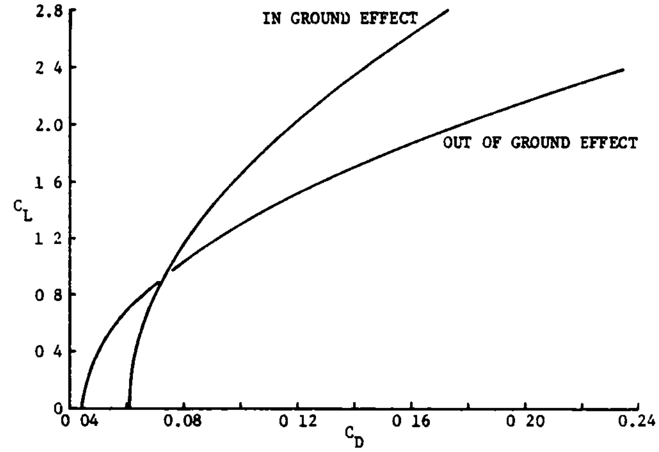

Figure 55. Takeoff Drag Polar - Two-Body MB2 Aircraft

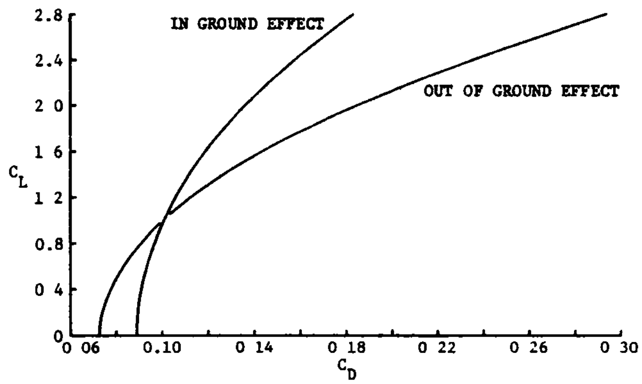

Figure 56. Takeoff Drag Polar - Three-Body MB3 Aircraft

AIRCRAFT	C_L	C_D	δ_f	$C_{L_{MAX}}$
SINGLE BODY REFERENCE SBR	1.696	0.1644	26.15	2.44
TWO-BODY MB1	1.678	0.1632	31.13	2.42
TWO-BODY MB2	1.909	0.1714	21.37	2.75
THREE-BODY MB3	1.947	0.1863	36.92	2.80

Figure 57. Climb-Out Configuration Data - Point Design Aircraft

2.7.1.5 Takeoff Distance

The estimated takeoff distances for the four point design aircraft are given as a function of gross weight in Figure 58. All aircraft are sized to provide a takeoff distance of 3200.4 m (10,500 ft) at their respective design gross weight. At 50 percent of design gross weight, the variation between the aircraft in takeoff distance is less than 45.7 m (150 ft).

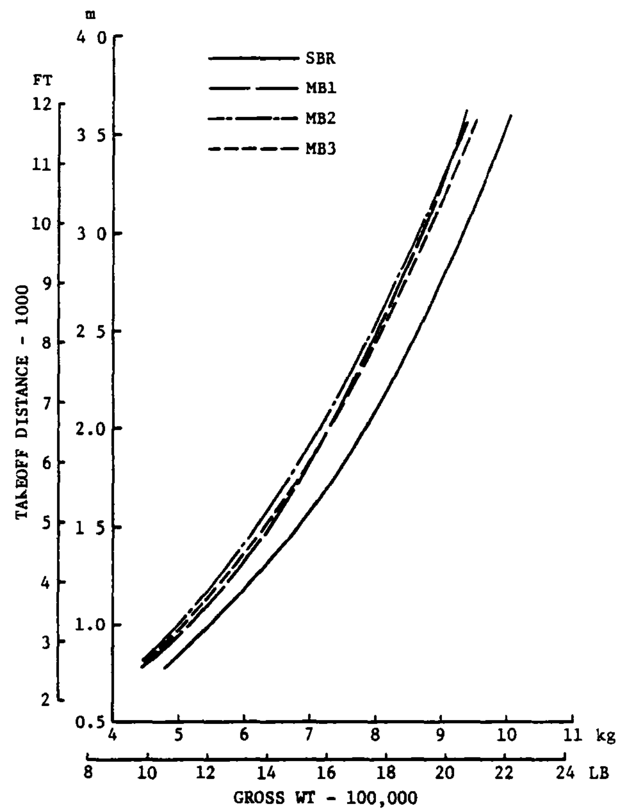

Figure 58. Takeoff Distance vs Gross Weight

2.7.1.6 Mission Performance

Payload-range and block fuel data for the point design aircraft are shown in Figures 59 through 62. Since all aircraft have the same design mission, these curves are very similar. All of the aircraft have large wings which provide more fuel volume capacity than is required for the design mission. The fuel tankage is limited to an amount which exceeds the design mission fuel requirement by one percent providing a slight design margin and a minimum fuel system weight. As a result, the payload-range diagram does not include the usual "Y" point. Increased range cannot be obtained by replacing payload with fuel at the design gross weight but can be obtained by a reduction in payload. The range capability of these aircraft can be increased

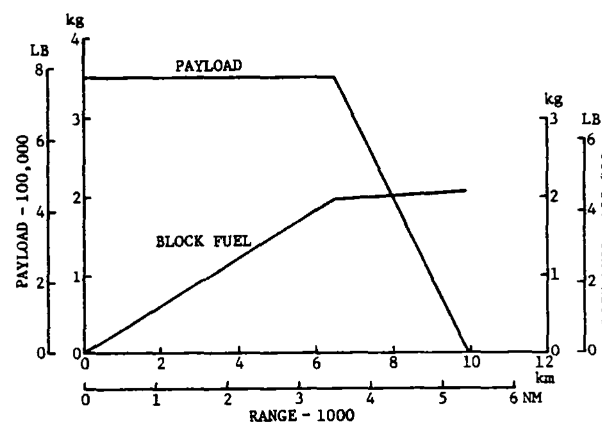

Figure 59. Payload-Range-Block Fuel Comparison - Single Body Reference SBR Aircraft

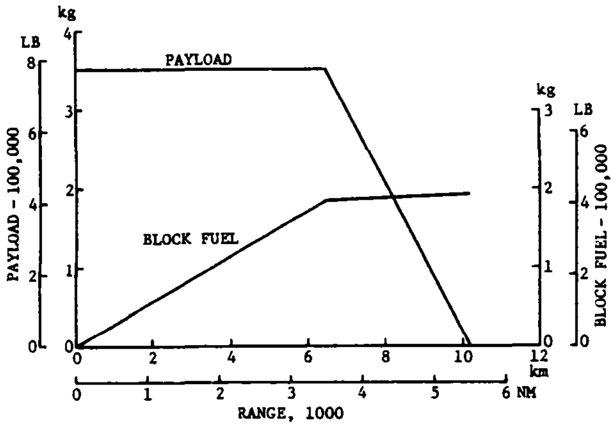

Figure 60. Payload-Range-Block Fuel Comparison - Two-Body MB1 Aircraft

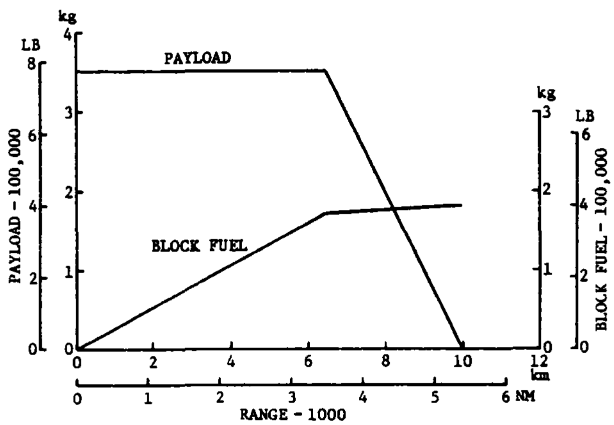

Figure 61. Payload-Range-Block Fuel Comparison - Two-Body MB2 Aircraft

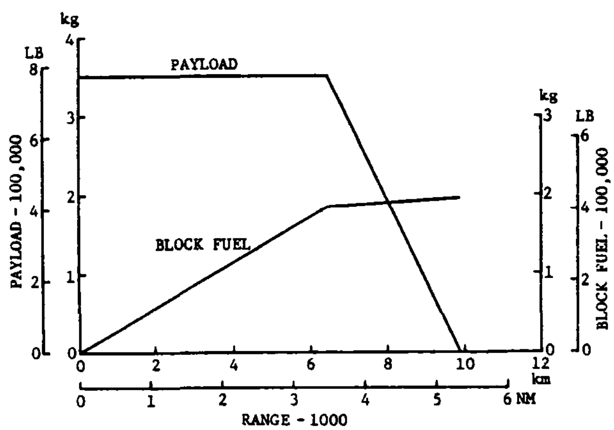

Figure 62. Payload-Range-Block Fuel Comparison - Three-Body MB3 Aircraft

significantly, without a significant increase in aircraft size, by providing additional fuel tanks and increased fuel system weight. The ferry range capability of these aircraft varies from 9,895.2 to 10,206.4 km (5343 to 5511 n.m.).

2.7.2 Stability and Control

The stability and control analyses performed for each point design aircraft consists of a detailed estimation of all the stability and control derivatives, calculations of the static and dynamic stability characteristics, evaluation of the control capabilities, and comparison with present and proposed specifications, including a flying qualities discussion.

The stability and control derivatives are estimated using results from the Digital Datcom computer program. In addition, revisions to the Digital Datcom output or handbook methods are used where the Digital Datcom methods are inadequate for this type of configuration.

Initial static stability characteristics are calculated in the Generalized Aircraft Sizing and Performance program. These results are checked and expanded using more detailed calculation methods reflecting the final configuration.

The dynamic stability characteristics are calculated using two, three-degree-of-freedom analysis computer programs. Roots, modal parameters, and aircraft response to control inputs are calculated in these programs.

The control capabilities of the point design aircraft are analyzed in detail. Study of the roll control capability resulted in a recommendation for a more practical specification for large aircraft roll control capability. The yaw and pitch control effectiveness are shown to be sufficient. Control capability is also discussed in the section on specification and flying qualities.

The flying qualities of the point design aircraft are compared to the MIL-F-8785B(ASG) Military Specification, "Flying Qualities of Piloted Aircraft," Reference 7. Lockheed's experience in applying these specifications to the flying qualities of large aircraft, noted in Reference 8, indicates that these specifications have limitations in their application to large aircraft. Therefore, this comparison is used as a guideline only. Possible problem areas in the flying qualities of multibody aircraft are identified, specifically roll maneuvers and accelerations at the pilot station during maneuvers.

The problem of defining acceptable flying qualities for a very large aircraft with the pilot located far from the roll axis, and with limited control capability is very complex. A flight simulation study of the problem was recognized as being invaluable. Lockheed's efforts were expanded to provide the necessary stability derivatives and physical descriptions required for studying the point design aircraft on NASA's moving base simulator. Appendix E is a compilation of these data.

2.7.2.1 Stability and Control Derivatives

Detailed estimates of the stability and control derivatives are prepared for the point design aircraft. Figures 63 through 66 list these derivatives for two flight conditions. The majority of the calculations are made with the Digital Datcom computer program. However, revisions to the results are made to reflect the peculiarities of the multibody aircraft. The remaining derivatives are calculated using Datcom or other handbook methods. In addition, adjustment factors based on C-5 flight test data are applied to the estimates of lateral control effectiveness.

The largest corrections encountered in the estimation of these derivatives

UNITS 1/RAD	LANDING CASE	CRUISE CASE
C_{L_α}	5.04	5 04
$C_{M_\alpha}^*$	-0 252	-0 252
C_{M_α}	-5 56	-7 92
C_{M_q}	-25 5	-29 7
$C_{M_{\delta_e}}$	-0 925	-0 764
$C_{L_{\delta_e}}$	0 216	0 179
$C_{M_{i_H}}$	-2 42	-2.77
$C_{L_{i_H}}$	0 566	0 646
C_{n_β}	0 0981	0 103
C_{l_β}	-0.139	-0 00981
C_{y_β}	-0.407	-0.425
C_{n_p}	-0.0526	-0 0178
C_{l_p}	-0 473	-0 578
C_{y_p}	0 164	0 0920
C_{n_r}	-0.123	-0.127
C_{l_r}	0.120	0.0647
C_{y_r}	0	0
$C_{n_{\delta_r}}$	-0.0558	-0 0404
$C_{l_{\delta_r}}$	0 00463	0 00618
$C_{y_{\delta_r}}$	0 123	0 0887
$C_{n_{\delta_a}}$	-0.0226	--
$C_{l_{\delta_a}}$	-0 161	--

*(5% EFFECTIVE S M.)

S REF = 1617 7 m^2 (17,413 FT^2)

b REF = 120.17 m (394 25 FT)

$\bar{c}$ REF = 14.883 m (48 829 FT)

CG = 35% $\bar{c}$

Figure 63. Stability and Control Derivatives - Single Body Reference SBR Aircraft

UNITS 1/RAD	LANDING CASE	CRUISE CASE
C_{L_α}	5 10	5 10
$C_{M_\alpha}^*$	-0 255	-0 255
C_{M_α}	-3 64	-5 03
C_{M_q}	-20 67	-23 5
$C_{M_{\delta_e}}$	-0 785	-0 619
$C_{L_{\delta_e}}$	0 202	-0 160
$C_{M_{i_H}}$	-1 94	-2 14
$C_{L_{i_H}}$	0 516	0 559
C_{n_β}	0 0899	0 0991
C_{l_β}	-0 143	-0 00144
C_{y_β}	-0.567	-0 566
C_{n_p}	-0 0610	-0.0233
C_{l_p}	-0 504	-0 625
C_{y_p}	0.186	0 108
C_{n_r}	-0.0881	-0 0934
C_{l_r}	0 122	0 0579
C_{y_r}	0	0
$C_{n_{\delta_r}}$	-0.0461	-0 0340
$C_{l_{\delta_r}}$	0 00509	0.00614
$C_{y_{\delta_r}}$	0.129	0 0951
$C_{n_{\delta_a}}$	-0.0141	--
$C_{l_{\delta_a}}$	-0 125	--

*(5% EFFECTIVE S M.)

S REF = 1,454 3 m^2 (15,654 FT^2)

b REF = 118 77 m (389.67 FT)

$\bar{c}$ REF = 12 994 m (42 631 FT)

CG = 33% $\bar{c}$

Figure 64. Stability and Control Derivatives - Two-Body MB1 Aircraft

UNITS 1/RAD	LANDING CASE	CRUISE CASE
C_{L_α}	5 21	5.21
C_{M_α} *	-0.261	-0 261
C_{M_α}	-4 90	-7 47
C_{M_q}	-16 4	-19 5
$C_{M_{\delta_e}}$	-0 788	-0 655
$C_{L_{\delta_e}}$	0 206	0 174
$C_{M_{i_H}}$	-1 83	-2 07
$C_{L_{i_H}}$	0 501	0 559
C_{n_β}	0 0734	0 0818
C_{l_β}	-0 131	-0 00118
C_{y_β}	-0 589	-0 545
C_{n_p}	-0 0808	-0 0480
C_{l_p}	-0 642	-0.793
C_{y_p}	-0 00596	0 0303
C_{n_r}	-0 0793	-0 0804
C_{l_r}	0 204	0 225
C_{y_r}	0	0
$C_{n_{\delta_r}}$	-0 0423	-0 0258
$C_{l_{\delta_r}}$	0 00479	0 00473
$C_{y_{\delta_r}}$	0.128	0 0779
$C_{n_{\delta_a}}$	-0 00377	—
$C_{l_{\delta_a}}$	-0.142	—

*(5% EFFECTIVE S M.)

S REF = 1,457 6 m^2 (15,689 FT^2)

b REF = 125 1 m (410.5 FT)

$\bar{c}$ REF = 12 62 m (41 39 FT)

CG = 34% c

Figure 65. Stability and Control Derivatives - Two-Body MB2 Aircraft

UNITS 1/RAD	LANDING CASE	CRUISE CASE
C_{L_α}	5.33	5 33
C_{M_α} *	-0 267	-0 267
C_{M_α}	-7 32	-11 2
C_{M_q}	-23.4	-27 9
$C_{M_{\delta_e}}$	-1 28	-1 06
$C_{L_{\delta_e}}$	0.353	0 293
$C_{M_{i_H}}$	-2 89	-3 32
$C_{L_{i_H}}$	0 840	0 974
C_{n_β}	0.0982	0 106
C_{l_β}	-0 140	-0 0104
C_{y_β}	-0 942	-0.905
C_{n_p}	-0.0805	-0 0470
C_{l_p}	-0 647	-0 847
C_{y_p}	-0.0209	0 0225
C_{n_r}	-0.0736	-0 0728
C_{l_r}	0.208	0 232
C_{y_r}	0	0
$C_{n_{\delta_r}}$	-0 0511	-0.0312
$C_{l_{\delta_r}}$	0 0108	0 00877
$C_{y_{\delta_r}}$	0 204	0 125
$C_{n_{\delta_a}}$	-0.00365	—
$C_{l_{\delta_a}}$	-0.139	—

*(5% EFFECTIVE S.M.)

S REF = 1,352 2 m^2 (14,555 FT^2)

b REF = 130 23 m (427 27 FT)

$\bar{c}$ REF = 11 24 m (36.89 FT)

CG = 31% $\bar{c}$

Figure 66. Stability and Control Derivatives - Three-Body MB3 Aircraft

involve the wing-body interference effects and the effect of the body offset from the aircraft centerline. The wing-body interference effects for multibody aircraft are based on superimposing the effects for single body aircraft. Simple equations are derived for the effect of body and tail offset on the derivative components, but further study is necessary to more exactly define these effects. Suggestions for future work in these areas are discussed in the Research and Technology Recommendations section.

Two flight conditions are chosen to represent the cases of most interest in the operational flight envelope of the aircraft. These conditions are landing approach (1.3 V_S at sea level) and cruise (M = 0.8 at 10,668.0 m (35,000 ft). The stability level shown for all aircraft represents an effective five percent static margin (dC_m/dC_L = -0.05).

2.7.2.2 Static Stability

The longitudinal static stability parameters are initially calculated in the tail sizing section which is run as a subroutine to the GASP Program. These results are checked for validity during the point design phase of the study. The tail sizing criteria are discussed in Section 2.3.3. Longitudinal static stability as discussed here refers to dC_m/dC_L, the change in pitching moment with a lift change.

Static margin is defined as the distance from the total aircraft center of gravity to the total aircraft aerodynamic center in percent of the mean aerodynamic chord, positive if the center of gravity is forward. A positive effective static margin is necessary for a statically stable aircraft. Conventional aircraft designs usually have a minimum positive three percent static margin (i.e. dC_m/dC_L = -0.03).

The multibody aircraft incorporate the concept of reduced longitudinal static stability to decrease horizontal tail size, with an augmentation system increasing the effective stability to give good flying qualities. As discussed in the ground rules, the horizontal is sized for negative eight percent static margin (representing the maximum instability that is still controllable). All of the point design aircraft meet this minimum static margin limit of negative eight percent. With the augmentation system operational, the effective stability is at least five percent static margin.

Note that the tail is sized for negative eight percent static margin at landing approach conditions. The assumption is made that for the high speed condition, the aircraft is less

unstable. Flexibility effects play a much more important role in this aspect than estimates which could be made for Mach effects on a rigid wing. As previously mentioned, a detailed structural design is required for a flexible analysis and that is beyond the scope of this study. Static stability is therefore assumed to be at the design condition (negative eight percent static margin) for the cruise case. This assumption is plausible - the C-5A conforms to it. Assuming a 5 percent static margin as the base, going to the multibody design condition of minus 8 percent reduces the horizontal tail by the following percentages: single body reference 27 percent; two-body MB1 25 percent; two-body MB2 25 percent; three-body MB3 17 percent.

Directional static stability is also initially set in the GASP program and checked in the point design. The tail sizing program sizes the vertical tail for engine out trim or minimum directional stability, whichever is more critical. Based on Lockheed's large transport aircraft experience, a minimum c_{n_β} of 0.086 per rad (0.0015 per degree) is defined as sufficient to give good flying qualities. For the point design aircraft, the minimum directional stability is the critical sizing criteria. Figure 67 shows the requirement and the detailed point design estimates of the directional stability. All aircraft appear to have sufficient directional stability even though the two-body MB2 aircraft is slightly under the preliminary goal level.

AIRCRAFT	C_{n_β} (1/DEG)
SINGLE BODY SBR	0.0017
TWO-BODY MB1	0.0016
TWO-BODY MB2	0.0013
THREE-BODY MB3	0.0017

- PRELIMINARY GOAL 0.0015
- LANDING APPROACH CASE

Figure 67. Directional Stability - Point Design Aircraft

In summary, all of the point design aircraft have adequate static stability characteristics.

2.7.2.3 Dynamic Stability

Dynamic stability modal parameters and aircraft response to control inputs are computed by three-degree-of-freedom analysis computer programs for the longitudinal and the lateral-directional motions. These two computer programs use linear aerodynamic models.

Figures 68 through 71 present the dynamic stability modal parameters for the point design aircraft. Note that the longitudinal parameters are computed for an effective five percent static margin, which is the normal aug-

LONGITUDINAL	LANDING	CRUISE
PHUGOID (5% EFFECTIVE SM)		
DAMPING RATIO	0 367	0 0498
NATURAL FREQUENCY (RAD/SEC)	0 0817	0.0364
PERIOD (SEC)	82 7	173.0
SHORT PERIOD (5% EFFECTIVE SM)		
DAMPING RATIO	(CRITICALLY DAMPED)	0 909
NATURAL FREQUENCY (RAD/SEC)		0.585
PERIOD (SEC)		25 7
TIME CONSTANT (SEC)	2.45	2 15
LATERAL - DIRECTIONAL		
ROLL MODE		
TIME CONSTANT (SEC)	0 910	0 781
SPIRAL MODE		
T DOUBLE (SEC)	74 8*	189 0
DUTCH ROLL		
DAMPING RATIO	0 111	0.120
NATURAL FREQUENCY (RAD/SEC)	0 412	0.605
FREQUENCY - DAMPING PRODUCT	0.0457	0.0726
PERIOD (SEC)	15 3	10 5
LONGITUDINAL		
PITCH SAS INOPERATIVE		
AFT CG (-8% SM)		
T DOUBLE (SEC)	9 84	8.63

*TIME TO HALF AMPLITUDE SINCE STABLE

Figure 68. Modal Parameters - Single Body Reference SBR Aircraft

LONGITUDINAL	LANDING	CRUISE
PHUGOID (5% EFFECTIVE SM)		
DAMPING RATIO	0 284	0.0424
NATURAL FREQUENCY (RAD/SEC)	0 0946	0 0407
PERIOD (SEC)	69 3	155 0
SHORT PERIOD (5% EFFECTIVE SM)		
DAMPING RATIO	0 957	0.826
NATURAL FREQUENCY (RAD/SEC)	0 558	0 714
PERIOD (SEC)	38 7	15 6
TIME CONSTANT (SEC)	1 97	1.58
LATERAL - DIRECTIONAL		
ROLL MODE		
TIME CONSTANT (SEC)	1.97	1 90
SPIRAL MODE		
T DOUBLE (SEC)	277 6*	189 0
DUTCH ROLL		
DAMPING RATIO	0 0255	0 106
NATURAL FREQUENCY (RAD/SEC)	0 334	0 498
FREQUENCY - DAMPING PRODUCT	0 0085	0 0528
PERIOD (SEC)	18 8	12 7
LONGITUDINAL		
PITCH SAS INOPERATIVE		
AFT CG (-8% SM)		
T DOUBLE (SEC)	7 32	4 93

*TIME TO HALF AMPLITUDE SINCE STABLE

Figure 69. Modal Parameters - Two-Body MB1 Aircraft

LONGITUDINAL	LANDING	CRUISE
PHUGOID (5% EFFECTIVE SM)		
DAMPING RATIO	0 271	0.0366
NATURAL FREQUENCY (RAD/SEC)	0.112	0.0434
PERIOD (SEC)	58 2	145 0
SHORT PERIOD (5% EFFECTIVE SM)		
DAMPING RATIO	0.970	0 841
NATURAL FREQUENCY (RAD/SEC)	0 524	0 753
PERIOD (SEC)	49.2	15 4
TIME CONSTANT (SEC)	1 97	1.58
LATERAL - DIRECTIONAL		
ROLL MODE		
TIME CONSTANT (SEC)	1.58	1 32
SPIRAL MODE		
T DOUBLE (SEC)	94 3	61 5
DUTCH ROLL		
DAMPING RATIO	0 0902	0 120
NATURAL FREQUENCY (RAD/SEC)	0 312	0 489
FREQUENCY - DAMPING PRODUCT	0.0281	0 0587
PERIOD (SEC)	20.2	13 0
LONGITUDINAL		
PITCH SAS INOPERATIVE		
AFT CG (-8% SM)		
T DOUBLE (SEC)	6.26	3 25

Figure 70. Modal Parameters - Two-Body MB2 Aircraft

LONGITUDINAL	LANDING	CRUISE
PHUGOID (5% EFFECTIVE SM)		
DAMPING RATIO	0.343	0 0517
NATURAL FREQUENCY (RAD/SEC)	0.101	0.0421
PERIOD (SEC)	66 2	149 0
SHORT PERIOD (5% EFFECTIVE SM)		
DAMPING RATIO	(CRITICALLY DAMPED)	(CRITICALLY DAMPED)
NATURAL FREQUENCY (RAD/SEC)		
PERIOD (SEC)		
TIME CONSTANT (SEC)	2.46	1.24
LATERAL - DIRECTIONAL		
ROLL MODE		
TIME CONSTANT (SEC)	1 36	1 11
SPIRAL MODE		
T DOUBLE (SEC)	52 7	65 8
DUTCH ROLL		
DAMPING RATIO	0 134	0 121
NATURAL FREQUENCY (RAD/SEC)	0 384	0 597
FREQUENCY - DAMPING PRODUCT	0 0515	0 0722
PERIOD (SEC)	16.5	10 6
LONGITUDINAL		
PITCH SAS INOPERATIVE		
AFT CG (-8% SM)		
T DOUBLE (SEC)	7 11	4 36

Figure 71. Modal Parameters - Three-Body MB3 Aircraft

mentation operative case. This represents the level of stability that the pitch stability augmentation system is assumed to provide, as discussed in Section 2.2.3.

Also shown in Figures 68 through 71 are the longitudinal time to double amplitude at the aft center of gravity position with the stability augmentation system inoperative. This is the negative eight percent static margin condition for which the horizontal tail is sized, representing the least stable condition that the aircraft can reach. In some instances the mode is critically damped as noted in Figures 68 and 71.

The results of the dynamic stability analysis are used in Section 2.7.2.5. Even though the parameters are shown for an effective five percent static margin, it is not meant to be implied that the resulting modal parameters as such would provide good flying qualities. Augmentation systems will have to be tailored to the needs of each configuration.

2.7.2.4 Control Capability

This section discusses details of the control capabilities of the point design aircraft.

A comparison of the point design aircraft roll, yaw, and pitching acceleration capability with other Lockheed transports is shown in Figure 72. No requirements on these angular accelerations exist and these data are presented for comparison only. The C-130 is built to be highly maneuverable, and the C-141 and C-5A are also built to the military specifications for maneuverability, which are more demanding than civil specifications.

AIRCRAFT	RAD/SEC^2		
	$\dot{\phi}$	$\dot{\psi}$	$\dot{\theta}$
SINGLE BODY SBR	0 175	0.031	0 074
TWO-BODY MB1	0 069	0 022	0 104
TWO-BODY MB2	0.071	0 020	0.090
THREE-BODY MB3	0 083	0 031	0 261
C-130H	0 500	0.182	0 300
C-141B	0 310	0 070	0 150
C-5A	0 400	0.066	0 123

• LANDING APPROACH PHASE

Figure 72. Control Power - Point Design Aircraft

One example of control requirements is the ability to land in a crosswind. The required rudder and aileron deflections to land in a 1.6 rad (90 degrees) crosswind are presented in Figure 73. All of the point design aircraft can achieve a zero crab angle touchdown in an 18.0 m/sec (35 kt) crosswind.

Roll control capability is a problem area for large multibody aircraft for several reasons:

- o Roll inertia is large due to body spanwise spacing.

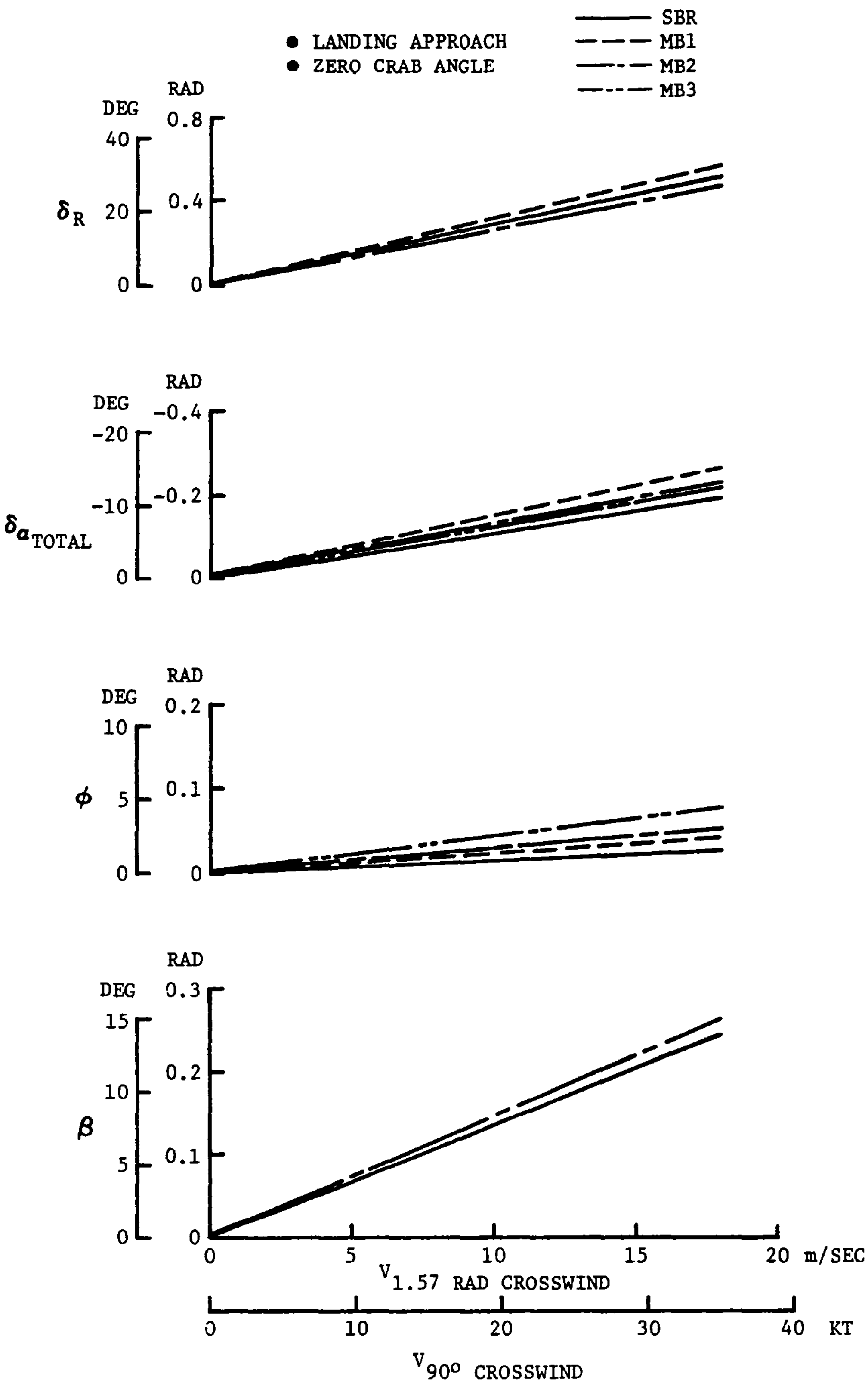

Figure 73. Crosswind Capability - Point Design Aircraft

- o The bodies placed out along the span cut into wing area which would otherwise be available for positioning control surfaces, such as ailerons or spoilers.
- o Experience in large aircraft has shown that the roll control specifications presently available are insufficient and impractical for very large aircraft.

The severity of the lateral control problem is shown by noting the tradeoffs that occur and the resulting aircraft response as the bodies move outboard. Ailerons are used on the outboard 30 percent of the semispan and their effectiveness is relatively constant. However the spoilers are used only outboard of the bodies and their effectiveness is a function of the area outboard which is shown to be rapidly decreasing. Problems associated with roll control and its effect on configuration development were recognized early in the study. Appendix C provides a description of the logic used in developing study ground rules.

It is obvious that roll control becomes increasingly difficult with fuselages located off the aircraft centerline. Quantifying exactly where the cut-off should be is not easily done. The Civil Regulations are not very specific, and the Mil Spec requirements - even though more specific—are known to be inadequate for very large aircraft. MIL Spec 8785B quantifies roll capability by specifying the time required to bank 0.52 rad (30 degrees). Figure 74 shows

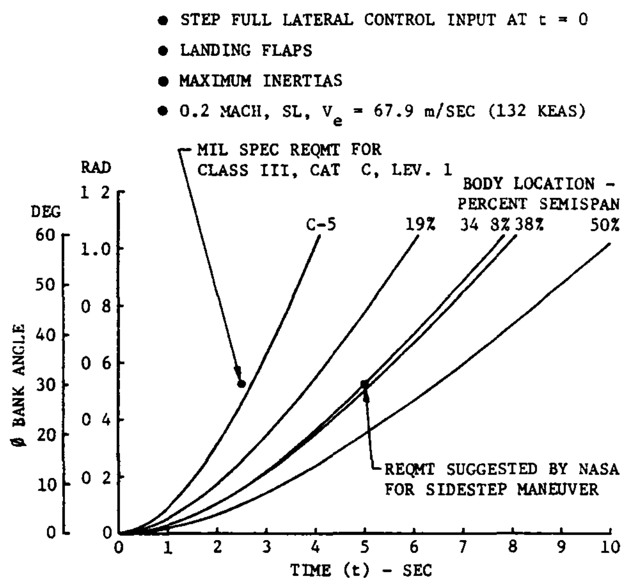

Figure 74. Roll Time Histories - Two-Body Aircraft

how the two-body aircraft and the C-5 compare with such a standard. The requirement shown is for Level 1 - the desired normal capability. The specification allows the time to increase to 3.2 and then 4.0 seconds for Levels 2 and 3, where Level 3 is termed as being able to land safely. The revised version of the Specification (8785C) allows the time to increase to 6.0 seconds for Level 3. The C-5 does not meet the requirement but is judged to have good flying qualities.

A different approach to establishing a required level of roll capability is to perform the true mission of the

aircraft on a flight simulator with a pilot in the loop. During the C-5 development, a lateral offset maneuver on landing approach was used as an evaluation task. The final selected C-5 configuration was able to perform the maneuver using 50 percent of its available control with a four degree/second maximum roll rate and limiting bank angle to 0.26 rad (15 degrees). An analysis of a similar task was made for the two-body aircraft. The results are presented in Figures 75and 76. The three solid lines of Figure 75 show the lateral displacement which can be achieved while using 50, 75 and 100 percent of the lateral control as a function of fuselage position. A capability similar to that of the C-5 (noted on both figures) can be obtained by permitting more of the available control to be used and/or by allowing the roll rate to increase.

A flight simulation study is presently underway at NASA-Langley to aid in the development of criteria for the multibody concept. Final results will not be available in time to be incorporated into this study. Initial results, however, confirm that the maneuver is a good test of required capability. The ability to achieve a 0.52 rad (30 degrees) bank angle in approximately five seconds was equated with a satisfactory pilot rating for

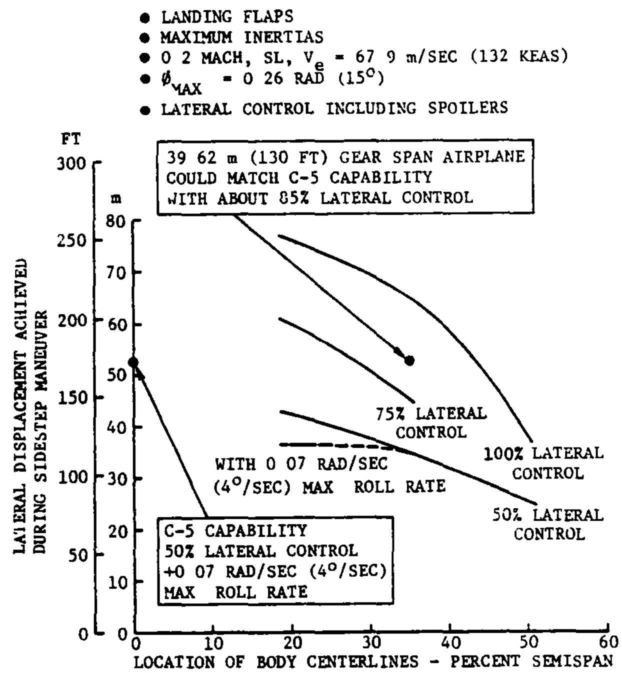

Figure 75. Sidestep Maneuver Capability - Two-Body Aircraft

successfully completing the offset maneuver. All of the point design aircraft can meet this roll requirement as shown in Figure 77.

2.7.2.5 Specification and Flying Qualities

In this section, the flying qualities of the point design aircraft are discussed and compared to specifications and requirements. The civil requirements, FAR Part 25, are not very detailed in their specifications on flying qualities. MIL-F-8785B (ASG), Military Specification, "Flying Qualities of Piloted Aircraft," Reference 7,

BODY POSITION - % SEMISPAN	LATERAL CONTROL -PERCENT MAXIMUM	MAXIMUM ROLL RATE -RAD/SEC (DEG/SEC)	MAXIMUM BANK ANGLE -RAD (DEG)	MINIMUM WING TIP CLEARANCE -m (FT)	MAX. Δ C_L DUE TO LAT. CONTROL
19.0	50	0.12 (6.6)	0.19 (11.0)	16 (52)	0.25
19.0	75	0.17 (9.6)	0.25 (14.5)	12 (40)	0.41
19.0	100	0.20 (11.2)	*0.26 (15.0)	8 (25)	0.57
34.8	50	0.09 (5.0)	0.15 (8.5)	18 (60)	0.14
34.8	75	0.12 (6.9)	0.21 (12.1)	15 (48)	0.23
34.8	100	0.15 (8.8)	0.26 (15.0)	11 (37)	0.32
50.0	50	0.06 (3.2)	0.10 (5.8)	20 (65)	0.06
50.0	100	0.11 (6.4)	0.17 (10.0)	17 (56)	0.13
(C-5)	50	*0.07 (4.0)	0.21 (12.0)	16 (54)	0.15

*CONSTRAINED TO THIS MAXIMUM VALUE

Figure 76. Sidestep Maneuver Characteristics - Two-Body Aircraft

AIRCRAFT	TIME (SEC)
SINGLE BODY SBR	2.7
TWO-BODY (MB1)	4.5
TWO-BODY (MB2)	4.8
THREE-BODY (MB3)	4.75

• FULL LATERAL CONTROL

Figure 77. Time to Bank 0.52 Rad (30 Degrees) - Point Design Aircraft

is much more detailed and provides a more meaningful way to evaluate flying qualities. For this reason, the Military Specification is used for the comparison in this study, even though these are civil aircraft. Also, the limitations of MIL-F-8785B (ASG) are better known.

Specification - Previous experience with applying these specifications to the flying qualities of the C-5A indicates that these specifications have limitations in their application to large aircraft. They appear to be too stringent in some areas and, therefore, will be used as guidelines only. No attempt is made to evaluate or redefine MIL-F-8785B (ASG) here, but its limitations are discussed below, along with suggested preliminary specifications.

The most significant discrepancy between MIL-F-8785B (ASG) and demonstrated large aircraft flying qualities is in lateral control. Reference 8 suggests that the requirements are too stringent. Based on C-5A experience, the sidestep maneuver on landing approach in Figure 78 is defined as a practical test of lateral control capability for large transport aircraft. Preliminary results from NASA flight simulations confirm the suitability of the maneuver as a specification on lateral control capability and that a minimum time of 5.0 seconds to bank 0.52 rad (30 degrees) is needed for an aircraft this size to complete the maneuver. Therefore, 0.52 rad (30 degrees) $t \leq 5.0$ seconds is used as a preliminary specification for lateral control capability for the point design aircraft.

Reference 8 shows that the dutch roll frequency-damping product requirements for Level 2 flying qualities (yaw damper inoperative) are too high relative to the demonstrated acceptable performance of the C-5A. The point design aircraft show similar performance.

Reference 8 recommends that the maximum roll mode time constant requirement be significantly relaxed for aircraft with the flight crew station located at any significant distance from the principal roll axis. This is due to the recognition of the "sidekick" characteristic, which is a lateral acceleration during an abrupt rolling maneuver felt at the pilot station because of the significant vertical distance from the principal roll axis. This effect is barely noticeable on the C-5A, but could be more pronounced in larger aircraft. The multibody aircraft flight station would experience both lateral and vertical accelerations, due to the large vertical and horizontal displacements from the principal roll axis. For example, assuming

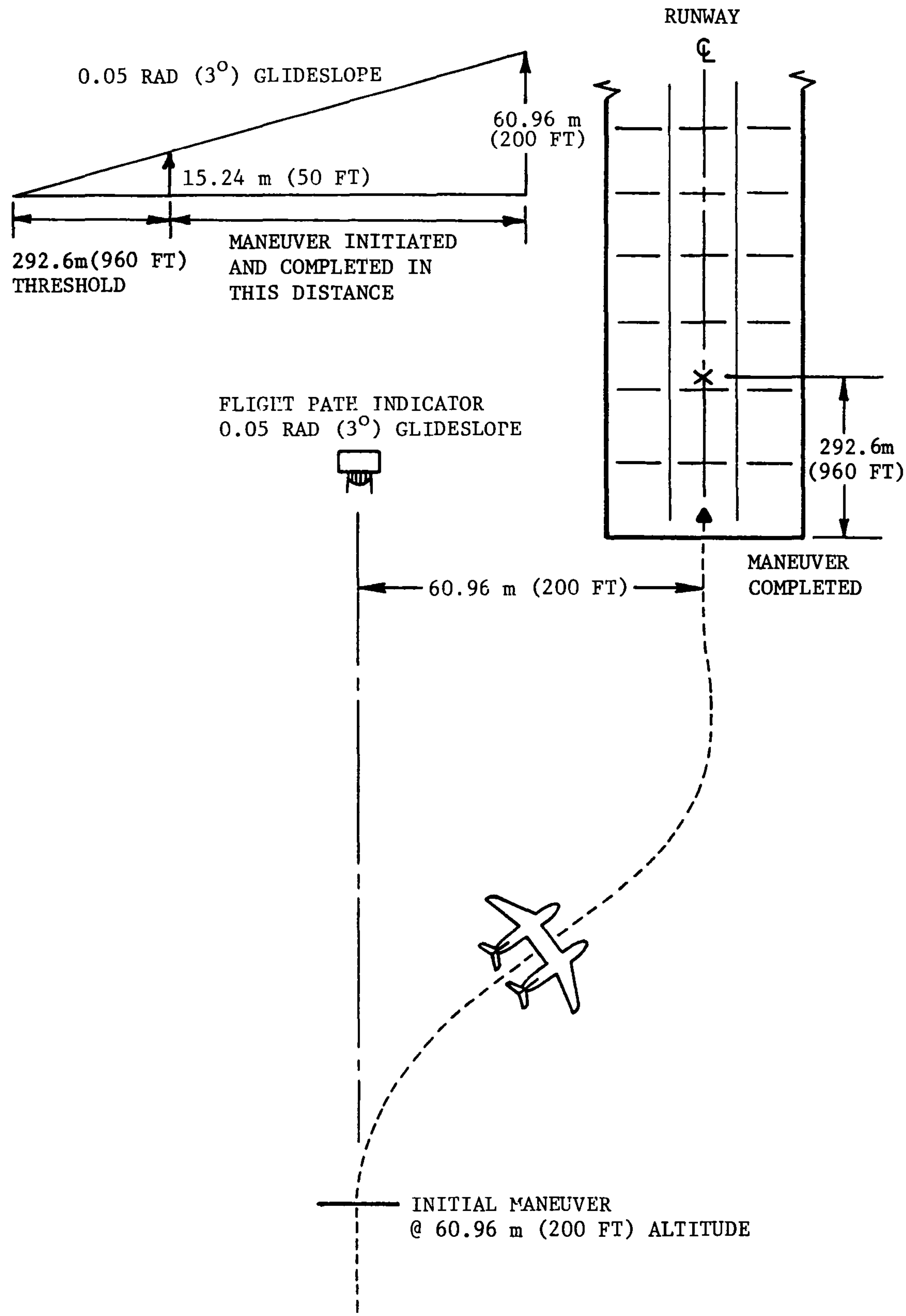

Figure 78. Sidestep on Landing Approach Maneuver

equivalent C-5A roll capabilities and locating the pilot 30.5 m (100 ft) laterally from the principal roll axis, the pilot would feel a vertical acceleration of 0.6 g during an abrupt roll maneuver. If a roll rate of 0.52 rad (30 degrees) per second developes, then the pilot would feel almost 0.9 g lateral acceleration. This would be a totally unacceptable condition.

Further study is necessary to define a requirement for this condition. Perhaps a minimum roll mode time constant could limit the pilot vertical acceleration during abrupt roll maneuvers, and a maximum roll rate requirement could limit the pilot lateral acceleration. Note that the present requirement in MIL-F-8785B (ASG) is a maximum roll mode time constant, and Reference 8 shows that this requirement could aggrevate a "sidekick" type characteristic. If further study should prove that the crew offset is unacceptable, then a crew location on the aircraft centerline of rotation should be investigated. An immediate problem associated with this location would be in providing visibility guidance, possibly through electronic means.

Reference 8 shows that the short period frequency requirements are too high relative to the proven good performance of the C-5A. The multibody aircraft show similar characteristics.

As discussed in Section 2.3.3, the point design aircraft incorporate the concept of reduced longitudinal static stability to decrease the horizontal tail size, with an augmentation system increasing the effective stability to give good flying qualities. If the pitch stability augmentation system becomes inoperative, though, the aircraft still must be controllable. Previous Lockheed studies on large aircraft handling qualities have shown that an aircraft with a time to double amplitude for a pitch instability of no less than 5.0 seconds is controllable. Therefore, for the point design aircraft, a preliminary specification of $T_{double} \geq 5.0$ seconds for the unaugmented aircraft is applied in addition to MIL-F-8785B (ASG) specifications for the augmented aircraft.

Flying Qualities - The following paragraphs discuss the actual comparisons of the point design aircraft flying qualities to the specification. The specification used for comparison are for Class III aircraft, which are heavy transport aircraft. Category B requirements are used for the cruise case, and Category C requirements are used for the landing approach case. Performance is considered adequate if the augmented aircraft meets Level 1 flying qualities, which are defined as

clearly adequate for the mission flight phase. Level 2 is defined as adequate flying qualities but with an increased pilot workload or mission effectiveness degradation, or both. Level 3 is defined as flying qualities such that the aircraft is controllable but the pilot workload is excessive or the mission effectiveness is inadequate, or both. It also states that Category A and B can be safely terminated and C (landing and takeoff) can be completed. Comparisons are made with preliminary specifications on lateral control and unaugmented pitch stability. These comparisons with the requirements are not meant to imply that the characteristics shown are the final ones the aircraft would have. They are meant more as an indication of what additional functions have to be added with an augmentation system.

Note that all specification comparisons for augmentation operating case (normal) use data based on the effective five percent static margin analysis. Augmentation inoperative cases use data based on the negative eight percent static margin analysis since that is the true critical condition.

The Level 1 requirement on the phugoid damping ratio is that it be greater than or equal to 0.04. Data from Figures 68 through 71 show that this requirement is met in all cases except the cruise case for the MB2 aircraft. The phugoid damping ratio for the MB2 aircraft is very close to the specification and is acceptable considering the accuracy of the calculation.

The Level 1 requirement on short period damping is $0.35 < \zeta_{SP} < 1.3$ for Category C, and $0.3 < \zeta_{SP} < 2.0$ for Category B. Data from Figures 68 through 71 show that all point design aircraft meet these requirements, except for the aperiodic cases of the three-body MB3 and the single body reference aircraft.

Figures 79 and 80 show the MIL-F-8785B (ASG) specifications on short period frequency along with the preformance of the point design aircraft. The short period frequencies are too low to meet the Level 1 specification which is as expected. Reference 8 shows that the C-5A also has short period frequencies that are in general below the specification, yet its short period flying qualities are rated good.

The longitudinal dynamic stability analysis results for the point design aircraft with the pitch stability augmentation system inoperative are shown at the bottom of Figures 68 through 71. Note that this analysis is done at the critical stability point of negative eight percent static margin. The preliminary specification of T double ≥ 5.0 seconds is met by all aircraft for

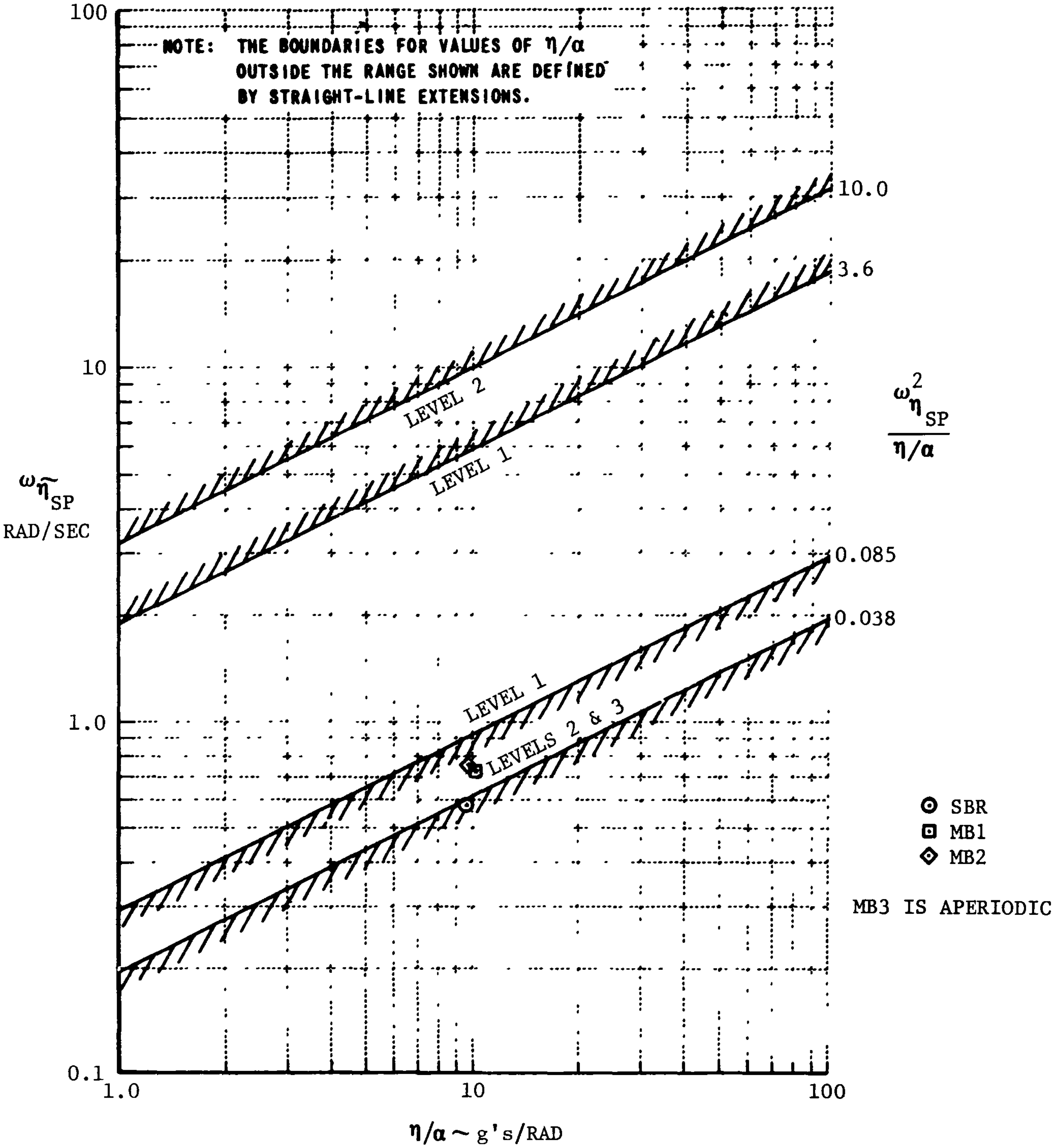

Figure 79. MIL-F-8785B (ASG) Short Period Frequency Requirements - Category B Flight Phases

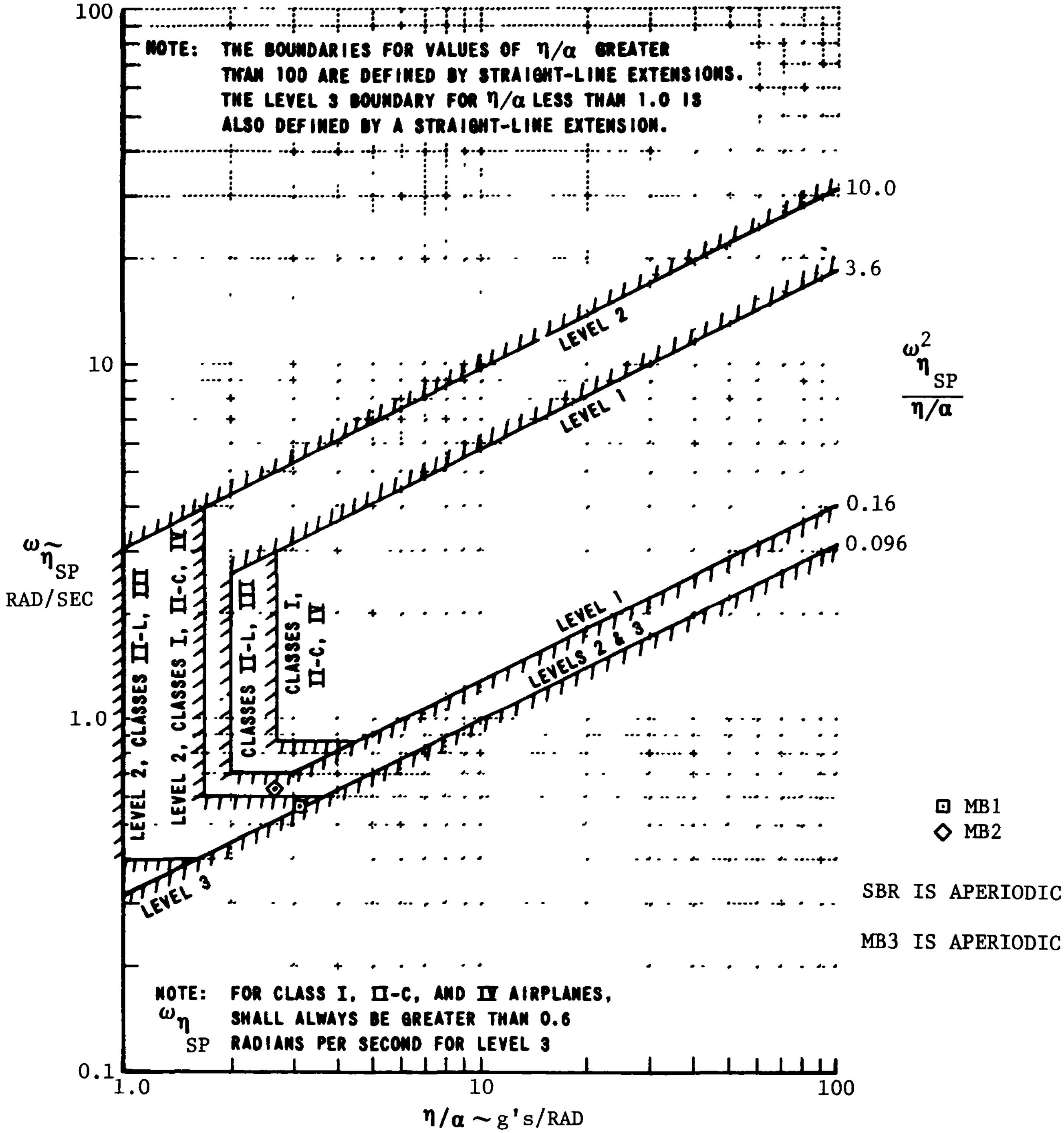

Figure 80. MIL-F-8785B (ASG) Short Period Frequency Requirements - Category C Flight Phases

the landing approach case. The multi-body cruise configurations, however, are not quite stable enough to meet this preliminary specification. Different stability levels were checked and a negative six percent static margin limit allowed the specification to be met for both the cruise and landing approach case. Note again that this is a rigid aircraft analysis, and a full elastic analysis would be necessary to validate the cruise case characteristics. It is anticipated that the cruise stability level would actually be greater than that of the landing case.

The lateral-directional oscillation or Dutch roll mode requirements call for a minimum damping ratio of 0.08 for Level 1 and 0.02 for Level 2. The minimum frequency requirement is given as 0.4 rad/sec for all levels. A combination requirement is given also as a minimum frequency damping ratio product of 0.15 for Level 1 and 0.05 for Level 2. Figures 68 through 71 show these values for the point design aircraft. A comparison shows that all point design aircraft are Level 1 in damping ratio except the landing case of the two-body MB1 which is Level 2. the single body reference aircraft meets the Level 1 frequency requirements, but the multibody aircraft are Level 1 in cruise only. All aircraft are Level 2 for the damping - frequency product except for the landing case of the two-body MB1 and MB2 and the SBR aircraft. These characterisitics are generally acceptable for a large aircraft which is unaugmented. Conventional augmentation systems should provide good flying qualities. (Reference 8 shows similar comparisons with similar discrepancies for the C-5 unaugmented.)

The roll mode time constant requirement is for a value no greater than 1.4 for Level 1 or 3.0 for level 2. These values for the point design aircraft are again shown in Figures 68 through 71. The single body reference and three-body MB3 aircraft are Level 1, the two-body MB1 aircraft is Level 2, and the two-body MB2 aircraft is Level 2 for landing and Level 1 for the cruise case.

Spiral stability is stipulated by requiring the time to double amplitude be at least 20 seconds for Level 1. The spiral mode is usually designed to be slightly unstable. The value of time to half amplitude if stable, or time to double amplitude if unstable, as presented in Figures 68 through 71 show that all aircraft meet level 1. If anything, this shows that the spiral mode may be a little too stable.

The requirements on roll rate oscillations after a step aileron input and bank angle oscillations after an aileron pulse are shown in Figures 81 and 82

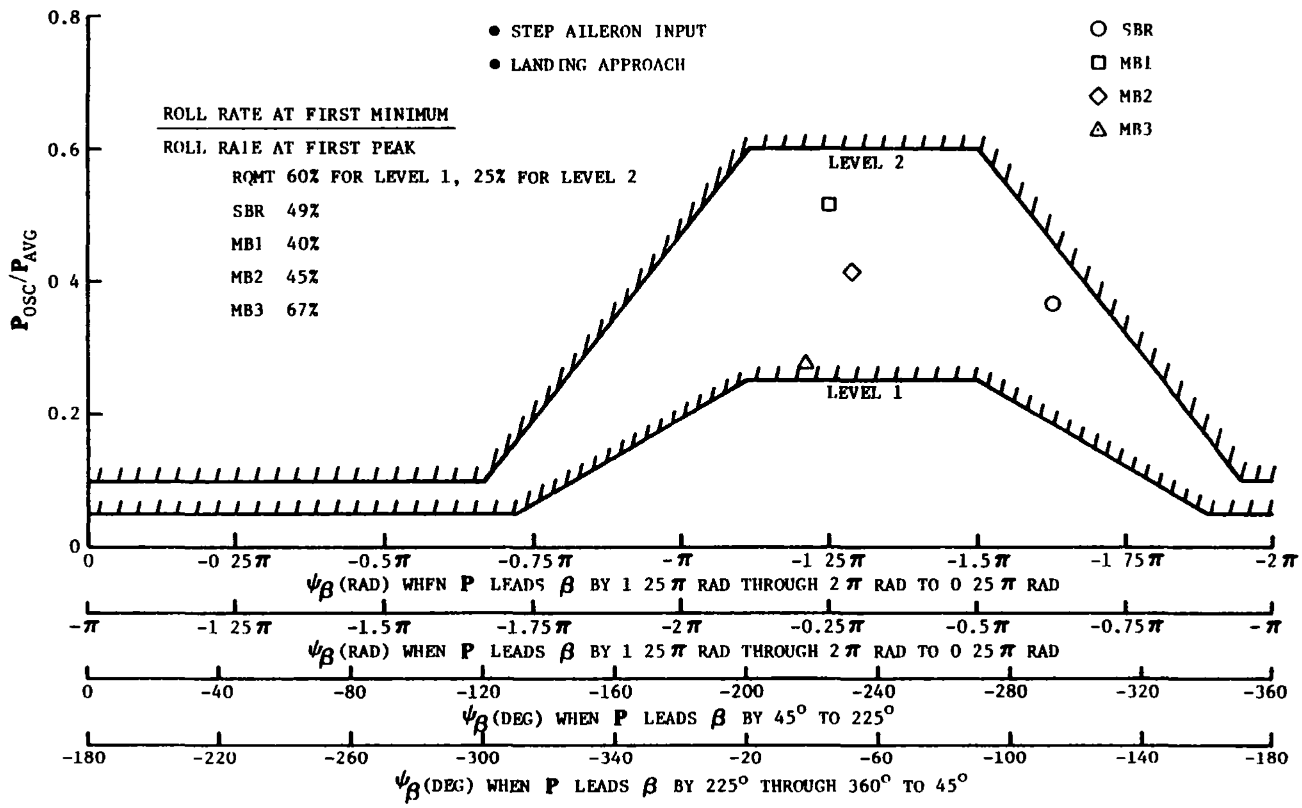

Figure 81. MIL-F-8785B (ASG) Roll Rate Oscillation Limitations - Category C Flight Phases

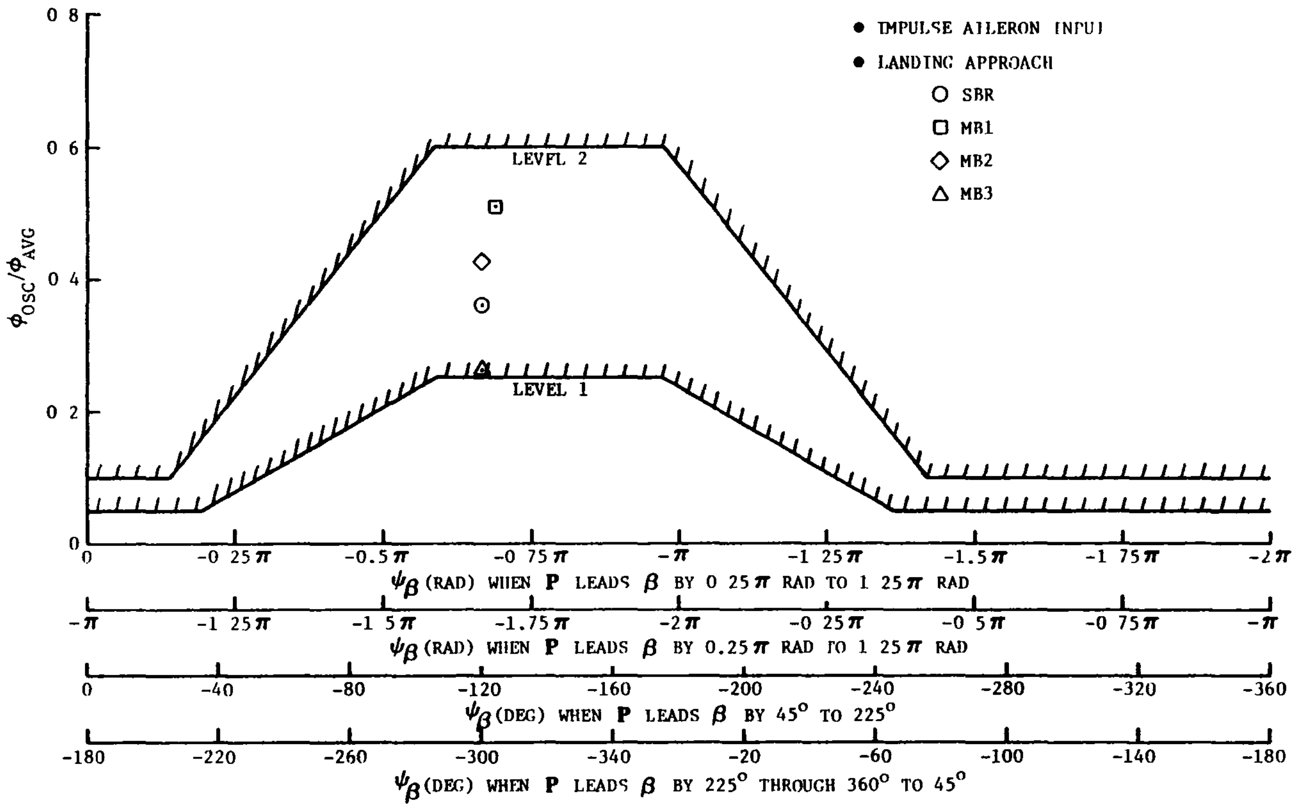

Figure 82. MIL-F-8785B (ASG) Bank Angle Oscillation Limitations - Category C Flight Phases

along with the point design aircraft performances. All aircraft meet the Level 2 requirement. Figure 83 shows the sideslip excursions for all point design aircraft after a step aileron input. The requirements and performance are used to compute the parameters for Level 1 and Level 2 performance. All aircraft are outside Level 1 and Level 2 boundaries. Note that these results are for unaugmented aircraft. A turn coordinator - type augmentation system will improve the point design aircraft performances in these areas.

The time to achieve 0.52 rad (30 degrees) bank angle using a full lateral control step input is shown in Figure 77 for all point design aircraft. All the configurations meet the preliminary specification of achieving the 0.52 rad (30 degrees) in less than 5.0 seconds, which is considered the requirement for a successful sidestep maneuver. As previously explained, this is considered a more realistic requirement than the 2.5 seconds for Level 1 of the Mil Spec. which none of the aircraft meet.

Summary - This comparison with MIL-F-8785B (ASG), Reference 7, is presented as a guideline in determining

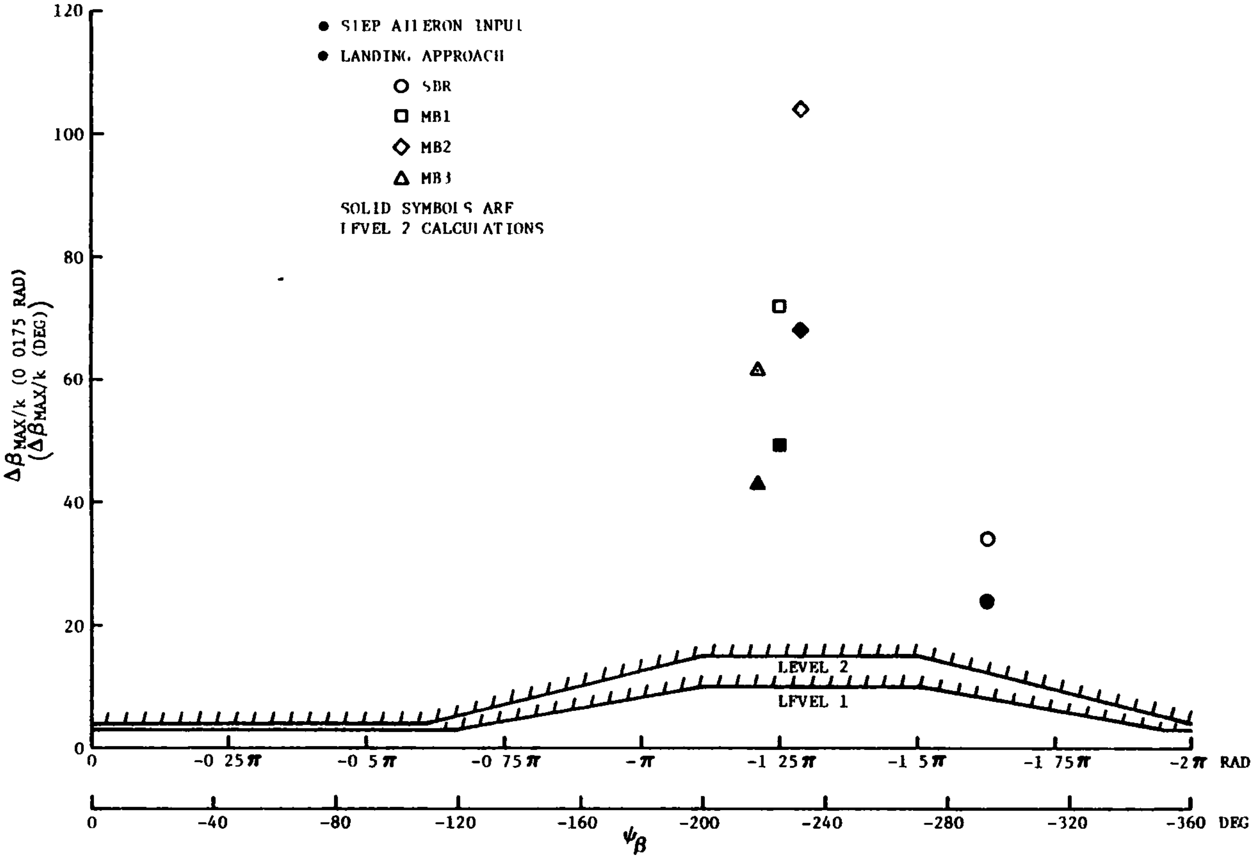

Figure 83. MIL-F-8785B (ASG) Sideslip Excursion Limitations - Category C Flight Phases

the acceptability of the flying qualities of the point design aircraft. C-5A experience noted in Reference 8 has shown that the specifications may be limited in application to large aircraft in the following areas:

- o Minimum frequency for short period
- o Dutch roll frequency-damping product
- o Lateral control effectiveness - sidestep maneuver proposed as more practical than 0.52 rad (30 degrees) ϕ in 5.0 seconds.
- o Roll mode time constant - "Side-kick" characteristics

An additional specification is added for the pitch stability augmentation system inoperative case: T double $\geq$ 5.0 seconds.

The actual comparison shows that the point design aircraft have Level 1 flying qualities for the majority of the requirements. The exceptions are listed below, along with short explanations:

- o Short period frequency are below the requirements, using an effec-

tive five percent static margin, but so is the C-5A and its short period response is rated good. Therefore, the point design aircraft are assumed acceptable in this area also.

- o With the pitch stability augmentation system inoperative, the cruise case just misses the T double $\geq$ 5.0 seconds. If the minimum static margin were changed to approximately negative six percent, the requirement could be met. A full elastic analysis is necessary to verify if that would be necessary.

- o Dutch roll frequency is low.

- o Dutch roll frequency damping product is low. A yaw damper will probably be required.

- o The roll mode time constants are about half Level 2 for all cases shown. These requirements should probably be relaxed in order to prevent unacceptable "Sidekick" type characteristics during roll maneuvers.

- o Roll rate and bank angle oscillation for step aileron input are Level 2. Sideslip excursions do not even meet Level 2 capabilities. A turn coordinator augmentation system will improve these characteristics.

- o The preliminary requirement on lateral control capability of 0.52 rad (30 degrees) t $\leq$ 5.0 seconds is met by all aircraft. Therefore all aircraft should be able to successfully complete the sidestep maneuver, a practical test of lateral control capability for large aircraft.

The performance of all of the point design aircraft relative to these specification is very similar. No one aircraft has any noticeably better performance than any other.

The point design aircraft appear to have acceptable flying qualities within the preliminary proposed specifications for large aircraft based on MIL-F-8785B (ASG), or can reach acceptable levels with the incorporation of conventional augmentation systems.

2.7.2.6 Flight Simulation

A six degree of freedom moving base flight simulation is to be conducted by NASA-Langley to investigate the peculiarities of the multibody configuration in the low-speed flight regime. The three multibody point design aircraft are to be evaluated as well as the single body reference aircraft and a spanloader concept from a previous study. These studies are expected to include an evaluation of flying qualities specifications, with emphasis on the problems of lateral control capability and the offset of the pilot from the roll axis. New or unforseen flying qualities problems could be identified during the course of the study. Comparisons of flying qualities will be made between the single body, multibody, and spanloader concepts.

The data for constructing these flight simulations are presented in

Appendix E. They consist of geometry, weights, stability derivatives, drag polars, ground effects, engine data, and three-views for each configuration.

2.7.3 Structures

The point design aircraft, as explained in Section 2.3.2, are first generated using statistical based structural analysis methods which provide preliminary weights and mass distributions. These parametric aircraft are next subjected to analysis by detailed analytical computer programs which include structural, balance, and inertia analyses. Based upon the results of the detailed analyses, the statistical methods are revised. This iterative process continues until the statistical and detailed methods provide comparable results.

2.7.3.1 Fuel Management

Fuel system tankage is provided for each of the point design aircraft equal to that required for mission fuel (design point payload and range) plus a one percent margin. The available fuel tank volume contained within the wing contours of each of the point design aircraft far exceeds the required volume. Therefore, it is necessary to define the location and size of each fuel tank and the sequence of fuel usage from each tank such that the effects on loads, balance, and moments of inertia can be determined.

Three tanks of equal volume are used within each wing semispan, one at each semispan extreme and the other at the midpoint of the semispan. This provides one tank per engine and equal fuel usage from each tank. This tankage configuration is selected to minimize center of gravity travel due to fuel burn and the maximum possible wing structure inertia load relief.

2.7.3.2 Structural Analysis

The primary benefit to be derived from the multibody concept is the wing flight load relief provided by the body inertia loads. To assure this benefit is quantified within reasonable accuracy consistent with preliminary design analyses, a detailed structural analysis is performed to verify the predicted wing weight. If the results of these two analyses are not in agreement, the statistical methods are revised and the Analytical Structural Weight Estimating Routine (ANSWER) program is rerun. This procedure is repeated until comparable results are obtained.

The ANSWER program is a semi-analytical beam theory program which estimates the wing box weight based on external loads, mass distributions,

stiffness requirements, and geometric definition. The secondary structure is estimated by statistical methods.

External geometry such as area, span, chord, and thickness distribution is obtained directly from GASP. The internal structural arrangement such as spar location, rib spacing, and bulkhead locations are determined by experience or trade studies. In this case, the spars are located at 15 percent and 65 percent chord, respectively. The best rib spacing is about 1.27m (50 in.).

A survey of external loads is conducted to establish a set of critical loads to be used in the analysis. From this survey, five load cases are selected as being representative of the most critical loading conditions. These are presented in Figure 84. There are two gust cases, maximum gross and zero fuel weights at the most critical gust condition. Two maneuver conditions are considered, maximum gross and zero fuel weights at maximum speed at sea level. There is one ground condition which is a 2g taxi case. These load cases are used for all point design aircraft.

The inertia loads are based on fuel distribution, engine locations, body location, and wing mass distribution. These are added to the airloads derived from the conditions in Figure 84 to determine net external loads. Stiffness requirements are developed by flutter analysis programs which interact with the structural analysis programs to give the best mix between structural strength and stiffness.

WEIGHT	SPEED		ALTITUDE		LOAD FACTOR	GUST VELOCITY	
	m/sec	kts	m	ft		m/sec	ft/sec
Zero Fuel Weight	180	350	6096	20,000	-	15	50
Gross Weight	180	350	6096	20,000	-	15	50
Zero Fuel Weight	211	410	0	0	2.5	-	-
Gross Weight	211	410	0	0	2.5	-	-
Gross Weight	0	0	0	0	-2.0	-	-

Figure 84. Critical Flight Loading Conditions - Summary

2.7.3.3 Flutter Analysis

The data presented in this section are the primary results of the flutter analysis. Detailed data are contained in Appendix D.

Flutter boundaries for the single body reference and two-body MB1 aircraft are greater than the 20 percent margin requirements for zero and mission fuel and zero and full cargo loadings at the minimum structural weight level. Summary curves for mission fuel and no cargo, the most critical of conditions analyzed for both aircraft, are illustrated in Figures 85 and 86. Altitude versus flutter velocity summaries for no cargo, both fuel conditions, and Mach 0.5 and 0.8 are shown in Appendix D for both aircraft. There are no weight penalties because of flutter on these two aircraft. The minimum structural weight two-body MB2 and three-body MB3 aircraft had flutter boundaries inside the 20 percent margin requirements; the three-body aircraft had flutter instabilities within the flight envelope. Both of these aircraft required resizing of the wing stiffness to achieve adequate flutter margins.

Flutter boundaries and optimum stiffness distributions are calculated by using two separate computer programs. The first uses a more detailed aerodynamic and structural representation, and is used to define flutter points at several altitude, fuel, cargo, and Mach number conditions. The second uses a simpler mathematical model, computes flutter velocity derivatives, and redistributes stiffness and weight along the wing span, but for only one altitude, Mach number, fuel, and cargo condition. This condition is generally the most critical determined

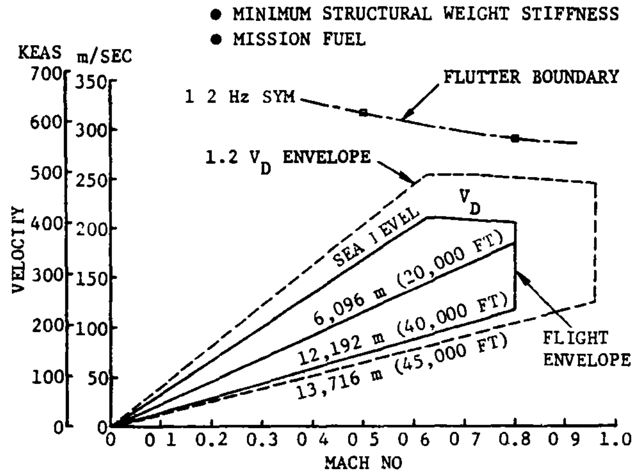

Figure 85. Wing Flutter Results - Single Body Reference Aircraft

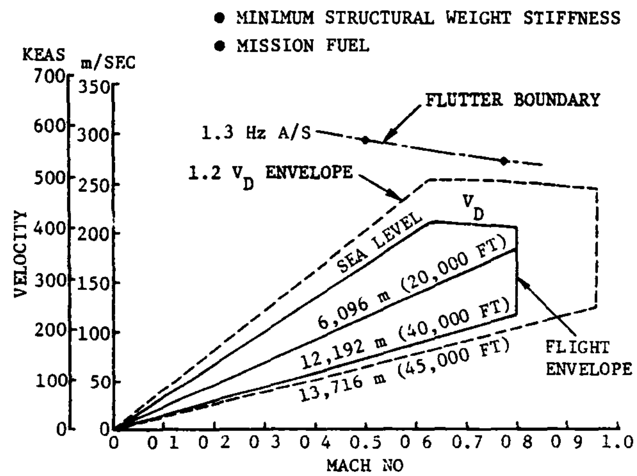

Figure 86. Wing Flutter Results - Two-Body MB1 Aircraft

necessary to add torsional stiffness to both the inner and outer wing to stabilize two antisymmetric flutter modes, by the first program. Flutter optimization is used only when the flutter boundary of a configuration lies within the 20 percent flutter margin requirements.

Figure 87 shows that the minimum structural weight two-body MB2 aircraft fluttered inside the flight envelope, thus requiring stiffness resizing. Flutter optimization methods are employed to arrive at a minimum weight penalty that will ensure this configuration to be free of flutter and meet the flutter margin requirements. Flutter derivatives are computed and the wing resized by adding stiffness to the areas where the flutter derivatives are the largest. All of the stiffness required to stabilize this flutter mode is added to the outer wing, Figure 88. The wing weight penalty due to flutter is 2041 kg (4500 lb) for the two-body MB2 aircraft. During the structural resizing process no other flutter modes became critical; hence, the flutter derivatives along the span tended to be quite uniform, which establishes this stiffness distribution as being close to an optimum weight. Flutter boundaries, for the optimum stiffness distribution of the two-body MB2 aircraft, are illustrated in Figure 89 for no cargo and mission fuel. Altitude versus

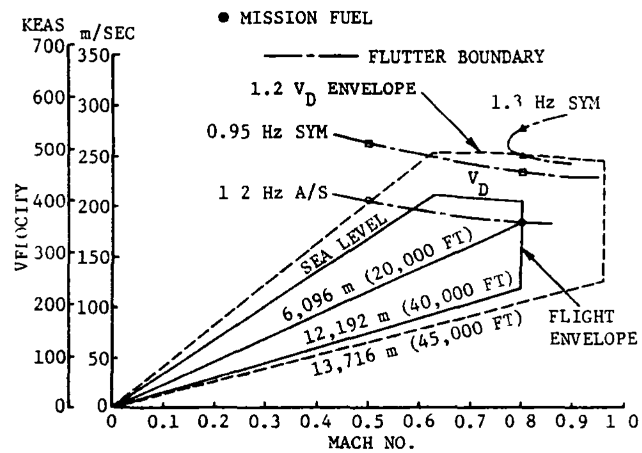

Figure 87. Wing Flutter Results - Minimum Stiffness - Two-Body MB2 Aircraft

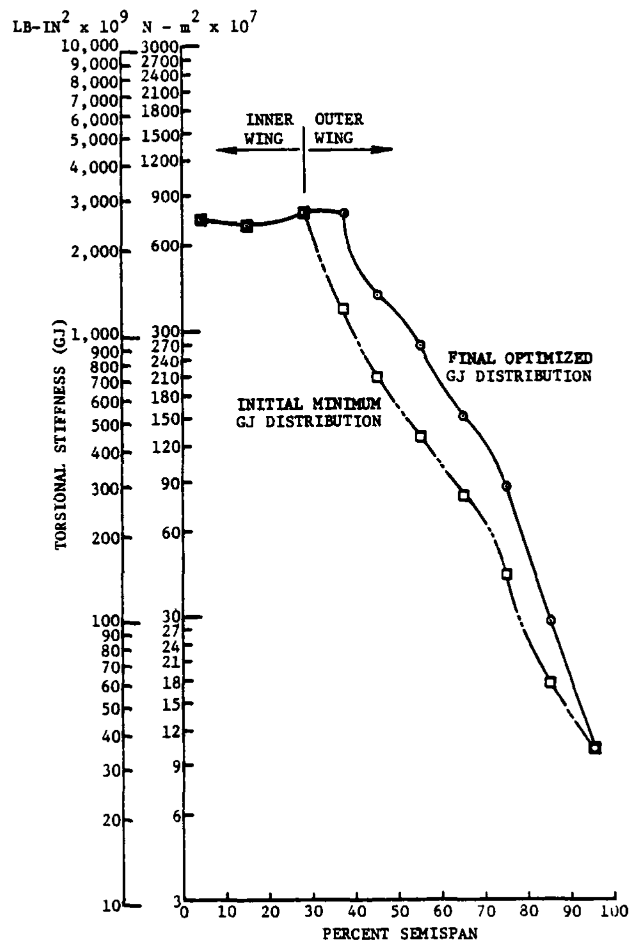

Figure 88. Wing Torsional Stiffness - Two-Body MB2 Aircraft

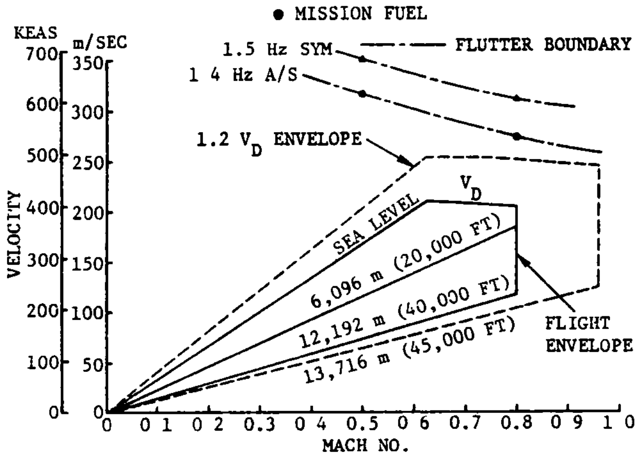

Figure 89. Wing Flutter Results - Optimum Stiffness - Two-Body MB2 Aircraft

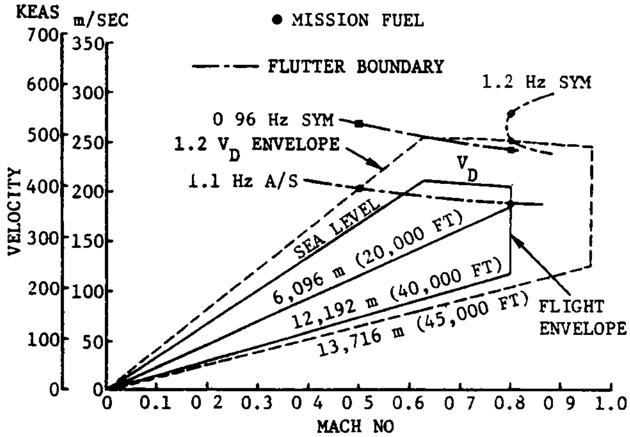

Figure 90. Wing Flutter Results - 40 Percent Increase in Center Wing Stiffness - Two-Body MB2 Aircraft

flutter velocity summaries are given in Appendix D for Mach 0.5 and 0.8, mission and zero fuel, no cargo, and both symmetries. Additional flutter analyses are presented that illustrate the effect of increasing only the stiffness in the center wing. Two increases of 40 and 80 percent are summarized, and no appreciable improvement is noted in Figures 90 and 91. These results are verified by the flutter optimization program, as very small flutter derivatives are computed for the center wing. Minimal flutter velocity increases are noted for stiffness increases in the center wing. These results demonstrate, within the limits of the analysis performed, that flutter is primarily caused by the outer wing. Hence, additional stiffness benefits of a horizontal tail, which connects the two fuselages, will do nothing toward increasing the flutter velocity for this two-body MB2 aircraft.

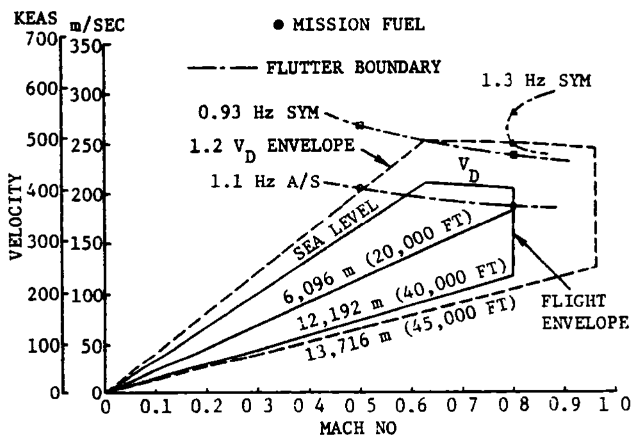

Figure 91. Wing Flutter Results - 80 Percent Increase in Center Wing Stiffness - Two-Body MB2 Aircraft

Data plots relating to the following modes and conditions for the two-body MB2 aircraft are in Appendix D: altitude versus flutter velocity for zero fuel and mission fuel at Mach 0.5 and 0.8 for the 80 percent stiffness increase; results of the vibration analysis with optimum wing stiffness distribution for both fuel conditions

in symmetric and antisymmetric modes; velocity-frequency and velocity damping.

Flutter speeds derived for the initial three-body MB3 aircraft are inside the flight envelope. It is one at 0.5 Hz and the other at 0.9 Hz, shown in Figures 92 and 93. The lowest flutter velocity mode at 0.9 Hz, for the initial design, is more stable when the stiffness of the outer wing is increased. Optimum stiffness changes, i.e., the greatest increase in flutter velocity with the least wing weight penalty for this flutter mode, occurs between 40 and 80 percent semispan and is shown in Figure 94. As this mode is stabilized, another flutter mode, 0.5 Hz, involving inner wing torsion with the outer bodies moving in an antisymmetric manner, becomes critical.

Optimum stiffness increases for this mode is applied from 0 to 30 and 50 to 70 percent semispan. Final stiffness values that relocate the antisymmetric flutter boundaries outside the 20 percent flutter margin requirements are applied generally over the entire wing with minimum changes around the outer bodies. Weight penalties are 4310.0 kg (9502 lb) for the inner wing and 2048.9 kg (4517 lb) for the outer wing.

During the flutter optimization process, symmetric flutter velocities are computed to be considerably above the critical antisymmetric flutter velocity; hence, the stiffness curves are based on optimizing this critical mode. Optimum stiffness values are derived without the effects of pylon, engine, fuselage, and empennage aerodynamics. Final flutter boundary results include these aerodynamic effects and are used as a basis of comparison to ensure that all reasonable flutter mechanisms are

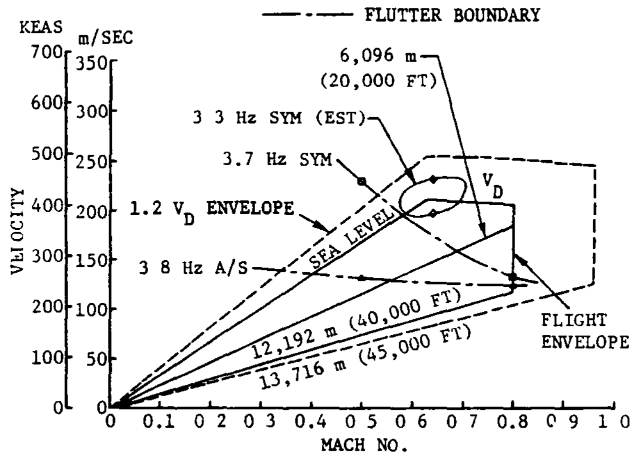

Figure 92. Wing Flutter Results - Initial Design Stiffness - Zero Fuel - Three-Body MB3 Aircraft

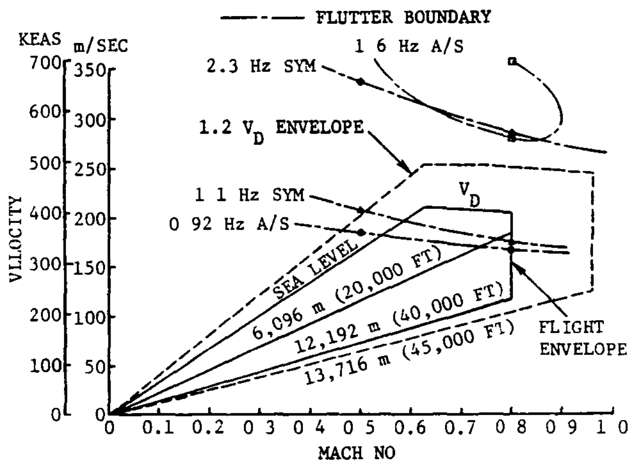

Figure 93. Wing Flutter Results - Initial Design Stiffness - Mission Fuel - Three-Body MB3 Aircraft

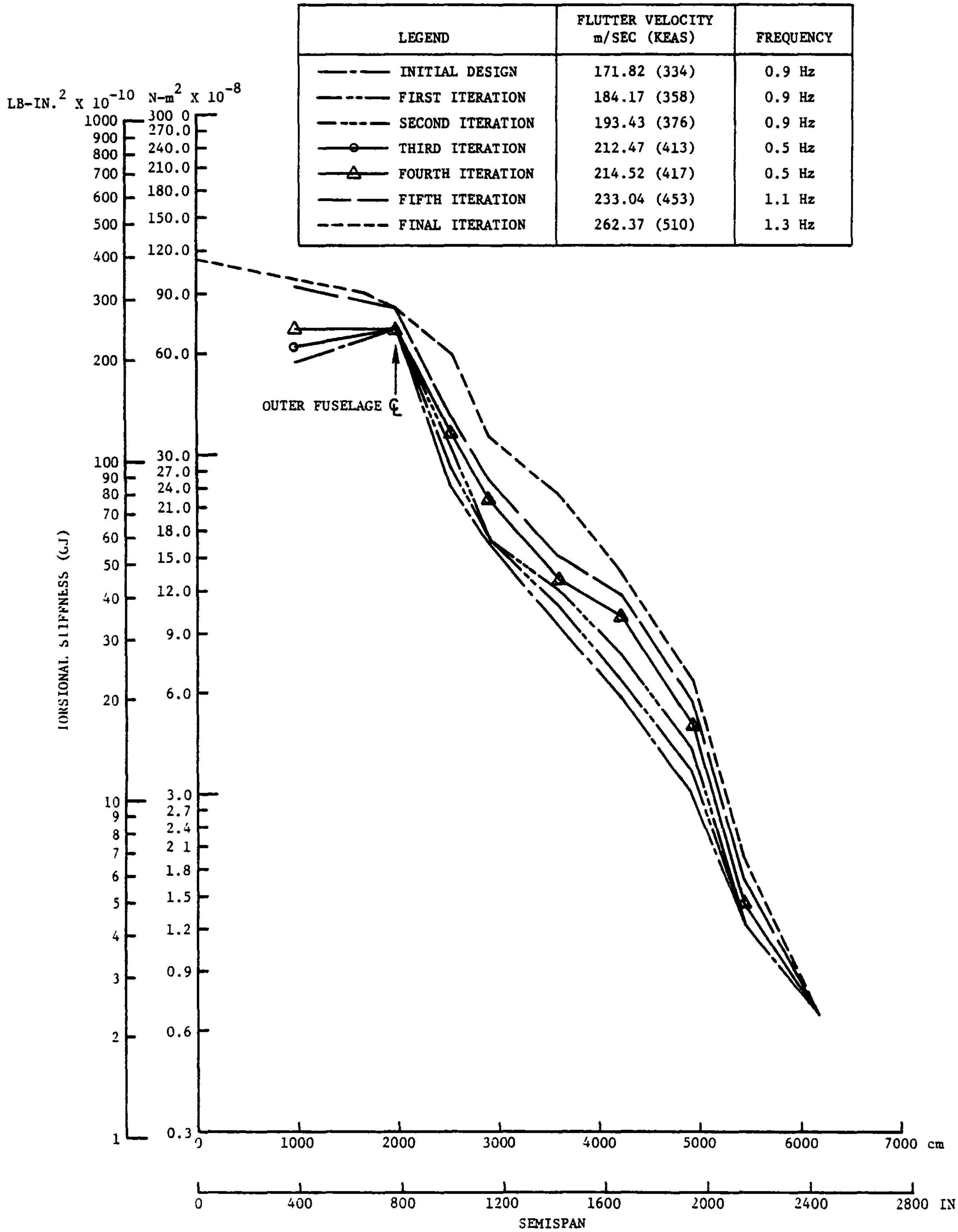

Figure 94. Wing Flutter Stiffness Optimization - Three-Body MB3 Aircraft

analyzed while computing optimum stiffness distributions. Antisymmetric flutter results, without the additional aerodynamic effects, are deemed conservative; however, the symmetric results are unconservative for the three-body configuration. Symmetric flutter, as shown in Figure 95, is computed to be inside the 20 percent flutter margin requirements but outside the flight envelope; to remove this instability will require additional stiffness increases to the outer wing. This conclusion is drawn by raising the required symmetric flutter velocity in the optimization program and computing the stiffness changes to stabilize this mode. Approximate weight increases are 453.6 kg (1000 lb) for the outer wing. No flutter boundary verification or aircraft resizing is conducted for this additional stiffness increase.

As an alternative to increasing wing stiffness alone, a slab tail is considered and discussed in Section 2.6.2. It is rejected for several reasons. Symmetric flutter involves bending of the center wing and torsion due to opposing motion of the center and outer bodies. Antisymmetric flutter is the result of opposing motion of the outer bodies with the center body contributing little to the relative bending or torsion of the center wing; thus, torsional or bending stiffness benefits of a slab horizontal tail would do little

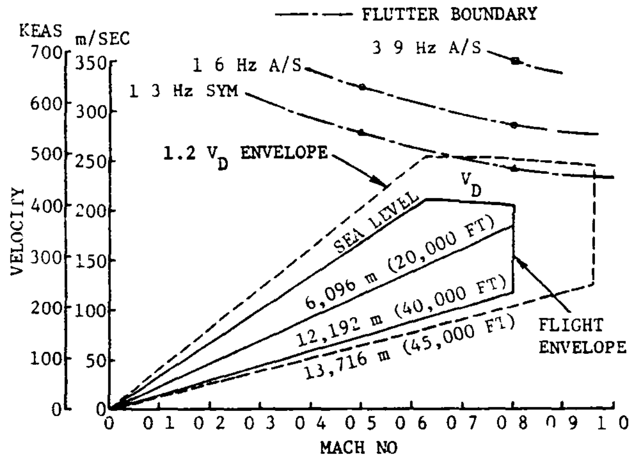

Figure 95. Wing Flutter Results - Optimum Stiffness - Mission Fuel - Three-Body MB3 Aircraft

to stabilize flutter for the three-body MB3 aircraft. A slab tail will tend to stabilize an antisymmetric mode since it ties the two outboard fuselages together. It will not, however, do anything towards stabilizing a symmetric mode. Figures 92 and 93 show that both symmetric and antisymmetric flutter modes are critical. It will be necessary, therefore, to stiffen the wing center section even for a slab tail configuration. The slab tail will weigh about 3175.1 kg (7000 lb) more than the two tee-tails and there will be some wing stiffness penalty for symmetric flutter. In addition, it is expected that a slab tail will encounter flutter and divergence problems associated with elevator rotation and tail bending as well as torsional stiffness. Addition of a slab horizontal tail does not effectively stabilize symmetric

flutter and provides minimal benefits for antisymmetric flutter.

2.7.3.4 Weight, Balance, and Moment of Inertia

The point design aircraft are subjected to a detailed weight, balance, and inertia analysis. A group weight statement is developed for each aircraft which reflects the distribution of weight between structure, systems, equipment, payload, and fuel. A center of gravity envelope is developed which is consistent with the aircraft general arrangement, the fuel sequence, and the stability and control requirements. Similarly, envelopes for the four components of moment of inertia are developed. In addition, a payload loading envelope is calculated for each point design aircraft. This envelope defines the most forward and most aft allowable payload c.g. for any given payload.

A group weight statement and the results of the analyses for each of the point design aircraft are given in Figures 96 through 111.

ITEM	POUNDS	KILOGRAMS
STRUCTURE	(634789)	(287935)
WING	270949	122900
HORIZONTAL TAIL	9607	4358
VERTICAL TAIL	7833	3553
FUSELAGE	231541	105025
NOSE LANDING GEAR	12247	5555
MAIN LANDING GEAR	81964	37179
NACELLE	7955	3608
PYLON	12693	5757
PROPULSION SYSTEM	(117826)	(53445)
ENGINES	93035	42200
FUEL SYSTEM	6161	2794
THRUST REVERSERS	15630	7090
MISCELLANEOUS	3000	1361
SYSTEMS AND EQUIPMENT	(51348)	(23291)
AUXILIARY POWER SYSTEM	2211	1003
SURFACE CONTROLS	15382	6973
INSTRUMENTS	2847	1291
HYDRAULIC AND PNEUMATIC	7168	3251
ELECTRICAL	5477	2484
AVIONICS	2400	1089
FURNISHINGS	9188	4168
AIR CONDITIONING & ANTI-ICE	6284	2850
AUXILIARY GEAR EQUIPMENT	391	177
WEIGHT EMPTY	(803963)	(364671)
OPERATING EQUIPMENT	16897	7665
OPERATING WEIGHT	(820860)	(372336)
CARGO	771618	350000
ZERO FUEL WEIGHT	(1592478)	(722336)
FUEL	519209	235509
GROSS WEIGHT	(2111687)	(957845)
AMPR WEIGHT	(660322)	(299517)

Figure 96. Group Weight Summary - Single-Body Reference Aircraft

2.7.4 FAR 36 Noise Compliance

FAR 36 noise certification analyses are conducted for each of the point design aircraft. The multibody aircraft have a small acoustical advantage over the single body reference aircraft, however, all the aircraft have predicted noise levels considerably in excess of the Stage 3 noise limits. The analysis includes noise contributions from the propulsion system (the dominant noise source), the airframe, and the engine jet efflux impinging on the flap. The principal reasons for the aircraft noise level exceedances are: (a) the engine-designed for fuel efficiency - has a higher noise level than current engines when installed with the same amount of acoustic treatment in the nacelle and (b) the aircraft altitude over the takeoff flyover noise measurement point is typically 198.1 m

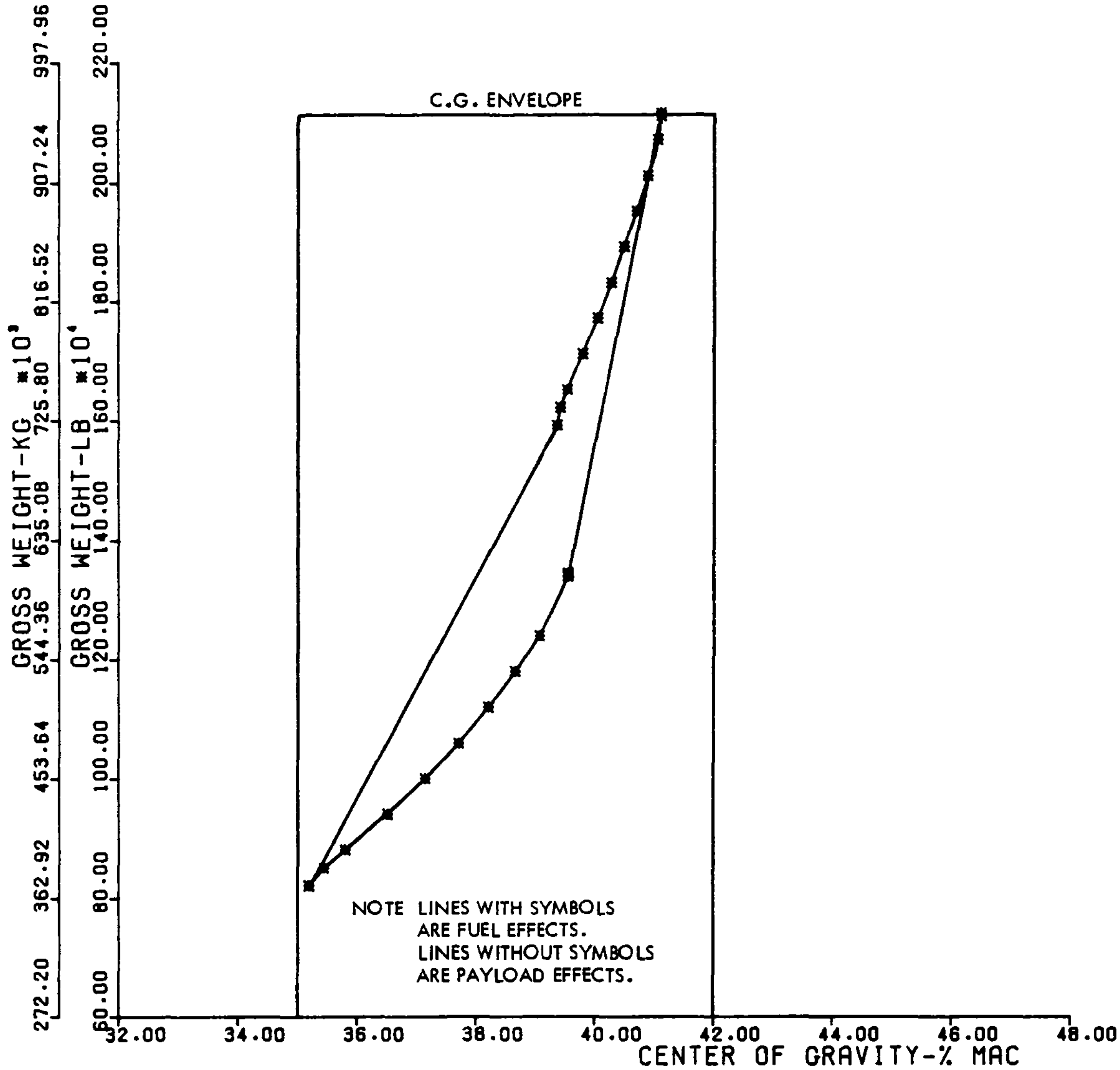

Figure 97. Center of Gravity Envelope - Single Body Reference Aircraft

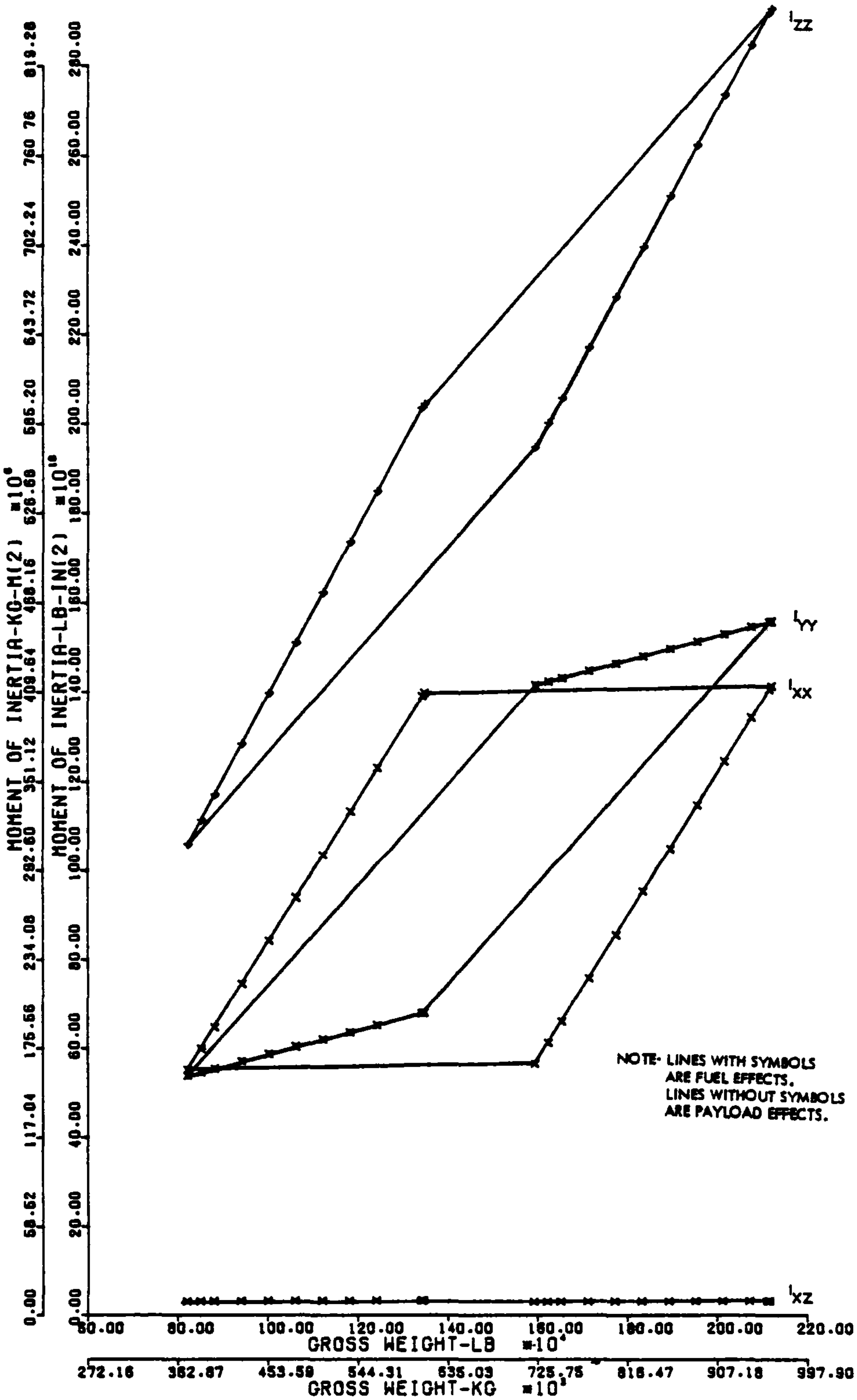

Figure 98. Moment of Inertia Envelope - Single Body Reference Aircraft

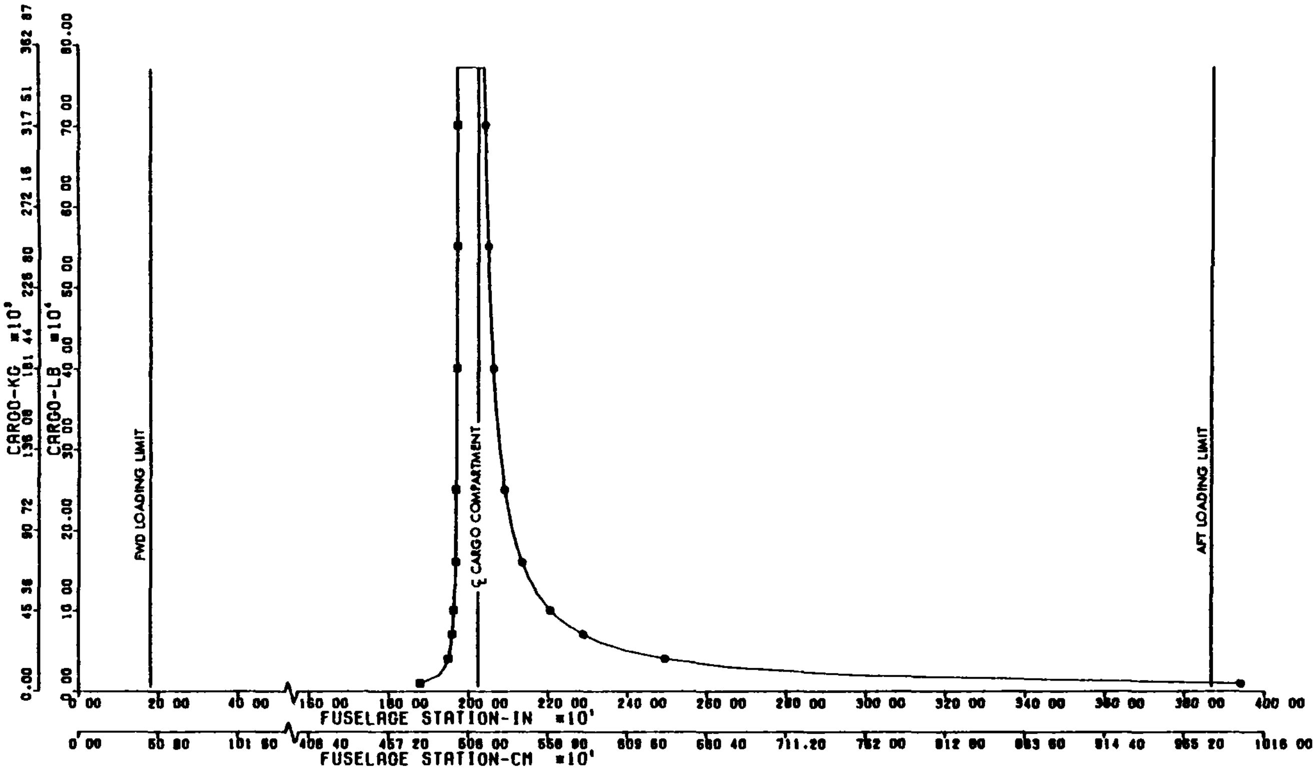

Figure 99. Payload Loading Envelope - Single Body Reference Aircraft

ITEM	POUNDS	KILOGRAMS
STRUCTURE	(536973)	(243567)
WING	197341	89512
HORIZONTAL TAIL	10645	4829
VERTICAL TAIL	8020	3639
FUSELAGE	236153	107117
NOSE LANDING GEAR	8514	3862
MAIN LANDING GEAR	56982	25846
NACELLE	7525	3413
PYLON	11793	5349
PROPULSION SYSTEM	(109661)	(49741)
ENGINES	86035	39025
FUEL SYSTEM	5952	2700
THRUST REVERSERS	14453	6555
MISCELLANEOUS	3221	1461
SYSTEMS AND EQUIPMENT	(50086)	(22719)
AUXILIARY POWER SYSTEM	2082	944
SURFACE CONTROLS	13649	6191
INSTRUMENTS	3119	1415
HYDRAULIC AND PNEUMATIC	6361	2885
ELECTRICAL	6095	2766
AVIONICS	2400	1089
FURNISHINGS	9946	4511
AIR CONDITIONING & ANTI-ICE	6070	2753
AUXILIARY GEAR EQUIPMENT	364	165
WEIGHT EMPTY	(696720)	(316027)
OPERATING EQUIPMENT	16621	7539
OPERATING WEIGHT	(713341)	(323566)
CARGO	771618	350000
ZERO FUEL WEIGHT	(1484959)	(673566)
FUEL	484224	219640
GROSS WEIGHT	(1969183)	(893206)
AMPR WEIGHT	(574023)	(260372)

Figure 100. Group Weight Summary - Two-Body MB1 Aircraft

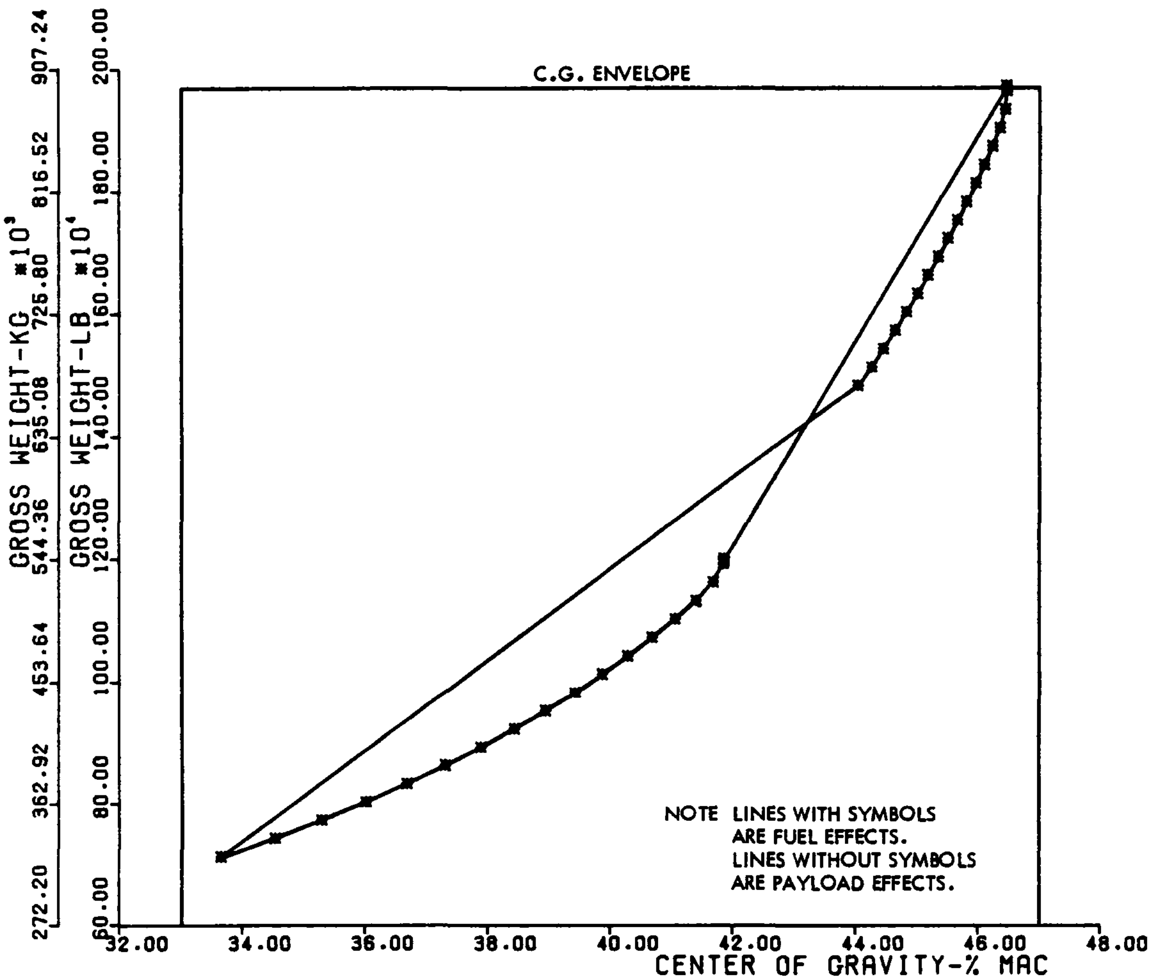

Figure 101. Center of Gravity Envelope - Two-Body MB1 Aircraft

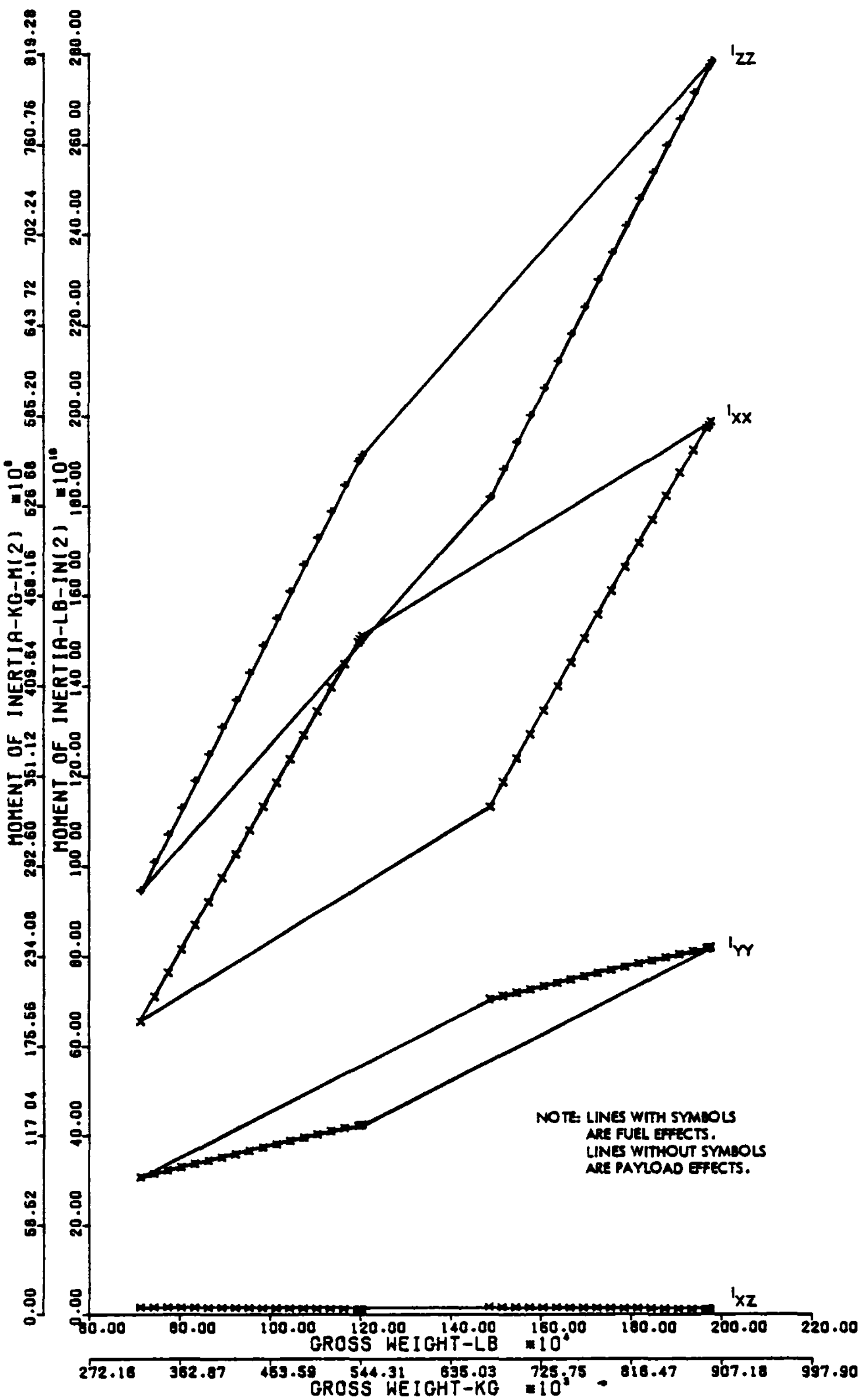

Figure 102. Moment of Inertia Envelope - Two-Body MB1 Aircraft

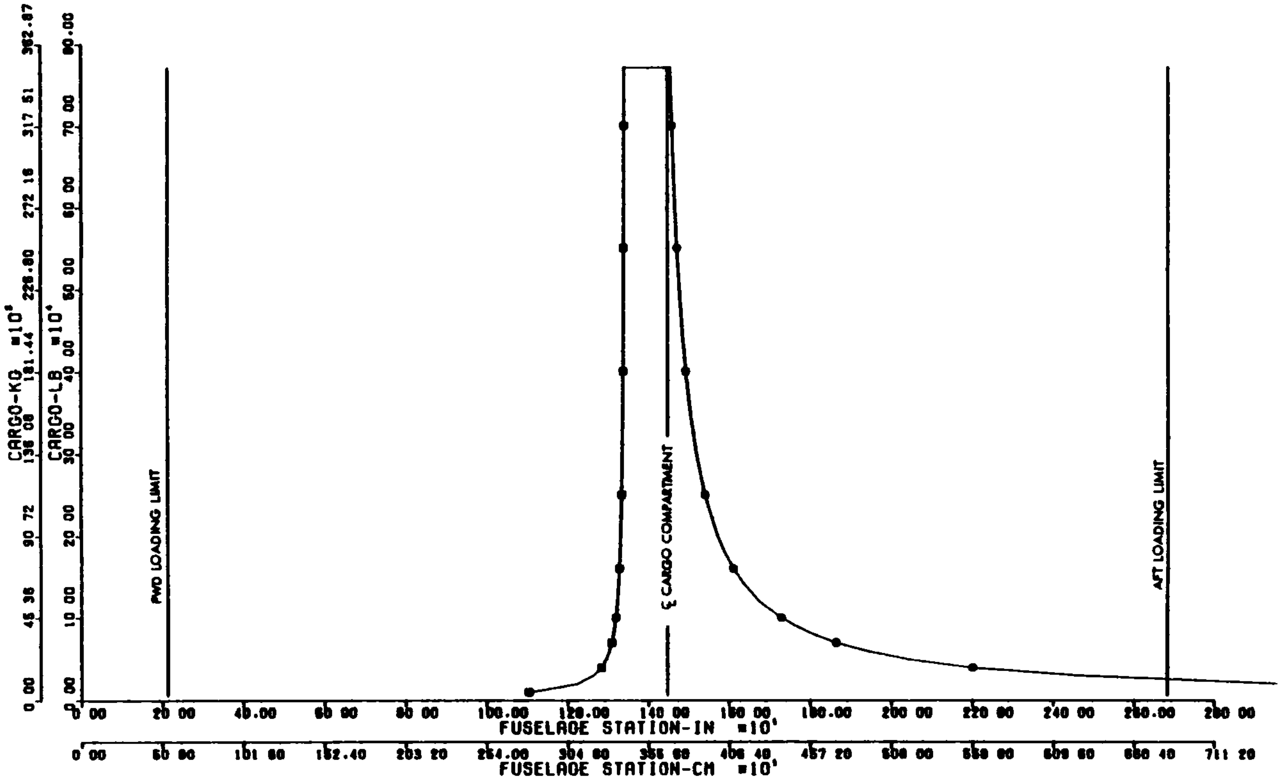

Figure 103. Payload Loading Envelope - Two-Body MB1 Aircraft

ITEM	POUNDS	KILOGRAMS
STRUCTURE	(571698)	(259318)
WING	232714	105557
HORIZONTAL TAIL	10729	4867
VERTICAL TAIL	8158	3700
FUSELAGE	236282	107176
NOSE LANDING GEAR	8567	3887
MAIN LANDING GEAR	57332	26005
NACELLE	7066	3205
PYLON	10850	4921
PROPULSION SYSTEM	(100818)	(45730)
ENGINES	78739	35715
FUEL SYSTEM	5763	2614
THRUST REVERSERS	13227	6000
MISCELLANEOUS	3089	1401
SYSTEMS AND EQUIPMENT	(50226)	(22782)
AUXILIARY POWER SYSTEM	2078	942
SURFACE CONTROLS	13796	6258
INSTRUMENTS	3154	1431
HYDRAULIC AND PNEUMATIC	6429	2916
ELECTRICAL	6004	2723
AVIONICS	2400	1089
FURNISHINGS	9946	4511
AIR CONDITIONING & ANTI-ICE	6056	2747
AUXILIARY GEAR EQUIPMENT	363	165
WEIGHT EMPTY	(722742)	(327830)
OPERATING EQUIPMENT	16378	7429
OPERATING WEIGHT	(739120)	(335259)
CARGO	771618	350000
ZERO FUEL WEIGHT	(1510738)	(685259)
FUEL	453886	205879
GROSS WEIGHT	(1964624)	(891138)
AMPR WEIGHT	(607155)	(275401)

Figure 104. Group Weight Summary - Two-Body MB2 Aircraft

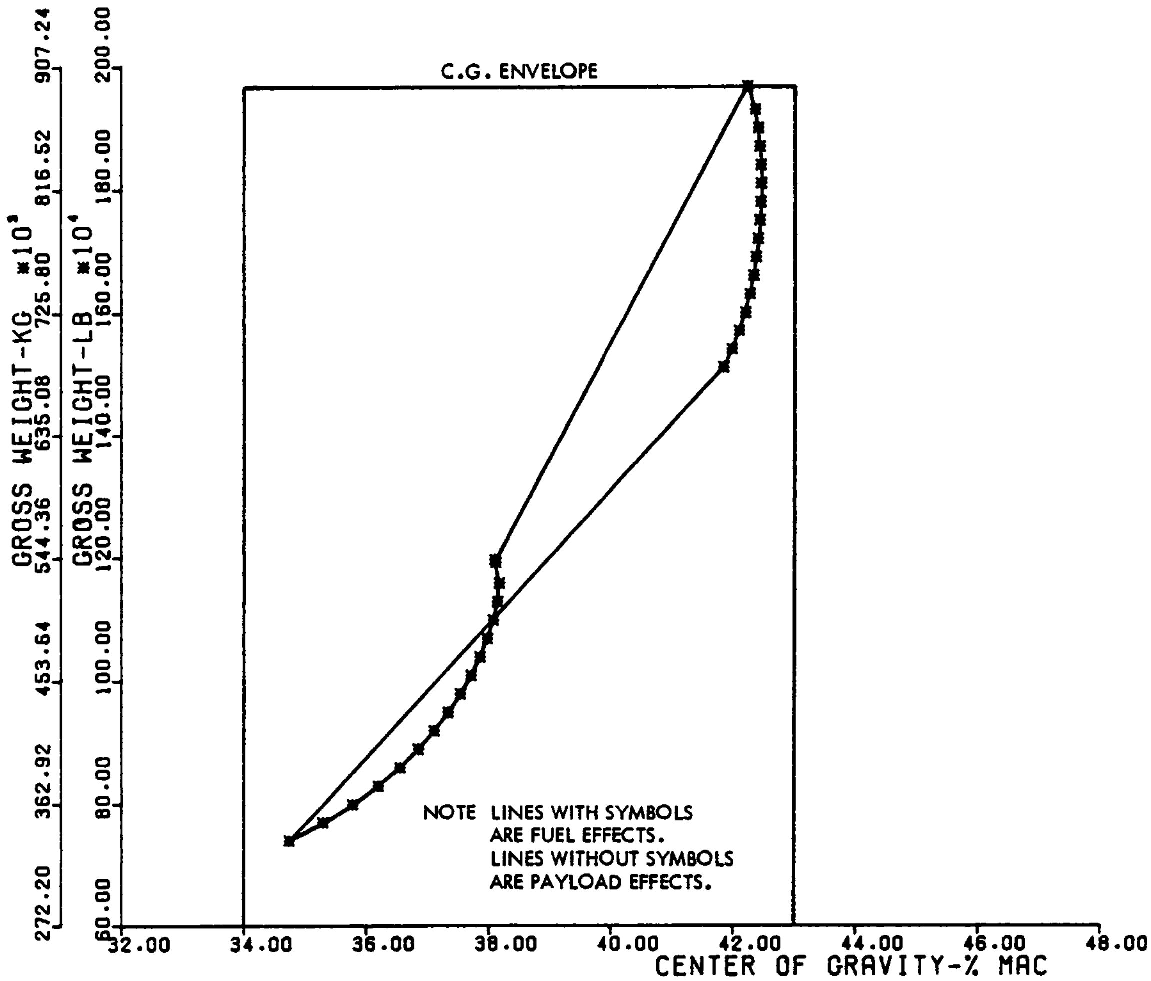

Figure 105. Center of Gravity Envelope - Two-Body MB2 Aircraft

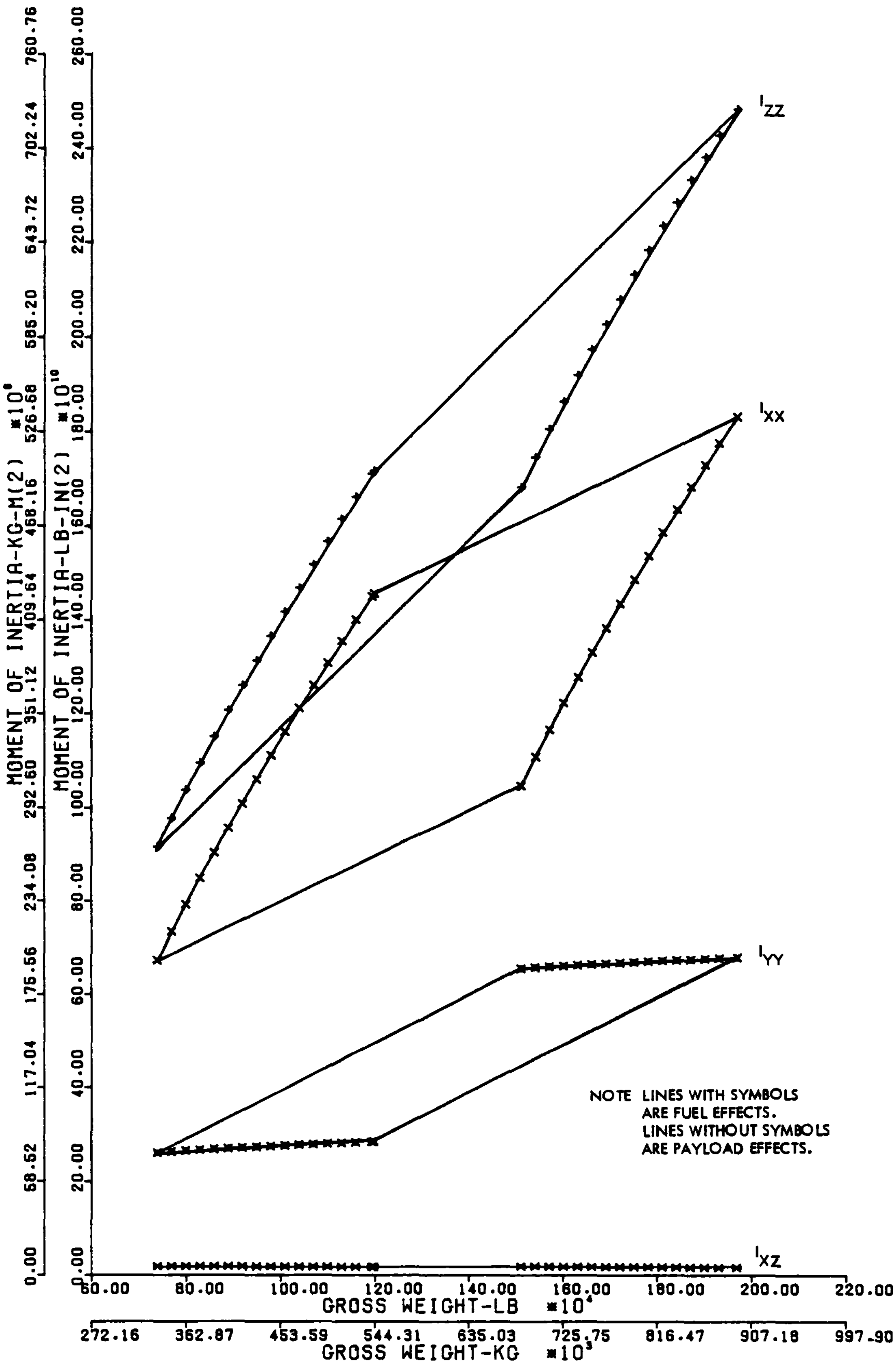

Figure 106. Moment of Inertia Envelope - Two-Body MB2 Aircraft

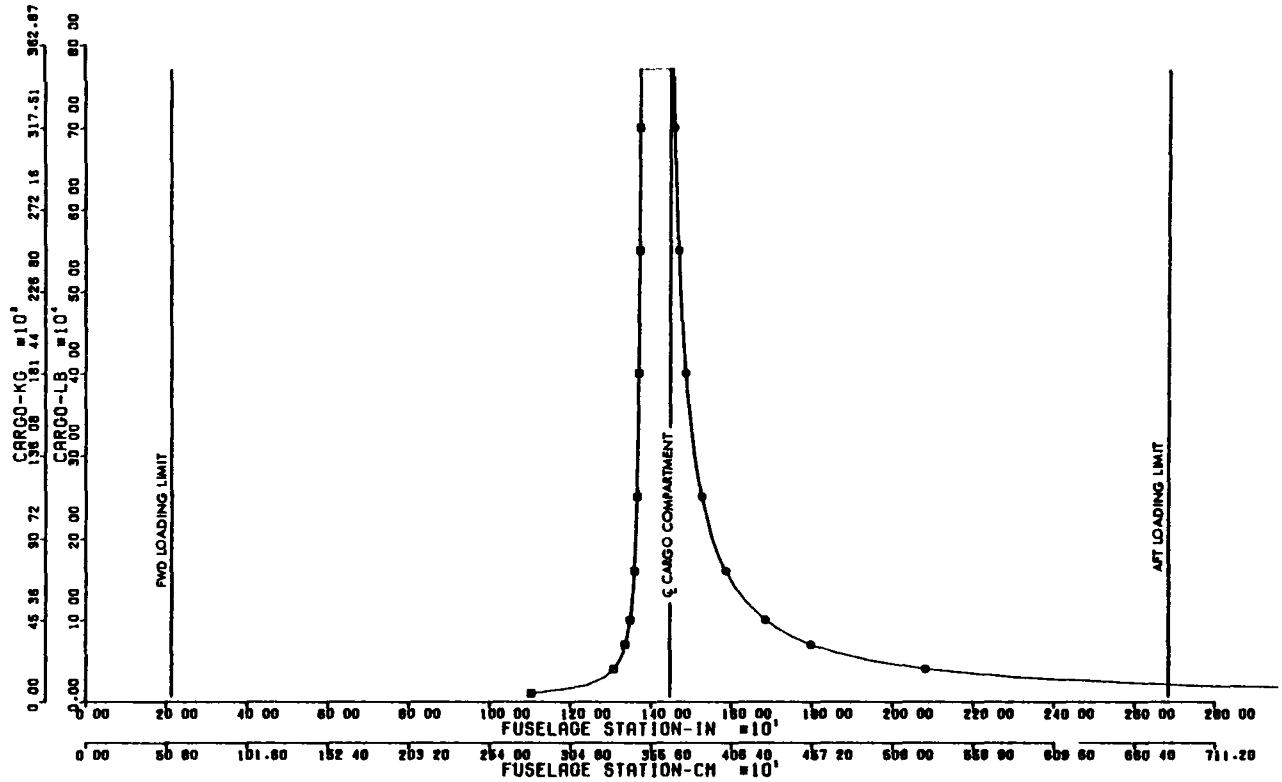

Figure 107. Payload Loading Envelope - Two-Body MB2 Aircraft

ITEM	POUNDS	KILOGRAMS
STRUCTURE	(562791)	(255278)
WING	224540	101850
HORIZONTAL TAIL	14774	6701
VERTICAL TAIL	10835	4915
FUSELAGE	226916	102927
NOSE LANDING GEAR	8646	3922
MAIN LANDING GEAR	57862	26246
NACELLE	7493	3399
PYLON	11725	5318
PROPULSION SYSTEM	(108637)	(49277)
ENGINES	85513	38788
FUEL SYSTEM	5980	2699
THRUST REVERSERS	14366	6516
MISCELLANEOUS	2808	1274
SYSTEMS AND EQUIPMENT	(51813)	(23502)
AUXILIARY POWER SYSTEM	2106	955
SURFACE CONTROLS	14126	6408
INSTRUMENTS	3308	1500
HYDRAULIC AND PNEUMATIC	6583	2986
ELECTRICAL	6383	2895
AVIONICS	2400	1089
FURNISHINGS	10453	4742
AIR CONDITIONING & ANTI-ICE	6085	2760
AUXILIARY GEAR EQUIPMENT	369	167
WEIGHT EMPTY	(723241)	(328056)
OPERATING EQUIPMENT	16618	7538
OPERATING WEIGHT	(739859)	(335594)
CARGO	771618	350000
ZERO FUEL WEIGHT	(1511477)	(685594)
FUEL	484197	219628
GROSS WEIGHT	(1995674)	(905222)
AMPR WEIGHT	(600452)	(272360)

Figure 108. Group Weight Summary - Three-Body MB3 Aircraft

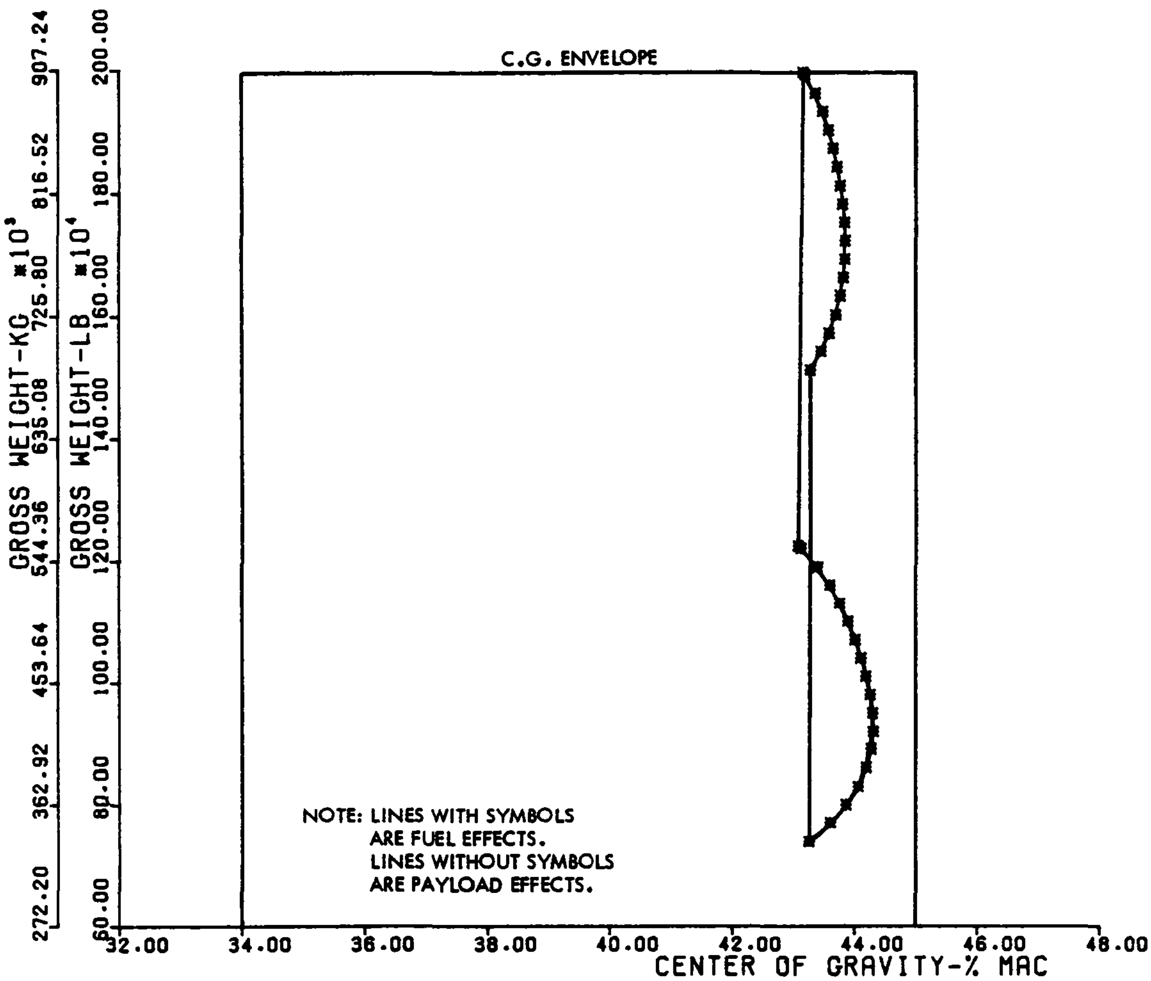

Figure 109. Center of Gravity Envelope - Three-Body MB3 Aircraft

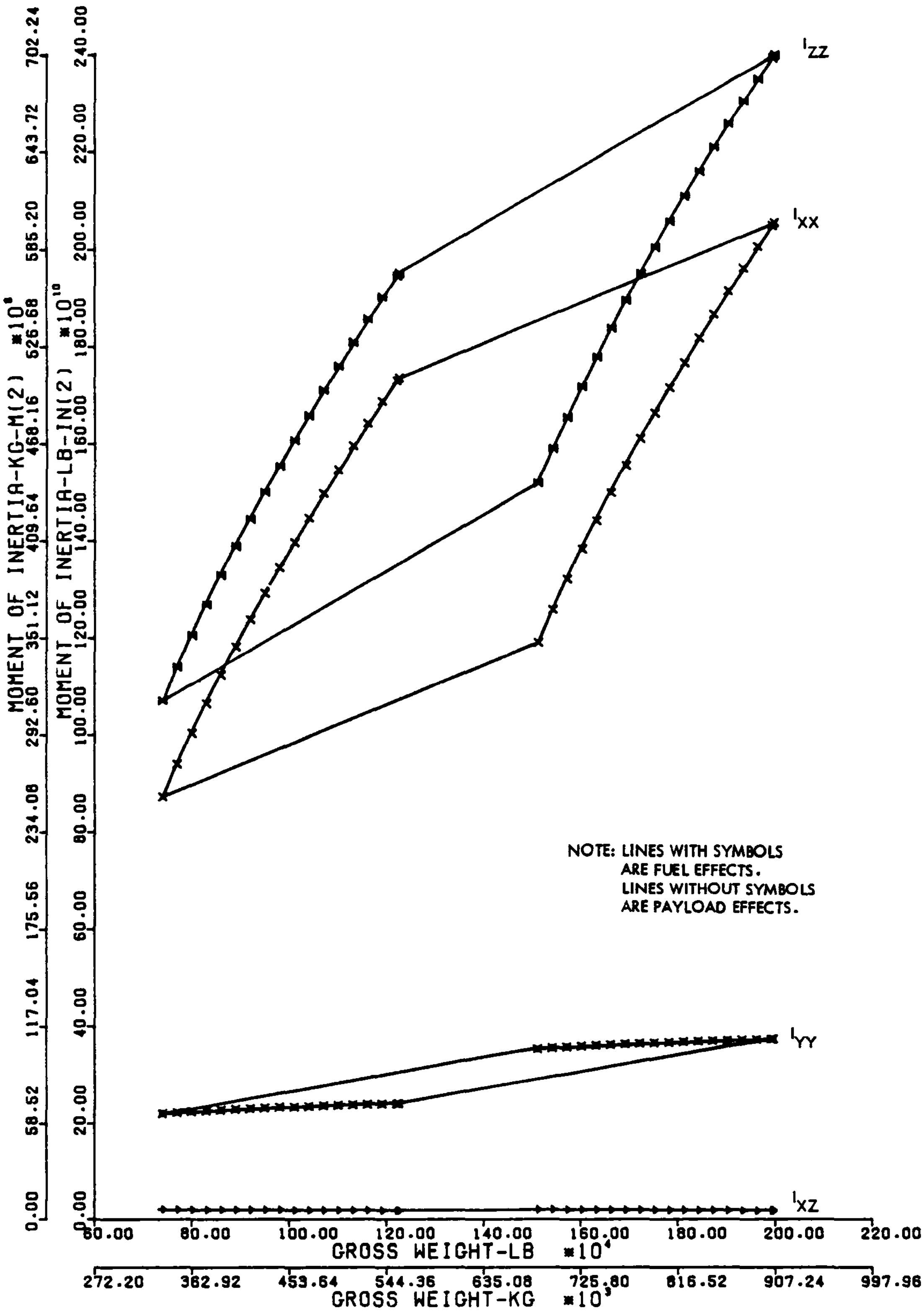

Figure 110. Moment of Inertia Envelope - Three-Body MB3 Aircraft

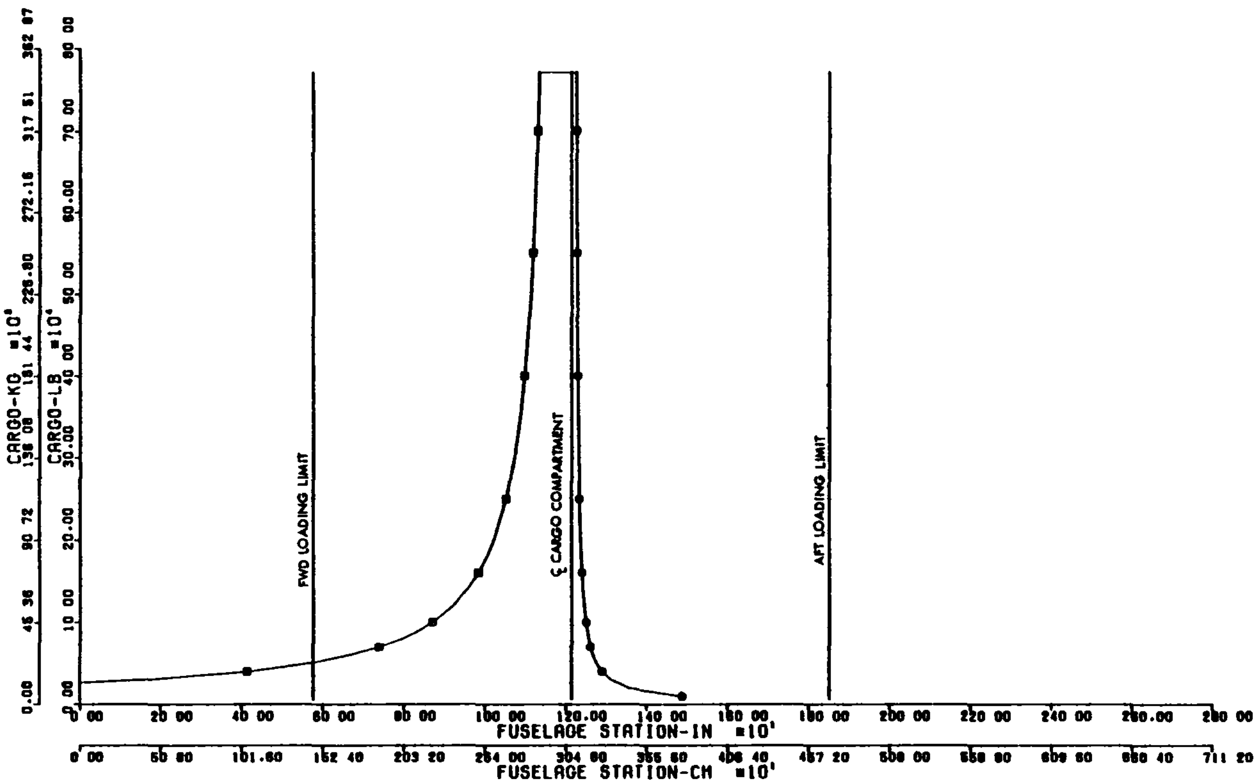

Figure 111. Payload Loading Envelope - Three-Body MB3 Aircraft

(650 ft) which precludes the use of cutback. The exceedance problem is aggravated by the fact that the Stage 3 limits have a ceiling limit for weights greater than about 362,874 kg (800,000 lb). Nominal compliance with the limits typically requires airplane noise reductions of 3 EPNdB at the takeoff sideline location, 10 EPNdB at the takeoff flyover location, and 6 EPNdB at the approach flyover location. In practice, the need for an acoustic design tolerance will increase these noise reduction requirements. Aircraft noise reduction can be obtained by the use of alternate engines designed for low-noise, more nacelle acoustic treatment, and improved aircraft FAR 36 performance. These noise reductions will probably not be sufficient to ensure Stage 3 compliance. Aircraft operation at reduced takeoff and landing weights which provide compliance with the Stage 3 limits when necessary is possible, though not economically feasible. Considerable noise reduction could be obtained by mounting the engines above the wing and fuselages. Relaxation of the Stage 3 noise limits to permit a continued increase in allowable noise with weight above 362,874 kg (800,000 lb) may be possible. Design of any aircraft on the order of 907,185 kg (2,000,000 lb) gross weight which will meet the FAR 36 Stage 3 ceiling limits is a challenging problem!

2.7.4.1 Requirements and Design Approach

New commercial aircraft are required to comply with the noise requirements of FAR Part 36, Stage 3 limits shown in Figure 112. Compliance with the noise limits must eventually be shown by demonstration, and the test procedures are shown in Figure 113. The noise limits are a function of takeoff gross weight (TOGW) except above 385,554 kg (850,000 lb) when the noise limits become constant. In these acoustic analyses, aircraft certification noise predictions are made for the conditions shown in Figure 113. Aircraft noise predictions are nominal levels, whereas the noise limits are "not-to-be-exceeded" noise levels. To ensure demonstration compliance with the not-to-be-exceeded limits, part of the prediction procedure also requires the assessment of a noise design tolerance to cover prediction, design, and test uncertainties.

Airport noise restrictions are becoming increasingly promulgated and enforced; they can take the form of daytime limits, nighttime limits, and nighttime curfews. These restrictions are aimed primarily at the noisier (non-FAR 36 complying) aircraft. Some of the nighttime restrictions are far more stringent than the Stage 3 requirements.

There is active discussion concerning the imposition of even lower noise certification limits for future new type designs, e.g., Stage 4 limits. For this study, the Stage 3 limits are as-

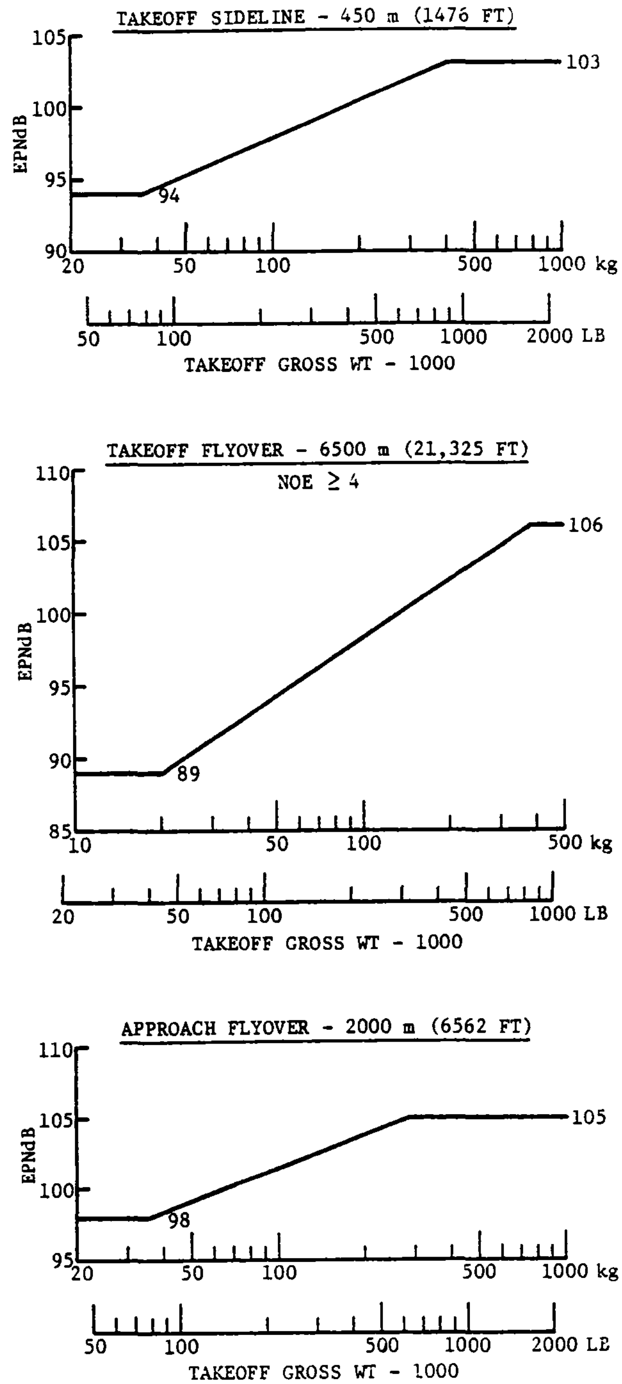

Figure 112. FAR 36 Stage 3 Noise Limits

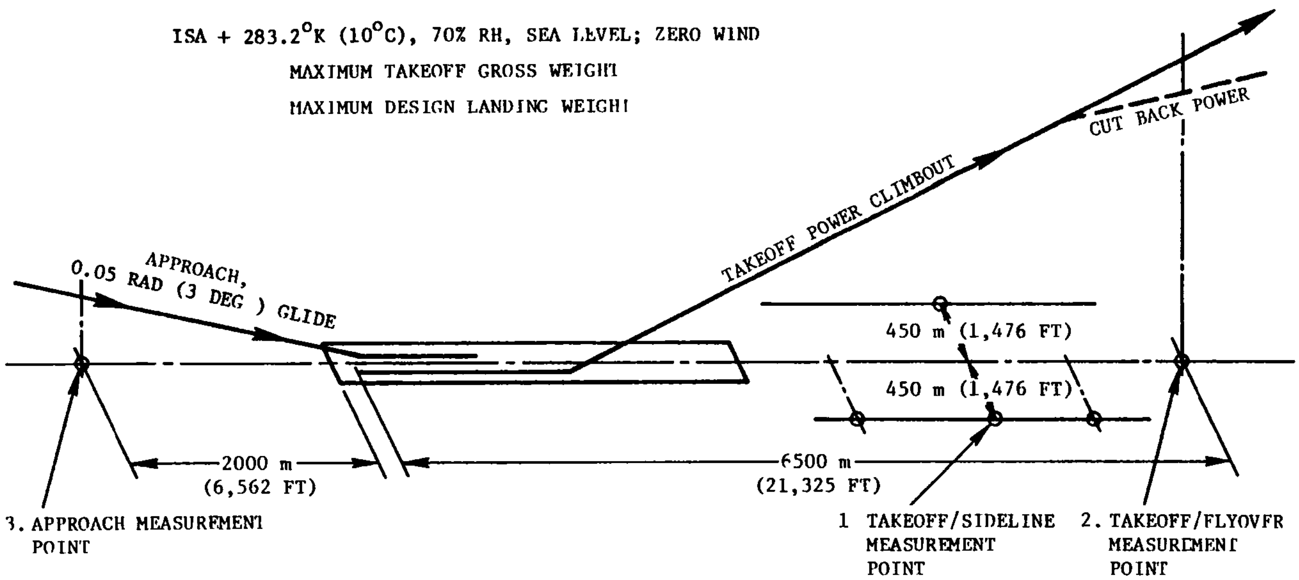

Figure 113. FAR 36 Noise Demonstration Procedure

sumed to be the applicable limits, for aircraft introduced into service in 1990, and a design tolerance is not included.

2.7.4.2 Aircraft Noise Sources

The four point design aircraft which are acoustically analyzed are shown in Figures 25 through 28. The principal aircraft design parameters are summarized in Figure 114. Aircraft flyover total noise is made up of contributions from the propulsion system, possible jet flap interaction, and from the airframe, as discussed below.

The engines are based on the Pratt and Whitney STF 477 which have a fan pressure ratio of 1.70, a by-pass ratio of 8.0, and an overall pressure ratio of 45. This engine cycle has been optimized for fuel efficiency. Even though it has a single-stage fan with no inlet guide vanes, the high fan tip speeds and overall pressure ratios lead to noise levels higher than current commercial engines.

The engine is installed in an acoustically treated nacelle which has extensive wall treatment in the inlet, fan discharge, and turbine discharge sections. Propulsion noise is the dominant aircraft noise source.

The engines are conventionally mounted below the wings. The flaps are continuous along the trailing edge without spanwise gaps behind the engines. Thus, for small spacings between wing and pylon, additional noise can be generated depending upon engine efflux velocity (power setting) and flap deflection. This noise source can

METRIC UNITS

					AIRPLANE PERFORMANCE PARAMETERS OVER THE TAKEOFF FLYOVER MEASUREMENT POINT			AIRPLANE PERFORMANCE PARAMETERS OVER THE APPROACH FLYOVER MEASUREMENT POINT		
AIRCRAFT	TOGW kg	NUMBER OF FUSELAGES	ENGINE SSLT N	NUMBER OF ENGINES	FLAP DEFLECTION RAD	V_2 + 5.14 TAS m/SEC	HEIGHT AT 6.5 km, m	FLAP DEFLECTION RAD	1.3 V_s + 5.14 TAS m/SEC	POWER SETTING %
SBR	957,987	1	330,948	6	0.45	83.85	192.94	0.86	80.25	41
MB1	893,123	2	308,707	6	0.54	82.83	194.46	0.87	81.28	39
MB2	891,309	2	285,576	6	0.37	81.28	202.69	0.82	74.08	39
MB3	905,370	3	306,927	6	0.65	80.77	200.86	0.87	80.25	34

CUSTOMARY UNITS

					AIRPLANE PERFORMANCE PARAMETERS OVER THE TAKEOFF FLYOVER MEASUREMENT POINT			AIRPLANE PERFORMANCE PARAMETERS OVER THE APPROACH FLYOVER MEASUREMENT POINT		
AIRCRAFT	TOGW LB	NUMBER OF FUSELAGES	ENGINE SLST LB	NUMBER OF ENGINES	FLAP DEFLECTION °	V_2 + 10 KTAS	HEIGHT AT 21,325 FT, FT	FLAP DEFLECTION DEG.	1.3 V_s + 10 KTAS	POWER SETTING %
SBR	2,112,000	1	74,400	6	26	163	633	49	156	41
MB1	1,969,000	2	69,400	6	31	161	638	50	158	39
MB2	1,965,000	2	64,200	6	21	158	665	47	144	39
MB3	1,996,000	3	69,000	6	37	157	659	50	156	34

Figure 114. FAR 36 Performance Parameters - Point Design Aircraft

be significant on takeoff and approach.

The airframe noise component is most important on approach; it's principal subcomponents are the landing gear system (wheels and wells) and the high-lift system (wing leading edge slats and trailing edge flaps). The noise estimates show that the large landing gear required for these aircraft can be a particularly significant noise source.

2.7.4.3 FAR 36 Performance

The predicted FAR 36 aircraft performance characteristics are summarized in Figure 114. Typically the aircraft achieves an altitude over the takeoff flyover location of 198.1 m (650 ft). FAR 36 permits a power cutback - hence a noise reduction - when the aircraft has achieved an altitude of 210.0 m (689 ft). (For maximum noise reduction benefit, this minimum cutback altitude should be achieved just prior to the noise measurement point). None of the point design aircraft achieves this altitude and thus cannot take advantage of this noise reduction technique. If an altitude of 243.8 m (800 ft) could be attained, reduction of approximately 4 EPNdB would be obtained through a combination of increased altitude and allowable cutback. Included in all the aircraft performance estimates are some penalties associated with the acoustic treatment in the nacelle, e.g., a weight increase, a thrust loss, and an SFC increase.

2.7.4.4 Aircraft Noise Levels

The predicted aircraft noise levels at the three noise certification points are summarized in Figures 115 and 116. The single body reference aircraft is the heaviest and the noisiest. All the multibody aircraft have a small acoustical advantage over the single body reference aircraft which arises principally because of their smaller engines, slightly better climb out performance, and lower power settings required on approach. The three-body MB3 aircraft is the least noisy being an average 1.4 EPNdB less noisy at each location. It also has the highest wing aspect ratio. However, all the aircraft exceed the Stage 3 limits at all locations. These areas are typically 3 EPNdB at the sideline location, 10 EPNdB at the takeoff flyover location, and 6 EPNdB at the approach flyover location. The principal causes of these exceedances are:

(a) The propulsion system has high noise levels.

(b) The aircraft do not attain an altitude over the takeoff flyover noise measurement point which is high enough to allow a power cutback.

	FAR 36 MEASURE POINTS			ΣΔ EPNdB REF LIMIT OVER THREE POINTS	ΣΔ EPNdB REF SBR OVER THREE POINTS
	TAKEOFF SIDELINE 450 m (1,475 FT)	TAKEOFF FLYOVER 6500 m (21,325 FT)	APPROACH FLYOVER 2000 m (6,562 FT)		
STAGE 3 LIMIT, EPNdB →	103	106	105		
SBR, NOISE LEVEL, EPNdB (REF. LIMIT, ΔEPNdB)	106 3 (+3 3)	116 2 (+10 2)	112 5 (+7 5)	+21.0	REF
MB1, NOISE LEVEL, EPNdB (REF LIMIT, ΔEPNdB)	106.0 (+3.0)	115 8 (+9 8)	111 8 (+6.8)	+19 6	-1 4
MB2, NOISE LEVEL, EPNdB (REF LIMIT, ΔEPNdB)	105 6 (+2 6)	115 0 (+9 0)	111.6 (+6 6)	+18 2	-1 8
MB3, NOISE LEVEL, EPNdB (REF LIMIT, ΔEPNdB)	105 9 (+2 9)	115 4 (+9 4)	109 6 (+4.6)	+16.9	-4 1

Figure 115. FAR 36 Noise Levels - Point Design Aircraft

(c) The Stage 3 noise limits have a ceiling value for aircraft weights greater than about 362,874 kg (800,000 lb).

2.7.4.5 Stage 3 Compliance Design

For nominal FAR 36 compliance, aircraft noise reductions of 10 EPNdB are required on takeoff and 6 EPNdB on approach. Should an acoustic design tolerance be required, larger noise reductions will be needed. A reduction of the aircraft noise levels could be obtained in the following ways:

(a) Consideration of alternate, less noisy engines (turbofans or profans, about 5 dB less noisy).

(b) Incorporation of more acoustic treatment in the nacelles (probably acoustic flow splitters).

(c) Improvement of FAR 36 takeoff and landing performance (this could provide some small noise reductions, and possibly some operating restrictions on flap settings).

(d) Operation of the aircraft at reduced weights (which show Stage 3 compliance) only at airports where such compliance is necessary and obtain a deviation for maximum weight operation at non-noise sensitive airports.

(e) Placement of engines over the wings and fuselages to provide acoustic shielding, as shown schematically in Figure 117.

The design of a multibody aircraft weighing about 907,185 kg (2,000,000 lb), or any other type of very heavy aircraft, requiring compliance with the FAR 36 Stage 3 noise limits is a formidable noise control task.

2.7.4.6 FAR 36 Compliance vs Aircraft Size

These aircraft will probably perform unique missions which will require operation from special runways; it may be possible to obtain exemption from Stage 3 requirements.

One of the causes of the Stage 3 exceedance is that the noise limits are constant at weights greater than about

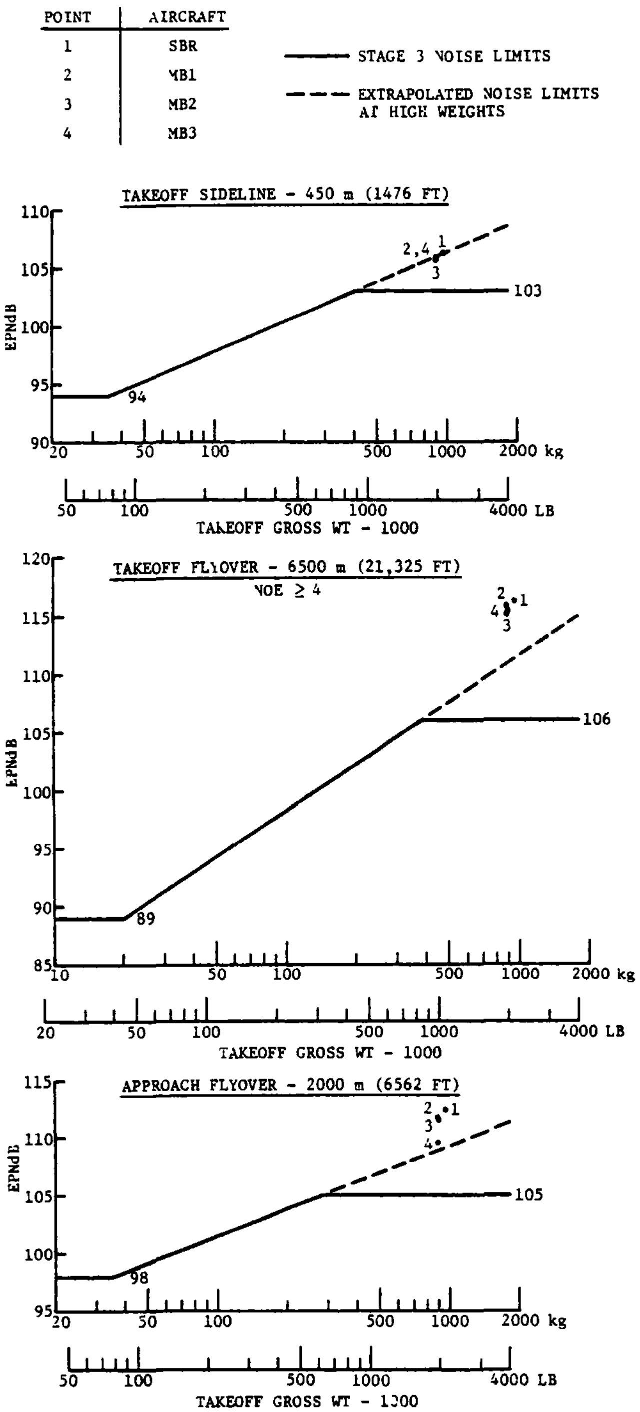

Figure 116. FAR 36 Noise Levels vs Gross Weight - Point Design Aircraft

362,874 kg (800,000 lb). This requires that a 907,185 kg (2,000,000 lb) aircraft should make no more noise than a 362,874 kg (800,000 lb) aircraft; thus considerably more noise control must be built into the heavier airplanes. The Stage 3 noise limit constants originate from the regulatory desire to place a ceiling on single event flyover noise and were established before aircraft maximum weights of more than 453,592 kg (1,000,000 lb) were being considered. If the Stage 3 limits were changed to allow a continuation of the increase of noise with weight, as shown in Figure 116, compliance would be considerably eased. FAR 36, as it is currently written, discriminates against very heavy aircraft - regardless of how efficient and productive they may be. In effect, FAR 36 places a limit on allowable commercial aircraft size.

2.7.5 Configuration Design

The structural arrangement concept, basic dimensions, and general aircraft characteristics are given in Figures 118 through 121 for two-body MB2 type aircraft. Although these data were prepared for an earlier version of the point design MB2 aircraft, conceptual definition is the same; however, small dimensional differences do occur. Data are shown in terms of buttock lines, waterlines, fuselage stations, and wing stations. The data in Figure 118 show the fuselage and cargo compartment geometry and the location of the major components relative to the fuselage.

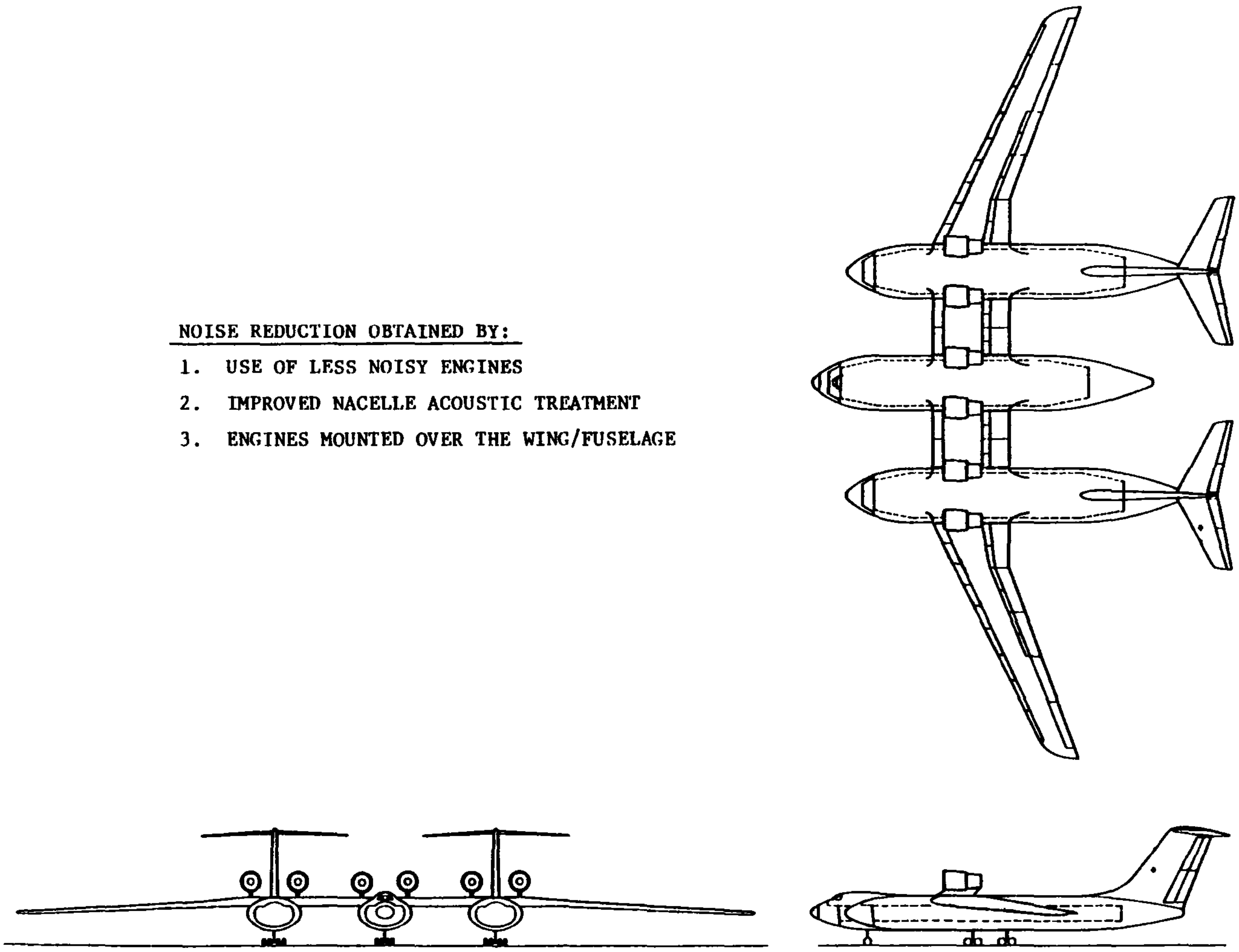

Figure 117. Possible Stage 3 Configuration - Three-Body MB3 Aircraft

Basic wing data, geometry, and locations of major structural members and manufacturing breaks are shown in Figure 119. The wing structure consists of a two-spar single cell primary structure, made up of an inner panel between the fuselages, and a center and outer panel mounted outboard of each fuselage. The inner wing panel is unswept. The lower surface lies on a waterline plane which is aligned with the ceiling of the cargo compartment and the carry-thru structure in the fuselage. The center and outer wing panels have 0.47 rad (26.73 degrees) leading edge sweep and have an anhedral of 0.05 rad (3 degrees) measured between the wing reference and waterline planes. The wing twist schedule is linear, with the maximum twist occurring at the centerline of the total wing, proceeding to zero twist at the

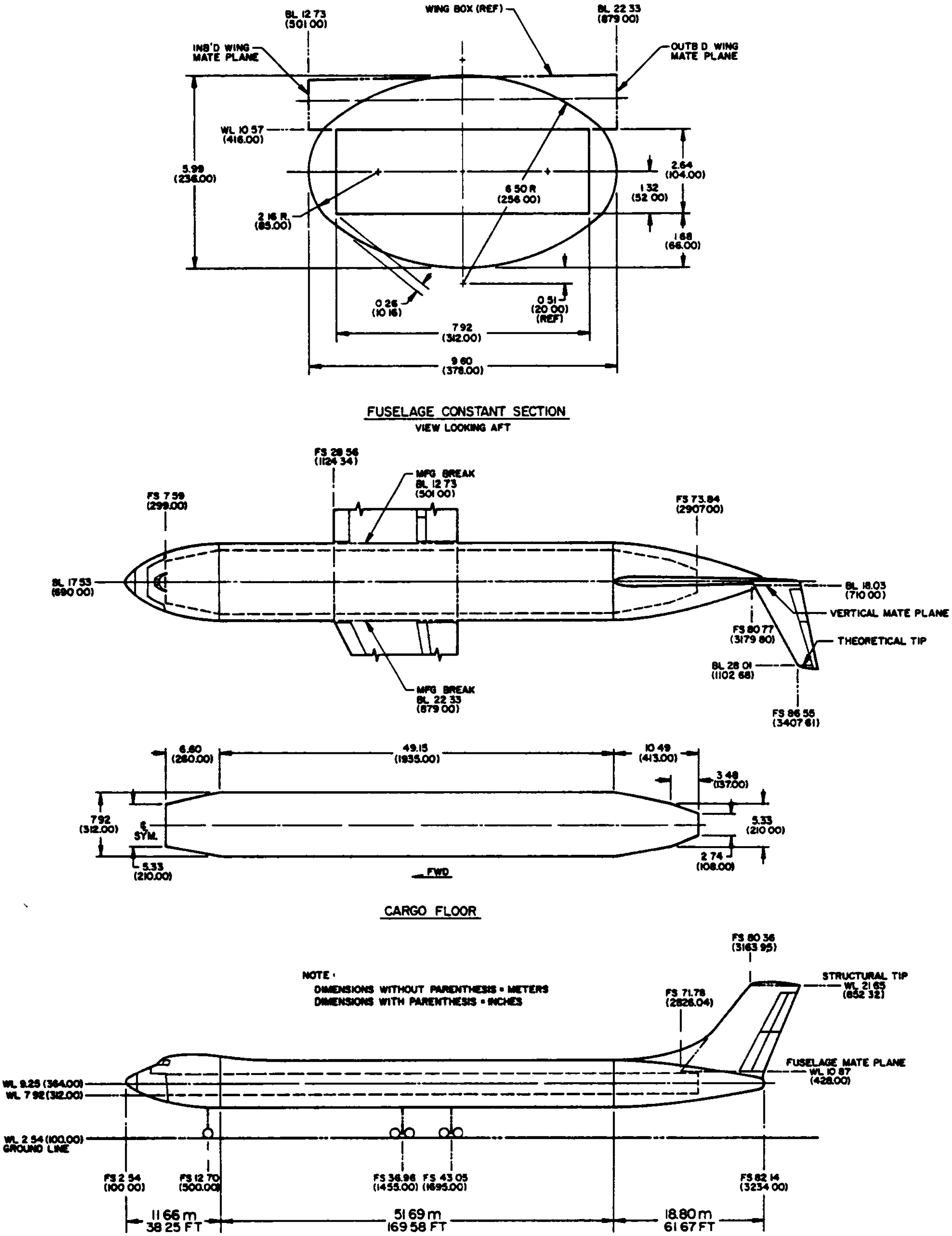

Figure 118. Fuselage Basic Dimensions and Structural Arrangement - Two-Body MB2 Aircraft

WING DATA

SPAN - THEORETICAL TIP	125 13 m (410 54 FT)	
ASPECT RATIO	10 74 (AERO)	11 18 (GEOM)
AREA	1,458 SQ m (15,689 SQ FT)	

CHORD LENGTH	m	(FT)	t/C - %
ROOT	15 39	50 50	10 81
INB'D BREAK	15 39	50 50	12 70
OUTB'D BREAK	10 88	35 70	11 11
MAC	12 62	41 39	-
STRUCTURAL TIP	6 50	21 32	11 67
THEORETICAL TIP	6 22	20 40	11 73

	INNER PANEL		CENTER PANEL		OUTER PANEL	
SWEEP ANGLE	RAD	(DEG)	RAD	(DEG)	RAD	(DEG)
LEADING EDGE	0	0	0 47	26 73	0 47	26 73
FWD BEAM	0	0	0 40	23 17	0 45	25 70
25 % CHORD LINE	0	0	0 36	20 70	0 44	25 00
AFT BEAM	0	0	0 17	10 00	0 39	22 13
TRAILING EDGE	0	0	0	0	0 34	19 52

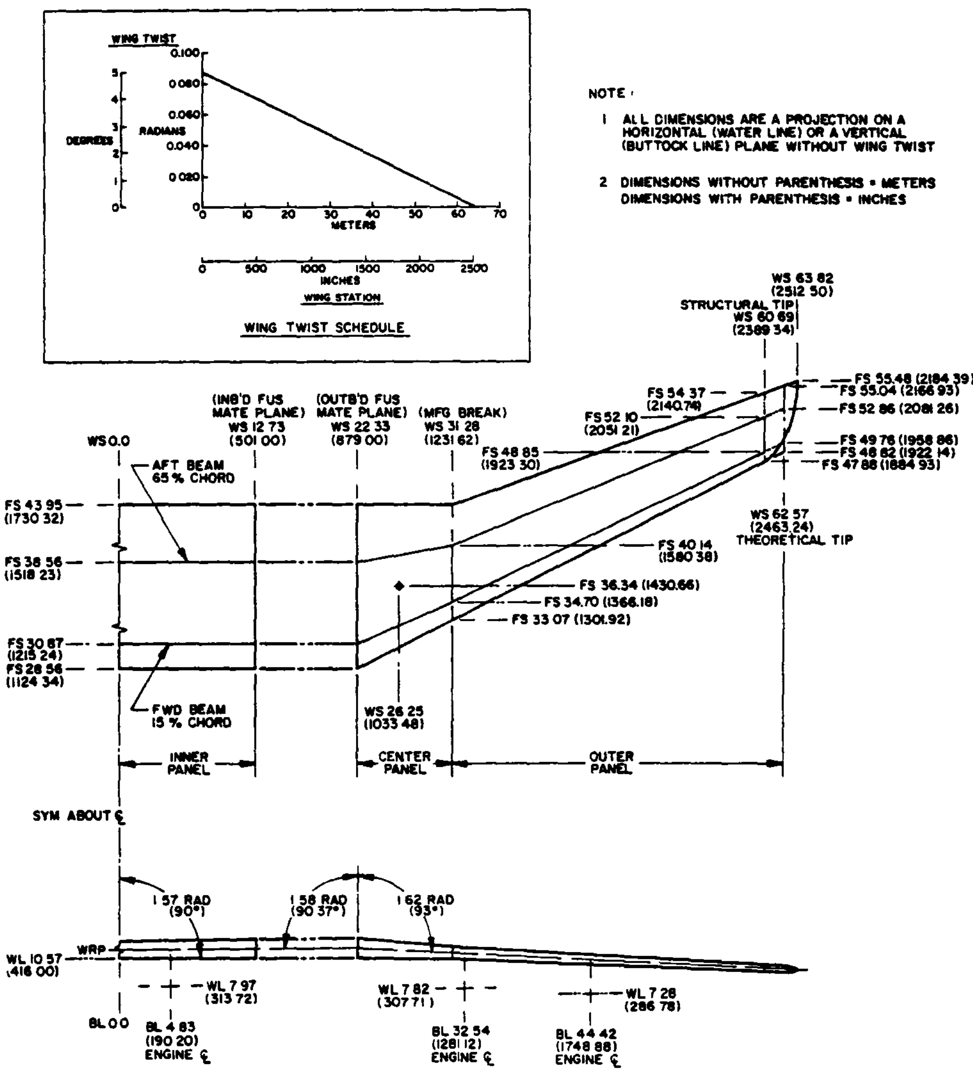

Figure 119. Wing Basic Dimensions and Structural Arrangement - Two-Body MB2 Aircraft

VERTICAL STABILIZER

SPAN	10 78 m (35 36 FT)
ASPECT RATIO	1 30
t/C-%	10 50
AREA	89 34 SQ m (961 69 SQ FT)

CHORD LENGTH	m	(FT)
ROOT	10 36	34 00
MAC	8 46	27 77
TIP	6 22	20 40

SWEEP ANGLE	RAD	(DEG)
LEADING EDGE	0 67	38 53
FWD BEAM	0 65	37 15
25 % CHORD LINE	0 61	35 00
AFT BEAM	0 50	28 65
70 % HINGE LINE	0 49	27 80
85 % HINGE LINE	0 44	25 15
TRAILING EDGE	0 39	22 38

NOTE:
DIMENSIONS WITHOUT PARENTHESIS = METERS
DIMENSIONS WITH PARENTHESIS = INCHES

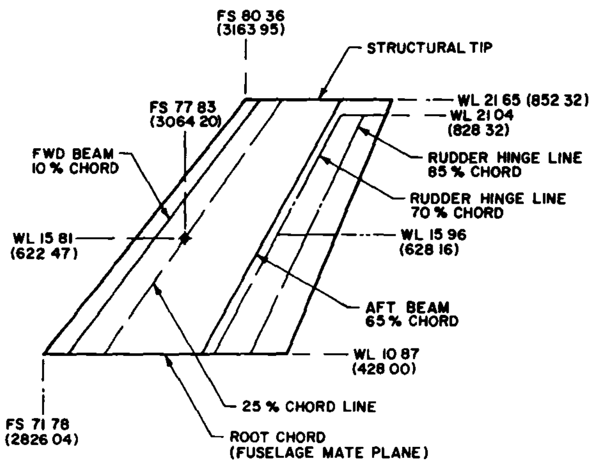

Figure 120. Vertical Stabilizer Basic Dimensions and Structural Arrangement - Two-Body MB2 Aircraft

HORIZONTAL STABILIZER

SPAN - THEORETICAL TIP	20 96 m (68 78 FT)
ASPECT RATIO	5 00 (AERO) 5 20 (GEOM)
t/C-%	8 00
AREA	87 90 SQ m (946 18 SQ FT)

CHORD LENGTH	m	(FT)
ROOT	5 99	19 65
VERT MATE PLANE	5 73	18 80
MAC	4 45	14 60
STRUCTURAL TIP	2 51	8 23
THEORETICAL TIP	2 40	7 86

SWEEP ANGLE	RAD	(DEG)
LEADING EDGE	0 50	28 90
FWD BEAM	0 48	27 37
25 % CHORD LINE	0 44	25 00
AFT BEAM	0 32	18 22
ELEVATOR HINGE LINE	0 29	16 43
TRAILING EDGE	0 21	11 82

NOTE:
DIMENSIONS WITHOUT PARENTHESIS = METERS
DIMENSIONS WITH PARENTHESIS = INCHES

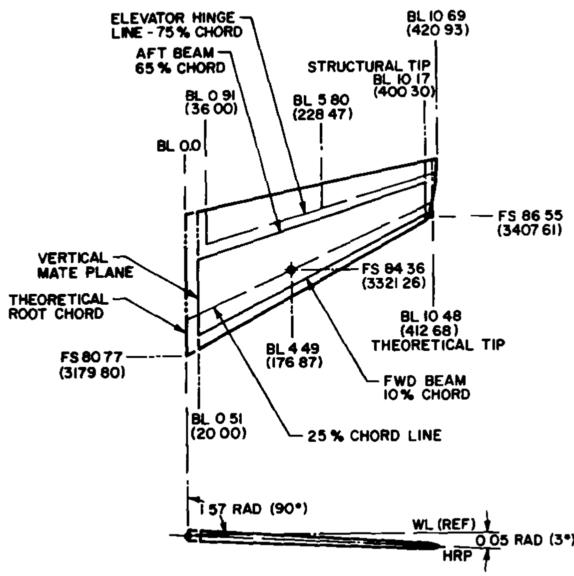

Figure 121. Horizontal Stabilizer Basic Dimensions and Structural Arrangement - Two-Body MB2 Aircraft

wing tip. The engine, nacelle, and pylon locations are shown for the semispan wing shown in Figure 119.

The empennage, which is a tee-tail configuration, consists of a fixed vertical stabilizer with a horizontal stabilizer incorporating trim capability mounted at the tip. The empennage data and geometric description are shown in Figures 120 and 121. The structural design of both stabilizers is similar to that of the wing primary structure. The structure consist of single cell box beams having spars located at 10 and 65 percent of the surface chords. Both stabilizers have fixed leading edges and the vertical stabilizer has a split double acting rudder. The horizontal stabilizer has a split elevator. The vertical stabilizer has 0.61 rad (35 degrees) of sweep measured at the 25 percent chordline (1/4 c). The sweep of the horizontal at 1/4 c is the same as that shown in Figure 119 for the wing. The anhedral is also the same as that of the center and outer wing panels.

2.7.5.1 Landing Gear Concept

Landing gear concepts for the single body and multibody aircraft are as discussed below. Each aircraft has four eight wheel bogie main gears and a rotation angle of 0.14 rad (8 degrees). The single body reference and the three-body MB3 aircraft have a four-wheel nose gear while the two-body MB1 and MB2 aircraft have a two-wheel nose gear on the centerline of each fuselage. All gears utilize 1.32m x 0.52m (52.00 in. x 20.50 in.) tires with a load capacity of 28,349.5 kg (62,500 lb). Tire and wheel spacing is shown in Figure 122.

Single Body Aircraft - The single body reference aircraft has an articulating main gear similar to the C-5 in that it rotates 1.6 rad (90 degrees) about the strut and retracts laterally about a trunnion for stowage between frames underneath the cargo floor. External pods are required only to house the structural frames, the trunnion, and the retract mechanism. The outboard main gear doors operate mechanically as a function of the gear extend and retract motion and, consequently, are not subjected to failures of an independent system. The inboard doors are mid-point folding, slide track operating, with an independent actuation system.

Lateral spacing of the struts is 13.3m (43.5 ft) and cargo floor height above ground is 7.8m (25.5 ft). This elevation is expected to present logistics problems in cargo handling functions. The floor height is a function of the 0.14 rad (8 degrees) rotation angle, fore and aft location of the

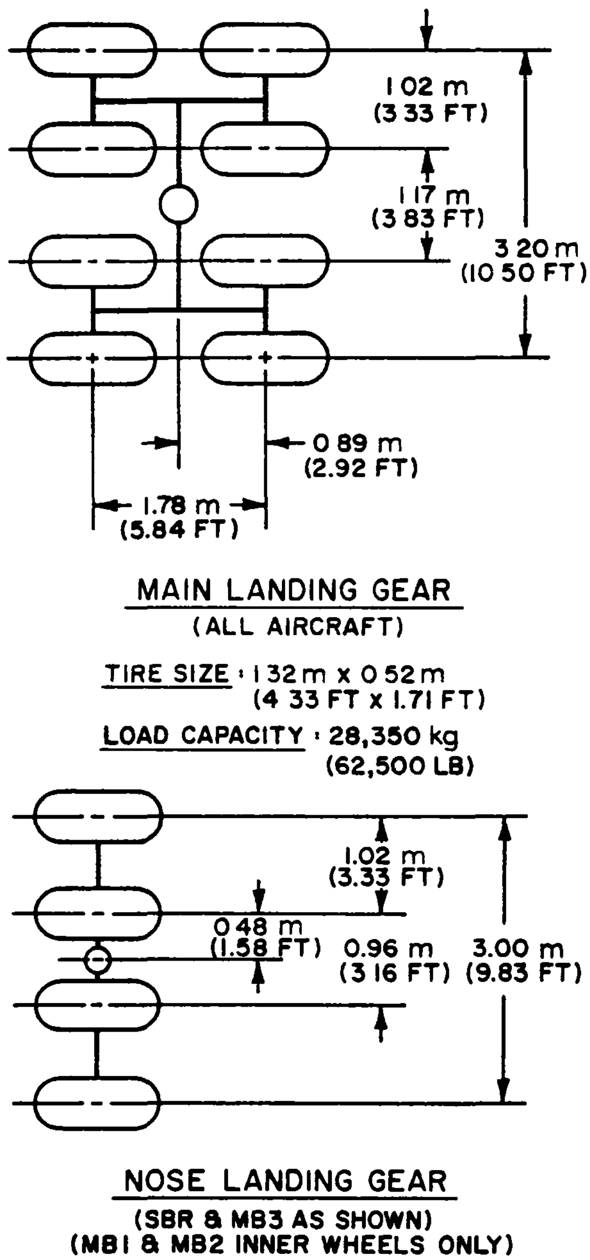

Figure 122. Wheel and Tire Spacing - Multibody Aircraft

main gear, and the 111.3m (365 ft) length required of the fuselage for the 350,000 kg (771,618 lb) payload. The floor height, as it relates to the maximum gross weight vertical cg height, and the lateral spacing, result in a tip over angle of 1.2 rad (68 degrees). This equates to a maximum allowable 0.40g turn.

The nose gear retracts forward (free fall) and is stowed underneath the cargo floor. The door operates mechanically as a function of the gear extend and retract motion. External fairings are not required for the nose gear. Extended and retracted positions are shown in Figure 123.

Two-Body Aircraft - The two-body aircraft (MB1 and MB2) have two tandem eight-wheel bogie main gears located on each fuselage centerline, laterally spaced at 39.6m (130 ft) for the two-body MB1 and 35.1m (115 ft) for the two-body MB2 aircraft. Main and nose gears retract forward (free fall) and are stowed underneath the cargo floor. External fairings are not required for the main gear nor for the two-wheel nose gear. Nose and main gear doors operate mechanically as a function of the gear extend and retract motion, hence, they do not require an independent system. Cargo floor height above ground is 5.39m (17.7 ft). Due to this height, the lateral spacing of the gears, and forces of 1.0g down and 0.50g side (turn), the tip over angle is approximately 0.40 rad (23 degrees) as shown in Figure 124. This permits a full 0.50g turn for the two-body aircraft. The maximum angle permitted for a full 0.50g turn is 1.10 rad (63.4 degrees).

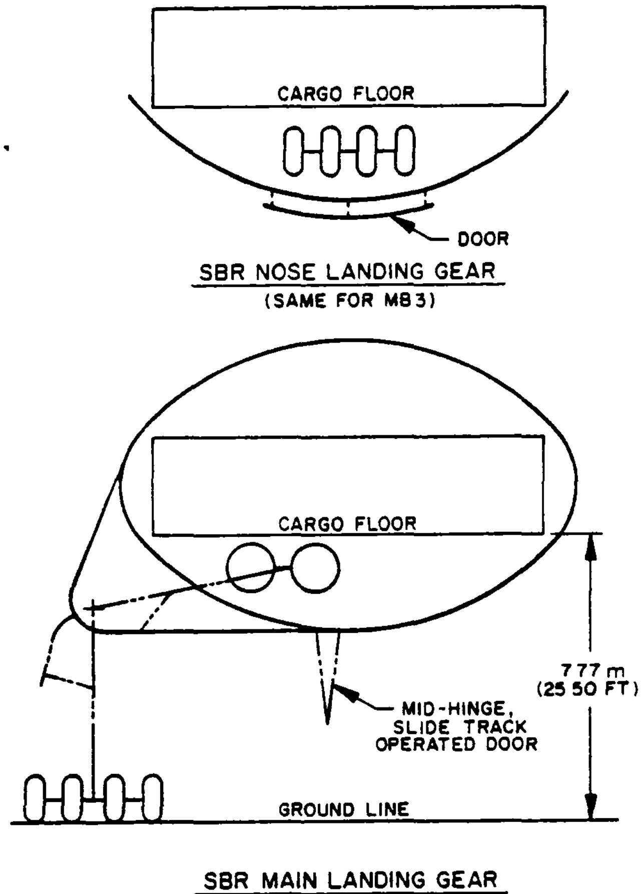

Figure 123. Landing Gear Concept - Single Body Reference Aircraft

Extended and retracted positions are shown in Figure 125.

Three-Body Aircraft - The three-body MB3 aircraft has two tandem eight-wheel bogie main gears located on each outboard fuselage centerline, laterally spaced at 39.6m (130 ft). Main and nose gear retraction, stowage, and door operation are the same as the two-body MB1 and MB2 aircraft. The four-wheel nose gear is located forward on the center fuselage centerline. Cargo floor height above ground is 4.1m (13.5 ft). The tip over angle is 0.42 rad (24 degrees) permitting a full 0.50g turn. Extended and retracted positions of the nose gear are representative of the nose gear in Figure 123 and those of the main gear in Figure 125.

2.7.6 Cost Analysis

The point design cost analysis includes both aircraft fly-away cost and direct operating cost (DOC). Sub-level breakdowns of each of these major cost elements are given for the four point design aircraft.

2.7.6.1 Fly-Away Cost

Fly-away cost consists of all cost elements associated with the purchase of the aircraft, such as research and development, airframe production, and engine costs. Fly-away cost summaries are given in Figure 126 for each of the point design aircraft.

The single body reference aircraft is representative of the aircraft used to develop the fly-away costing data base. The only costing adjustment made is to account for the oval fuselage shape as compared to the more conventional circular fuselage shape. This necessitates the addition of structure in the upper portion of the fuselage to react kick loads and to stabilize upper frames in compression. This structural change requires an approximate increase

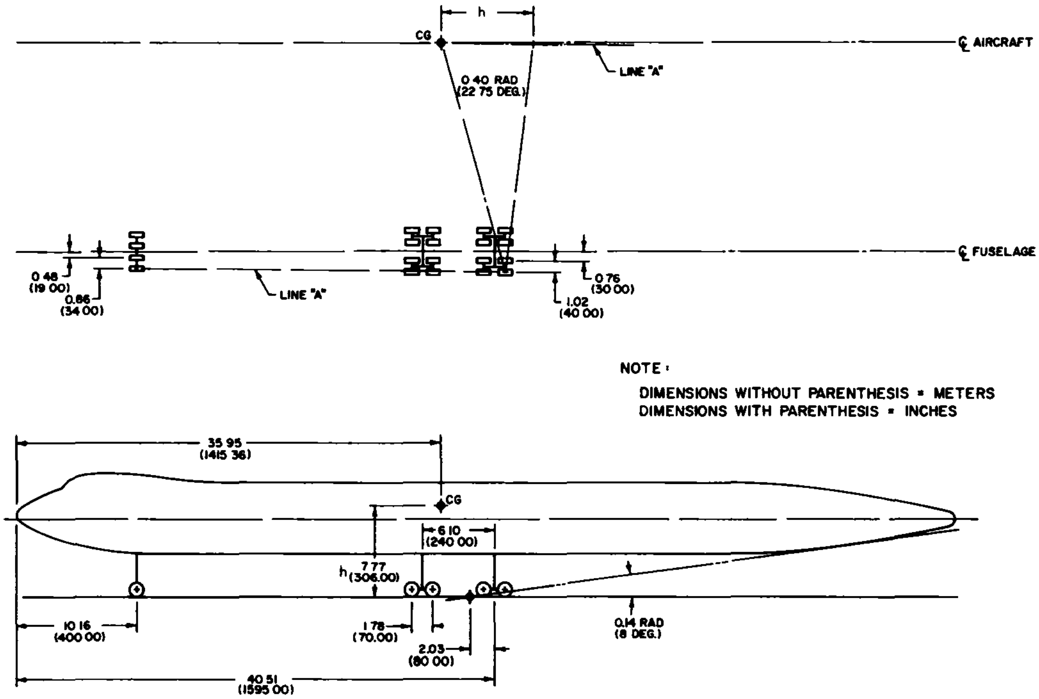

Figure 124. Tip Over Angle Geometry - Two-Body MB2 Aircraft

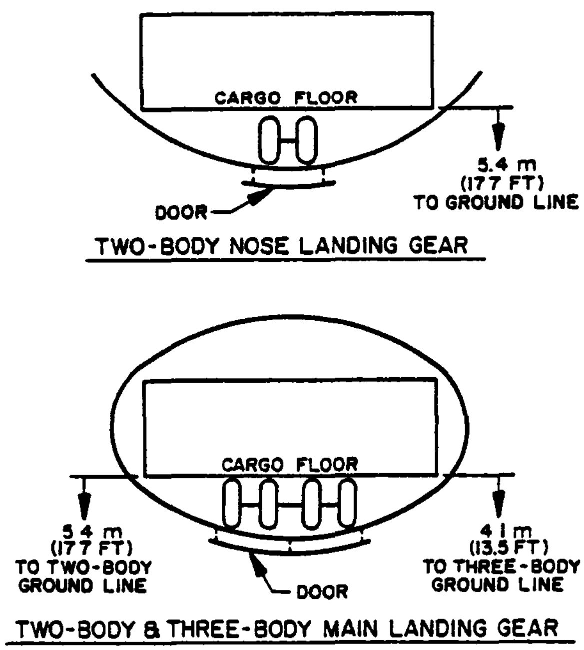

Figure 125. Landing Gear Concept - Multibody Aircraft

RESEARCH, DEVELOPMENT, TEST, AND ENGINEERING COSTS*				
	SBR	MB1	MB2	MB3
TECHNICAL DATA	1,728	1,653	1,651	1,667
DESIGN ENGINEERING	38,394	36,737	36,684	37,049
TOOLING	25,455	24,004	23,957	24,275
TEST ARTICLE	6,002	4,992	5,184	5,376
FLIGHT TEST	1,585	1,498	1,496	1,515
SPECIAL SUPPORT EQUIPMENT	461	441	440	445
SPARES	3,171	2,693	2,761	2,865
TOTAL	76,796	72,018	72,173	73,192
AIRFRAME PRODUCTION COST*				
WING	37,611	28,252	32,780	31,739
EMPENNAGE	5,898	5,856	5,919	7,787
FUSELAGE	37,240	29,601	29,616	30,214
NOSE LANDING GEAR	546	414	416	425
MAIN LANDING GEAR	2,887	2,175	2,186	2,170
CONTROLS	3,237	2,889	2,919	2,985
NACELLE/PYLON	6,178	5,747	5,297	5,715
ENGINE INSTL	314	301	286	300
FUEL SYSTEM	2,450	2,311	2,187	2,309
MISC PROPULSION	845	927	878	775
THRUST REVERSERS	6,106	5,458	4,806	5,410
INSTRUMENTS	783	870	881	930
HYDRAULICS	3,432	3,000	3,036	3,118
ELECTRICAL	2,136	2,477	2,425	2,641
AVIONICS (INSTL & RACKS)	112	112	112	112
FURNISHINGS	2,006	2,226	2,225	2,383
ENVIRONMENTAL	822	796	795	798
APU	256	242	241	244
SYSTEM INTEGRATION	6,357	5,561	5,755	5,760
TOTAL	119,216	99,215	102,761	105,815
FLY-AWAY COST SUMMARY*				
RDT&E	76,796	72,018	72,173	73,192
AIRFRAME PRODUCTION	119,216	99,215	102,761	105,815
SUSTAINING ENGINEERING	18,852	15,677	16,298	16,941
PRODUCTION TOOLING MAINT	16,649	13,845	14,393	14,961
QUALITY ASSURANCE	7,678	6,385	6,638	6,900
AIRFRAME WARRANTY	8,120	6,756	7,004	7,231
AIRFRAME FEE	25,577	21,282	22,064	22,777
ENGINE COST	29,782	28,493	27,133	28,396
AVIONICS COST	1,100	1,100	1,100	1,100
TOTAL	303,772	264,771	269,564	277,313

* 1,000$

Figure 126. Fly-Away Cost Summary - Point Design Aircraft

in fuselage labor cost of 4.3 percent over that required for a conventional fuselage.

The two-body aircraft require that consideration be given to commonlity of components within the airframe to a degree not previously included in conventional aircraft. Using weight as the primary measure of commonality, an assessment is made of each structural component to determine the percent of structure having multiple usage which results in reduced airframe cost due to the additional "learning" that results during manufacturing. This additonal learning is relative to the cost data base used for estimating conventional aircraft. These commonality cost factors for both two-body aircraft, MB1 and MB2, are given below:

COMPONENT	COMMONALITY COST FACTORS MATERIAL	LABOR
Wing	1.0	1.0
Vertical Stabilizer	0.9675	0.8197
Horizontal Stabilizer	0.9662	0.8037
Fuselage	0.9616	0.7744
Landing Gear	0.9609	0.7698
Nacelle	1.0	1.0

An additional factor, component unit weight, must be considered when two-body commonality is assessed relative model. Within the model, costs are to the conventional aircraft costing developed for each major structural component as a function of total weight. For example, in the case of the two-body MB1 aircraft, total fuselage weight is 107,117.6 kg (236,154 lb). However, this total weight is composed of two fuselage unit weights of 53,558.8 kg (118,077 lb). Therefore, a sizing factor is used to modify the cost model to reflect this multiple unit production requirement for each aircraft. These factors for the two-body MB1 and MB2 aircraft are:

COMPONENT	SIZING FACTOR MATERIAL	LABOR
Wing	1.0	1.0
Vertical Stabilizer	0.917	1.19
Horizontal Stabilizer	1.0	1.0
Fuselage	0.89	1.09
Landing Gear	1.07	1.36
Nacelle	1.0	1.0

These same procedures described for the two-body aircraft are used to develop the appropriate cost factors for the three-body MB3 aircraft. The resulting factors are:

COMP.	COMMONALITY MAT'L	LABOR	SIZING MAT'L	LABOR
Wing	1.0	1.0	1.0	1.0
Emp.	0.966	0.804	0.917	1.190
Fus.	0.956	0.750	0.842	1.170
Ldg. Gear	0.884	0.984	1.104	1.527
Nacelle	1.0	1.0	1.0	1.0

Cumulative average aircraft cost for the point design aircraft is given as a function of weight empty in Figure 127. The cost increment between these cost curves is a measure of the cost benefit attributed to airframe commonality.

2.7.6.2 Direct Operating Cost

Direct operating cost for each of the point design aircraft is given in Figure 128. Also given in this figure is a breakdown of the costs associated with performing the design point mission of 6482.0 km (3500 nm) at 100 percent load factor. As seen from these data, the maximum multibody trip cost dollar savings occur for the fuel and oil expenditure. The depreciation expenditure is also significantly reduced for the multibody aircraft.

DOC vs Fuel Price Comparison - Figure 129 shows the effect of fuel price increases on DOC for the four point design aircraft. The aircraft are first optimized at a fuel price of 34.34 ¢/l (1.30 $/gal) and then non-optimally performed as the fuel price increases to a maximum of 68.68 ¢/l (2.60 $/gal). It can be seen on the figure that as the fuel price doubles, DOC increases approximately 50 percent.

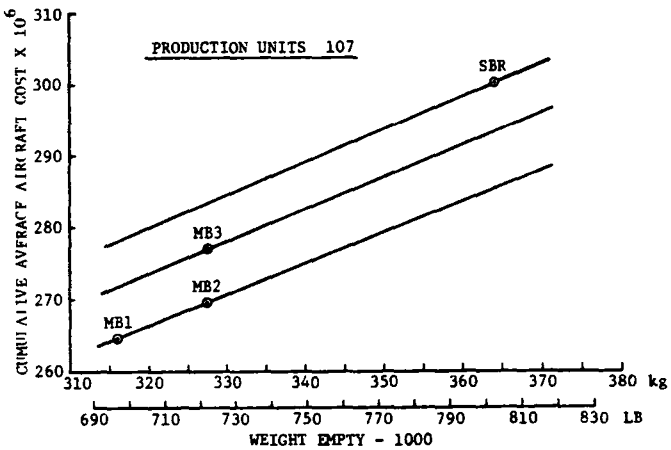

Figure 127. Cumulative Average Aircraft Cost

AIRCRAFT → / ↓ COST ITEM	SINGLEBODY (SBR)		MULTIBODY					
			MB1		MB2		MB3	
	$	%	$	%	$	%	$	%
CREW	5,289	3.3	5,144	3.5	5,143	3.6	5,173	3.5
FUEL & OIL	84,642	52.5	78,999	53.8	73,984	51.8	78,931	52.8
INSURANCE	12,233	7.6	10,662	7.3	10,863	7.6	11,172	7.5
AIRCRAFT LABOR	1,712	1.1	1,497	1.0	1,569	1.1	1,556	1.0
AIRCRAFT MATERIAL	5,641	3.5	4,864	3.3	4,994	3.5	5,126	3.4
ENGINE LABOR	813	0.5	795	0.5	777	0.5	794	0.5
ENGINE MATERIAL	4,297	2.7	4,111	2.8	3,917	2.7	4,098	2.7
MAINTENANCE BURDEN	5,049	3.1	4,585	3.1	4,693	3.3	4,700	3.1
DEPRECIATION	41,447	25.7	36,219	24.7	36,833	25.9	37,896	25.5
*TRIP COST - TOTAL	161,123	100.0	146,876	100.0	142,775	100.0	149,446	100.0
DOC ¢/AMgkm (¢/ATNM)	7.10 (11.93)		6.47 (10.87)		6.29 (10.57		6.58 (11.06)	

*6482 km (3500 NM)

Figure 128. Direct Operating Cost Summary

	DOC		FUEL PRICE
————	¢/AMgkm	=	10.7746 X [$/1] + 3.39
	(¢/ATNM	=	4.7769 X [$/GAL] + 5.70)
— — ———	¢/AMgkm	=	10.3669 X [$/1] + 3.13
	(¢/ATNM	=	4.6000 X [$/GAL] + 5.26)
——— – ———	¢/AMgkm	=	10.3378 X [$/1] + 2.92
	(¢/ATNM	=	4.5923 X [$/GAL] + 4.90)
— — — — —	¢/AMgkm	=	9.2895 X [$/1] + 3.10
	(¢/ATNM	=	4.1308 X [$/GAL] + 5.19)

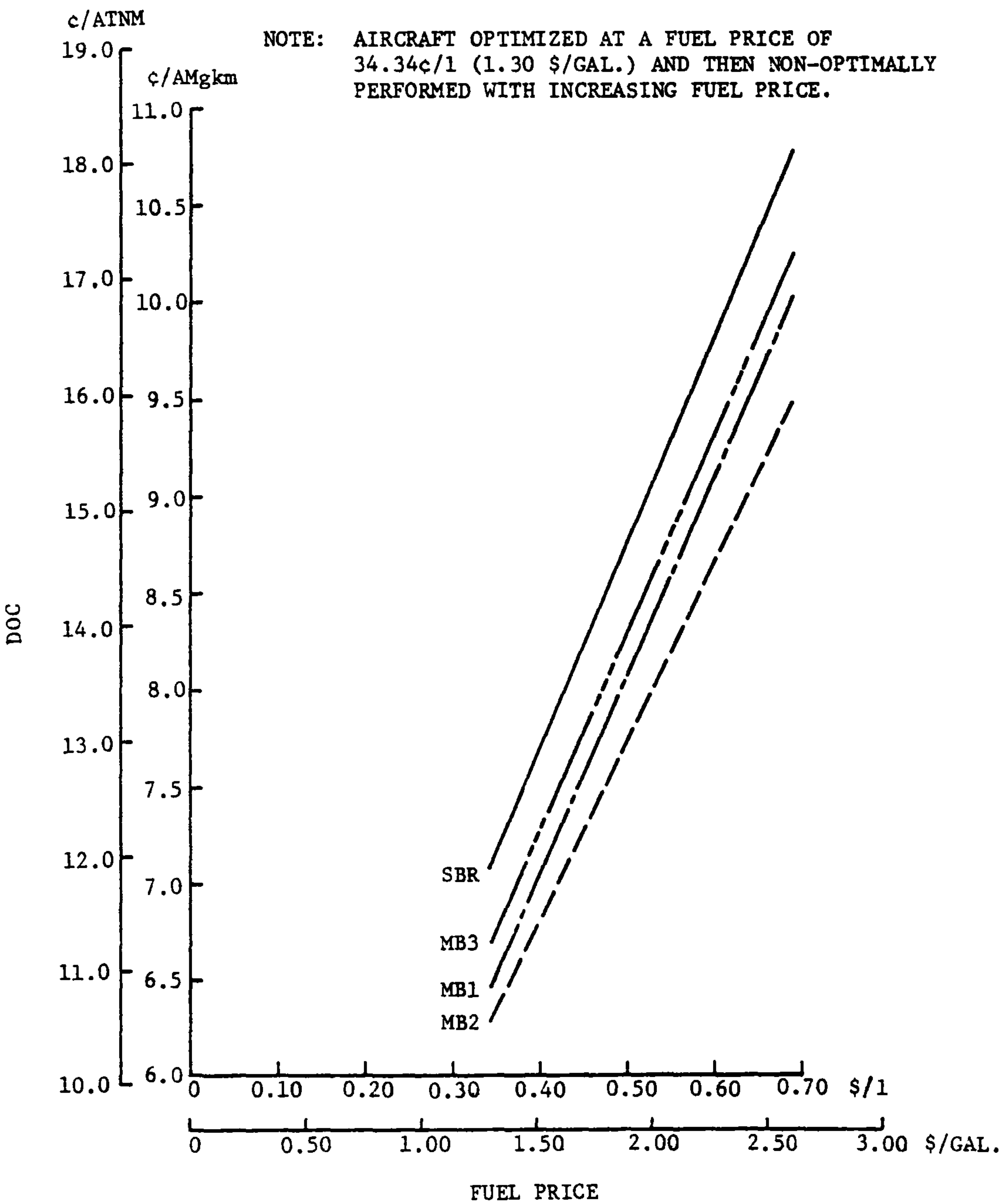

Figure 129. DOC vs Fuel Price Comparison

3.0 SENSITIVITY STUDIES

Sensitivity studies were conducted at the conclusion of the point design analysis such that the influence which a number of design and operational parameters have on aircraft characteristics is defined. These studies include variations in cruise power setting (aircraft thrust-to-weight), payload magnitude, wing spanwise body location, fuel price, and cargo container configuration.

Only the single body reference and two-body MB2 aircraft are evaluated, except for the nonstandard container study which also includes the three-body MB3 aircraft. It is noted that the baseline aircraft used within each of these sensitivity studies vary from the point design aircraft definitions and are identified as a part of the study definition.

The primary figure-of-merit used to compare the sensitivity alternatives is direct operating cost. However, data are included for comparisons of all aircraft major parameters, such as weight, drag, and cost.

The results provided by the point design analyses and these sensitivity studies are used to define the final aircraft of Section 4.0.

3.1 CRUISE POWER SETTING

The point design aircraft are sized to provide a five percent available thrust margin during cruise. In other words, cruise power setting (η) is fixed at 95 percent. Previous studies have indicated the possibility of obtaining lower DOCs or trip costs at cruise power settings less than 95 percent. Decreased cruise power settings require an increase in aircraft thrust-to-weight (T/W) ratio for a given field length requirement and allows an increased initial wing loading.

The cruise power setting sensitivity analysis is conducted for each of the four aircraft types. The analysis is based upon the point design single body reference and two-body MB1 aircraft, and the point design two-body MB2 and three-body MB3 aircraft, as modified to satisfy the results of the point design structural flutter analysis. The two-body MB2 aircraft is used to illustrate the sensitivity analysis in Figure 130. The upper curve provides trip cost as a function of both aspect ratio and cruise power setting, from which it is seen that the minimum trip cost occurs at a cruise power setting of 88.5 percent and an aspect ratio of 11.62. It is shown by the lower curves that, at this power setting and aspect ratio, aircraft T/W and wing loading are in-

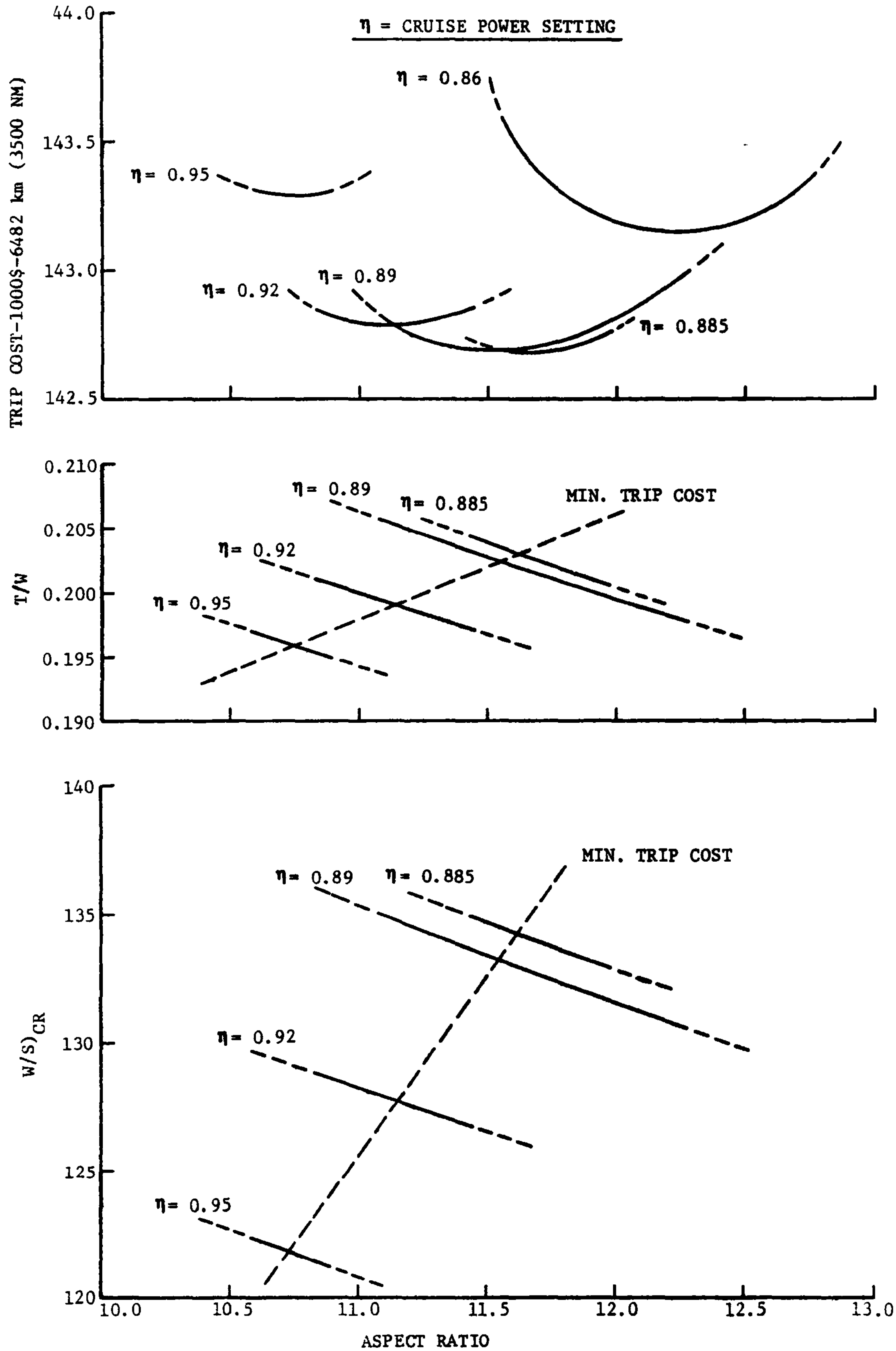

Figure 130. Cruise Power Sensitivity - Two-Body MB2 Aircraft

creased as compared to the 95 percent power setting values.

Similar analyses of the single body reference, two-body MB1, and three-body MB3 aircraft indicate the optimum cruise power settings to be 92, 95, and 95 percent, respectively. The trip cost reductions provided for the two-body MB2 and single body reference aircraft are, however, relatively small, 0.40 and 0.16 percent, respectively, as a result of the power setting decrease.

3.2 PAYLOAD PARAMETRIC

Three payload values 75,000, 167,000 and 258,000 kg (165,347, 368,172, and 568,793 lb), in addition to the point design payload value of 350,000 kg (771,618 lb), are investigated for both the single body reference and the two-body MB2 aircraft. Wing stiffness corrections required as a result of the point design analysis have been incorporated into these aircraft. The 350,000 kg (771,618 lb) two-body MB2 point design aircraft has a body separation distance of 35.1m (115 ft), which in terms of percent wing semispan equates to 28 percent. To maintain the same relative impact of body location on wing weight, the 28 percent semispan location is used as a common location for all two-body payload values. The fuselage physical separation distance, therefore, decreases as payload decreases.

Trip cost, $ per 6,482.0 km (3500 nm), is shown in Figures 131 and 132 as a function of single body and two-body aircraft wing aspect ratio, respectively, for the four payload values. As seen, the two-body minimum trip cost aspect ratio values are greater than those of the single body aircraft. This result is influenced by the reduction in wing weight realized by the two-body aircraft as compared to the single body aircraft at a given aspect ratio. However, the wing bending relief afforded by the multibody concept is not used in total to reduce wing structural weight. A part of this benefit is used to increase wing aspect ratio at an expense to the wing weight reduction that would otherwise be achieved at a constant aspect ratio. In other words, within limits, it is more advantageous when optimizing the aircraft to provide minimum DOC, to reduce fuel weight than to reduce wing weight. Wing weight is a function of wing loading and aspect ratio, as these parameters increase in magnitude, wing weight also increases. As shown in Figure 133, both aspect ratio and wing loading are higher for the multibody aircraft than for the single body aircraft. Although, as also shown in this figure, multibody aircraft wing weight is less than that of

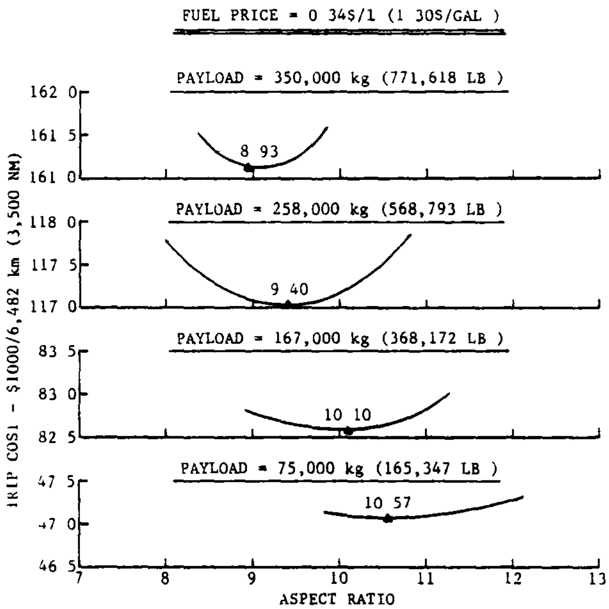

Figure 131. Aspect Ratio Selection - Single Body Reference Aircraft Payload Sensitivity

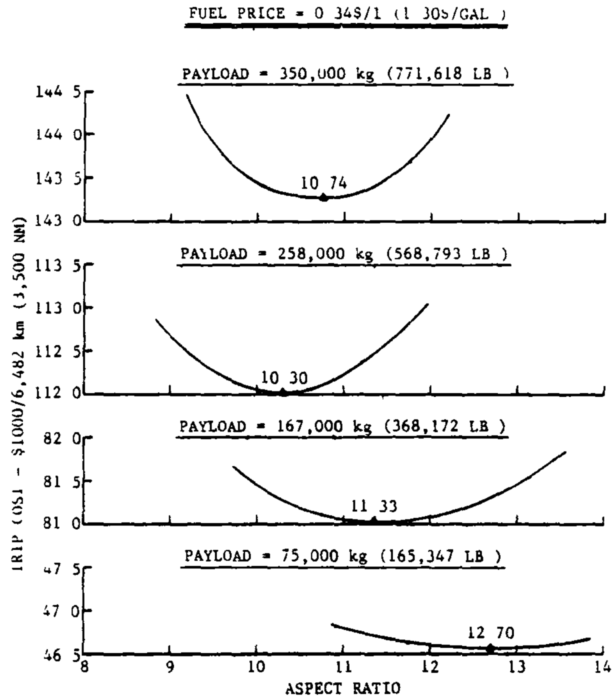

Figure 132. Aspect Ratio Selection - Two-Body Aircraft Payload Sensitivity

the single body aircraft. Wing weight reductions vary from about 0.4 percent at the lower payload value up to 12.4 percent at the highest payload. Comparisons of single body and multibody aircraft for a fixed aspect ratio and wing loading would yield higher percent savings for the multibody aircraft.

Aircraft are defined for each of the minimum trip cost aspect ratio values indicated in Figures 131 and 132 with resulting characteristics data summarized in Figure 133. Fuselage drag vs payload is given in Figure 134. As expected, two-body fuselage drag is higher than that of the single body aircraft at all payload values. This is primarily due to the higher fuselage wetted area required to contain the payload in two vs one fuselage as shown in Figure 135. Due to geometric constraints, step functions occur within the wetted area data between the discrete payload values evaluated, therefore, straight line increments are shown in Figure 135 only to illustrate wetted area trends.

Payload per pound of operating weight and per pound of fuel as a function of payload, as shown in Figure 136, are used to illustrate structural and aerodynamic efficiency, respectively. From these curves it is shown that the single body aircraft provides the better structural concept between payload values of approximately 75,000 and

PAYLOAD - kg	75,000		167,000		258,000		350,000	
DATA ITEM ↓ / AIRCRAFT TYPE →	SBR	MB2	SBR	MB2	SBR	MB2	SBR	MB2
Wing								
Aspect Ratio	10.57	12.70	10 10	11.33	9.40	10.30	8.93	10.74
Area - SQ. m	360.6	334.3	781.5	740.4	1289.3	1192.1	1617.7	1464 6
Sweep - Radians	0.610	0 436	0 610	0.436	0.610	0 436	0 610	0.436
Loading - kN/SQ.m	5 83	6.36	5 52	5.84	5.11	5.36	5.66	5.83
Span - m	61 75	65 17	88 85	91 59	110.06	110.79	120.15	125 39
Weight - kg	22,249	22,153	53,465	48,453	88,110	77,292	122,901	107,619
Weight - kg/SQ m	61 7	66 3	68 4	65.4	68.4	64.8	76.0	73 5
Fuselage								
Length - m	62 30	54 96	76.47	65.44	86.62	63.98	111 53	79.61
Width - m	6.31	4 02	9 60	6.30	12 25	9.60	12.25	9.60
Height - m	5.58	3.84	6 00	5 56	7.71	6.00	7.71	6.00
Weight - kg	28,762	32,550	50,480	58,491	70,035	74,965	105,025	107,207
Weight - kg/SQ m	27.8	25 0	30 9	26 9	30.4	28.3	34.3	31.3
Empennage								
Area - SQ m	80.7	81.7	162.3	184.9	278.2	295 6	310.8	354 5
Weight - kg	2,087	2,132	4,128	4,518	6,695	6,922	7,911	8,568
Weight - kg/SQ m	25 8	26.1	25 4	24.5	24 1	23.4	25.4	24 4
Propulsion								
Engines - Number	4	4	4	4	4	4	6	6
Thrust/Eng - 1000 N	120 9	117 7	237 4	232.6	349.7	339.3	330.8	286.3
System Wt - kg	12,764	11,993	25,383	24,780	38,261	37,358	53,447	45,863
Landing Gear								
Max Tread Width - m	7.32	21 94	10.60	29 35	16 98	34.75	16 98	38.77
Weight - kg	7,276	7,394	14,991	15,082	30,858	22,326	42,733	29,992
Aircraft Weight - 1000 kg								
Structure	62 8	66.5	127.6	131 0	202.3	187 9	287 9	261.5
Operating	88 3	92 1	171 9	175.3	265 3	249.8	372 4	337.7
Fuel	56 9	55.8	112 6	110.7	166.8	161 8	235 5	206 4
Gross	220.2	222 9	451.5	453.0	690.1	669 5	957.9	894.1
Performance								
Cruise L/D	20.25	21 05	21 15	21 65	21.94	21.94	21.48	23.16
Block Fuel - 1000 kg	47.7	46 7	94.2	92.7	139.5	135.4	196 9	172.6
Mg km/l - Fuel	8.19	8.36	9 23	9 38	9 63	9.92	9.25	10.55
Ferry Range - km	9,238	9,079	9,573	9,484	9,656	9,699	9,930	9,971
Economic								
Aircraft Price - $M	94.7	94.0	161.3	156 5	225 2	210 0	316.5	270.9
DOC-¢/AMgkm @ $0 34/l	9 65	9.54	7 63	7 49	7 01	6.71	7 10	6 32
Efficiency Factors								
Fuselage	0 424	0.485	0 402	0 424	0 335	0.402	0 335	0 402
ML/D	16.20	16.84	16.92	17 32	17 55	17.55	17 18	18.53
Aircraft Price/Payload - $/kg	1,263	1,253	966	937	873	814	868	774

Figure 133. Aircraft Characteristics Summary - Payload Parametric (Metric Units) (Sheet 1 of 2)

PAYLOAD - LB	165,347		368,172		568,793		771,618	
DATA ITEM ↓ / AIRCRAFT TYPE →	SBR	MB2	SBR	MB2	SBR	MB2	SBR	MB2
Wing								
Aspect Ratio	10.57	12.70	10 10	11.33	9 40	10.30	8.93	10 74
Area - SQ. FT	3,882	3,598	8,412	7,970	13,878	12,832	17,413	15,765
Sweep - Degree	35.0	25.0	35 0	25 0	35.0	25 0	35.0	25 0
Loading - LB /SQ. FT.	121.8	132 9	115.2	122 0	106.8	112.0	118.2	121.8
Span - FT.	202.6	213.8	291 5	300.5	361.1	363.5	394.2	411 4
Weight - LB	49,050	48,840	117,870	106,820	194,250	170,400	270,950	237,260
Weight - LB /SQ FT.	12 64	13.57	14 01	13.40	14.00	13 28	15.56	15 05
Fuselage								
Length - FT	204.4	180.3	250.9	214.7	284 2	209 9	365 9	261 2
Width - FT	20.7	13.2	31.5	20.67	40 2	31.5	40 2	31.5
Height - FT	18 3	12.6	19 7	18.25	25.3	19.7	25.3	19.7
Weight - LB	63,410	71,760	111,290	128,950	154,400	165,270	231,540	236,350
Weight - LB /SQ FT	5.70	5.13	6.33	5 50	6 23	5 80	7 02	6 42
Empennage								
Area - SQ FT	869	879	1,747	1,990	2,995	3,182	3,345	3,816
Weight - LB	4,600	4,700	9,100	9,960	14,760	15,260	17,440	18,890
Weight - LB /SQ. FT	5.29	5.35	5.21	5 01	4 93	4.80	5 21	5 00
Propulsion								
Engines - Number	4	4	4	4	4	4	6	6
Thrust/Eng - LB	27,170	26,450	53,360	52,280	78,620	76,280	74,360	64,370
System Wt - LB.	28,140	26,440	55,960	54,630	84,350	82,360	117,830	101,110
Landing Gear								
Max Tread Width - FT	24 0	72.0	34.8	96.3	55 7	114 0	55 7	127.2
Weight - LB	16,040	16,300	33,050	33,250	68,030	49,220	94,210	66,120
Aircraft Weight - 1000 LB								
Structure	138 4	146 7	281 3	288.8	446.0	414 3	634.8	576.6
Operating	194.7	203 1	379.0	386.5	584.8	550.7	820 9	744.4
Fuel	125.5	123 0	248 2	244 0	367 7	356.6	519.2	455.1
Gross	485.5	491.4	995.4	998.7	1521 3	1476.1	2111 7	1971.1
Performance								
Cruise L/D	20.25	21.05	21 15	21 65	21.94	21.94	21.48	23 16
Block Fuel - 1000 LB.	105.1	103.0	207.6	204.3	307.5	298.5	434.2	380.6
Ton NM/GAL Fuel	18 45	18.83	20.79	21.13	21.69	22.34	20.84	23.77
Ferry Range - NM	4,988	4,902	5,169	5,121	5,214	5,237	5,362	5,384
Economic								
Aircraft Price - $M	94 7	94 0	161.3	156.5	225.2	210.0	316 5	270.9
DOC - ¢ATNM @ $1 30/GAL	16.21	16 03	12.82	12.58	11 77	11.27	11 93	10 61
Efficiency Factors								
Fuselage	0.424	0 485	0 402	0 424	0 335	0.402	0 335	0 402
ML/D	16 20	16.84	16.92	17.32	17 55	17.55	17.18	18 53
Aircraft Price/Payload - $/LB	573	568	438	425	396	369	394	351

Figure 133. Aircraft Characteristics Summary - Payload Parametric (Customary Units) (Sheet 2 of 2)

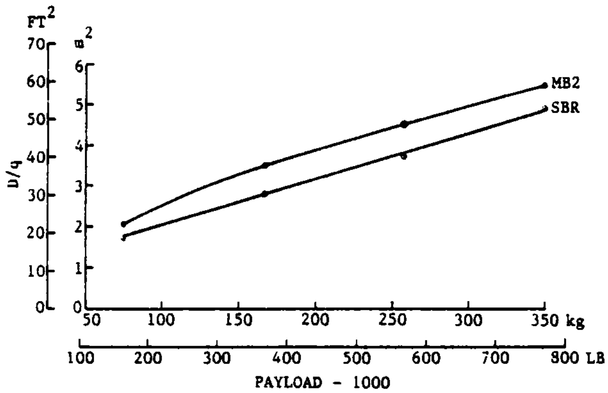

Figure 134. Fuselage Drag vs Payload

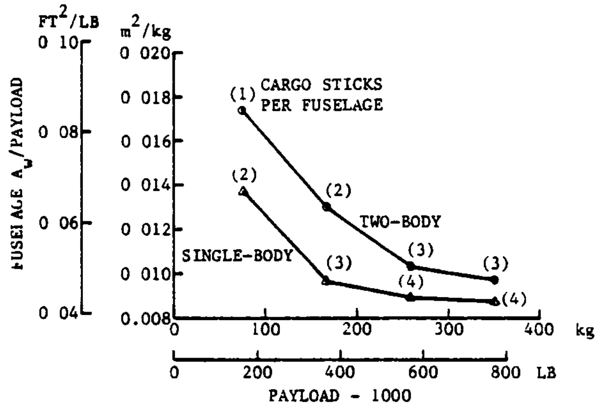

Figure 135. Fuselage Wetted Area vs Payload

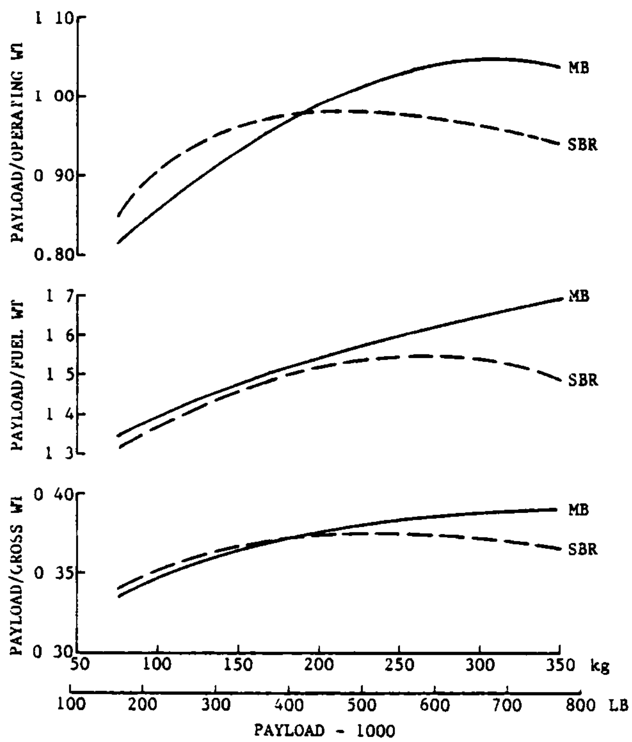

Figure 136. Weight Fractions

200,000 kg (165,347 and 440,925 lb), whereas aerodynamic efficiency is better at all payload values for the multibody aircraft. The payload to gross weight fraction, also shown in Figure 136, indicates the improved aerodynamic efficiency of the multibody is not sufficient to overcome the structural benefit of the single body aircraft at payload values less than approximately 167,000 kg (368,172 lb).

Including the economic influence in this comparison, as shown in Figure 137, multibody aircraft price and direct operating cost are lower than those of the single body aircraft at all payload values. DOC is a function of both aircraft price and the operational cost per flight hour (crew, fuel, maintenance, etc.) of the aircraft. As shown in Figure 137, the two-body MB2 aircraft price is less than that of the single body reference aircraft, although the multibody aircraft has the higher structural weight at the two lower study payloads, 75,000 and 167,000 kg (165,347 and 368,172 lb), which would indicate a higher price. The lower price is a function of the "learning curve cost reduction" advantage provided by commonality of structural component usage on the multibody aircraft.

The major element of the aircraft operating cost per hour is fuel cost. As previously shown, the multibody aircraft have the lower fuel consumption and, thereby, the lower incurred fuel cost at all payloads.

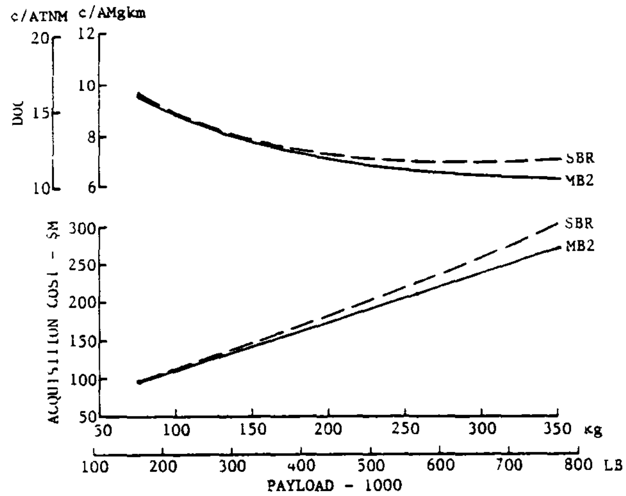

Figure 137. Economic Comparison

This lower fuel cost and aircraft price combine to provide the multibody aircraft with the lowest DOC at all payloads. The DOC advantage at the two lower payloads, 75,000 and 167,000 kg (165,347 and 368,172 lb), is somewhat insignificant, being only 1.1 and 1.9 percent, respectively. The DOC advantage increases to 4.2 and 11.1 percent at the two higher payload values, 258,000 and 350,000 kg (568,793 and 771,618 lb).

The overall conclusion drawn from these data is that to provide a significant competitive advantage, the multibody payload requirement should exceed 258,000 kg (568,793 lb). Although not studied here, the data included in this analysis indicate the multibody advantage would increase as design point

range increases, or where maximum flight endurance is a mission requirement.

It is noted that based upon the ground rule of this study, that all multibody aircraft body locations are constrained to 28 percent semispan, it is possible that a penalty is imposed on the lower payload aircraft. Using this constraint, the resulting physical fuselage separation distance and landing gear centerline width are given in Figure 138. As seen from this curve, the 350,000 kg (771,618 lb) payload aircraft has a 35.1m (115 ft) gear centerline separation which is felt to be compatible with existing 45.7m (150 ft) runway widths. The minimum payload value aircraft has a gear separation of approximately 18.3m (60 ft), well under 35.1m (115 ft) allowable for runway compatibility. Therefore, body separation can be increased at this payload value thus improving the structural efficiency, while maintaining runway compatibility. To what extent the body can be relocated outboard requires a detailed aerodynamic, structural, and stability and control analysis. However, some guidance is provided by the body location sensitivity study which indicates a body location up to 40 percent semispan is feasible. Using this percent, the gear centerline width would increase to approximately 25.3m (83 ft) for the 75,000 kg (165,347 lb)

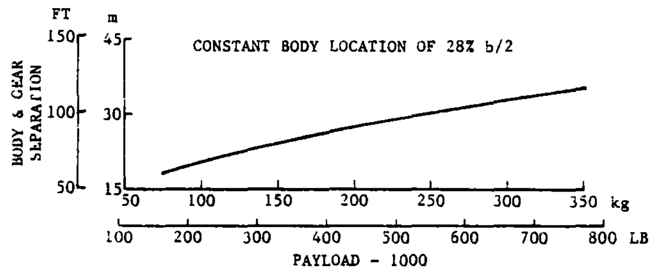

Figure 138. Body and Gear Centerline Separation vs Payload

payload aircraft. This same procedure could be applied to the 167,000 and 258,000 kg (368,172 and 568,793 lb) aircraft, but to a lesser extent as indicated by separation distances given in Figure 138.

3.3 BODY SPANWISE LOCATION SENSITIVITY

The two-body MB2 point design aircraft is configured with a body centerline separation distance of 35.1m (115 ft), or as a function of percent wing semispan, the bodies are located at 28 percent. To define the influence of body location on aircraft characteristics, three additional body locations are evaluated, 17, 39, and 50 percent semispan. Wing stiffness corrections required as a result of the point design analysis are incorporated into the aircraft evaluated at these various body locations.

Characteristics summary data are given in Figure 139 for aircraft optimized to provide minimum DOC when sized for each of the body locations. The primary benefit to be realized by the

BODY LOCATION - % SEMISPAN	17	28	39	50
BODY SEPARATION - METERS → / ↓ DATA ITEM	21.8	35.1	49.9	62.4
Wing				
Aspect Ratio	11.41	10.74	11.50	10.85
Area - SQ. m	1,443	1,465	1,425	1,435
Sweep - Radians	0.436	0.436	0.436	0.436
Loading - kN/SQ.m	6.08	5.83	5.92	5.98
Span - m	128.29	125.39	127.98	124.75
Weight - kg	122,506	107,619	101,977	108,458
Weight - kg/SQ. m	84.9	73.5	71.6	75.6
Fuselage				
Length - m	79.61	79.61	79.61	79.61
Width - m	9.60	9.60	9.60	9.60
Height - m	6.00	6.00	6.00	6.00
Weight - kg	107,461	107,207	107,089	107,243
Weight - kg/SQ. m	31.4	31.3	31.3	31.3
Empennage				
Area - SQ. m	366.1	354.5	339.6	328.6
Weight - kg	8,804	8,568	8,301	8,169
Weight - kg/SQ. m	24.1	24.2	24.4	24.9
Propulsion				
Engines - Number	6	6	6	6
Thrust/Eng. - 1000 N	295.0	286.3	279.9	289.9
System Wt. - kg	47,337	45,863	44,724	46,466
Landing Gear				
Max. Tread Width - m	38.77	38.77	38.77	38.77
Weight - kg	30,785	29,992	29,620	30,096
Aircraft Weight - 1000 kg				
Structure	278.0	261.5	255.0	262.2
Operating	355.6	337.7	329.9	339.2
Fuel	212.4	206.4	202.3	208.8
Gross	917.9	894.1	882.2	898.0
Performance				
Cruise L/D	23.08	23.16	23.36	22.97
Wing Span Efficiency - %	0.83090	0.93580	0.94312	0.97761
Block Fuel - 1000 kg	177.6	172.6	169.1	174.5
Ferry Range - km	10,147	9,971	9,877	9,856
Economics				
Aircraft Price - $M	281.2	270.9	266.2	272.0
DOC - ¢/AMgkm @ 0.34/1	6.51	6.32	6.20	6.36
Efficiency Factors				
Fuselage	0.402	0.402	0.402	0.402
ML/D	18.46	18.53	18.69	18.38
Aircraft Price/Payload - $/kg	803	774	761	777

Figure 139. Body Location Data Summary - Two-Body MB2 Aircraft (Metric Units) (Sheet 1 of 2)

	BODY LOCATION - % SEMISPAN			
	17	28	39	50
BODY SEPARATION - FEET → / ↓ DATA ITEM	71.6	115.0	163.8	204.6
Wing				
Aspect Ratio	11.41	10.74	11.50	10.85
Area - SQ. FT.	15,529	15,765	15,334	15,449
Sweep - Degree	25	25	25	25
Loading - LB./SQ. FT.	127.0	121.8	123.6	124.9
Span - FT.	420.9	411.4	419.9	409.3
Weight - LB.	270,080	237,260	224,820	239,110
Weight - LB./SQ. FT.	17.39	15.05	14.66	15.48
Fuselage				
Length - FT.	261.2	261.2	261.2	261.2
Width - FT.	31.5	31.5	31.5	31.5
Height - FT.	19.7	19.7	19.7	19.7
Weight - LB.	236,910	236,350	236,090	236,430
Weight - LB./SQ. FT.	6.43	6.42	6.41	6.42
Empennage				
Area - SQ. FT.	3,941	3,816	3,655	3,537
Weight - LB	19,410	18,890	18,300	18,010
Weight - LB./SQ. FT.	4.93	4.95	5.01	5.09
Propulsion				
Engines - Number	6	6	6	6
Thrust/Eng. - LB.	66,320	64,370	62,930	65,170
System Wt. - LB.	104,360	101,110	98,600	102,440
Landing Gear				
Max. Tread Width - FT.	127.2	127.2	127.2	127.2
Weight - LB.	67,870	66,120	65,300	66,350
Aircraft Weight - 1000 LB.				
Structure	612.8	576.6	562.1	578.1
Operating	783.9	744.4	727.4	747.8
Fuel	468.2	455.1	445.9	460.3
Gross	2,023.7	1,971.1	1,944.9	1,979.7
Performance				
Cruise L/D	23.08	23.16	23.36	22.97
Wing Span Efficiency - %	0.83090	0.93580	0.94312	0.97761
Block Fuel - 1000 LB.	391.5	380.6	372.8	384.8
Ferry Range - NM	5,479	5,384	5,333	5,322
Economics				
Aircraft Price - $M	281.2	270.9	266.2	272.0
DOC - ¢/ATNM @ $1.30/GAL.	10.94	10.61	10.41	10.69
Efficiency Factors				
Fuselage	0.402	0.402	0.402	0.402
ML/D	18.46	18.53	18.69	18.38
Aircraft Price/Payload - $/LB	364	351	345	353

Figure 139. Body Location Data Summary - Two-Body MB2 Aircraft (Customary Units) (Sheet 2 of 2)

multibody concept is a reduction in the magnitude of the cruise mode wing bending moment and thereby a reduction in wing weight. It would also be expected that, as body semispan location increases, this bending relief would also increase and wing weight would decrease. However, as shown in Figure 140, the two-body MB2 aircraft wing weight decreases for locations out to approximately 40 percent then begins to increase as the body is located further outboard.

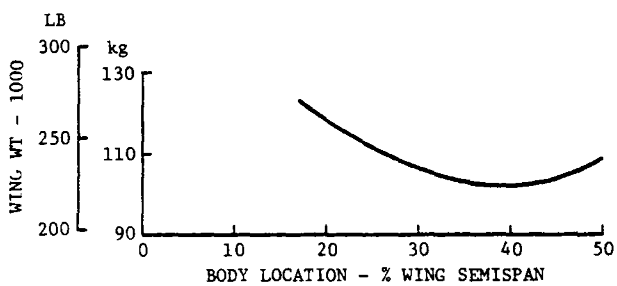

Figure 140. Wing Weight vs Body Location - Two-Body MB2 Aircraft

Wing bending moment for the various body locations is shown as a function of wing semispan in Figure 141. Both up bending and down bending moment cases are shown for the critical load conditions, 2.5g flight maneuver and 2.0g taxi, respectively. As seen from the figure, the peak bending moment at the outboard side of the body is decreased for both flight and taxi conditions as the body is moved outboard from the 17 to 50 percent semispan location. However, as the body is moved from the 39 percent location to the 50 percent location, the flight bending moment imposed on the wing center section changes from an up bending moment to a down bending moment and exceeds the taxi down bending moment at the 50 percent body location. This wing center section moment reversal, coupled with the reduction in center wing chord and thickness that occurs as the body is moved outboard, results in the wing weight increase outboard of the 39 percent body location as shown in Figure 141.

Although the wing span efficiency increases as the bodies are moved outboard, the cruise lift-to-drag ratio decreases from the 39 to the 50 percent body location as shown in Figure 139. Wing aspect ratio also decreases when the body is relocated from the 39 to the 50 percent semispan location, offsetting the increased span efficiency. It is assumed that the wing optimizes at a lower aspect ratio to reduce the impact of the wing weight increase that occurs between the 39 and 50 percent location as previously explained.

The optimum body location based upon direct operating cost is approximately 39 percent semispan as shown in Figure 142. It is noted however, that the aircraft evaluated by this analysis have coincident fuselage and landing gear centerlines. Thus, the 39 percent body location aircraft requires a runway

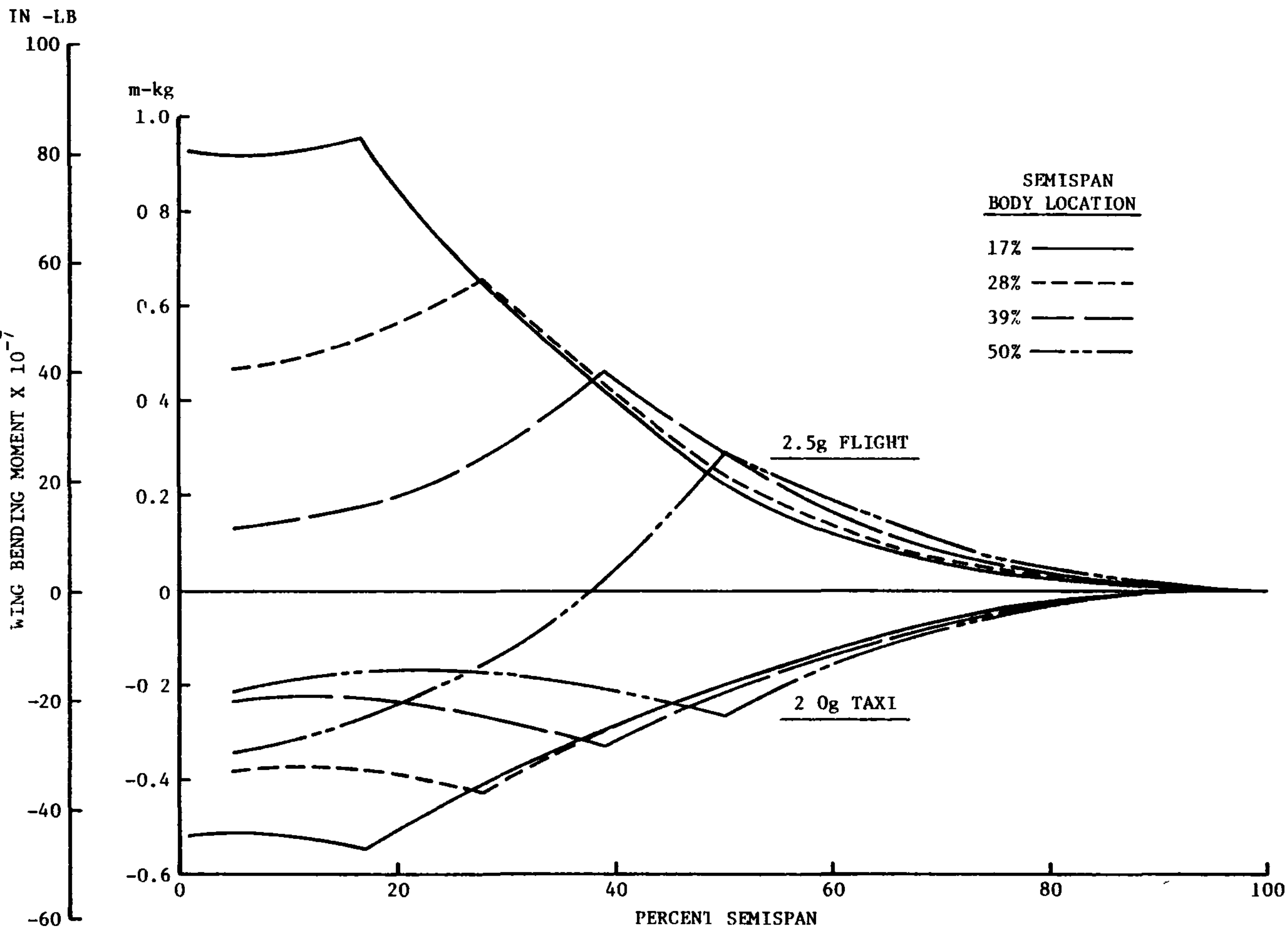

Figure 141. Wing Bending Moment vs.Wing Semispan and Body Location

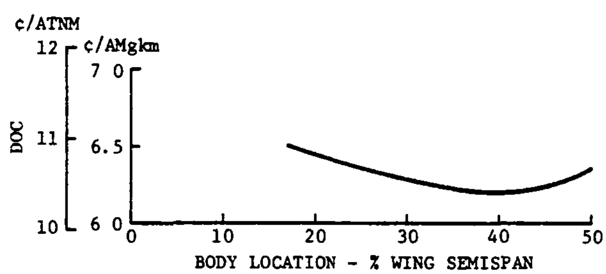

Figure 142. DOC vs Body Location

width greater than 50.0m (164 ft). To avoid this excessive runway width problem, the gear centerline location must be moved inboard along the wing box beam. This outboard displacement of the fuselage weight from the gear load reaction plane imposes a critical down bending moment on the wing during the landing mode. Reacting this moment requires a wing structural weight increase which diminishes the wing weight benefit derived by the fuselage outward movement. Additional data on this subject is included in Appendix C.

The severity of the lateral control problem is shown by noting the tradeoffs that occur and the resulting aircraft response as the bodies move outboard. Ailerons are used on the outboard 30 percent of the semispan and their effectiveness is relatively constant. However, the spoilers are used only outboard of the bodies and their effectiveness is a function of the area outboard of the body which decreases as the body is moved outboard. As body position moves from 19 to 50 percent semispan, the available rolling moment decreases by 55 percent while the required rolling moment, represented by the inertia, increases by a little over 50 percent. Initial studies described in Appendix C recognize and address this problem.

The data shown in Appendix C are based on early estimates of inertias. More detailed analyses produced during the sensitivity study show the problem to be even more severe as the fuselages are moved outboard. Figure 143 shows the roll and yaw inertias used for the preliminary analysis and for the sensitivity study. The later estimates show a sharper increase as the body location in percent semispan gets greater. The resulting performance, bank angle as a function of time, is shown in Figure 144.

It is obvious that roll control becomes increasingly difficult with fuselages located off the aircraft centerline. Quantifying exactly where the cut-off should be is not easily done. As discussed in Section 2.7.3, the civil regulations are not very specific. The military specification requirements, even though more specific, are known to be inadequate for very large aircraft. MIL-Spec 8785B quantifies roll capability by specifying the time required to bank 0.52 rad (30 degrees).

Discussions concerning hard criteria to define roll requirements are presented in Section 2.7.3 and Appendix C. It can be summarized here in connection with Figure 144 by stating that the ability to reach 0.52 rad (30 degrees) of bank in approximately five seconds appears to be a reasonable guide. A cross plot of these data shows the maximum body location for that requirement to be 32.5 percent. Since this is

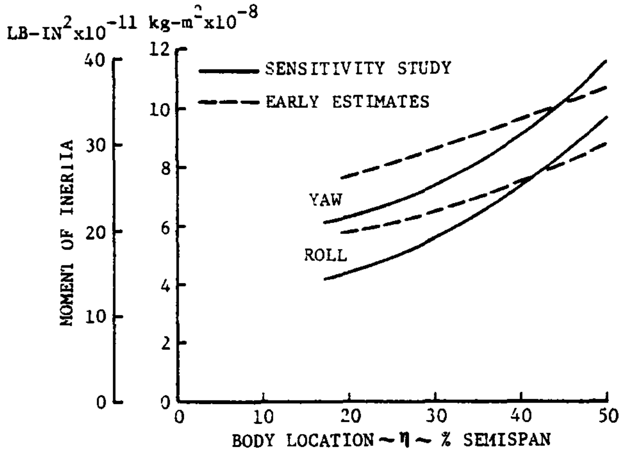

Figure 143. Maximum Moment of Inertia as a Function of Body Location

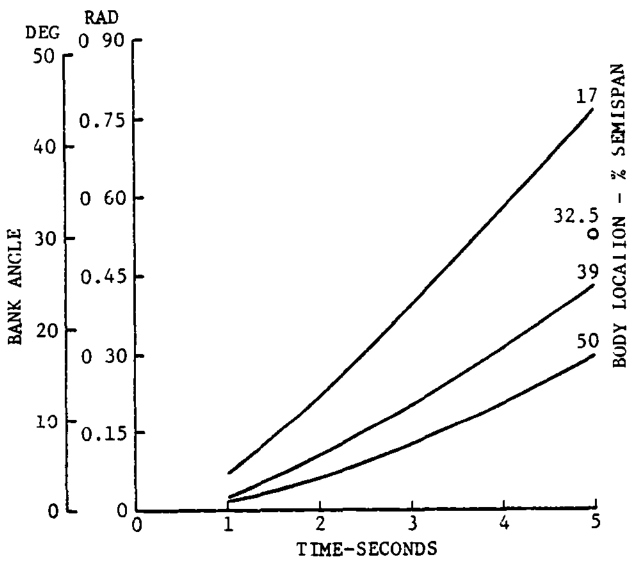

Figure 144. Maximum Bank Angle as a Function of Time- Body Location Sensitivity

not an exacting requirement, locations close to that should be considered as feasible at this time if they appear more optimum from an overall performance viewpoint. Roll capability, however, deteriorates rapidly, with a location of 50 percent providing only half of the chosen criteria.

Based upon the above data, the point design body location of 28 percent semispan is considered within the optimum body location range. To better define the optimum location requires additional investigations such as wind tunnel tests, flight simulator evaluation, and detailed structural analyses, all of which are beyond the scope of this study.

3.4 FUEL PRICE SENSITIVITY

The direct operating cost data produced as a part of the point design analysis are based upon a fuel price of 34.34 ¢/l (1.30 $/gal). In view of the current and projected price instability that exists in the world fuel market, the effects of three additional fuel prices, (17.17, 51.51 and 68.68 ¢/l) (0.65, 1.95, and 2.60 $/gal), on the single body reference and two-body MB2 aircraft are evaluated. Based upon the results of the cruise power setting sensitivity study, all aircraft defined within this analysis are cruise power optimized. Wing stiffness requirements are also increased for the two-body aircraft to meet flutter requirements.

Single body reference and two-body MB2 aircraft characteristics optimized to provide minimum DOC at each of the fuel price values are given in Figure 145. Trend curves of the more significant characteristics are given in Figure 146. As fuel price increases,

FUEL PRICE - $/LITER	0.17		0.34		0.52		0.69	
DATE ITEM / AIRCRAFT TYPE	SBR	MB2	SBR	MB2	SBR	MB2	SBR	MB2
WING								
ASPECT RATIO	8.46	9.91	9.21	11.62	10.02	12.22	10.34	12.65
AREA - SQ m	1,598	1,426	1,567	1,339	1,554	1,338	1,528	1,360
SWEEP - Radians	0.61	0.44	0.61	0.44	0.61	0.44	0.61	0.44
LOADING - kN/SQ.m	5.71	5.96	5.87	6.43	5.97	6.48	6.07	6.40
SPAN - m	116.25	118.87	120.09	124.69	124.75	127.86	126.03	131.16
WEIGHT - kg	116,650	98,320	125,480	114,270	136,070	121,420	140,260	127,430
WEIGHT - kg/SQ m	72.99	68.94	80.12	85.34	87.54	90.76	91.01	93.64
FUSELAGE								
LENGTH - m	111.53	79.61	111.53	79.61	111.53	79.61	111.53	79.61
WIDTH - m	12.25	9.60	12.25	9.60	12.25	9.60	12.25	9.60
HEIGHT - m	7.71	6.00	7.71	6.00	7.71	6.00	7.71	6.00
WEIGHT - kg	104,970	107,120	105,060	107,280	105,170	107,370	105,230	107,430
WEIGHT - kg/SQ m	34.27	31.30	34.27	31.35	34.32	31.39	34.32	31.39
EMPENNAGE								
AREA - SQ m	305	341	304	329	303	332	301	339
WEIGHT - kg	7,830	8,350	7,780	8,140	7,760	8,180	7,720	8,300
WEIGHT - kg/SQ m	25.63	24.51	25.63	24.71	25.58	24.66	25.63	24.51
PROPULSION								
ENGINES - NUMBER	6	6	6	6	6	6	6	6
THRUST/ENG - N	335,440	293,140	337,440	298,080	341,400	298,790	346,430	296,390
SYSTEM WT - kg	54,250	47,020	54,560	47,670	55,210	47,760	56,060	47,350
CRUISE POWER SETTING η	0.95	0.95	0.92	0.88	0.89	0.87	0.87	0.87
LANDING GEAR								
MAX TREAD WIDTH - m	16.98	38.77	16.98	38.77	16.98	38.77	16.98	38.77
WEIGHT - kg	42,500	29,740	42,880	30,230	43,400	30,480	43,660	30,690
AIRCRAFT WEIGHT - 1000 kg								
STRUCTURE	281.5	251.9	290.8	268.4	302.0	275.9	306.7	282.3
OPERATING	366.6	329.1	376.2	346.1	388.2	353.8	393.6	359.7
FUEL	238.0	210.2	233.5	202.1	230.3	200.1	229.3	199.0
GROSS	954.6	889.2	959.7	898.2	968.5	903.9	973.0	908.7
PERFORMANCE								
CRUISE L/D	21.11	22.50	21.81	24.05	22.51	24.57	22.81	24.90
BLOCK FUEL - 1000 kg	199.1	175.8	195.2	168.8	192.5	167.1	191.6	166.2
Mg km/l - FUEL	9.143	10.350	9.338	10.790	9.458	10.896	9.516	10.958
FERRY RANGE - km	10,101	10,251	9,953	10,058	9,775	9,938	9,734	9,808
ECONOMIC								
AIRCRAFT PRICE - $M	300.9	266.5	305.8	275.1	312.1	279.2	315.1	282.3
DOC - ¢/AMgkm @ $0.34/l	5.23	4.67	7.09	6.29	8.92	7.87	10.74	9.45
EFFICIENCY FACTORS								
FUSELAGE	0.335	0.402	0.335	0.402	0.335	0.402	0.335	0.402
ML/D	16.89	18.00	17.45	19.24	18.01	19.66	18.25	19.92
AIRCRAFT PRICE/PAYLOAD - $/kg	860	761	874	786	892	798	900	807

Figure 145. Aircraft Characteristics Summary - Fuel Price Sensitivity (Metric Units (Sheet 1 of 2)

wing aspect ratio increases with a corresponding increase in aircraft structural weight and a decrease in block fuel. The combination of these two weight elements results in an increase in gross weight as fuel price increases.

Comparing single body reference and two-body MB2 aircraft fuel price effects, the gross weight benefit of the two-body aircraft decreases as fuel price increases. At a fuel price of 17.17 ¢/l (0.65 $/gal) the gross weight of the two-body MB2 aircraft is 6.8 percent less than that of the single body reference aircraft, where at a price of 68.68 ¢/l (2.60 $/gal), this percent reduction is reduced to 6.6

FUEL PRICE $/GAL →	0 65		1 30		1 95		2 60	
AIRCRAFT TYPE → / ↓ DATA ITEM	SBR	MB2	SBR	MB2	SBR	MB2	SBR	MB2
WING								
ASPECT RATIO	8 46	9 91	9 21	11 62	10 02	12 22	10 34	12 65
AREA - SQ FT	17,200	15,350	16,862	14,409	16,728	14,400	16,452	14,644
SWEEP - DEGREE	35	25	35	25	35	25	35	25
LOADING - LB./SQ FT	119 30	124 50	122 50	134 30	124 70	135 30	126 80	133 70
SPAN - FT	381 40	390.00	394 00	409 10	409 30	419 50	413 50	430 30
WEIGHT - LB	257,170	216,760	276,630	251,920	299,980	267,680	309,230	280,930
WEIGHT - LB /SQ FT	14 95	14.12	16 41	17 48	17 93	18 59	18 64	19 18
FUSELAGE								
LENGTH - FT.	365.90	261 20	365 90	261 20	365 90	261 20	365 90	261 20
WIDTH - FT	40 20	31.50	40 20	31 50	40 20	31 50	40 20	31 50
HEIGHT - FT	25 30	19 70	25 30	19.70	25 30	19 70	25 30	19 70
WEIGHT - LB	231,430	236,170	231,610	236,520	231,870	236,700	231,990	236,840
WEIGHT - LB /SQ FT	7 02	6.41	7.02	6 42	7 03	6 43	7 03	6 43
EMPENNAGE								
AREA - SQ FT.	3,287	3,670	3,268	3,545	3,265	3,570	3,243	3,645
WEIGHT - LB	17,260	18,410	17,160	17,940	17,110	18,030	17,030	18,300
WEIGHT - LB./SQ FT	5.25	5 02	5 25	5 06	5 24	5 05	5 25	5 02
PROPULSION								
ENGINES - NUMBER	6	6	6	6	6	6	6	6
THRUST/ENG - LB	75,410	65,900	75,860	67,010	76,750	67,170	77,880	66,630
SYSTEM WT. - LB	119,600	103,670	120,280	105,090	121,720	105,290	123,590	104,390
CRUISE POWER SETTING η	0.95	0.95	0.92	0 88	0.89	0 87	0 87	0 87
LANDING GEAR								
MAX TREAD WIDTH - FT.	55 7	127 20	55 7	127 20	55 7	127 20	55 7	127 20
WEIGHT - LB	93,700	65,560	94,530	66,650	95,690	67,200	96,250	67,660
AIRCRAFT WEIGHT - 1000 LB.								
STRUCTURE	620.5	555 3	641.0	591.7	665.9	608 3	676 1	622.3
OPERATING	808 2	725 5	829 3	763.0	855.8	779 9	867.8	793 1
FUEL	524.7	463 4	514.8	445 5	507 7	441.1	505.6	438 7
GROSS	2,104 5	1,960 4	2,115.7	1,980 1	2,135 1	1,992.7	2,145 0	2,003 4
PERFORMANCE								
CRUISE L/D	21.11	22 50	21 81	24 05	22.51	24 57	22 81	24 90
BLOCK FUEL - 1000 LB.	438 9	387.5	430 4	372 2	424 3	368 5	422 4	366 4
TON NM/GAL FUEL	20.600	23.320	21 040	24.310	21.310	24.550	21.440	24 690
FERRY RANGE - NM	5,454	5,535	5,374	5,431	5,278	5,366	5,256	5,296
ECONOMIC								
AIRCRAFT PRICE - $M	300 9	266 5	305 8	275 1	312.1	279 2	315 1	282 3
DOC - ¢ATNM	8 78	7 84	11 91	10 56	14 99	13 23	18.04	15 88
EFFICIENCY FACTORS								
FUSELAGE	0 335	0 402	0 335	0 402	0 335	0 402	0 335	0 402
ML/D	16 89	18 00	17 45	19 24	18.01	19 66	18 25	19 92
AIRCRAFT PRICE/PAYLOAD - $/LB	390	345	396	357	405	362	408	366

Figure 145. Aircraft Characteristics Summary - Fuel Price Sensitivity (Customary Units) (Sheet 2 of 2)

percent. The opposite trend occurs for DOC. At a fuel price of 17.17 ¢/l (0.65 $/gal) the DOC of the two-body MB2 aircraft is 10.7 percent less than that of the single body reference aircraft, where at a price of 68.68 ¢/l (2.60 $/gal), this percent reduction increases to 12.0 percent. Thus, as fuel price increases, the operating cost benefit of this multibody aircraft also increases.

To illustrate the advantage of the two-body MB2 aircraft in terms of annual dollar savings, the annual operating cost of the two aircraft are compared. Each aircraft is assumed to fly 4000 hours per year with each flight being flown at the design point range

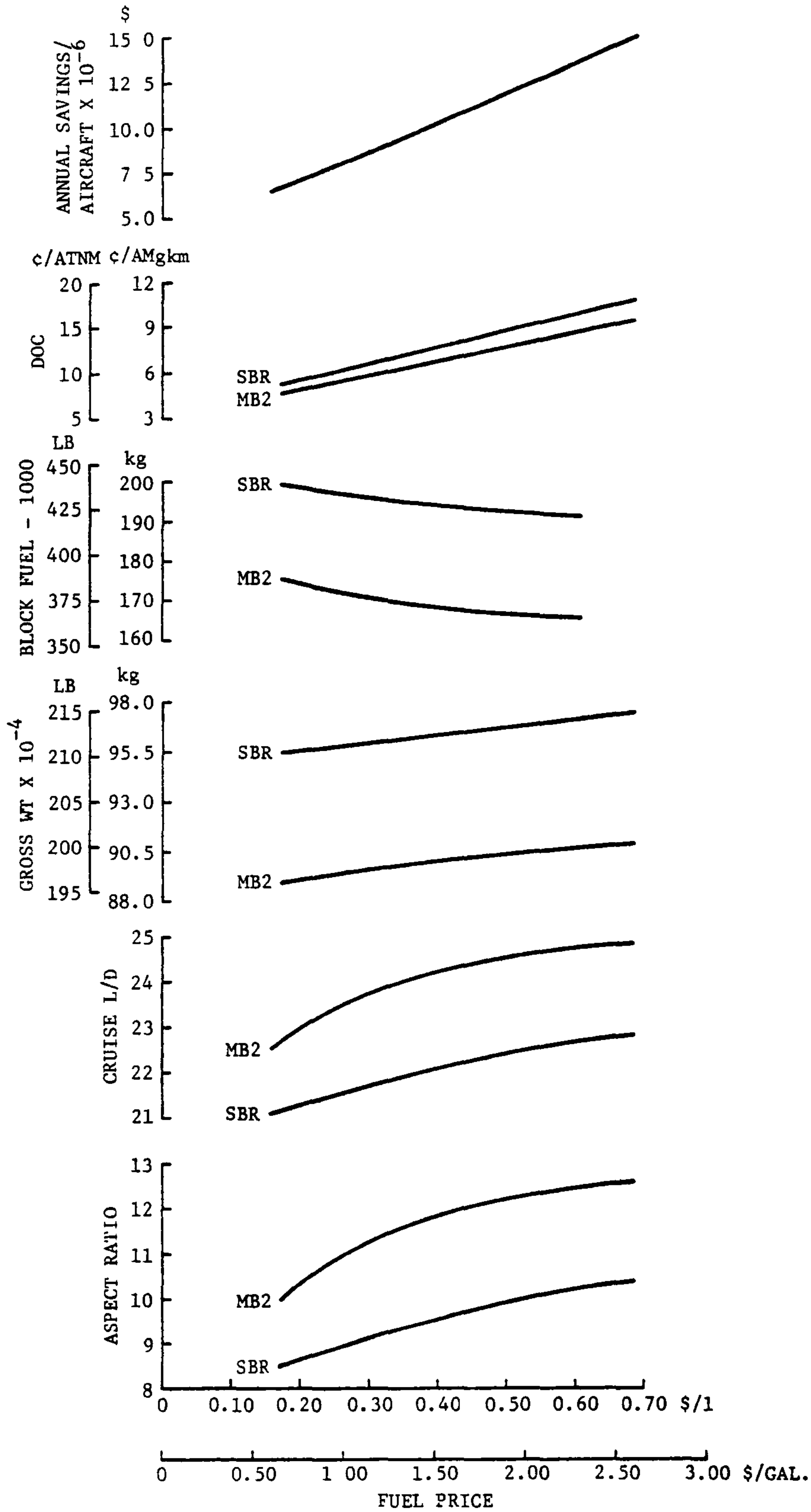

Figure 146. Fuel Price Sensitivity

of 6482.0 km (3500 nm) with a block time of 7.8 hours. Therefore, based upon approximately 512 flights/year, the annual savings provided by the two-body MB2 aircraft are shown in the upper curve of Figure 146. Savings vary from 6.5 million dollars at the low end of the fuel price scale to 15 million at the high end of the scale.

DOC elements as a function of fuel price are shown for both aircraft in Figure 147. At a fuel price of 34.34 ¢/1 (1.30 $/gal), fuel cost is approximately 50 percent of the total DOC. Increasing the fuel price by a magnitude of two, 68.68 ¢/1 (2.60 $/gal), results in approximately 67 percent of the DOC being attributed to fuel cost.

3.5 NONSTANDARD CONTAINER

The aircraft used in the nonstandard container sensitivity study were developed prior to aircraft point design definition. They are, however, sufficiently comparable for a credible evaluation and comparison. The nonstandard aircraft configurations are not redesigned for contour or underfloor containers since this would result in a disparate comparison.

A sensitivity study on the maximum utilization of the cargo compartment for payload is conducted on the single body, two-body, and three-body aircraft with optimized thrust-to-weight ratios as shown in the Cruise Power Setting Sensitivity Study (Section 3.1). Each of these aircraft has an efficient oval fuselage cross section shape with little wasted space. The cargo compartment height is sufficient for the roller height above the floor, the container, and 10.2 cm (4.0 inches) clearance to overhead structure. Nonstandard containers are used in the forward and aft fuselage tapered sections, in concert with the standard containers, to increase the container/fuselage efficiency in these areas. The floor plans and container arrangements are shown in Figures 148, 149, and 150 along with the containers' weights, volumes, and payload capability at approximately 160.2 kg/m^3 (10 lb/ft^3) density.

The utilization of nonstandard containers on floor areas previously unused reduces the length of the fuselage and cargo compartment by approximately 3.1m (10 feet) for all three aircraft.

A comparison of the three standard container (STD) configurations and the resulting nonstandard container (NSC) alternate is shown in Figure 151.

The fuselage efficiency is the cross section area of the container divided by the cross section area of the fuselage measured at the fuselage constant section. The fuselage efficiency for the four-stick single body reference aircraft is 0.3347, and 0.4022 for the

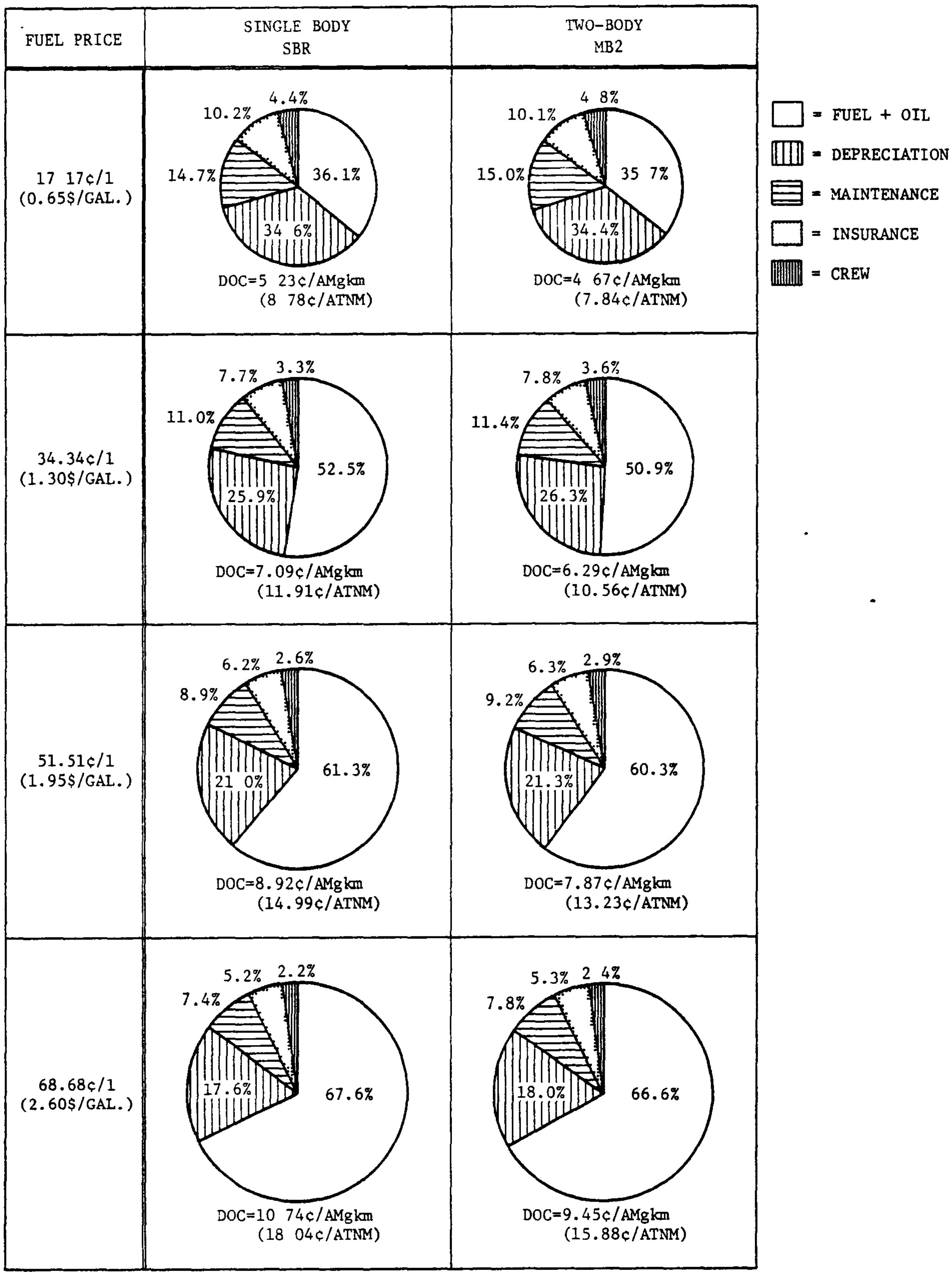

Figure 147. DOC Element Comparison - Fuel Price Sensitivity

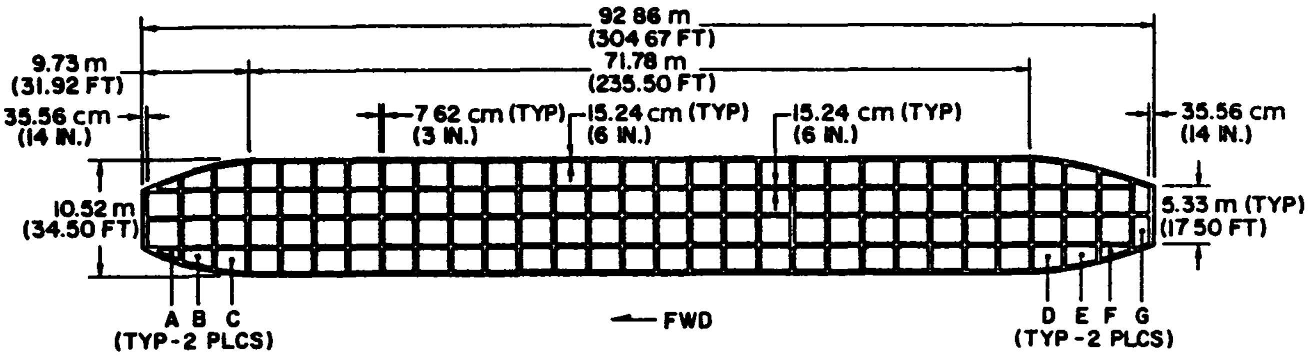

CONTAINER CODE	NET VOLUME		TARE WEIGHT		TOTAL WT-kg	TOTAL WT-LB
	CU.m.	CU.FT.	kg	LB	158 kg/m³ DENSITY	9.87 LB/FT³ DENSITY
STANDARD*	16.4	580	499	1100	3096	6825
A	4.0	141	182	401	814	1795
B	9.8	346	364	802	1913	4216
C	14.1	498	447	985	2675	5895
D	15.0	531	459	1013	2838	6256
E	11.9	420	425	938	2306	5083
F	6.8	241	310	684	1389	3062
G	10.6	376	375	826	2059	4537

*2.44m X 2.44m X 3.05m
(8 FT X 8 FT X 10 FT)

Figure 148. Standard/Nonstandard Container Arrangement - Single Body Reference Aircraft

three-stick two-body and three-body aircraft. These values do not change for the NSC aircraft as all changes occur forward and aft of the fuselage constant section. The percent decrease in fuselage length and total wetted area for the NSC aircraft is attributed to deplugging the fuselage in the constant section. The payload removed from the constant section is added in non-standard containers and evenly distributed in the tapered forward and aft cargo floor areas. The percent decrease in the total fuselage wetted areas is progressively larger as the number of fuselages for an aircraft increases. This indicates that there is more unused space in the two- and three-body aircraft than in the single body aircraft.

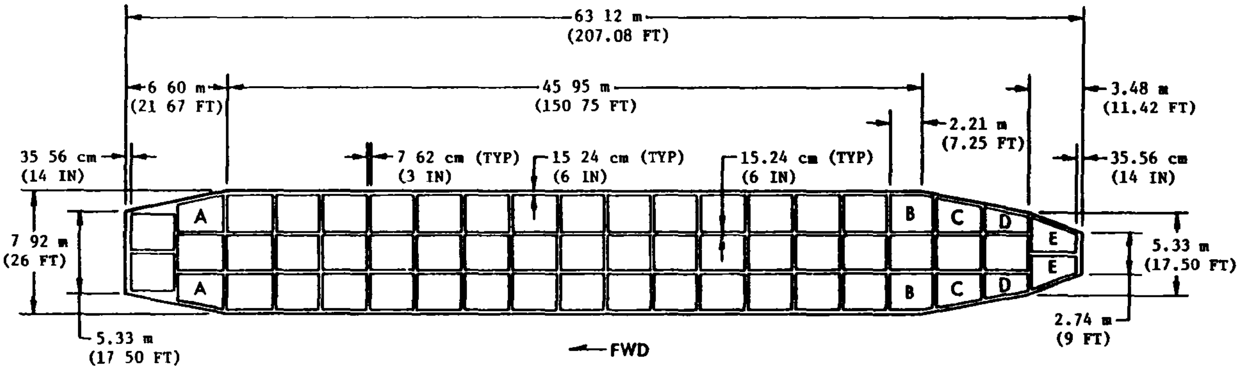

CONTAINER CODE	NET VOLUME		TARE WEIGHT		TOTAL WT-kg	TOTAL WT-LB
	CU. m	CU. FT	kg	LB	160 kg/m^3 DENSITY	9.99 LB/FT^3 DENSITY
STANDARD*	16.4	580	499	1100	3124	6888
A	14.4	507	459	1011	2754	6071
B	15.8	559	489	1077	3019	6656
C	12.9	457	438	965	2507	5526
D	9.2	324	363	800	1830	4034
E	12.1	426	428	944	2356	5195

*2.44 m x 2.44 m x 3.05 m
(8' x 8' x 10')

Figure 149. Standard/Nonstandard Container Arrangement - Two-Body MB2 Aircraft

The percentage weight decreases shown in Figure 151 increase progressively with the number of fuselages affected. The gross weight decrease is 0.6 percent for the single body, 1.7 percent for the two-body, and 2.0 percent for the three-body aircraft. The decrease in mission fuel and increased productivity, which is Mg km/kg fuel (ton nm/lb fuel), is 0.9, 1.7, and 2.0 percent, respectively, for the above aircraft. The decrease in acquisition cost and DOC is 0.8 percent for the single body aircraft, and between 2 and 3 percent for the multibody aircraft. Some of the advantages of using nonstandard containers are diminished by the higher initial cost of the containers due to low demand, logistic problems, and higher container weight to

payload accommodated ratios.

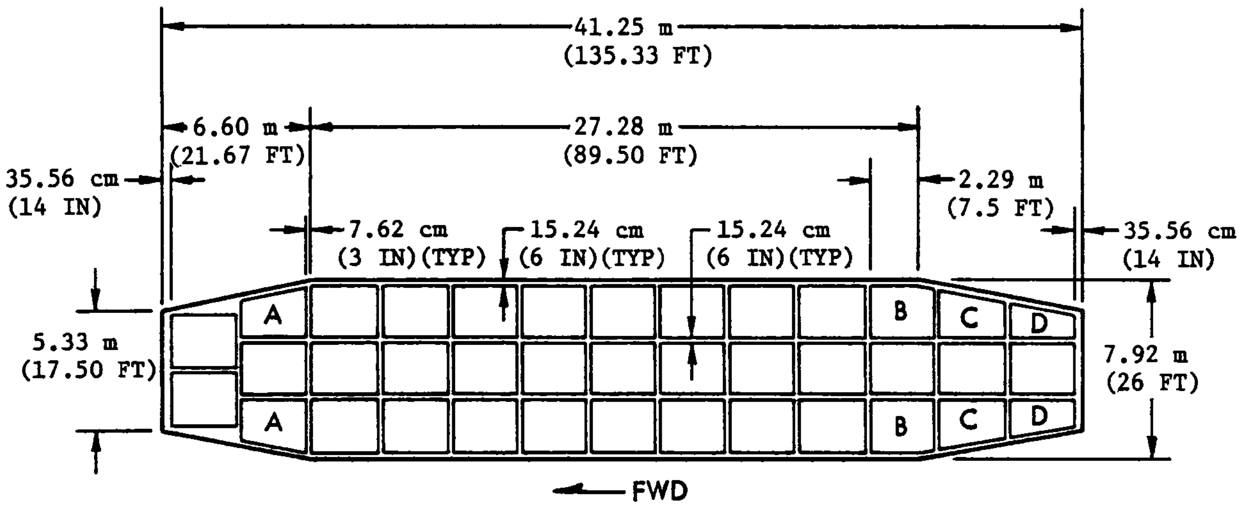

CONTAINER CODE	NET VOLUME		TARE WEIGHT		TOTAL WT-kg	TOTAL WT-LB
	CU. m	CU. FT	kg	LB	160 kg/m^3 DENSITY	9.99 LB/FT^3 DENSITY
STANDARD*	16.4	580	499	1100	3180	7010
A	14.3	506	459	1011	2799	6171
B	15.8	559	489	1077	3072	6773
C	13.5	476	451	995	2649	5841
D	10.5	371	381	840	2094	4616

*2.44 m x 2.44 m x 3.05 m
(8' x 8' x 10')

Figure 150. Standard/Nonstandard Container Arrangement - Three-Body MB3 Aircraft

IDENTIFY (CONTAINER)	SBR (STD)	SBR (NSC)	%* DECREASE (INCREASE)	MB2 (STD)	MB2 (NSC)	%* DECREASE (INCREASE)	MB3 (STD)	MB3 (NSC)	%* DECREASE (INCREASE)
FUSELAGE									
NUMBER	1	1	0.0	2	2	0.0	3	3	0.0
EFFICIENCY	0.3347	0.3347	0.0	0.4022	0.4022	0.0	0.4022	0.4022	0.0
LENGTH - m	111.53	108.41	2.8	79.60	76.53	3.9	60.86	57.74	5.1
WETTED AREA - m^2 (TOTAL)	3,064	2,967	3.2	3,421	3,269	4.5	3,711	3,478	6.3
WEIGHTS - kg									
FUSELAGE	105,057	100,629	4.2	107,238	100,938	5.9	102,929	94,647	8.0
STRUCTURE	290,753	287,759	1.0	265,442	255,100	3.9	255,282	243,398	4.7
OPERATING	376,164	372,567	1.0	342,417	330,850	3.4	335,613	322,187	4.0
FUEL	233,509	231,423	0.9	201,849	198,447	1.7	219,629	215,275	2.0
GROSS	959,665	953,995	0.6	894,257	879,289	1.7	905,234	887,453	2.0
PERFORMANCE									
Mg-km/1 FUEL	9.33	9.41	(0.9)	10.80	10.98	(1.7)	9.92	10.12	(2.0)
COST									
ACQUISITION $\$10^6$	305.8	303.5	0.8	273.1	266.3	2.5	277.3	269.3	2.9
DOC ¢/AMgkm**	7.09	7.03	0.8	6.26	6.14	2.0	6.58	6.43	2.3

$$* \ \% = 100 \times \frac{\text{NON-STANDARD CONTAINER-COMPARISON AIRCRAFT}}{\text{COMPARISON AIRCRAFT}}$$

** FUEL COST - 34.34 ¢/LITER

Figure 151. Standard vs Nonstandard Container Aircraft Comparison (Metric Units) (Sheet 1 of 2)

IDENTITY (CONTAINER)	SBR (STD)	SBR (NSC)	%* DECREASE (INCREASE)	MB2 (STD)	MB2 (NSC)	%* DECREASE (INCREASE)	MB3 (STD)	MB3 (NSC)	%* DECREASE (INCREASE)
FUSELAGE									
NUMBER	1	1	0.0	2	2	0.0	3	3	0.0
EFFICIENCY	0.3347	0.3347	0.0	0.4022	0.4022	0.0	0.4022	0.4022	0.0
LENGTH - FT	365.91	355.66	2.8	261.17	251.08	3.9	199.67	189.42	5.1
WETTED AREA - SQ FT (TOTAL)	32,983	31,934	3.2	36,828	35,188	4.5	39,939	37,437	6.3
WEIGHTS - LB									
FUSELAGE	231,610	221,850	4.2	236,420	222,530	5.9	226,920	208,660	8.0
STRUCTURE	641,000	634,400	1.0	585,200	562,400	3.9	562,800	536,600	4.7
OPERATING	829,300	821,370	1.0	754,900	729,400	3.4	739,900	710,300	4.0
FUEL	514,800	510,200	0.9	445,000	437,500	1.7	484,200	474,600	2.0
GROSS	2,115,700	2,103,200	0.6	1,971,500	1,938,500	1.7	1,995,700	1,956,500	2.0
PERFORMANCE									
TNM/GAL FUEL	21.02	21.21	(0.9)	24.33	24.74	(1.7)	22.34	22.79	(2.0)
COST									
ACQUISITION $\$10^6$	305.8	303.5	0.8	273.1	266.3	2.5	277.3	269.3	2.9
DOC ¢/ATNM**	11.91	11.81	0.8	10.52	10.31	2.0	11.06	10.81	2.3

* $\% = 100 \times \dfrac{\text{NON STANDARD CONTAINER-COMPARISON AIRCRAFT}}{\text{COMPARISON AIRCRAFT}}$

** FUEL COST 1.30 $ GALLON

Figure 151. Standard vs Nonstandard Container Aircraft Comparison (Customary Units) (Sheet 2 of 2)

4.0 FINAL AIRCRAFT DEFINITIONS

The final single body and multibody aircraft configurations are given in Figures 152 through 155. Characteristics data for each of these aircraft are summarized in Figure 156. The two-body MB1 aircraft is unchanged from the initial point design definition. However, as a result of the point design analysis, it is necessary to revise the remaining three aircraft.

The cruise power setting (aircraft thrust-to-weight ratio) is revised to provide an improved thrust match condition for the single body aircraft. This results in a slightly higher gross weight aircraft but a lower fuel consumption. The benefit derived is a lower DOC, 7.09 ¢/AMgkm (11.91¢/ATNM) for the final aircraft as compared to 7.10¢/AMgkm (11.93¢/ATNM) for the point design aircraft.

The two-body MB2 aircraft cruise power setting is also revised. In addition, its wing weight is increased as a result of critical flutter conditions encountered with the point design aircraft. As compared to the point design two-body MB2 aircraft, the final two-body MB2 aircraft has a higher gross weight but lower fuel weight and direct operating cost.

The point design three-body MB3 aircraft also was found to have a critical flutter condition requiring the wing weight of the final aircraft to be increased. An increase in aircraft thrust-to-weight ratio is not beneficial to this aircraft, thus the final three-body MB3 aircraft has an increase in gross weight and DOC when compared to the point design aircraft.

A detailed explanation of these point design thrust-to-weight ratio and wing weight changes can be found in paragraphs 3.1 and 2.7.3.3, respectively.

SPEED	0.80 MACH
PAYLOAD	350,000 kg (771,618 LB)
RANGE	6,482 km (3,500 NM)
OPERATING WT.	376,164 kg (829,300 LB)
GROSS WT.	959,665 kg (2,115,700 LB)
BLOCK FUEL	195,226 kg (430,400 LB)
ASPECT RATIO	9.21
DOC	7.09 ¢/AMgkm @ 34.34¢ PER LITER
	(11.91 ¢/ATNM @ 1.30$ PER GAL.)

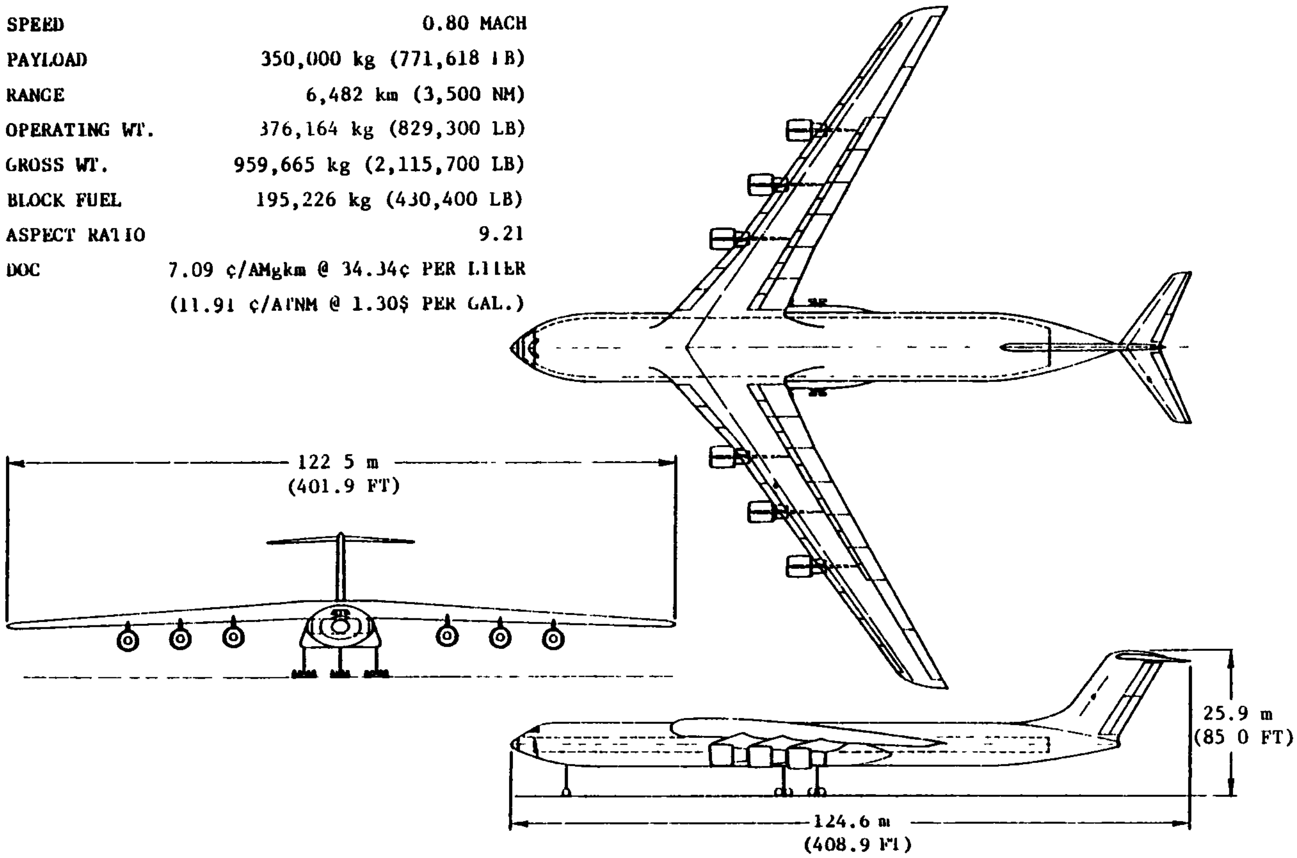

Figure 152. Single Body Reference SBR Aircraft - Final

SPEED	0.80 MACH
PAYLOAD	350,000 kg (771,618 LB)
RANGE	6,482 km (3,500 NM)
OPERATING WEIGHT	323,547 kg (713,300 LB)
GROSS WEIGHT	893,214 kg (1,969,200 LB)
BLOCK FUEL	183,796 kg (405,200 LB)
ASPECT RATIO	9.70
DOC	6.47 ¢/AMgkm @ 34.34¢ PER LITER
	(10.87 ¢/ATNM @ 1.30$ PER GAL.)

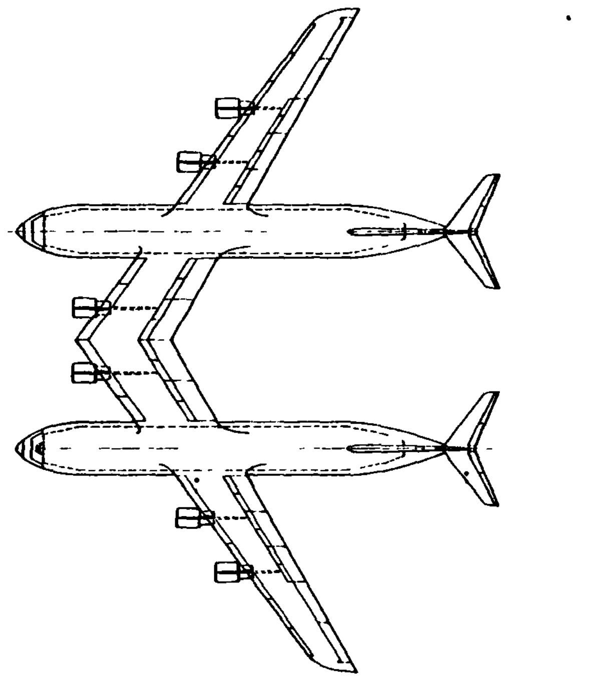

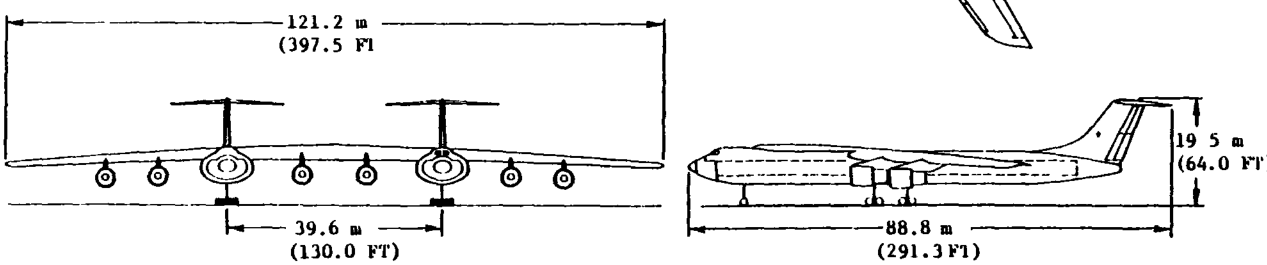

Figure 153. Two-Body MB1 Aircraft - Final

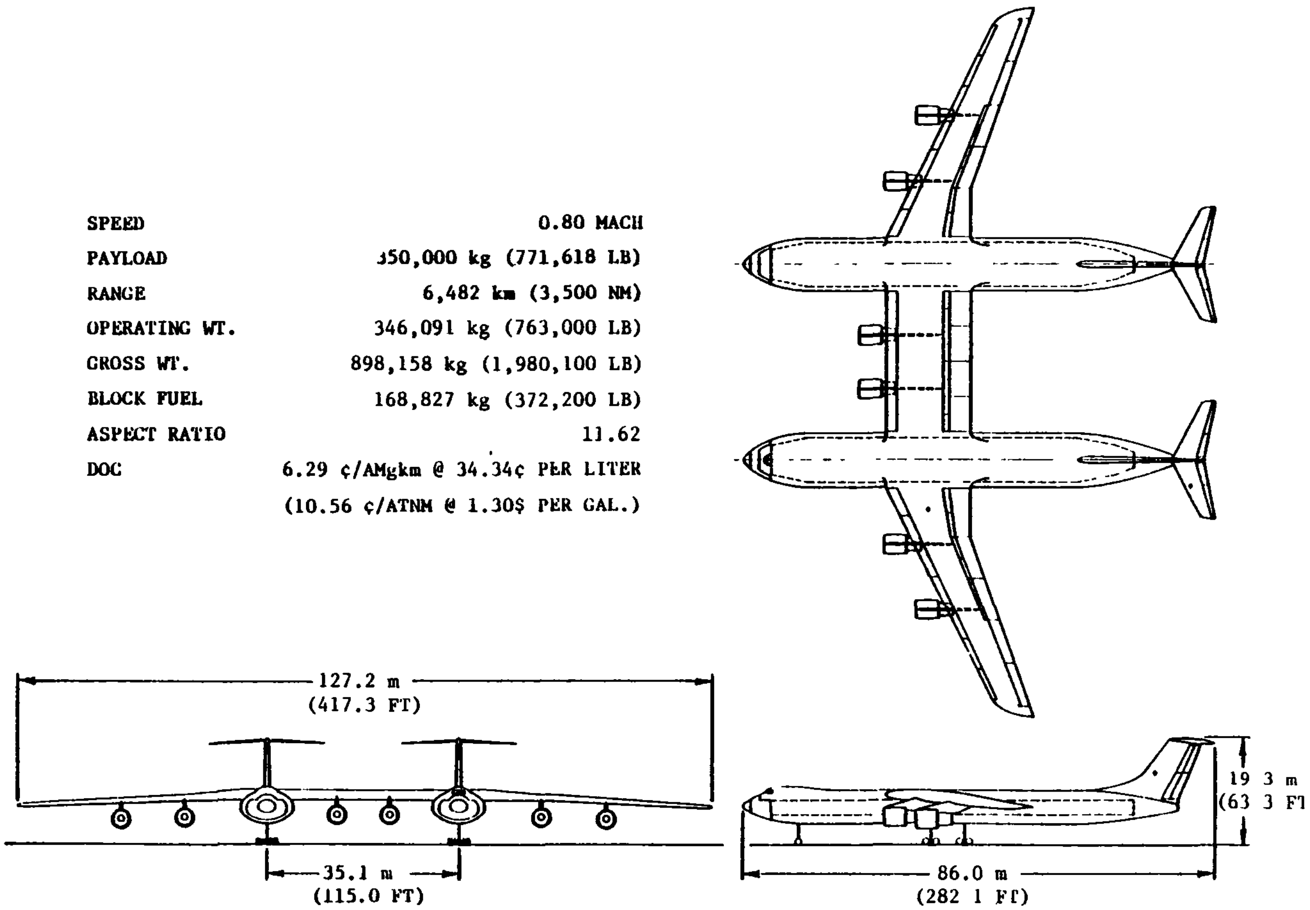

Figure 154. Two-Body MB2 Aircraft - Final

SPEED	0.80 MACH
PAYLOAD	350,000 kg (771,618 LB)
RANGE	6,482 km (3,500 NM)
OPERATING WT.	338,845 kg (747,025 LB)
GROSS WT.	913,490 kg (2,013,900 LB)
BLOCK FUEL	187,904 kg (414,257 LB)
ASPECT RATIO	11.83
DOC	6 69 ¢/AMgkm @ 34.34¢ PER LITER
	(11.24 ¢/ATNM @ 1.30$ PER GAL.)

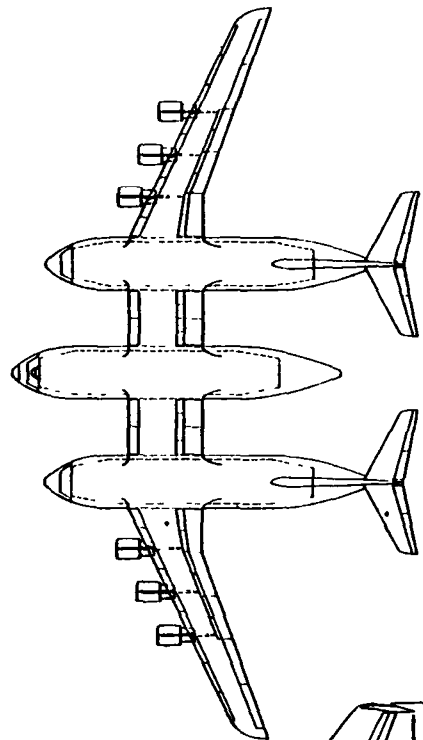

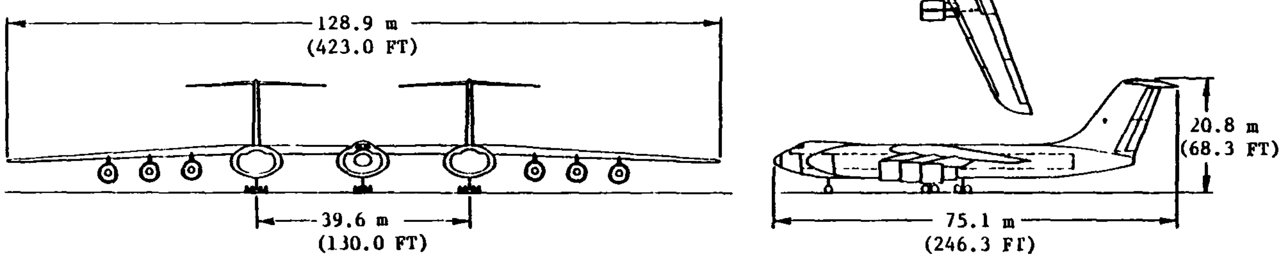

Figure 155. Three-Body MB3 Aircraft - Final

DATA ITEM ↓ / AIRCRAFT TYPE →	SINGLE BODY SBR	MULTIBODY		
		MB1	MB2	MB3
Wing				
Aspect Ratio	9.21	9.70	11.62	11.83
Area - SQ. m	1566.5	1454.3	1338.6	1348.0
Sweep - Radians	0.610	0.610	0.436	0.436
Loading - kN/SQ. m	5.87	5.87	6.43	6.47
Span - m	120.09	118.78	124.70	126.25
Weight - kg	125,477	89,512	114,269	103,238
Weight - kg/SQ. m	80.1	61.6	85.3	76.6
Fuselage				
Length - m	111.53	79.61	79.61	60.87
Width - m	12.25	9.60	9.60	9.60
Height - m	7.71	6.00	6.00	6.00
Weight - kg	105,057	107,116	107,284	102,997
Weight - kg/SQ. m	34.3	31.3	31.3	27.5
Floor Height Above Ground - m	7.77	5.39	5.41	4.11
Empennage				
Area - Sq. m	303.6	347.9	329.3	531.6
Weight - kg	7,784	8,469	8,137	11,471
Weight - kg/SQ. m	25.6	24.4	24.7	21.6
Propulsion				
Engines - Number	6	6	6	6
Thrust/Eng. - 1000 N	337.4	308.8	298.1	315.3
System Wt. - kg	54,558	49,741	47,668	50,698
Cruise Power Setting η	0.92	0.95	0.88	0.95
Landing Gear				
Max Tread Width - m	16.98	43.34	38.77	43.34
Weight - kg	42,878	29,710	30,232	30,386
Aircraft Weight - 1000 kg				
Structure	290.8	243.6	268.4	257.1
Operating	376.2	323.5	346.1	338.8
Fuel	233.5	219.6	202.1	224.7
Gross	959.7	893.2	898.2	913.5
Performance				
Cruise L/D	21.81	21.46	24.05	21.48
Block Fuel - 1000 kg	195.2	183.8	168.8	187.9
Mg km/l - Fuel	9.34	9.91	10.79	9.69
Ferry Range - km	9,953	10,206	10,058	10,023
Ecomonic				
Aircraft Price - $M	305.8	264.8	275.1	279.5
DOC - ¢/AMgkm @ $0.34/l	7.09	6.47	6.29	6.69
Efficiency Factors				
Fuselage	0.335	0.402	0.402	0.402
ML/D	17.45	17.17	17.92	17.78
Aircraft Price/Payload - $/kg	874	757	786	799

Figure 156. Final Aircraft Characteristics Summary (Metric Units) (Sheet 1 of 2)

DATA ITEM / AIRCRAFT TYPE	SINGLE BODY SBR	MULTIBODY MB1	MULTIBODY MB2	MULTIBODY MB3
Wing				
Aspect Ratio	9.21	9.70	11.62	11.83
Area - SQ. FT.	16,862	15,654	14,409	14,510
Sweep - Degree	35	35	25	25
Loading - LB./SQ.FT.	122.5	122.6	134.3	135.2
Span - FT.	394.0	389.7	409.1	414.2
Weight - LB.	276,630	197,340	251,920	227,600
Weight - LB./SQ. FT.	16.41	12.61	17.48	15.69
Fuselage				
Length - FT.	365.9	261.2	261.2	199.7
Width - FT.	40.2	31.5	31.5	31.5
Height - FT.	25.3	19.7	19.7	19.7
Weight - LB.	231,610	236,150	236,520	227,070
Weight - LB/SQ. FT.	7.02	6.41	6.42	5.64
Floor Height Above Ground-FT.	25.50	17.67	17.74	13.50
Empennage				
Area - SQ. FT.	3,268	3,745	3,545	5,722
Weight - LB.	17,160	18,670	17,940	25,290
Weight - LB./SQ. FT.	5.25	4.99	5.06	4.42
Propulsion				
Engines - Number	6	6	6	6
Thrust/Eng. - LB.	75,860	69,410	67,010	70,880
System Wt. - LB.	120,280	109,660	105,090	111,770
Cruise Power Setting η	0.92	0.95	0.88	0.95
Landing Gear				
Max. Tread Width - FT.	55.7	142.2	127.2	142.2
Weight - LB.	94,530	65,500	66,650	66,990
Aircraft Weight - 1000 LB.				
Structure	641.0	537.0	591.7	566.7
Operating	829.3	713.3	763.0	747.0
Fuel	514.8	484.2	445.5	495.3
Gross	2,115.7	1,969.2	1,980.1	2,013.9
Performance				
Cruise L/D	21.81	21.46	24.05	21.48
Block Fuel - 1000 LB.	430.4	405.2	372.2	414.3
Ton NM/GAL. Fuel	21.04	22.32	24.31	21.84
Ferry Range - NM	5,374	5,511	5,431	5,412
Economic				
Aircraft Price - $M	305.8	264.8	275.1	279.5
DOC - ¢ATNM @ 1.30 $/GAL.	11.91	10.87	10.56	11.24
Efficiency Factors				
Fuselage	0.335	0.402	0.402	0.402
ML/D	17.45	17.17	17.92	17.18
Aircraft Price/Payload - $/LB	396	343	357	362

Figure 156. Final Aircraft Characteristics Summary (Customary Units) (Sheet 2 of 2)

5.0 BENEFIT SUMMARY

The aircraft used to define the potential benefits of the multibody aircraft concept are those previously identified under Paragraph 4.0. Each of the multibody aircraft is compared to the single body aircraft, thus defining the potential benefit of the multibody concept. Comparisons are also made between the multibody aircraft to define the multibody concept which provides the maximum potential benefit.

5.1 WEIGHT COMPARISON

Structural weight comparisons of the multibody aircraft to the single body reference aircraft are shown in Figure 157. Wing component weight of the two-body MB1 aircraft realizes the maximum wing weight reduction when compared to the single body reference aircraft. However, it is noted that the wing aspect ratio of the two-body MB1 aircraft is the lowest of the three multibody concepts, thus incurring the minimum weight penalty as a function of aspect ratio. Shown in Figure 158 are variations in both total wing weight and wing weight per unit of wing area as a function of aspect ratio for each of the three multibody aircraft and the single body reference aircraft. All aircraft sized to provide the wing data

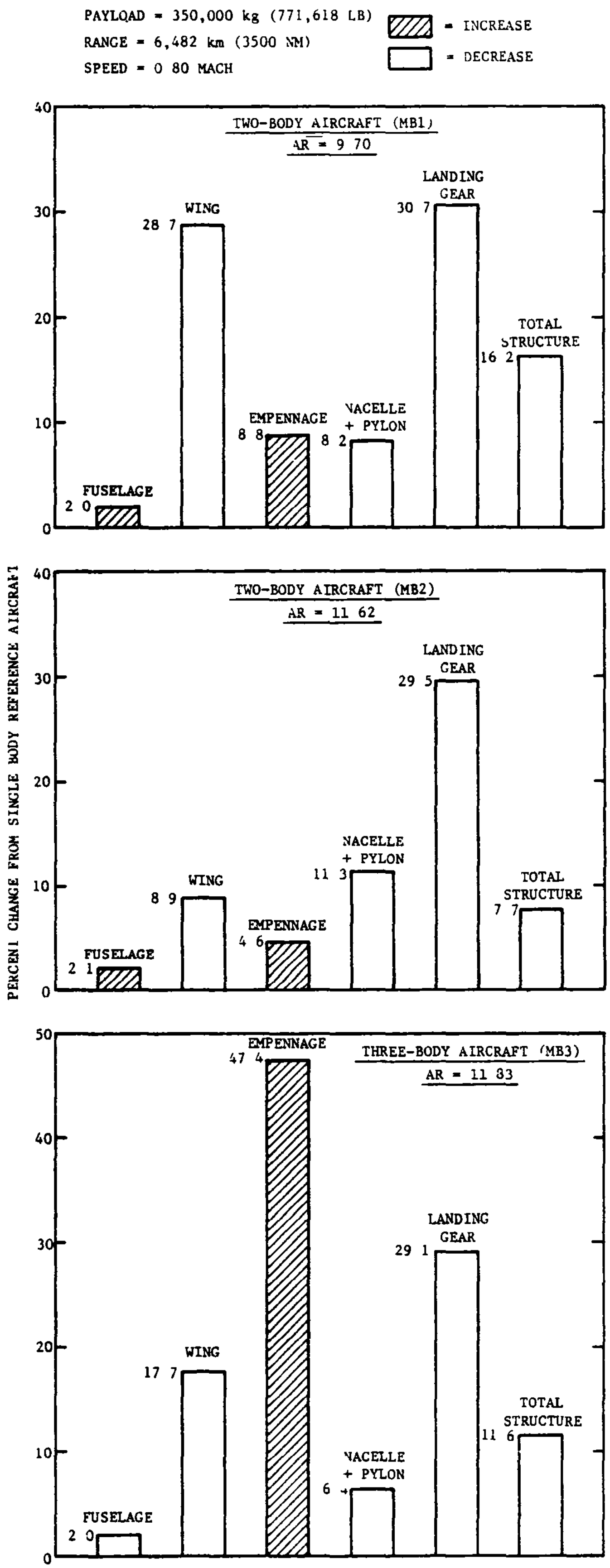

Figure 157. Structural Weight Comparison

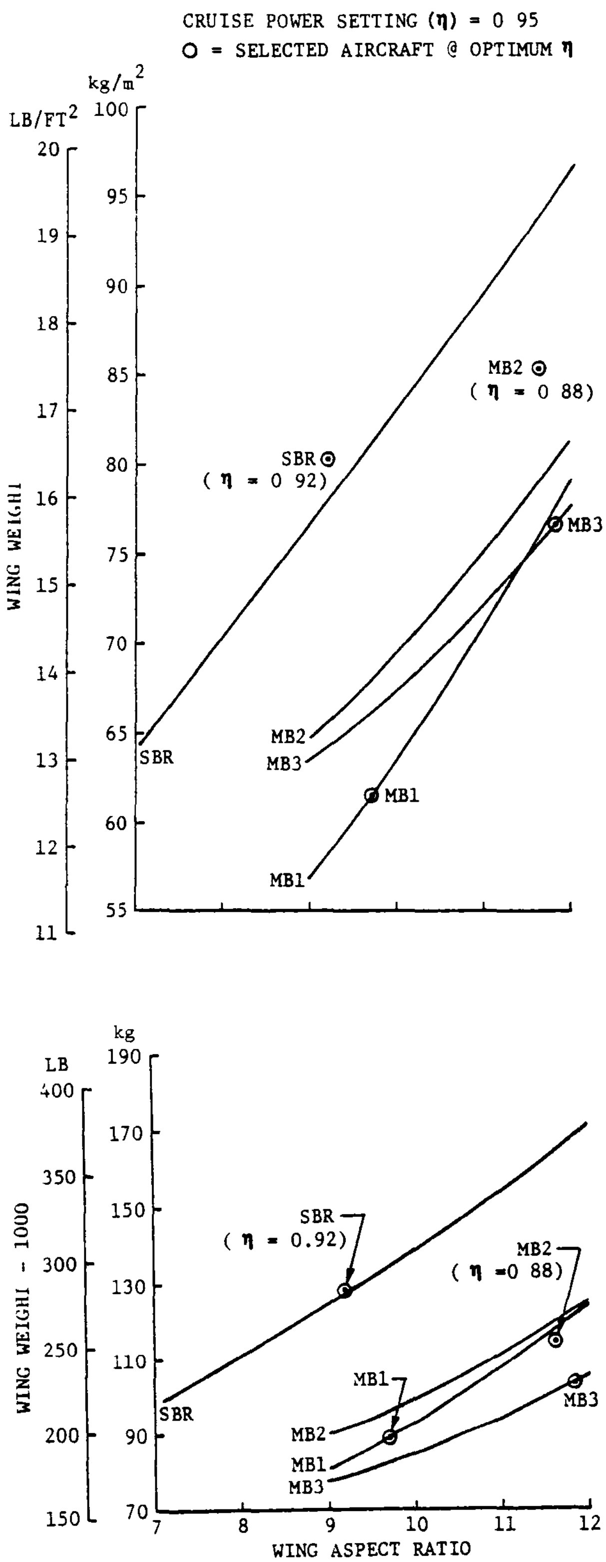

Figure 158. Wing Weight vs Aspect Ratio Comparison

in this figure are required to meet takeoff performance with engine thrust constrained to provide a cruise power setting of 0.95. Target points are used in the figure to identify the cruise power optimized aircraft. As seen from the total wing weight curve in Figure 158, the three-body MB3 aircraft has the lowest wing weight for all aspect ratio values. This lower weight of the three-body MB3 wing is influenced by the location of all six engines outboard of the fuselage, thus providing additional bending relief when compared to the two, two-body aircraft. The two, two-body aircraft have four engines located outboard of the fuselages and two inboard. The additional engine on the outer wing of the three-body MB3 aircraft causes more nose-down twist, as shown in Figure 159. The additional twist tends to shift the airloads inboard and reduce the net bending moment, as shown in Figure 160. The result is that the wing unit weight is less than that of the two-body MB2 wing.

From the wing weight per unit of wing area curve shown in Figure 158, it is seen that the two-body MB1 aircraft has the lower unit weight of the multibody concepts up to an aspect ratio of approximately 11.5. This is primarily a result of the lower wing loading shown as a function of aspect ratio in

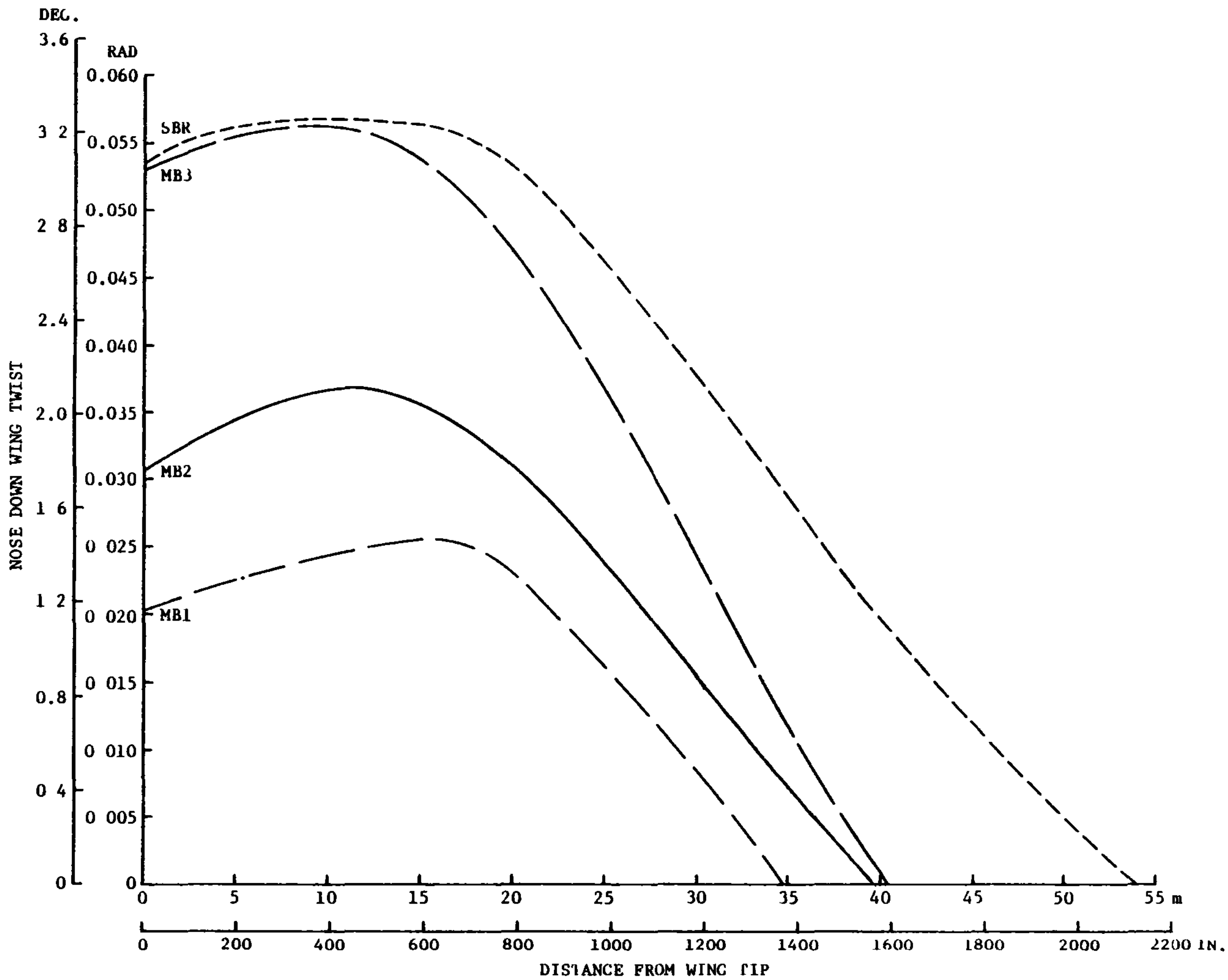

Figure 159. Wing Twist at 2.5g Dive Speed - Mission Fuel

Figure 161. It is also of interest to note in this figure that the single body reference aircraft has the minimum wing loading for any given aspect ratio, yet, as shown in Figures 158 and 161, it has the maximum weight values. This is an indication of the weight advantage afforded by the bending relief provided by the multibody concepts. Figures 160 and 162 show the critical up bending and down bending moments for the four point design wings. The single body wing loads continue to increase from tip to root as expected. The multibody wing loads, however, increase to the point where the body is located and then show a dramatic decrease in load on the inboard section. This causes a decrease in the multibody aircraft wing weight compared to the single body aircraft wing.

The unit weight of the three-body is the lowest of the four point design aircraft. This is due to the fact that the center body has no empennage or main landing gear loads. The two out-

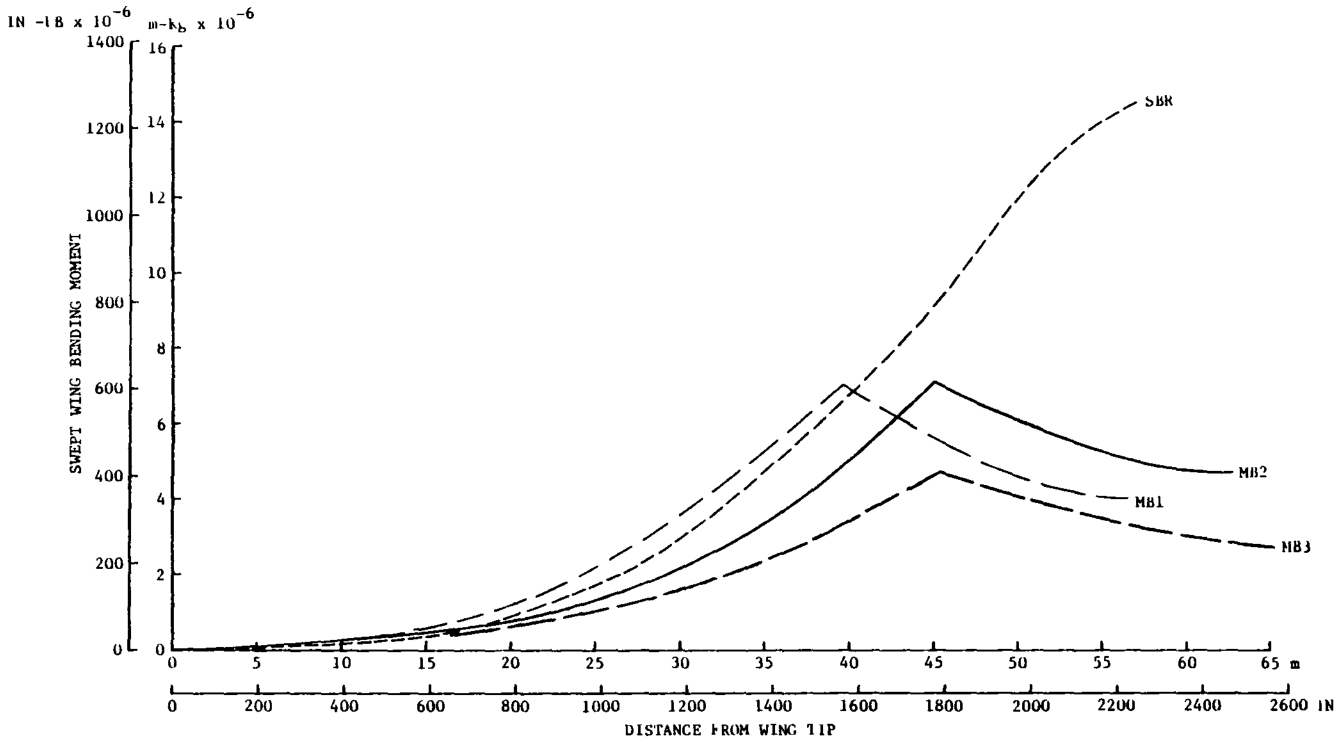

Figure 160. Swept Wing 2.5g Up Bending Moments

board bodies have the same unit weight as the two-body aircraft, but the center body is lighter because of the reduced loads. The net effect is that the overall unit weight of the three-body fuselage is lightest.

The single body aircraft requires the minimum weight empennage as indicated in Figure 157. Although the weight per unit area of the multibody empennage configurations is slightly less than that of the single body, a greater area is required resulting in a higher total weight. The shorter multibody fuselage bodies reduce the empennage tail arms and thereby increase tail area requirements.

The landing gear on the three multibody point design aircraft is about 30 percent lighter than that of the single body reference aircraft. There are three basic reasons for this. On the single body reference aircraft, the gear must be mounted on the sides of the fuselage as far apart as possible to provide for roll stability during ground operations. This requires beaming the landing gear loads into the fuselage structure. The multibody configurations allow the main gear to be mounted in the center of the fuselages which results in a much more efficient landing gear support structure. Due to the underfloor depth at the fuselage

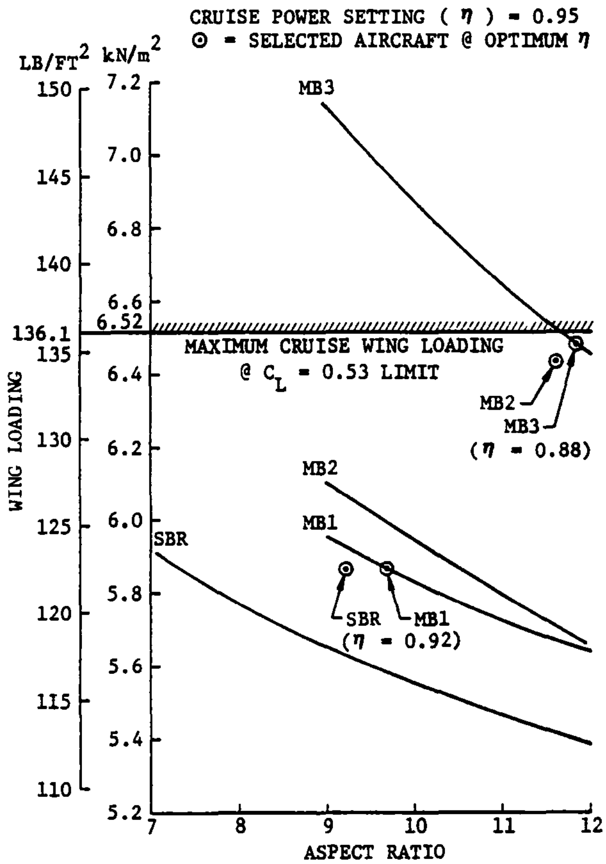

Figure 161. Wing Loading vs Aspect Ratio Comparison

centerline, most of the gear can be stowed internally rather than externally as on the single body reference aircraft. For this reason, there is no need for the large main landing gear fairing normally seen on a high wing cargo aircraft. Also, due to shorter fuselages, the multibody aircraft use a shorter gear strut for meeting aircraft rotation requirements. The combination of these effects allows for a much simpler and lighter main landing gear design.

The reduction in weight of these structural components results in the total structural weight of the two-body MB1 and MB2, and three-body MB3 aircraft being 16.2, 7.7, and 11.6 percent lighter than that of single body aircraft, respectively, as seen in Figure 163.

The remaining two major weight groups which define aircraft weight empty are the propulsion system and systems and equipment. The multibody propulsion system weight reductions vary from 7.1 percent to 12.6 percent when compared to the single body aircraft as shown in Figure 163. The multibody propulsion system weight benefits from both an overall reduction in aircraft weight and drag, resulting in a lower thrust and physical size requirement. Systems and equipment are relatively independent of aircraft concept and, as shown, remain approximately constant in weight for the four aircraft.

The resulting effect of these component weight reductions is a reduction in aircraft operating weight--14.0, 8.0, and 9.9 percent for the two-body MB1 and MB2, and three-body MB3 aircraft, respectively.

The synergistic influence of the multibody aircraft weight, thrust, and drag reductions is a reduction in both mission fuel and gross takeoff weight. As seen in Figure 163, these reductions

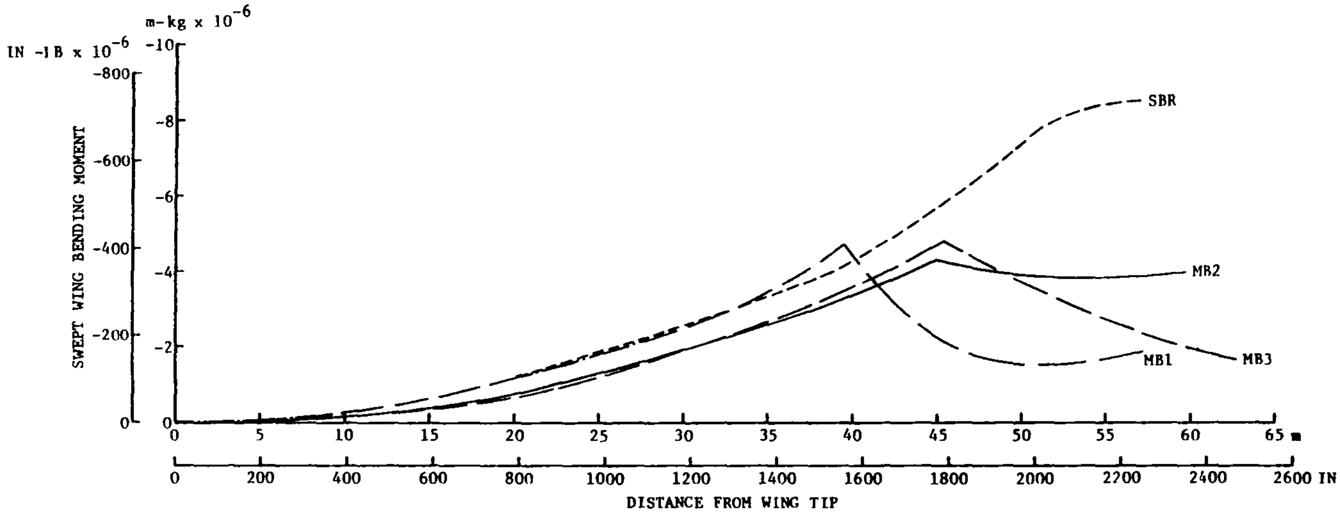

Figure 162. Swept Wing Down Bending Moments - 2.0g Taxi - Mission Fuel

in zero fuel and gross weight are 7.2 and 6.9 percent, respectively, for the two-body MB1 aircraft, 4.1 and 6.4 percent for the two-body MB2 aircraft, and 5.1 and 4.8 percent for the three-body MB3 aircraft. Weight fraction comparison data are provided in Figure 164 for each of the aircraft. No major changes occur in the distribution of the aircraft weight as the aircraft concept is changed.

5.2 STABILITY AND CONTROL COMPARISONS

The stability, control, and flying qualities analyses do not indicate that an advantage is gained by use of the multibody concept. However, the analyses have not shown a reason to believe that the multibody aircraft cannot achieve good flying qualities.

One method of showing the level of difficulty involved in achieving good flying qualities is to compare how the unaugmented aircraft meet the specific requirements of military specifications. The three multibody aircraft and the single body reference aircraft are compared to six longitudinal and thirteen lateral-directional cirteria. They are then ranked one through four on each criterion, (with one being top ranked), and a weighted average is compiled.

Using this technique, the final "longitudinal" ranking as to decreasing capacity to meet the criteria is the two-body MB1, two-body MB2, single body reference, and three-body MB3 aircraft with weighted averages of 12, 13, 16, and 19, respectively. The differences in these weighted averages show that there is no major problem with any aircraft in the longitudinal mode and, indeed, two of the multibody aircraft are ranked above the single body aircraft.

METRIC UNITS - 1000 kg

ITEM - WT. \ AIRCRAFT	SINGLE BODY SBR	MULTIBODY					
		MB1	Δ%	MB2	Δ%	MB3	Δ%
STRUCTURE	290.7	243.6	16.2	268.4	7.7	257.1	11.6
PROPULSION	54.6	49.8	8.8	47.7	12.6	50.7	7.1
SYSTEMS & EQUIPMENT	23.2	22.7	2.1	22.3	4.1	23.5	(1.4)
WEIGHT EMPTY	368.5	316.1	14.2	338.7	8.1	331.3	10.1
OPERATING EQUIPMENT	7.7	7.5	1.8	7.4	3.9	7.6	1.3
OPERATING WEIGHT	376.2	323.5	14.0	346.1	8.0	338.9	9.9
PAYLOAD	350.0	350.0		350.0		350.0	
ZERO FUEL WEIGHT	726.2	673.5	7.2	696.1	4.1	688.9	5.1
FUEL	233.5	219.6	5.9	202.1	13.5	224.7	3.8
GROSS WEIGHT	959.7	893.2	6.9	898.2	6.4	913.5	4.8
CUSTOMARY UNITS - 1000 LB							
STRUCTURE	640.9	537.0	16.2	591.7	7.7	566.7	11.6
PROPULSION	120.3	109.7	8.8	105.1	12.6	111.8	7.1
SYSTEMS & EQUIPMENT	51.2	50.1	2.1	49.1	4.1	51.9	(1.4)
WEIGHT EMPTY	812.4	696.8	14.2	746.7	8.1	730.4	10.1
OPERATING EQUIPMENT	16.9	16.6	1.8	16.3	3.9	16.7	1.3
OPERATING WEIGHT	829.3	713.3	14.0	763.0	8.0	747.1	9.9
PAYLOAD	771.6	771.6		771.6		771.6	
ZERO FUEL WEIGHT	1600.9	1484.9	7.2	1534.6	4.1	1518.7	5.1
FUEL	514.8	484.2	5.9	445.5	13.5	495.3	3.8
GROSS WEIGHT	2115.7	1969.2	6.9	1980.1	6.4	2014.0	4.8

$$\Delta\% = 100\left[\frac{MB - SBR}{SBR}\right]$$

(xx) = Increase

Figure 163. Component Weight Comparison

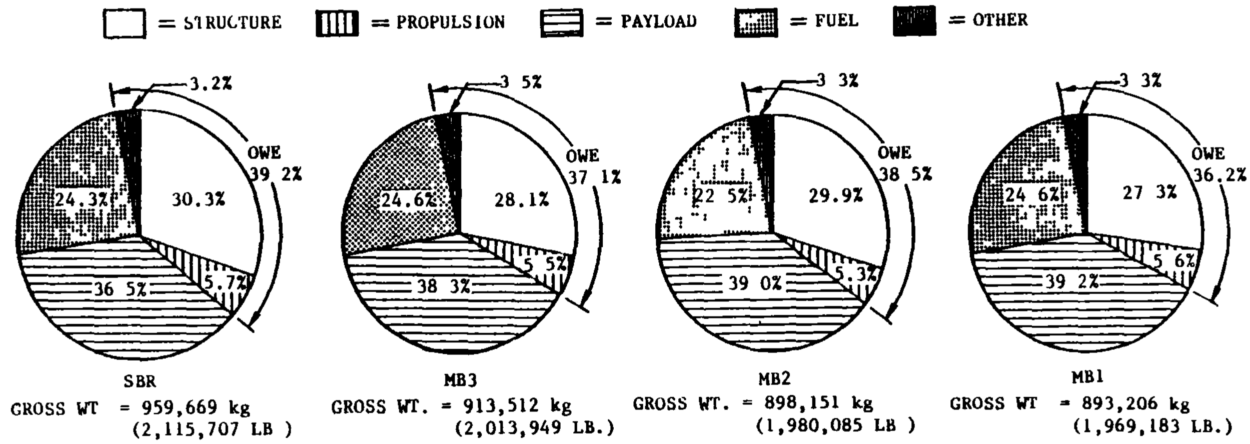

Figure 164. Weight Fraction Comparison

A similar ranking of the lateral-directional mode is as follows: Single body reference, three-body MB3, two-body MB2, and two-body MB1 aircraft, with averages of 23.5, 26.5, 39.5, and 40.5, respectively. The spread in averages is more conclusive for this comparison and indicates, as expected, that the aircraft with the highest roll inertia will require the maximum augmentation.

The most important result of the stability and control analyses is that roll control will limit the fuselage spanwise location. With this knowledge, it is extremely important that roll criteria be adequately defined and innovative control concepts be further explored.

5.3 FLY-AWAY AND DIRECT OPERATING COST COMPARISONS

All fly-away cost elements as shown in Figure 165 are less for the multi-body aircraft than for the single body aircraft, with the exception of the wing and landing gear cost per pound. The increased wing cost reflects the additional complexity of the multiple wing joints at the fuselage mating planes. The large percent decrease in fuselage cost per pound incorporates the effect of commonality of structural components used in the production of the multiple fuselage concepts. The additional multibody landing gear costs result from size (weight), materials, and complexity. Figure 166 shows the strong influence of size on landing gear costs when expressed as dollars per kg (lb) of structure. The multibody study considers this influencing driver as well as complexity, commonality, and materials. The resulting cost per pound of structure values show the multibody designs with a higher cost per pound. This results from the multibody main landing gears being lighter than the single body gear, therefore taking a

METRIC UNITS

AIRCRAFT → / ↓ ITEM	SINGLE BODY SBR	MULTIBODY					
		MB1	Δ%	MB2	Δ%	MB3	Δ%
COST PER kg - $							
WING	306	315	(2.9)	309	(0.7)	311	(1.4)
EMPENNAGE	747	692	7.4	694	7.1	670	10.3
FUSELAGE	355	276	22.4	276	22.4	293	17.4
LANDING GEAR	79	88	(11.1)	86	(8.3)	86	(8.3)
NACELLE & PYLON	661	657	0.7	655	1.0	657	0.7
WEIGHT EMPTY	326	313	4.1	311	4.7	322	1.4
COST-MILLIONS $							
RDT&E	77.0	72.0	6.5	72.7	5.6	72.7	5.6
PRODUCTION	120.2	99.2	17.5	105.5	12.2	106.7	11.2
OTHER	108.6	93.6	13.8	96.9	10.8	100.1	7.8
FLY-AWAY	305.8	264.8	13.4	275.1	10.0	279.5	8.6

CUSTOMARY UNITS

AIRCRAFT → / ↓ ITEM	SINGLE BODY SBR	MULTIBODY					
		MB1	Δ%	MB2	Δ%	MB3	Δ%
COST PER POUND - $							
WING	139	143	(2.9)	140	(0.7)	141	(1.4)
EMPENNAGE	339	314	7.4	315	7.1	304	10.3
FUSELAGE	161	125	22.4	125	22.4	133	17.4
LANDING GEAR	36	40	(11.1)	39	(8.3)	39	(8.3)
NACELLE & PYLON	300	298	0.7	297	1.0	298	0.7
WEIGHT EMPTY	148	142	4.1	141	4.7	146	1.4
COST-MILLIONS $							
RDT&E	77.0	72.0	6.5	72.7	5.6	72.7	5.6
PRODUCTION	120.2	99.2	17.5	105.5	12.2	106.7	11.2
OTHER	108.6	93.6	13.8	96.9	10.8	100.1	7.8
FLY-AWAY	305.8	264.8	13.4	275.1	10.0	279.5	8.6

$\Delta\% = 100 \times \left[\frac{MB - SBR}{SBR}\right]$ (xx) = Increase

Figure 165. Fly-Away Cost Comparison

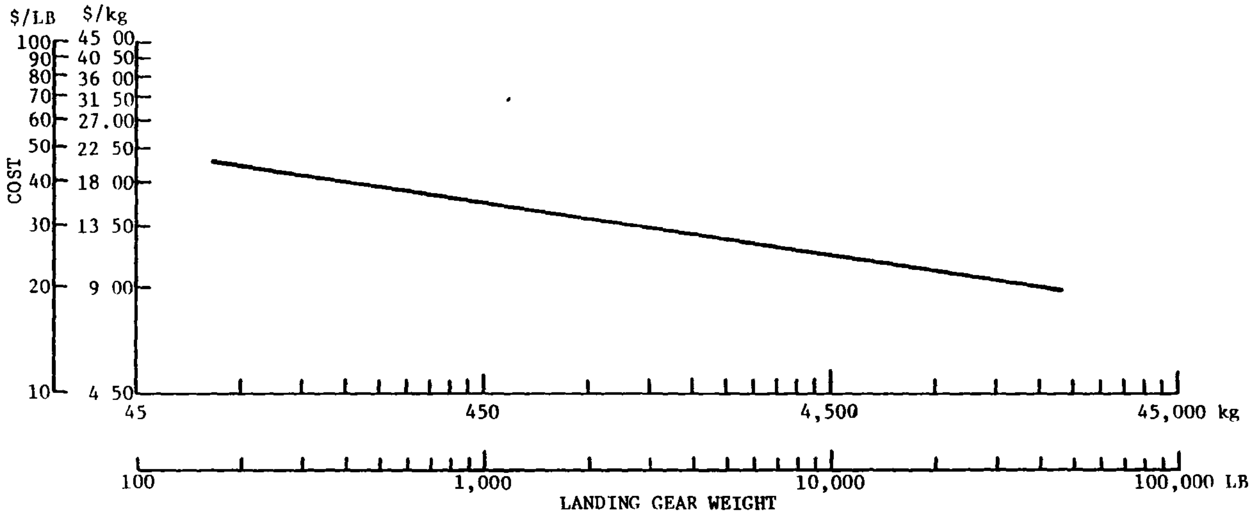

Figure 166. Landing Gear Cost - Parametric

higher dollar per kg (lb) value from the curve. This weight factor is the main driver in the equation for this study. The overall cost of the multi-body gears is still lower, due to reduced complexity, commonality, and gross weight advantages.

The fly-away costs of the multibody aircraft which consists of RDT&E, production, and 'other cost' are from 8.6 to 13.4 percent less than that of the single body aircraft. 'Other cost,' as used here, include costs such as engine cost, warranties, and profit.

Direct operating cost comparisons between the single body and multibody aircraft are given in Figure 167. DOC is subdivided into two major elements, fuel cost and 'other cost'. The 'other cost' element consists of crew, maintenance, insurance, and depreciation costs. As seen from the figure, at all fuel cost values the major reduction in DOC as compared to the single body aircraft is provided by the 'other cost' element for the two-body MB1 and three-body MB3 aircraft. Whereas, for the two-body MB2 aircraft the major DOC reduction occurs in the fuel cost element. These cost characteristics of the multibody aircraft result in the two-body MB2 aircraft providing the maximum DOC benefit at the baseline fuel price of 0.34 $/l (1.30 $/gal) and an increasing benefit as fuel price increases. Although the absolute DOC dollar savings of the two-body MB1 and three-body MB3 aircraft increase as fuel price increases, the percent savings decreases.

Direct operating cost is shown in Figure 168 subdivided into its five major cost elements--fuel and oil, depreciation, maintenance, insurance, and crew. The baseline fuel price of

METRIC UNITS

ITEM \ AIRCRAFT	SINGLE BODY SBR	MULTIBODY MB1	Δ%	MB2	Δ%	MB3	Δ%
FUEL & OIL COST ¢/AMgkm							
FUEL @ 17.17 ¢/1	1.85	1.70	8.0	1.60	13.5	1.78	3.9
FUEL @ 34.34 ¢/1	3.70	3.48	6.1	3.20	13.7	3.56	3.9
FUEL @ 51.51 ¢/1	5.55	5.27	5.0	4.80	13.5	5.34	3.8
FUEL @ 68.68 ¢/1	7.40	7.04	4.9	6.39	13.6	7.12	3.8
OTHER COST - ¢/AMgkm	3.39	2.99	11.8	3.09	8.8	3.13	7.6
TOTAL - ¢/AMgkm							
@ 17.17 ¢/1	5.24	4.69	10.5	4.69	10.5	4.91	6.3
@ 34.34 ¢/1	7.09	6.47	8.7	6.29	11.3	6.69	5.6
@ 51.51 ¢/1	8.93	8.26	7.6	7.89	11.7	8.47	5.2
@ 68.68 ¢/1	10.79	10.03	7.1	9.48	12.1	10.25	5.0

NOTE: AIRCRAFT OPTIMIZED @ 34.34 ¢/1 FUEL COST

CUSTOMARY UNITS

ITEM \ AIRCRAFT	SINGLE BODY SBR	MULTIBODY MB1	Δ%	MB2	Δ%	MB3	Δ%
FUEL & OIL COST-¢/ATNM							
FUEL @ 0.65 $/GAL	3.11	2.86	8.0	2.69	13.5	2.99	3.9
FUEL @ 1.30 $/GAL	6.22	5.84	6.1	5.37	13.7	5.98	3.9
FUEL @ 1.95 $/GAL	9.32	8.85	5.0	8.06	13.5	8.97	3.8
FUEL @ 2.60 $/GAL	12.43	11.82	4.9	10.74	13.6	11.96	3.8
OTHER COST-¢/ATNM	5.69	5.02	11.8	5.19	8.8	5.26	7.6
TOTAL - ¢/ATNM							
@ 0.65 $/GAL	8.80	7.86	10.5	7.88	10.5	8.25	6.3
@ 1.30 $/GAL	11.91	10.87	8.7	10.56	11.3	11.24	5.6
@ 1.95 $/GAL	15.01	13.87	7.6	13.25	11.7	14.23	5.2
@ 2.60 $/GAL	18.12	16.84	7.1	15.93	12.1	17.22	5.0

NOTE: AIRCRAFT OPTIMIZED @ 1.30 $/GAL FUEL COST

$$\Delta\% = 100\left[\frac{MB - SBR}{SBR}\right]$$

Figure 167. Direct Operating Cost Comparison

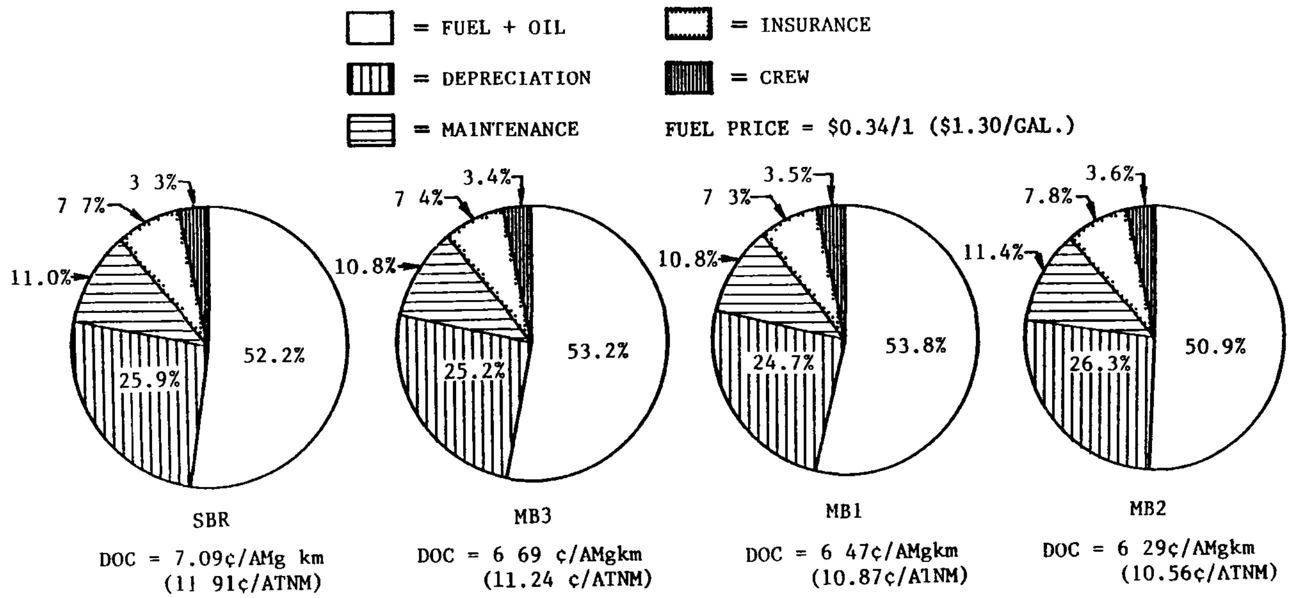

Figure 168. DOC Element Comparison

0.34 $/1 (1.30 $/gal) is used, and as seen at this value, fuel cost is slightly greater than 50 percent of the total DOC for all aircraft.

5.4 OPERATIONAL COMPARISON

Operational similarities of the four point design aircraft, shown in Figures 152 through 155, are that each provides for straight-in loading/unloading of cargo at floor height through a nose visor door opening. All payload is carried on a single floor level and all of the aircraft cargo floors contain rails, rollers, and tiedown fittings for securing the cargo.

Operational variations of these aircraft are discussed in the following paragraphs.

The single body reference aircraft has a cargo floor height of 7.8m (25.5 ft). This is a result of the fuselage length and the required 0.14 rad (8 degrees) rotation angle. This height requires that ground handling/support equipment have more flexibility than is required for the multibody aircraft which have floor heights of 5.4m (17.7 ft) and 4.1m (13.5 ft). Also, due to the landing gear strut length necessitated by this 7.8m (25.5 ft) height, and to strut location, the tip over angle of 1.2 rad (68 degrees) restricts this aircraft to a 0.40g turn. The multibody aircraft have the full 0.50g turn capability. Floor heights are shown in Figures 123 and 125.

Cg location for lateral control makes cargo loading of the single body

reference aircraft more flexible than that of the multibody aircraft due to rolling moments which will be created by unequal loading of the multibody fuselages. Although the quantity of equipment and personnel required for simultaneous loading of the fuselages are increased, the loading/unloading time of the multibody aircraft can be significantly reduced thereby increasing the availability of the aircraft to produce revenue.

The single body reference aircraft has a main gear strut spacing of 13.3m (43.5 ft), laterally, which permits ease of operation on conventional runways and taxiways. The multibody aircraft comparable gear spacing is 30.1m (115 ft) for the two-body MB2 aircraft and 39.6m (130 ft) for the two-body MB1 and three-body MB3 aircraft. Wing spans of the four aircraft range from 121m (397 ft) to 128.9m (423 ft) with none having a distinct advantage in complying with taxiway or ramp clearance requirements. Due to the single body reference aircraft floor height, the engines have a greater ground clearance than do those of the multibody aircraft which makes the engines less susceptible to foreign object damage.

The single body reference and the three-body MB3 aircraft have the pilot/roll axis at the aircraft centerline while the two, two-body aircraft have a pilot/roll axis offset. This subject is discussed in Section 2.7 with regard to a flight simulation program designed to define the effects of this offset.

5.5 TWO-BODY MB2 AIRCRAFT VS SPANLOADER

The spanloader aircraft discussed in this comparison is shown in Figure 169. It is the product of a study by Lockheed, under the direction of the NASA, "Technical and Economic Assessment of Span-Distributed Loading Cargo Aircraft Concepts," Reference 1. For convenience, the two-body MB2 aircraft is shown adjacently in Figure 170.

Figure 171 shows the basic differences in performance requirements, technology availability, cost basis, and aircraft characteristics. Items that are common to both aircraft are containers and payload density.

The advanced material application to structural components differs for the two aircraft. Figure 172 shows the percent component weight reduction realized by advanced material application for each aircraft when compared to aluminum material components. Appreciable differences exist primarily in the fuselage and empennage.

A comparison in aircraft geometry, weights, performance, and cost are shown in Figures 173, 174, 175, and 176, respectively. The extensive variation in most of the elements of the

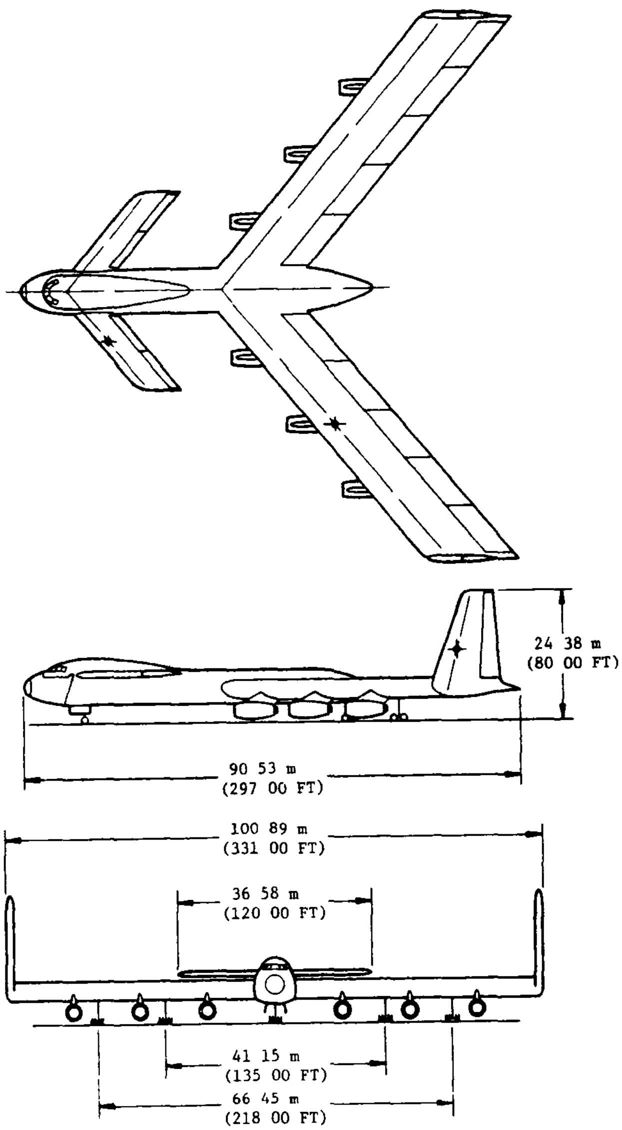

Figure 169. Spanloader - Comparison Aircraft

above parameters is consistent with the differences noted previously in Figure 171. It also emphasizes the fact that a direct comparison of any of these parameters does not necessarily reflect meaningful results.

Some points of comparison that are compatible, with consideration for required adjustments, are gear tread width, total productivity, and direct operating cost (DOC). The two-body MB2 aircraft has a gear tread width of 35.1m (115 ft) which is considered compatible with existing runways, while that of the spanloader is 66.4m (218 ft). Obviously, a stringent wing weight penalty would be inflicted if the spanloader tread width were reduced to 35.1m (115 ft). For an indication of this weight increase, reference is made to the "Peripheral Jet Air Cushion Landing System Spanloader Aircraft Study," Technical Report AFFDL-TR-3152, Volume 1, December 1979, Reference 9. In this study the same aircraft as shown in Figure 169 is used as the baseline aircraft for developing a peripheral jet air cushion landing system (PJ-ACLS) whereby the gear tread width is reduced to 22.9m (75 ft) and the outer wing is supported by a lower surface peripheral jet during taxi, takeoff, and landing. Prior to installing the PJ-ACLS, and with a gear tread width of 22.9m (75 ft), a wing weight penalty of 23,587 kg (52,000 lb) is incurred.

Aircraft productivity and DOC comparisons are normally made on an equal payload and/or a fixed task basis. The total productivity of the 216 spanloader fleet is 189.5 x 10^9 Mg-km (112.8 x 10^9 ton-nm) compared to 130.7 x 10^9 Mg-km (77.8 x 10^9 ton-nm) for the two-body fleet of 107, adjusted for the 4200 hour utilization rate of the span-

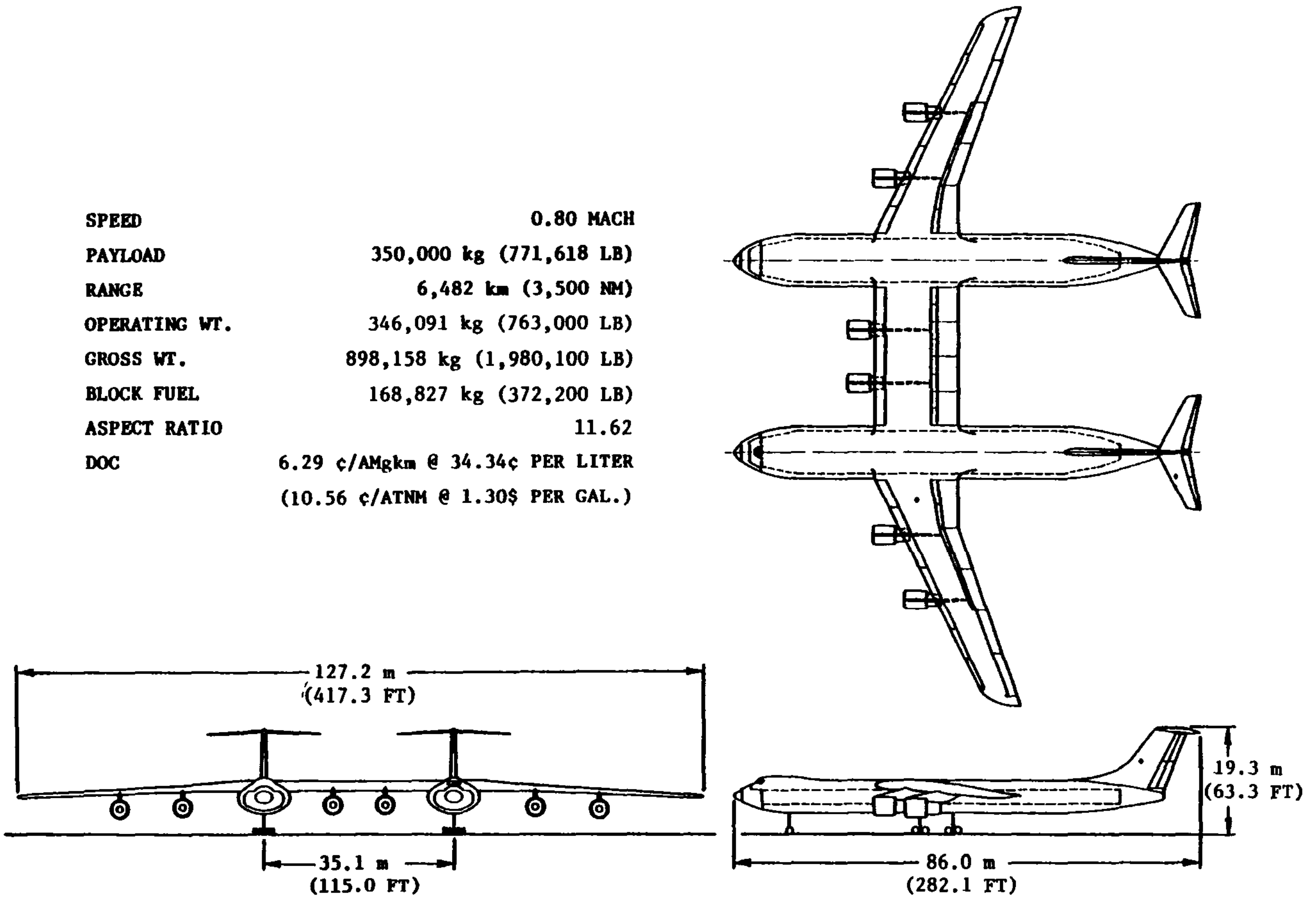

Figure 170. Two-Body MB2 Aircraft - Final

loader. Using the two-body total productivity of 130.7 x 10^9 Mg-km (77.8 x 10^9 ton-nm) as the fixed task, the spanloader production quantity is reduced from 216 to 149 aircraft. DOC for the spanloader in 1975 dollars is 4.04¢/AMgkm (6.78¢/ATNM) and that of the two-body aircraft in 1981 dollars is 6.29¢/AMgkm (10.56¢/ATNM), both as shown in Figure 176. All spanloader costs are subsequently escalated to 1981 dollar equivalents, and the resulting DOC is 7.58¢/AMgkm (12.73¢/ATNM) which is a 20 percent higher DOC than that of the two-body aircraft. The above noted reduction in the spanloader production quantity for the fixed task comparison substantially increases all spanloader costs shown in Figure 176; hence, the true DOC differential, though not recalculated, is considerably greater than 20 percent.

Although a complete competitive analysis of these two aircraft cannot be performed, indications are that the multibody configuration is a more productive and less costly aircraft than is the spanloader. Further verification

is dependent on future design and performance studies under the same mission requirements, guidelines, and ground rules.

ITEM / AIRCRAFT	TWO-BODY MB2	SPANLOADER
PAYLOAD	350,000 kg (771,618 LB)	272,155 kg (600,000 LB)
RANGE	6482 km (3500 NM)	5556 km (3000 NM)
SPEED - MACH	0.80	0.75
ALTITUDE - CRUISE	9754 m (32,000 FT)	10,668 m (35,000 FT)
TECHNOLOGY AVAILABILITY	1985	1990
COST BASIS	$ JAN 1, 1975	$ JAN 1, 1981
FAA FIELD LENGTH (MAX)	3200 m (10,500 FT)	3658 m (12,000 FT)
FUEL PRICE	34 ¢/l (1.30 $/GAL)	9.8 ¢/l (37 ¢/GAL)
CONTAINERS	2.44 m x 2.44 m x 3.05 m OR 6.10 m (8' x 8' x 10' OR 20')	2.44 m x 2.44 m x 6.10 m OR 12.20 m (8' x 8' x 20' OR 40')
DESIGN DENSITY - CARGO	160.18 kg/m^3 (10 LB/FT^3)	160.18 kg/m^3 (10 LB/FT^3)
CARGO DISTRIBUTION	33.3% EACH FUSELAGE	80% WING & 20% FUSELAGE
CARGO CAPABILITY	CONTAINERS ONLY	CONTAINERS OR OUTSIZE CARGO IN FUSELAGE - CONTAINERS ONLY IN WING
CARGO LOADING	NOSE VISOR	NOSE VISOR & WING TIP DOORS
PRODUCTION QUANTITY	107	216
UTILIZATION	4000 HRS/YR	4200 HRS/YR

Figure 171. Two-Body MB2 Aircraft/Spanloader Comparison - Basic Requirements

	ADVANCED MATERIAL COMPONENT PERCENT WEIGHT REDUCTION RELATIVE TO ALUMINUM COMPONENT	
COMPONENT / AIRCRAFT	TWO-BODY MB2	SPANLOADER
WING	18	20
FUSELAGE	12	22
HORIZONTAL TAIL	27	18
VERTICAL TAIL	27	18
NACELLES & PYLON	11	10
LANDING GEAR	3	0

Figure 172. Two-Body MB2 Aircraft/Spanloader Comparison - Advanced Material

ITEM ↓ / AIRCRAFT →	TWO-BODY MB2	SPANLOADER
WING		
SPAN - m (FT)	127.1 (417)	100.9 (331)
SWEEP - RAD (DEG)	0.44 (25)	0.70 (40)
THICKNESS RATIO	0.111	0.218
AREA - m^2 (FT^2)	1339 (14,409)	1725 (18,559)
ASPECT RATIO	11.62	5.9
OVERALL LENGTH - m (FT)	86.0 (282)	90.5 (297)
MAXIMUM HEIGHT - m (FT)	19.2 (63)	24.4 (80)
GEAR TREAD WIDTH - m (FT)	35.1 (115)	66.5 (218)

Figure 173. Two-Body MB2 Aircraft/Spanloader Comparison - Geometry

ITEM - WEIGHT kg (LB)	AIRCRAFT	
	TWO-BODY MB2	SPANLOADER
WING	114,269 (251,920)	109,592 (241,610)
OPERATING	346,091 (763,000)	248,750 (548,400)
PAYLOAD	350,000 (771,618)	272,155 (600,000)
FUEL	202,075 (445,500)	179,124 (394,900)
GROSS	898,158 (1,980,100)	700,029 (1,543,300)

Figure 174. Two-Body MB2 Aircraft/ Spanloader Comparison - Weights

ITEM ↓ / AIRCRAFT →	TWO-BODY MB2	SPANLOADER
CRUISE LIFT/DRAG RATIO	24.05	19.66
WING LOADING, kN/m^2 (LB/FT^2)	6.43 (134.3)	3.88 (81.0)
ENGINE THRUST, N (LB)	298,031 (67,000)	283,797 (63,800)
FAA FIELD LENGTH, m (FT)	3200 (10,500)	1829 (6000)
PAYLOAD/GROSS WT. FRACTION	0.390	0.389
Mg-km/1 FUEL	10.8	8.2
TON-NM/GAL. FUEL	24.3	18.4
STRUCTURAL WT/GROSS WT	0.299	0.268

Figure 175. Two-Body MB2 Aircraft/Spanloader Comparison - Performance

ITEM ↓ / AIRCRAFT →	TWO-BODY MB2 - 1981 $	SPANLOADER - 1975 $
UNIT COST, MILLIONS $		
ENGINES (6)	27.87	11.05
AIRFRAME	247.25	123.03
AIRCRAFT	275.12	134.08
DOC, ¢/AMgkm (¢/ATNM)	6.29 (10.56)	4.04 (6.78)

Figure 176. Two-Body MB2 Aircraft/Spanloader Comparison - Cost

6.0 CONCLUSIONS

Several conclusions have been reached based on the results of this study. Each one is presented in a highlighted single summary sentence and is followed by a brief discussion that explains and justifies the conclusion.

- **Reasonable span efficiencies can be obtained for multibody configurations, however, transonic code development and wind tunnel tests are required to optimize the configuration.**

  Wind tunnel test results demonstrate that reasonable span efficiencies can be obtained for double body configurations. However, a correlated transonic code which is capable of multibody analysis is required in order to optimize the wing design. This code, along with additional test data, can be used to develop wing camber and twist variations, wing-body filleting, and wing spanwise thickness variations which will optimize the aerodynamic configuration for a prescribed fuselage size, shape, and location.

- **Multibody aircraft have lower drag level than single body aircraft sized for same mission.**

  The lower drag level of the multibody results from both induced and profile drag reductions as compared to the single body aircraft. Lower induced drag levels are achievable for the multibody as the wing flight bending moment relief provided by the concept allows for the use of higher aspect ratio values. In addition, the multibody profile drag level is reduced by the lack of a need to provide landing gear housing external to the basic fuselage shape as is required by the single body aircraft.

- **Multibody aircraft wing weight and direct operating cost are minimized with the fuselage bodies located at approximately 40 percent wing semispan.**

  The peak bending moment which occurs at the outboard side of the body decreases for both flight and taxi conditions as the body is located at increasing percent semispan positions up to the most outboard location studied, 50 percent. However, a load reversal occurs on the wing center section with bodies located outboard of 40 percent semispan. The flight upbending moment changes to a down bending moment which exceeds the taxi down bending moment. Less wing chord and thickness are also available for moment reaction as the body is moved outboard. The combination

of load reversal and reduction in available structure result in a wing weight increase occurring outboard of the 40 percent body location, for the point design aircraft.

- **Design of any aircraft that has a gross weight on the order of 907,185 kg (2,000,000 lb) which will meet the FAR 36 Stage 3 noise ceiling limits is a challenging problem.**

Although this problem has been identified well before this study effort, its impact on the multibody study results warrants recognition. The study results indicate that if multibody benefits are to be maximized, the aircraft must be capable of transporting relatively high payloads with corresponding gross weights on the order of 907,185 kg (2,000,000 lb). All of the point design aircraft have predicted noise levels considerably in excess of the FAR 36 Stage 3 noise limits. The principal reasons for the noise level exceedances are: (a) the engine used is designed for fuel efficiency - not minimum noise level and (b) poor climb performance on takeoff prevents the use of throttle cutback over the takeoff flyover noise measurement point.

These two conditions could be improved by redesign - selection of a low noise level engine and improved climb performance. However, the noise exceedance problem is aggravated by the fact that the Stage 3 limits have a noise ceiling limit for weights greater than about 362,874 kg (800,000 lb).This problem cannot be improved by redesign and is a problem to be faced by all aircraft concepts where the benefits derived are maximized at high payload/gross weight values.

- **Stability and control analyses indicate that roll control capability will limit the fuselage spanwise location.**

When relocating the body position from 19 to 50 percent semispan for those aircraft studied, the available rolling moment decreases by 55 percent while the required rolling moment increases by slightly over 50 percent. Based upon a requirement to provide the ability to obtain 0.52 radians (30 degrees) of bank in approximately five seconds, the maximum semispan body location is about 33 percent. To define the optimum body location requires investigations such as wind tunnel test, flight simulator evaluation, and detailed structural analyses, all of which were beyond the scope of study encompassed by this report.

Study results indicate the maximum structural benefit is derived with the bodies located at approximately 40 percent semispan. Therefore, additional studies should concentrate on techniques to provide the required capability for body locations outboard of the 33 percent semispan location.

Roll control system requirements, as defined by this study, are based upon symmetrical loading of the multiple fuselage bodies. Future studies should be performed to define trim drag penalties incurred as a function of lateral imbalance.

- **Flying qualities criteria are unspecified for extremely large aircraft.**

The inadequacy of control design criteria to insure good flying qualities first became an item of concern with the C-5 size aircraft, 340,194 kg (750,000 lb) gross weight. This lack of criteria becomes an even greater concern with aircraft gross weights of 970,185 kg (2,000,000 lb) investigated by this study. The importance of roll criteria, as shown by its limiting effect on fuselage spanwise location, is a prime example of one criterion. There is a need for a thorough investigation of all criteria.

- **Crew location may be limited to the aircraft centerline of rotation if acceptable ride qualities are to be achieved.**

Ride qualities data are available for aircraft where the pilot and crew stations are offset from the aircraft centerline of rotation, such as the C-5 aircraft. However, the offset dimensions of the C-5 aircraft are insignificant when compared with the offset which occurs for a 30 to 40 percent semispan body location, 907,185 kg (2,000,000 lb) multibody aircraft.Until design control criteria are established for very large aircraft, exact crew accelerations will not be known. Using present control criteria would limit crew offset dimensions to less than those required for a viable multibody aircraft unless centerline crew provision are used. Further investigations are required to fully define the performance and weight penalties associated with this concept of crew location.

- **A competitive advantage is offered by the multibody study aircraft only at payload values in excess of 258,000 kg (568,793 lb).**

At the maximum payload evaluated, 350,000 kg (771,618 lb), the direct operating cost advantage for the multibody aircraft is about 11 percent. However, as payload is reduced to 258,000 kg (568,793 lb) this advantage decreases to about four percent. The advantage at payloads less than 258,000 kg (568,793 lb) becomes negligible.

The magnitude of the above direct operating cost advantages are not felt to be sufficient to provide the incentive necessary for commercial development. However, should a specific need be identified in the future for a very large payload capability civil transport, advantages which are not apparent in the DOC comparison exist for the multibody. The multibody fly-away-cost is less by about 9 to 15 percent, requiring less "up-front" and fleet investment capital. The multiple cargo loading access available on the multibody provides greater loading flexibility and reduced loading time. The cargo floor height of the multibody is compatible with existing ground loading equipment, whereas, the height of the single body reference aircraft would require new investments in both loading equipment and facilities. Finally, should fuel prices rise at a faster rate than the overall inflation rate (production labor & materials), the DOC advantage of the multibody would improve.

The study results indicate that should range capability exceeding the study value of 6482.0 km (3500 nm) or maximum flight endurance capability be a desired mission requirement, the advantage of the multibody would increase. This advantage would be in terms of reduced fuel consumption which has a direct influence on operating cost.

Although not evaluated, it should be stated that for applications of advanced composite materials on a more extensive basis than used within this study, the potential for the multibody advantage will tend to diminish. As advanced composite material application is increased for a wing of a given aspect ratio, total wing weight decreases thereby decreasing the weight penalty associated with flight bending moments. Thus the potential for weight reduction by providing the flight bending moment relief also decreases. The materials technology used is representative of 1985 maturity thus providing considerable latitude for increased advanced material usage.

This study represents the first detailed investigation of contemporary multibody aircraft, and it is limited by guidelines and constraints; however, requirements for further study of multibody aerodynamics, structures,

stability and control, and noise have been identified. Also, extensive work is required pertaining to dynamic loads, flight simulation, and tunnel testing before a final multibody configuration can be established. The study results do indicate that where it is desirable to transport very large payloads over relatively long distances, this final multibody configuration can offer advantages over a comparable single body aircraft.

7.0 RESEARCH AND TECHNOLOGY RECOMMENDATIONS

7.1 WIND TUNNEL TEST REQUIREMENTS

Considerable research and development is required before a multibody configuration can be placed in commercial service. A better understanding of the aerodynamic characteristics of this type configuration must be obtained in order to assure an acceptable level of risk in the design and development process. This knowledge can be obtained by experimental and theoretical methods; the knowledge gained in the wind tunnel must be understood, correlated, and adequately repeated with the theoretical methods so that these methods, which are relatively inexpensive when compared to wind tunnel tests, can be used to provide the basic information for the numerous design trade studies which are required.

Such a test program must define the basic lift, drag, stability, and loads characteristics for a systematic variation of multibody configurations in order to assure that all parameters of potential significance are evaluated and that the resulting configuration will be properly selected. These data are required for cruise performance evaluation as well as for evaluation of low speed performance, control, and handling characteristics.

Stability and control derivatives are based on conventional methods which are derived from experimental data. All static and dynamic analyses use these derivatives to define the aircraft. Since no experimental data are available for multibody configurations of the type developed in this study, it is imperative that experimental data be obtained for this discipline as well as for performance. Some purposes for such data include: verification of assumptions made with respect to interference effects of multibodies; verification of stability levels due to unusual load distributions, different fuselage projections, and body offsets; evaluation of control effectiveness due to unusual wing planform and body shapes; identification of unusual problems near stall such as pitch up and blanking of tail effectiveness in stall regions.

Many of the characteristics which require evaluation can be defined by testing semispan models and this is suggested because of the reduced costs associated with this type of test. On the other hand, some data requirements cannot be satisfied by this type of test. Full span evaluation of a three-body configuration is probably needed since the center body is very likely to be in the boundary layer of

the support system for semispan testing and the test data is likely to be unreliable. Most stability and control evaluations are also better accomplished with full span testing so that tail-on results can be obtained for longitudinal stability and control analysis and sideslip data can be obtained for use in evaluation of directional stability and control characteristics.

The influence of body location, wing planform concepts, and variations of airfoil section thickness and twist on roll capability could be investigated in semispan tests.

Fulfillment of empirical data requirements can be satisfied by a three-phase test program. The three phases of the proposed program are: (1) semispan high speed testing, (2) full span high speed testing and (3) full span low speed testing. The proposed multibody wind tunnel test program is summarized in Figure 177. Test objectives, test hours, and required model components are indicated. This program is based on the assumption that the same model is used for the full span high and low speed tests. Through this approach, only a new wing with flaps need be fabricated for the low speed test.

7.1.1 Phase I Semispan High Speed Testing

This phase of testing is divided into two parts. The first part (a) will be primarily devoted to the evaluation

PHASE	TYPE TEST OBJECTIVES	TUNNEL TEST TIME	MODEL COMPONENTS REQUIRED											
			W	B	HT	VT	NAC	PYL	FIL	FLAP	RUD	ELEV	AIL	SPLR
I	SEMISPAN, HIGH SPEED o Body size/location o Unswept center wing o High/low wing o Wing/body fillet o Triple-body o Longitudinal stability	280 HR	5	3	1	1	0	0	30	0	0	0	0	0
II	FULLSPAN, HIGH SPEED o Aero data base o S & C data base o Empennage selection o Triple-body	80 HR	1	3	5	4	6	6	1	0	4	5	1	3
III	FULLSPAN, LOW SPEED o Flap configuration o Flap aero data base o Flap S & C data base	80 HR	1	*	*	*	*	*	*	3	*	*	1	1

* Use parts from Phase II.

Figure 177. Multibody Wind Tunnel Test Summary

of variables which affect multibody cruise performance characteristics.

It is proposed that two trapezoidal wings having sweep angles of 0.44 and 0.61 rad (25 and 35 degrees) be designed. These wings should have a fixed aspect ratio and taper and should be pressure instrumented. The camber and twist definition of the wings will be defined using existing theoretical methods including the effect of body overpressures on the wing flow field.

Two bodies of different diameters and a one-half center body should be tested with each wing. The wings should be designed to accept the bodies at three spanwise locations. Fillets should be designed for each wing sweep/body location combination for both high and low wing configurations. The fillet configuration for one high and one low wing configuration will be modified, based on evaluation of the force, pressure, and flow visualization data to produce the effect of this variable. The result from this series of tests include:

(a) effect of wing sweep, wing location, body size, and body location on wing-body interference, body overpressures, drag rise characteristics, basic wing-body longitudinal stability characteristics and span efficiency.

(b) wing-body fillet design guidance.

(c) wing camber and twist design guidance.

(d) preliminary three-body characteristics.

The objective of Part (b) of the semispan testing is to resolve the effects of unswept center wing panels. Three wings are required which represent two body spanwise locations with the effect of the outboard panel wing "bat" and the center panel chord at one body location. As in Part (a), both high and low wing positions will be investigated as well as wing/body fillets effects. Bodies and empennage from Part (a) will be used as required. Results from the Part (b) testing include the following effects for unswept center wing configurations:

- Comparison with a straight taper wing
- Center wing panel chord/outer panel "bat"
- Body spanwise location
- High versus low wing position
- Preliminary three-body characteristics.

7.1.2 Phase II Full Span Model High Speed Test

Evaluation of the semispan test results and correlation of these results with theoretical methods will provide a firm base for selection of the full span two-body configuration. The test configuration should also reflect practical constraints, such as body location limitations imposed by anticipated runway and taxiway width. Three-body configurations will be generated by the addition of a center body to the two-body configurations.

The model must be designed to provide a complete evaluation of the characteristics of multibodies and should be configured to provide test data for evaluation of the following:

1. Aerodynamic Characteristics

The full span model must be designed to allow a component buildup of the lift and drag characteristics of the configuration. Evaluation of these buildup results will allow comparison of component characteristics with predicted levels and will define the interference drag characteristics of the configuration. These data will provide a reliable basis for trade studies between the performance, structural, and control requirements and indicate areas of potential improvement in the configuration.

2. Basic Stability Characteristics

The basic stability levels of multibody configurations require definition. The component buildup of the model required for drag analysis will also provide insight into the stability characteristics of these configurations. The effects of sideslip angle of the configuration characteristics must be determined.

3. Empennage Configuration

During the course of the current study, several empennage configurations were evaluated. For instance, a slab horizontal configuration spanning the area between the fuselages was compared to a twin tee-tail configuration. An evaluation test of several empennage configurations would provide an improved data base for use in empennage selection. The proposed test would include the following configurations:

- slab tail mounted on conventional upright vertical tails
- slab tail mounted on canted verticals in order to reduce horizontal tail span requirements
- high and low variations for slab and conventional tails

o rudder and elevator effectiveness

It would be desirable to test several tail sizes, locations, and shapes in order to evaluate the effectiveness of these configurations, all the way through deep stall regions. Rudder and elevator data should be obtained for all configurations; these data are especially important for the canted vertical configuration in order to provide information on the potential cross-coupling of control inputs resulting from a configuration of this type.

4. Roll Control Effectiveness

Ailerons and spoilers are required in order to evaluate the roll control effectiveness. While this evaluation could be accomplished during semispan testing, the results from the larger scale, full span model are considered more valid.

7.1.3 Full Span Low Speed Testing

Because of the high moments of inertia of multibodies, low speed maneuverability with conventional controls may not be acceptable. Side force generators or other innovative configurations aimed toward solution of this potential problem should be investigated.

In addition to the above configuration considerations, the impact of multibody configurations on flap effectiveness, flaps down L/D ratio, and flaps down stability levels must also be evaluated. Control effectiveness in the flapped configurations must be determined.

7.2 TRANSONIC CODE DEVELOPMENT

For a transonic code to be helpful in the analysis of multibody configurations, the code must be capable of modeling off-centerline bodies and should incorporate the capability of analyzing configurations consisting of a wing and multiple bodies, pylons, and nacelles.

Another application for a multibody code involves the optimization of the fillet design for the configuration. Fillet development is a matter of importance to these configurations because of the asymmetric nature of the wing body intersection and of the fillet which will be required. Effective fillet design is required because of its impact on span efficiency.

It is estimated that modification of an existing code will require a man-year and associated computer costs.

7.3 FLIGHT SIMULATION

Flight simulation should continue to be used as a method for helping to define design criteria. In particular,

the required control capability commensurate with the large transport aircraft mission needs to be defined. This will help to provide design constraints for fuselage location.

Another important area of future study is acceleration at the pilot, crew, or passenger stations during abrupt maneuvers. Anyone located at a spanwise distance from the aircraft's principal roll axis will experience significant vertical and lateral accelerations during these maneuvers. Limits on the accelerations could be determined using motion base flight simulations, provided the motion base system has enough acceleration capability. These limits on acceleration could be used to define limits on roll mode time constants, maximum roll rate, etc., as a function of station location.

7.4 STRUCTURES

There are several areas in the structures discipline which need more detailed study. They are considered to be outside the scope of the current multibody program, but they present problems which will require investigation before such a configuration can be built. The following list presents some of the problem areas:

Dynamic Loads - A detailed investigation of dynamic loads for both flight and ground conditions should be accomplished. It is possible that loads due to the dynamic response of a multibody configuration could be more critical than normal flight loads. Another possibility is that taxi loads will be higher, due to the possibility of the landing gear rolling over uneven surfaces.

Load Alleviation - It is expected that a load alleviation system will be very effective in reducing the effect of dynamic loads. This will be, however, a complex system because the elevators and rudders, as well as ailerons and spoilers, will affect wing loads. A system with this many control inputs will require a considerable amount of development work. A separate system using the landing gear struts is a possible solution to damp out any adverse dynamic taxi loads. This will require the strut to absorb excess deflections and will, therefore, not transfer the load to the wing structure.

Flutter Analysis - Although a very thorough preliminary design flutter analysis was performed during the study, a more detailed analysis is needed. The two configurations with unswept center section wings had flutter problems and the reasons are not well understood. It is expected that these two configurations will have cen-

ter wing stiffness problems. However, on the MB2 type configuration, the flutter problem is solved by the addition of outer wing stiffness. This is an unexpected result which will require more analysis to fully understand.

Material Application - Depending on the date of the initial design phase of the aircraft and material technology development programs, a wide variety of structural materials can be applied to a multibody aircraft. The study aircraft have graphite epoxy throughout the empennage, and the wing and fuselage secondary structure. The rest of the structure is conventional aluminum. A study to investigate the various possibilities might identify material applications which have a larger payoff for a multibody configuration.

Unsymmetrical Loadings - On a multibody configuration it is possible to load the payload in a manner which will result in an unsymmetric aircraft. This will cause not only a static unbalance where the lateral center of gravity is nonzero, but will also affect the aircraft moments of inertia. It is necessary to determine the limits of the allowable lateral unbalance.

LIST OF SYMBOLS/ABBREVIATIONS

ACFT	Aircraft
ACQ	Acquisition
A_c/A_f	Fuselage Efficiency = $\frac{\text{container x-sec area x no. of sticks}}{\text{fuselage x-sec area}}$
AEDC	Arnold Engineering & Development Center
ALT	Altitude
AR	Aspect Ratio
ASTF	Aeropropulsion Systems Test Facility
ATA	Air Transport Association
ATNM	Available - Ton - Nautical Mile
b	Wing span
BF	Block fuel
BL	Baseline
BPR	Bypass Ratio
c	Chord
CAB	Civil Aeronautics Board
C_{D_c}	Compressibility Drag Coefficient
CG	Center of Gravity
$CC_c lC$	Unit lift
$CC_l/C_{av}C_L$	Spanwise lift distribution
$\bar{c}$	Mean aerodynamic chord
C_{av}	Average chord
C_L	Total wing lift coefficient
C_l	Section lift coefficient
℄	Centerline
CU FT	Cubic feet
D, d	Fuselage body diameter
D_f/b	Diameter fuselage/wing span
d/[b/2]	Body width to wing semispan ratio
DOC	Direct Operating Cost

e	Wing span efficiency
EA	Elastic axis
EPNdB	Equivalent Perceived Noise Level - Decibels
ETA	Engine power setting and Percent Body Location
FAR	Federal Aviation Regulation
FT	Feet
FVR	Fuel Volume Ratio
GAL	Gallon
GASP	Generalized Aircraft Sizing and Performance
GW	Gross Weight
Hz	Hertz (cycles/sec)
I	Moment of Inertia
k	1000
KEAS	Knots Equivalent Airspeed
KTAS	Knots True Airspeed
Kts	Knots
KWSS	Secondary Structure Weight per unit total wing area and Mach number
L/D_e	Fuselage Fineness Ratio (Length/Equivalent Dia.)
L/D	Lift/Drag
LB	Pounds
M	Mach number
M_c	Cruise Mach number
MAC	Mean aerodynamic chord

max	Maximum
MB1	Two-Body Aircraft (Straight Taper Wing)
MB2	Two-Body Aircraft (Unswept Center Section Wing)
MB3	Three-Body Aircraft
N_E	Number of Engines
N_{z_u}	Ultimate load factor for gross weight
N_z	Ultimate load factor
NM	Nautical mile
NP	Neutral Point
NWLO	Nosewheel liftoff at rotation speed
OW	Operating weight
OWE	Operating weight empty
P&WA	Pratt and Whitney Aircraft Company
P	Roll acceleration (radians/sec)
PLD	Payload
PSF	Pounds per square foot
PSI,	Pounds per square inch
R_e	Wing mounted nacelle, pylon, and engine weight to gross weight ratio
R_{fus}	Wing mounted fuselage, payload, and tail weight to gross weight ratio
RS_{ow}	Outer wing to total wing area ratio
RS_{iw}	Inner wing to total wing area ratio
R_{tax}	Taxi to maneuver load factor ratio
R_{zfw}	Zero fuel weight to gross weight ratio
RDT&E	Research & Development Test & Engineering
RFP	Request for proposal
RNG	Gust to maneuver load factor ratio
RT	Rated thrust

S	Wing area
S_f	Wing frontal area
S_h	Horizontal tail area
S_w	Total wing area
SBR	Single Body Reference
SFC	Specific fuel consumption
SM	Static margin
SOW	Statement of Work
SQ FT	Square feet
SS	Semispan
STA	Station
STR	Structure
T	Thrust
t/c	Thickness to chord ratio
$(t/c)_e$	Equivalent wing thickness ratio (%)
$(t/c)_{eff}$	Effective thickness to chord ratio
$(t/c)_{ow}$	Outer wing effective thickness ratio (%)
$(t/c)_{iw}$	Inner wing effective thickness ratio (%)
Takeoff F/O	Flyover noise point
Takeoff S/L	Sideline noise point
TBD	To be determined
T.C.	Trip cost
T.O.	Takeoff
T.O. WT	Takeoff weight
TOD	Takeoff distance
TS, T_s	Tension stress
$\bar{V}$	Tail volume coefficient
V_e	Equivalent airspeed
V_h	Horizontal tail volume coefficient
V_s	Stall speed

V_{s1}	Stall speed with landing flaps
VLM	Vortex lattice method
V_v	Vertical Tail Volume Coefficient
w	Distance between fuselages
W	Weight
W_G	Gross weight
W_{ss}	Weight - Secondary Structure
W_w	Wing weight
W_{zf}	Zero fuel weight
W/S	Wing loading
x/c	Point location along chord
Y	Lateral CG location consistent with W_{zf}
Y/SS	Fuselage (CG) lateral location to semispan ratio
Y/b	Fuselage (CG) lateral location to wing span ratio
$(\Delta n_t)_{LG}$	Incremental inner wing coefficient for 2.0g taxi due to landing gear location inboard of fuselage
ϵ_{ea}	Unit chord location of elastic axis
η	Body location in percent semispan and engine power setting
η_{al}	Unit spanwise location of wing airload
$(\eta_{al})_{ow}$	Unit spanwise location of outer wing airload
η_b	Unit spanwise location of planform break
η_e	Engine location
η_{fus}	Unit spanwise location of fuselage centerline
η_{lg}	Unit spanwise location of main landing gear
η_m	Unit spanwise location of total wing mean chord

$\bar{\eta}_a$	Correction factor for effective lift
$(\bar{\eta}_a)_{ow}$	Outer wing correction factor
$(\bar{\eta}_a)_{iw}$	Inner wing correction factor
$\bar{\eta}_e$	Unit spanwise loaction of engine CG
$\bar{\eta}_g$	Gust correction factor
$\bar{\eta}_t$	Taxi correction factor for 2.0g taxi
Λ	Wing sweep angle
$\Lambda_{c/z}$	Mid-chord sweep angle
Λ_{le}	Leading edge sweep angle
λ	Taper ratio
λ_b	Break chord ratio
λ_e	Equivalent taper ratio
λ_r	Total root chord to reference wing root chord ratio
$\bar{\lambda}$	Total wing average chord to reference wing root chord ratio
ϕ	Bank angle
$C_{L_{max}}$	Maximum lift coefficient
C_{L_α}	Lift curve slope
C_{M_α}	Pitching moment curve slope
$C_{M_{z_1}}$	Pitching moment at zero lift
$C_{M_{\dot{\alpha}}}$	Pitching moment due to α
C_{M_q}	Pitching moment due to q
$C_{M_{\delta_e}}$	Pitching moment due to elevator deflection
$C_{L_{\delta_e}}$	Lift due to elevator deflection
$C_{M_{i_H}}$	Pitching moment due to stabilizer incidence
$C_{L_{i_H}}$	Lift due to stabilizer incidence

C_{n_β}	Yawing moment due to sideslip
C_{l_β}	Rolling moment due to sideslip
C_{Y_β}	Side force due to sideslip
C_{n_p}	Yawing moment due to roll rate
C_{l_p}	Rolling moment due to roll rate
C_{Y_p}	Side force due to roll rate
C_{n_r}	Yawing moment due to yaw rate
C_{l_r}	Rolling moment due to yaw rate
C_{Y_r}	Side force due to yaw rate
$C_{n_{\delta_r}}$	Yawing moment due to rudder deflection
$C_{l_{\delta_r}}$	Rolling moment due to rudder deflection
$C_{y_{\delta_r}}$	Side force due to rudder deflection
$C_{l_{\delta_a}}$	Rolling moment due to aileron deflection
$C_{n_{\delta_a}}$	Yawing moment due to aileron deflection
S_{ref}	Aircraft reference area
b_{ref}	Aircraft reference span
$\bar{c}_{ref}$	Aircraft reference mean aerodynamic chord
CG	Center of gravity, % c
I_{xx}	Roll moment of inertia
I_{yy}	Pitch moment of inertia
I_{zz}	Yaw moment of inertia

I_{xz}	Product of inertia
δ_f	Wing flap deflection
δ_e	Elevator deflection
i_h	Horizontal stabilizer incidence
δ_r	Rudder deflection
δ_a	Aileron deflection
V_s	Stall speed
V_{App}	Approach speed
M	Mach number
β	Sideslip angle
$\ddot{\phi}$	Roll acceleration
$\ddot{\psi}$	Yaw acceleration
$\ddot{\theta}$	Pitch acceleration
p	Roll rate
$\dot{p}$	Roll acceleration
n	Load factor
α	Aircraft angle of attack
α_{zl}	Aircraft angle of attack for zero lift
$\dot{\alpha}$	Rate of aircraft angle of attack change
q	Pitch rate
r	Yaw rate
T_{30^o}	Time to achieve a 30^o bank angle using full lateral control input
T_{double}	Time to double amplitude for a pitch axis instability
SM	Static margin
ϕ_{osc}/ϕ_{avg}	Ratio of the oscillatory component to the average component of bank angle following a rudder-pedals-free impulse aileron input (see reference 3)

ψ_β	Phase angle in a cosine representation of the dutch roll sideslip component (see reference 3)
p_{osc}/p_{avg}	Ratio of the oscillatory component to the average component of roll rate following a rudder-pedals-free impulse aileron input (see reference 3)
$\Delta\beta_{max}$	Maximum sideslip excursion occurring within 2 seconds or one half-period of the dutch roll, whichever is greater, for a step aileron command (see reference 3)
k	Ratio of commanded roll performance to the applicable roll performance requirement (see reference 3)
$\omega_{n_{sp}}$	Short period natural frequency
δ_{sp}	Short period damping ratio
$\omega_{n_{dr}}$	Dutch roll natural frequency
δ_{dr}	Dutch roll damping ratio
τ_r	Roll mode time constant
$T_{\phi\ double}$	Spiral mode time to double bank angle

REFERENCES

1. Johnston, William M., et al., "Technical and Economic Assessment of Span-Distributed Loading Cargo Aircraft Concepts," NASA CR-145034 (prepared by Lockheed-Georgia Company), August 1976.

2. Whitlow, David H. and Whitener, P. C., "Technical and Economic Assessment of Span-Distributed Loading Cargo Aircraft Concepts," NASA CR-144963 (prepared by Boeing Commercial Airplane Company), June 1976.

3. "Technical and Economic Assessment of Span-Loaded Cargo Aaircraft Concepts," NASAA CR-144962 (prepared by McDonnell douglas Corporation), January 1976.

4. Whitehead, Allen H., Jr., "Preliminary Analysis of the Span-Distributed-Load Concept for Cargo Aircraft Design," NASA TM X-3319, Langley Research Center, December 1975.

5. Hess, John L., "Calculation of Potential Flow About Arbitrary Three-Dimensional Lifting Bodies," Naval Air Systems Command, MDC J5679-01 (prepared by Douglas Aircraft Company, McDonnell Douglas Corporation), October 1972.

6. Miranda, Luis R., Elliot, Robert D., and Baker, William M., "A Generalized Vortex Lattice Method for Subsonic and Supersonic Flow Applications," National Aeronautics and Space Administration, Report 2865 (prepared by Lockheed-California Company), December 1977.

7. "Military Specification, Flying Qualities of Piloted Airplanes," MIL-F-8785 (ASG)-4, August 1969.

8. Silvers, Charles L., and Withers, Clifton C., "Evaluation of the Flying Qualities Requirements of MIL-F-8785B(ASG) using the C-5A Airplane," Air Force Flight Dynamics Laboratory, AFFDL-TR-75-3 (prepared by Lockheed-Georgia Company), March 1975.

9. Moore, J. W., et al., "Peripheral Jet Air Cushion Landing System-Spanloader Aircraft," Volume 1, Air Force Flight Dynamics Laboratory, AFFDL-TR-79-3152 (prepared by Lockheed-Georgia Company), December 1979.

1 Report No	2 Government Accession No	3 Recipient's Catalog No
NASA CR-165829		
4 Title and Subtitle MULTIBODY AIRCRAFT STUDY Volume I		5 Report Date JULY 1982 6 Performing Organization Code
7 Author(s) J.W. Moore; E. P. Craven; B. T. Farmer; J. F. Honrath; R. E. Stephens; C. E. Bronson, Jr.; R. T. Meyer; and J. H. Hogue		8 Performing Organization Report No LG81ER0259
9 Performing Organization Name and Address LOCKHEED-GEORGIA COMPANY 86 South Cobb Drive Marietta, Georgia 30063		10 Work Unit No 11 Contract or Grant No NAS1-15927
12 Sponsoring Agency Name and Address NATIONAL AERONAUTICS AND SPACE ADMINISTRATION Washington, D.C. 20546		13 Type of Report and Period Covered Contractor Report Sept 1979 thru Sept 1981 14

15 Supplementary Notes

NASA Program Manager: D. V. Maddalon

16 Abstract

The purpose of this report is to quantify and provide technical substantiation of the potential benefits of a multibody aircraft when compared to a single body aircraft. The analyses consist principally of a detailed point design analysis of three multibody and one single body aircraft, based on a selected payload of 350,000 kg (771,618 lb), for final aircraft definitions; sensitivity studies to evaluate the effects of variations in payload, wing semispan body locations, and fuel price; recommendations as to the research and technology requirements needed to validate the multibody concept.

Two, two-body, one, three-body, and one single body aircraft were finalized for the selected payload, with DOC being the prime figure-of-merit. When compared to the single body, the multibody aircraft showed a reduction in DOC by as much as 11.3 percent. Operating weight was reduced up to 14 percent, and fly-away cost reductions ranged from 8.6 to 13.4 percent.

Weight reduction, hence cost, of the multibody aircraft resulted primarily from the wing bending relief afforded by the bodies being located outboard on the wing.

Wind tunnel tests and flight simulation are recommended so as to better understand the aerodynamic characteristics in order to assure an acceptable level of risk in the design and development of a large multibody aircraft. For this same reason, further structural investigations are required in such areas as dynamic loads, load alleviation, unsymmetrical loads, flutter, and material application.

17 Key Words (Suggested by Author(s))	18 Distribution Statement
Multibody, Two-Body, Three-Body, Single Body, Point Design, Wing Span Efficiency, Load Distribution, Vorlax, Hess	Unclassified-Unlimited Subject Category - 05

19 Security Classif (of this report)	20 Security Classif (of this page)	21 No of Pages	22 Price*
Unclassified	Unclassified	241	

End of Document